

AD-A234 482

2

GL-TR-88-0111
ENVIRONMENTAL RESEARCH PAPERS, NO. 1002

Analysis of the IRAS Low Resolution Spectra

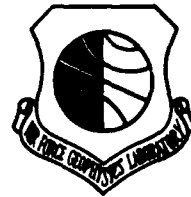
IRENE LITTLE-MARENIN



1 April 1988



Approved for public release; distribution unlimited



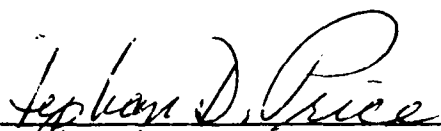
OPTICAL PHYSICS DIVISION PROJECT 7670
AIR FORCE GEOPHYSICS LABORATORY
HANSCOM AFB, MA 01731

UNCLASSIFIED

97 4 20 1988

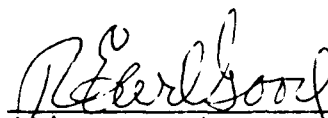
"This technical report has been reviewed and is approved for publication"

FOR THE COMMANDER



(Signature)

STEPHAN D. PRICE, Chief
Celestial Backgrounds Branch



(Signature)

R. EARL GOOD, Acting Director
Optical Physics Division

This document has been reviewed by the ESD public Affairs Office (PA) and is releasable to the National Technical Information Service (NTIS).

Qualified requestors may obtain additional copies from the Defense Technical Information Center. All others should apply to the National Technical Information Service.

If your address has changed, or if you wish to be removed from the mailing list, or if the addressee is no longer employed by your organization, please notify AFGL/DAA, Hanscom AFB, MA 01731. This will assist us in maintaining a current mailing list.

Do not return copies of this report unless contractual obligations or notices on a specific document requires that it be returned.

UNCLASSIFIED

SECURITY CLASSIFICATION OF THIS PAGE

REPORT DOCUMENTATION PAGE				Form Approved OMB No. 0704-0188	
1a. REPORT SECURITY CLASSIFICATION UNCLASSIFIED		1b. RESTRICTIVE MARKINGS			
2a. SECURITY CLASSIFICATION AUTHORITY		3. DISTRIBUTION / AVAILABILITY OF REPORT Approved for Public Release; Distribution unlimited			
2b. DECLASSIFICATION / DOWNGRADING SCHEDULE					
4. PERFORMING ORGANIZATION REPORT NUMBER(S) AFGL-TR-88-0111 ERP, No. 1002		5. MONITORING ORGANIZATION REPORT NUMBER(S)			
6a. NAME OF PERFORMING ORGANIZATION Air Force Geophysics Laboratory		6b. OFFICE SYMBOL (if applicable) OPC		7a. NAME OF MONITORING ORGANIZATION	
6c. ADDRESS (City, State, and ZIP Code) Hanscom AFB Massachusetts 01531-5000		7b. ADDRESS (City, State, and ZIP Code)			
8a. NAME OF FUNDING / SPONSORING ORGANIZATION		8b. OFFICE SYMBOL (if applicable)		9. PROCUREMENT INSTRUMENT IDENTIFICATION NUMBER	
8c. ADDRESS (City, State, and ZIP Code)		10. SOURCE OF FUNDING NUMBERS			
		PROGRAM ELEMENT NO. 62101F	PROJECT NO. 7670	TASK NO. 06	WORK UNIT ACCESSION NO. 13
11. TITLE (Include Security Classification) Analysis of the IRAS Low Resolution Spectra					
12. PERSONAL AUTHOR(S) Irene Little-Marenin					
13a. TYPE OF REPORT In-house		13b. TIME COVERED FROM _____ TO _____		14. DATE OF REPORT (Year, Month, Day) 1988 April 1	
				15. PAGE COUNT 178	
16. SUPPLEMENTARY NOTATION					
17. COSATI CODES			18. SUBJECT TERMS (Continue on reverse if necessary and identify by block number)		
FIELD	GROUP	SUB-GROUP	Infrared Astronomy, Stellar Spectra		
03	01				
03	02				
19. ABSTRACT (Continue on reverse if necessary and identify by block number)					
<p>Analysis of the IRAS low resolution spectra show that the 8-22 μm spectral range show a variety of emission features. The strongest features in spectra of M stars are the 10 and 18 μm silicate emission features. In addition a three-component feature with peaks at 10, 11 and 13.1 μm and a weak, broad 9-15 μm feature is present in many M variable stars. Most carbon stars show the 11.2 μm SiC emission feature as well as, in some cases, an unidentified 8-9 μm emission feature. The MS, S and SC stars show a range of emission features whose peaks range from 10 to 11.2 μm. The excess emission above the underlying photospheric continuum in the 8-22 μm region for S Mira variables shows a sharp increase for period greater than about 370 days.</p>					
20. DISTRIBUTION / AVAILABILITY OF ABSTRACT <input checked="" type="checkbox"/> UNCLASSIFIED / UNLIMITED <input type="checkbox"/> SAME AS RPT. <input type="checkbox"/> DTIC USERS			21. ABSTRACT SECURITY CLASSIFICATION Unclassified		
22a. NAME OF RESPONSIBLE INDIVIDUAL Stephan D. Price			22b. TELEPHONE (Include Area Code) (617) 377-4552		22c. OFFICE SYMBOL OPC

DD Form 1473, JUN 86

Previous editions are obsolete.

SECURITY CLASSIFICATION OF THIS PAGE

UNCLASSIFIED

Acknowledgements

I would like to thank the Air Force Office of Scientific Research for providing the University Resident Research Program, the Air Force Geophysics Laboratory/Optical Physics Division, Celestial Backgrounds Branch for their hospitality and Wellesley College for allowing me to be re-assigned to the Air Force in order to pursue this research opportunity. I specially would like to thank Len Marcotte for writing the original computer program to obtain the LKS spectra and Charles Wilton for modifying the program while working for me in the 1985 USAF-UES Summer Graduate Research Program. My special thanks are reserved for Stephan Price for making me welcome and providing support and to Paul LeVan for many interesting conversations. My collaborations with my colleagues at Wellesley College are gratefully acknowledged. Wendy Hagen Bauer made it possible to publish our technetium survey and Priscilla J. Benson introduced me to the intricacies of radio astronomy. Most important, my collaborations with my husband Stephen J. Little over the years has greatly increased my understanding of the fundamental issues involved in our research projects.



Accession For	
DTIC GRA&I	<input checked="" type="checkbox"/>
DTIC TAB	<input type="checkbox"/>
Unannounced	<input type="checkbox"/>
Justification	
By	
Distribution	
Availability	
Not	Special
A-1	

Contents

1. RESEARCH	1
1.1 M Stars	2
1.2 Carbon Stars	4
1.3 MS, S, and SC Stars	5
2. OTHER WORK	6
2.1 Other Research	6
2.2 Summer Students	7
2.3 Conferences	7
3. PUBLICATIONS	8
REFERENCES	
APPENDIXES	
A. ULTRAVIOLET, OPTICAL, INFRARED, AND MICROWAVE OBSERVATIONS OF HR 5110 (AP J COPYRIGHT)	11
B. CARBON STARS WITH SILICATE DUST IN THEIR CIRCUMSTELLAR SHELLS (AP J. COPYRIGHT NOTICE — SHE WORKED HERE ON AN AFOSR GRANT)	25
C. A WATER MASER ASSOCIATED WITH EU ANDROMEDAE: A CARBON STAR NEAR AN OXYGEN-RICH CIRCUMSTELLAR SHELL (AP J COPYRIGHT — BENSON WORKED AT WELLESLEY COLL., WHILE LITTLE-MARENIN WORKED HERE)	33
D. NEW CARBON STARS IDENTIFIED FROM LOW-RESOLUTION IRAS SPECTRA (A.J. COPYRIGHT — MULTIPLE AUTHORS)	39
E. A SEARCH FOR TECHNETIUM (TC II) IN BARIUM STARS (A.J. COPYRIGHT — LITTLE WORKED AT BENTLEY)	47

F.	ADDITIONAL LATE-TYPE STARS WITH TECHNETIUM (A.J. COPYRIGHT — ALL 3 GOT NSF OR AFGL MONEY)	53
G.	MASERS ASSOCIATED WITH TWO CARBON STARS: V778 CYGNI AND EU ANDROMEDAE (ACCEPTED BY AP J FOR PUBLICATION 15 JUL 88; TWO NON-GOVERNMENT AUTHORS)	71
H.	EMISSION FEATURES IN IRAS LRS SPECTRA OF MS, S, AND SC STARS (SUBMITTED TO AP J; LITTLE IS AT BENTLEY COLL)	97
I.	PAPERS PUBLISHED AS PART OF A CONFERENCE PROCEEDING (SPRINGER-VERLAG PROBABLE COPYRIGHT) CONF. TITLE: COOL STARS, STELLAR SYSTEMS, AND THE SUN	135
J.	SUMMER SCHOOL ON INTERSTELLAR PROCESSES: ABSTRACTS OF CONTRIBUTED PAPERS (NASA PUB)	147
K.	CONFERENCE DIGEST: SECOND HAYSTACK OBSERVATORY MEETING, PAPER ENTITLED WATER MASERS AROUND TWO SHORT PERIOD MIRAS: R. CETI AND RZ SCORPII. LITTLE-MARENIN, BENSON AND DICKINSON	153
L.	EMISSION FEATURES IN IRAS LRS SPECTRA OF MS, S. AND SC STARS, (PROC 5TH CAMBRIDGE WORKSHOP ON COOL STARS, STELLAR SYSTEMS AND THE SUN, SPRINGER VERLAG PROBABLE COPYRIGHT)	159
M.	NEW LATE-TYPE STARS WITH TECHNETIUM, AND MISSING LRS SPECTRA OF IRAS C AND S STARS, PUB AS POSTER PAPER ABSTRACTS IN BULL. AAAS.	169

Analysis of the IRAS Low Resolution Spectra

I have analyzed the emission characteristics in the low resolution spectra of cool celestial sources. This study concentrated on the emission characteristics of dust grain features that are produced in the circumstellar dust shells (CDS) of stars in the late stages of their evolution and on the determination of the amount of infrared excess produced by the CDS. I found that the spectra show a variety of emission features, most of which were previously not known.

1. RESEARCH

The Infrared Astronomical Satellite, IRAS, surveyed the sky in four wavelength bands centered on 12, 25, 60 and 100 μm . Spectra of sources brighter than about 8 Jy in the 8-22 μm region were also obtained by the Low Resolution spectrometer (LRS). Emission features from silicate dust grains at 10 and 18 μm and of silicon carbide dust grains at 11.2 μm are found in this spectral range. The LRS simultaneously scanned two overlapping wavelength ranges, one extending from 8-13.4 μm and the other from 11-22.6 μm . The resolution ($\Delta\lambda / \lambda$) of the spectrometer varied with wavelength from about 15 at the short wavelength end to about 60 at the long wavelengths. The two wavelength halves in general do not agree at 12 μm unless a linear baseline is subtracted from the usable portion of the spectrum.

The IRAS science team characterized the LRS spectra according to the shape of the energy distribution and type of emission and absorption features observed in the 8-22 μm region.¹ Typical spectra from oxygen-rich

(Received for Publication 25 March 1988)

¹IRAS Science Working Group. 1986, *Atlas of Low Resolution Spectra, Astr. Ap., (Suppl.), 65, 607.*

stars that have silicate dust grain emission features extending from about 8-14 μm with a maximum around 10 μm are characterized as 2n where n=1 to 9 measures the strength of the 10 μm emission. Many, but not all, 2n spectra also show the broad 18 μm emission feature due to the bending mode of silicates. Spectra of carbon-rich objects have SiC dust grain emission features between about 10 to 14 μm with a maximum around 11.2 μm . They are characterized as 4n where n=1 to 9 measures the strength of the SiC feature. No other emission features due to dust grains were recognized in the LRS characterization since no others were known at that time. Spectra characterized as 1n supposedly indicate a blue featureless continuum where n=1 to 9 is twice the spectral index in the 8-22 μm region. Hence, stars whose spectra show only a photospheric continuum ($T > 3000\text{K}$) are characterized as 18. The *Explanatory Supplement to the IRAS Catalogs and Atlases*, 1984, Chapter 9² has a complete discussion of the 10 different characterization classes.

During the late stages of stellar evolution, asymptotic giant branch (AGB) stars produce energy in hydrogen and helium burning shells. Thermal instabilities that develop in these stars can dredge up material from the nuclear processed regions, changing the surface compositions of the stars. In this evolutionary phase, stars evolve along the spectral sequence from M \rightarrow MS \rightarrow S \rightarrow (SC) \rightarrow C stars as classified by the optical appearance of their spectra. These changes are accompanied by light variability and increased mass loss with the consequence that the stars can develop extensive circumstellar dust shells. My research has focused on the type of emission features observed in the LRS spectra of the various spectral classes observed during the AGB phase and on the amount of infrared excess produced by the CDS. First, I will discuss the M stars and their emission features, second the C stars, and third the intermediate evolutionary stages: the MS, S and SC stars.

1.1 M Stars

Non-variable M stars have not yet reached the thermal instability phase of their evolution and, for the most part, their LRS spectra show only a featureless photospheric continuum indicating the absence of CDS. On the other hand, most of the variable M stars show both an infrared excess and dust grain emission features in the 8-22 μm region.

Roughly 35 percent of the variable M stars are characterized as 2n, that is, they have LRS spectra with silicate emission features; about 45 percent are 1n with the rest having a variety of other characterizations. I will first discuss the 2n spectra. To study the emission features I assume that the 8-22 μm emission is produced by a) the stellar photosphere, b) a continuum emission from the dust grains and c) a strongly wavelength dependent term due to the dust grains. Representing the first two terms with a black body energy distributions and subtracting it from the observed spectrum, we are left with the remaining strongly wavelength dependent emission feature term. The 10 μm silicate emission feature among the 2n stars shows variations from star to star. However, I find that the variable stars can be divided into three groups characterized by similar spectral shapes. The 10 μm feature of semiregular (SRa,b,c) and irregular Lb variables extends from 8.4 μm to $\sim 14 \mu\text{m}$ with a peak at $10 \pm 0.05 \mu\text{m}$. The FWHM (Full Width Half Maximum) is $2.1 \pm 0.15 \mu\text{m}$, but the feature is asymmetric with the ratio of the width of the short wavelength (rising) branch to the long wavelength (falling) branch of 0.6:1.5 at half intensity. The average silicate excess of Mira variables extends from 8-14 μm with a peak at 9.75 μm and a FWHM of 2.3 μm . The feature is also asymmetric but on the average has a less steeply rising branch than the

²*Explanatory Supplement to the IRAS Catalogs and Atlases*, 1984, Ed. C.A Beichman, G. Neugebauer, H.J. Habing, I.E. Clegg, T.J. Chester. Washington, DC: US Govt. Print. Office.

other long period variables (LPVs). However, the $10\ \mu\text{m}$ Mira feature shows much greater variation from star to star than that of the other LPVs. The shape of the Mira feature ranges from one identical to the SRs and Lbs to a much broader one which extends from $< 8\ \mu\text{m}$ to $\sim 14\ \mu\text{m}$ with a corresponding shift in the peak emission from 10 to $9.6\ \mu\text{m}$ and an increase in FWHM from 2.1 to $2.4\ \mu\text{m}$. In general the greater the contrast, C_T , (defined as the percent of emission above the underlying continuum at the wavelength of peak emission) the shorter the beginning wavelength of the rising branch. The above results were presented at the Summer School on Interstellar Processes held July 2-7, 1986 (Little-Marenin, Little and Price 1986).

Almost two thirds of the spectra of stars with weak emission features (those characterized as 21 and 22) irrespective of the variability type show a new type of emission feature with 3 components and emission peaks at 10 , 11 and $13.1\ \mu\text{m}$ and extending from about 8.8 to $15\ \mu\text{m}$. In M stars the $10\ \mu\text{m}$ peak is always strongest but the intensity of the other components varies greatly from star to star. A long wavelength feature that peaks at $19\ \mu\text{m}$, distinctly different from the $18\ \mu\text{m}$ bending mode feature of silicates, is also present. The dust grain or size distribution of dust grains or other mechanism that produces this emission has not yet been identified. It is not known how or if the feature is related to silicate dust (Little-Marenin and Price 1986).³

We decided to investigate the variables characterized as 1n (implying a featureless continuum) in greater detail since almost half of the Mira variables are characterized as 1n. Mass loss in Mira variables is expected to be high and hence circumstellar dustshell emission either as dust grain features or continuum dust emission should be observable. Of the 1n stars only those characterized as 18 or 17, with very few exceptions, show a featureless continuum that can be matched with temperatures hotter than about $1500\ \text{K}$ representative of the photospheric emission in the LRS. This unexpectedly includes about 2 percent of the Miras. Roughly half of the spectra that are characterized as 13, 14, 15 and 16 with S/N's larger than 10 show a relatively cool (500 - $800\ \text{K}$) featureless continuum most likely due to continuum (black body) emission from the dust grains in the CDS. The other half of the LRS spectra show various types of weak, broad emission features. Some of these resemble the 3-component feature discussed previously while others show a broad 9 - $15\ \mu\text{m}$ feature with a poorly defined peak around $11.4\ \mu\text{m}$ and FWHM ~ 4 - $4.5\ \mu\text{m}$. It is too broad to be due to SiC and has the wrong wavelength dependence to be associated with the usual silicate emission. It appears that the weak 1n and weak 2n (21, 22) features can be described as consisting of three components with peaks at roughly 10 , 11 and $13\ \mu\text{m}$. The contribution of the three components to the observed feature of any one star varies so that we observe a continuous range of spectral shapes from the $10\ \mu\text{m}$ silicate feature for which the 11 and $13\ \mu\text{m}$ contribution is small, to the 3-component feature with a larger contribution at 11 and $13\ \mu\text{m}$, to the 9 - $15\ \mu\text{m}$ feature for which the $10\ \mu\text{m}$ component is weaker than $11\ \mu\text{m}$ component. The weak 2n spectra have a larger percentage of 3-component features than the 1n spectra, otherwise there does not appear to be a significant difference between stars characterized as 13, 14, 15 and 16 or 21 and 22. If any, or all, of these features are produced by silicates is not yet known. Part of the research on the 1n spectra was obtained by Todd Strohmayer while on the 1987 USAF-UES Graduate Student Summer Support Program at AFGL.

The 8 - $22\ \mu\text{m}$ excess, defined as the percent of emission above an assumed photospheric continuum of $T=2500\ \text{K}$ ranges from 0 percent to about 300 percent. How the 8 - $22\ \mu\text{m}$ excess relates to the period of light variability and mass loss rate for these stars is presently being investigated.

³Little-Marenin, I.R. and Price, S.D. 1986, "The Shapes of the Circumstellar Silicate Feature," *Summer School on Interstellar Processes*, Grand Teton National Park, July 2-7, 1986, NASA Technical Memorandum 88342, pp. 137-138.

1.2 Carbon Stars

The LRS spectra of carbon stars show a much smaller variety in the emission features than do the M stars. I have only been able to identify two, possibly three, different emission features. The SiC feature is remarkably uniform among the C stars independent of the strength of the feature, unlike the $10\ \mu\text{m}$ silicate feature among the M stars. The maximum of the feature is found at $11.15 \pm 0.10\ \mu\text{m}$ with a FWHM of $1.6 \pm 0.15\ \mu\text{m}$.⁴

The SiC feature is uniform enough so that it can be used as a classification criterion. We have therefore, classified 176 stars as C stars from their LRS spectra (Little-Marenin, Ramsay, Stephenson, Little and Price 1987).⁵ Many, but not all C stars with enhanced ^{13}C , have spectra in which the emission feature is shifted to about $11.6\ \mu\text{m}$. A second fairly symmetrical emission feature, unknown before the LRS spectra became available, extends from about $8\text{-}10\ \mu\text{m}$ with an emission peak at $8.6\ \mu\text{m}$ and a FWHM of about $1.3\ \mu\text{m}$. The intensity of the feature varies greatly from star to star, at times being more intense than the SiC feature. No obvious correlations exist between photospheric abundances, such as the C/O, N/C or $^{12}\text{C}/^{13}\text{C}$ ratios determined by Lambert et al (1986),⁶ and the strength of the $8.6\ \mu\text{m}$ feature except that stars with larger C/O ratios (>1.04) appear to show the stronger $8.6\ \mu\text{m}$ features. The $8.6\ \mu\text{m}$ feature is not related to the presence of an s-process element since both stars with large s-process enhancements and no s-process enhancements, such as Y CVn, show the feature. A few C stars appear to have additional continuum emission in the $14\text{-}22\ \mu\text{m}$ region due to amorphous carbon.

Besides emission features, the LRS spectra of C stars also show photospheric absorption due to C_2H_2 and HCN around $14\ \mu\text{m}$. The short wavelength edge of the feature is difficult to define since it is blended with the SiC emission. The strength of the absorption shows a positive correlation with the photospheric C/O ratio. Other absorption bands of these two molecules have been observed around $3.1\ \mu\text{m}$ and $7.5\ \mu\text{m}$ in C star spectra.

The excess $8\text{-}22\ \mu\text{m}$ emission in carbon stars is small, ranging from 0 percent to a maximum of about 30 percent. These values are much smaller than the ranges of $8\text{-}22\ \mu\text{m}$ excesses observed in M stars. Even for C star Miras the typical value of the $8\text{-}22\ \mu\text{m}$ excess is only about 15 percent. The excess is primarily due to the dust emission from SiC. Amorphous carbon contributes only a few percent in a few stars. No C star Miras are known which are without an infrared excess of SiC emission feature. The relationship between the $8\text{-}22\ \mu\text{m}$ excess, period of light variability, and mass loss rates is being currently investigated.

Most unexpected was the discovery of three C stars with strong 10 and $18\ \mu\text{m}$ silicate emission features in their LRS spectra (Little-Marenin 1986).⁷ An additional four C stars were added to the list by Willems (1987).⁸ The presence of oxygen-rich material near the C stars is confirmed by the detection of the $22\ \text{GHz}$ water maser

⁴Little-Marenin, I.R., and Wilton, C., 1986, "Analysis of IRAS Low Resolution Spectra (LRS) of Carbon and M Variable Stars," *Cool Stars, Stellar Systems and the Sun*, Lecture Notes in Physics No. 254, eds. M. Zeilik and D.M. Gibson, (Springer-Verlag:Berlin), p. 420-422.

⁵Little-Marenin, I.R., Ramsay, M.E., Stephenson, C.B., Little, S.J. and Price, S.D. 1987, "New Carbon Stars Classified from IRS Low Resolution Spectra," *Artron. J.*, **93**, 663-668.

⁶Lambert, D.L., Gustafsson, B., Ericksson K., and Hinkle, K.H. 1986, *Astrophys. J. Suppl.*, **62**, 373.

⁷Little-Marenin, I.R. 1986, "Carbon Stars with Silicate Dust in Their Circumstellar Shells," *Ap. J. (Letters)*, **307**, L15-L19.

⁸Willems, F.J. 1987, (Ph.D thesis, University of Amsterdam).

emission line from two of the C stars, EU And⁹ and V778 Cyg.^{10,11} The positional agreement between the water maser and the optical counterpart to V778 Cyg was recently tightened to 0.5" by Deguchi et al (1988).¹² Also, the location of the C stars in IRAS color-color plots places them among the oxygen-rich M stars with moderately thick circumstellar dust shells. We interpret these C stars as being part of a binary system with a C and an M star component. The circumstellar dust shell around the M star produces the 10 and 18 μm silicate dust grain emission features and the water maser emission line while absorbing the visible light of the M star so that in the visible and near infrared region only the C star component is visible. We do not believe in the interpretation of Willems (1987) that the observations can be explained as the transition of an M into a C star, since the transit time of material through the CDS from which the maser and the silicate emission arises is only on the order of 50 years and the stars were classified as C stars more than 40 years ago

1.3 MS, S and SC Stars

Stellar evolution theory predicts, and observations confirm, that stars evolve from M->MS->S->(SC)->C stars during the late stages of AGB evolution. Helium shell flashing occurs at this stage of stellar evolution and the products of helium burning, primarily ¹²C and s-process elements, are mixed with the outer envelope during the third dredge-up. The C:O ratio changes progressively from about 0.4 in M stars to about 1.1 in C stars and s-process elements are enhanced from their solar value in M stars to about 100 times the solar value in C stars. Since stars develop CDS during their AGB phase of evolution, we searched for signatures of the changing photospheric composition in the dust grain emission features observed in the LRS spectra of these evolving stars.

We found that the typical emission feature of strong S stars (those with the greater amounts of s-process enhancements) show dust grain emission extending from about 9 to 14 μm , with a peak between 10.3-11 μm and a FWHM of 2.4 μm . This feature resembles neither the silicate, the 3-component or broad 9-15 μm feature observed in M stars nor the SiC feature observed in C stars. The exact carrier of this feature is not yet known, but we suspect that it may be due to a silicate dust grain combined with an s-process element such as Zr, Ba or La. A second possibility is that the 10.8 μm S star feature is produced by both silicate and SiC dust grains since it is possible to mimic the observed emission by co-adding the silicate and SiC emission features, as suggested by

⁹Benson, P.J. and Little-Marenin, I.R. 1987, "A Water Maser Associated with EU Andromedae: A Carbon Star Near an Oxygen-Rich Circumstellar Shell," *Ap. J. (Letters)*, **316**, L37-L40.

¹⁰Little-Marenin, I.R., Benson, P.J., and Little, S.J. 1987, "Water Masers Associated with Two Carbon stars: EU Andromedae and V778 Cygni," *Cool Stars, Stellar Systems and the Sun*, Fifth Cambridge Workshop, 1987, July 7-10, Boulder, CO, eds J.L. Linsky and R. Stencel (Heidelberg: Springer Verlag) p. 396.

¹¹Little-Marenin, I.R., Benson, P.J., and Dickinson, D.F. 1988 "Masers Associated with Two Carbon Stars: V778 Cygni and EU Andromedae" (in press, the *Astrophysical Journal*, 1988, July 15).

¹²Deguchi, S., Kawabe, R., Ukita, N., Nakada, Y., Onaka, T., Izumiura, H., and Okamura, S., "Position Confirmation of Water Maser Emission from V778 Cygni, a Carbon Star," 1988, *Ap. J.*, **325**, 795.

Little, Little-Marenin and Price (1987).¹³ I recommend that stars classified as M stars which show the 10.8 μm feature in their LRS spectra should be re-examined to see if the 10.8 μm feature can be used as a classification criteria for S stars in the mid-infrared.

The emission features of the S stars are in general quite weak, having an average contrast of about 27 percent. This may be the result of two effects: a) the circumstellar dust shells of these stars may have less material in them and hence not many dust grains are available, and/or b) since the C:O ratio in S stars is closer to unity than in M stars, less oxygen is available to form oxygen-bearing grains such as silicates. Support for hypothesis (a) is given by the fact that 8-22 μm emission excess shows a positive correlation with the mass loss rate of S stars implying that less material in the CDS produces fewer dust grains. The importance of hypothesis (b) can not be established until the exact carrier of the 10.8 μm feature has been identified.

MS stars are a transition phase between M and S stars and their LRS spectra show a variety of dust grain emission features ranging from spectra with the typical 10 μm silicate feature, to the 3-component feature, to the 10.8 μm S star feature. We interpret this to mean that the changing photospheric composition in MS stars produces different dust grain features in the 8-22 μm region depending on the exact abundances observed in the CDS.

SC stars are the transition phase between S and C stars. These stars are rare and only a few of them were bright enough to obtain their LRS spectra. Their spectra show emission features that range from the 10.8 μm S star feature to the 11.2 μm SiC feature, again implying that the changing photospheric composition of these transition objects produces dust grain features representative of the changing C:O ratio.

The 8-22 μm excess observed in MS, S, and SC stars correlates with their period of light variability. Specifically the excess shows a marked increase for $P > 370$ days implying that the amount of material able to emit in the 8-22 μm region increases markedly for the long τ period stars.¹⁴

2. OTHER WORK

2.1 Other Research

During my two years at AFGL I was able to finish and publish a 10 year survey of technetium (Tc) in late-type stars. Technetium has no stable isotopes and theory predicts that it is produced and mixed to the surface of stars in their late AGB phase of evolution. Its presence allows us to delineate those stars in which helium shell flashing has recently occurred and is still occurring. We found that only M Miras with $P > 300$ days show Tc in their atmosphere (Little, Little-Marenin and Bauer 1987).¹⁵ We are presently investigating if these stars have larger mass loss rates and stronger silicate emission features in their LRS. In a related project we were able to

¹³Little, S.J., Little-Marenin, I.R., and Price, S.D. 1987, "Emission Features in IRAS LRS Spectra of MS, S and SC Stars," *Cool Stars, Stellar Systems and the Sun*, Fifth Cambridge Workshop 1987, July 7-10, Boulder, CO, eds J.L. Linsky and R. Stencel (Heidelberg:Springer Verlag) p. 377.

¹⁴Little-Marenin, I.R. and Little, S.J. 1988, "Emission Features in IRAS LRS Spectra of MS, S and SC Stars," (submitted to the *Astrophysical Journal*).

¹⁵Little, S.J., Little-Marenin, I.R., and Bauer, W.H. 1987, "Additional Late Type Stars with Technetium," *Astron. J.*, **94**, 981-995.

show that ionized Tc (Tc II) is not observed in the ultraviolet spectra of barium stars obtained with the Ultraviolet Explorer Satellite (IUE). Hence barium stars are not in their AGB phase of evolution and their observed s-process enhancements are most probably related to the binary nature of these stars (Little-Marenin and Little 1987).¹⁶

In order to understand the nature of the C stars with silicate and water maser emission features in their spectra, we have been monitoring the water maser emission from EU And and V778 Cyg and about 10 other long period variable stars since March of 1987 at the 37 m Haystack Radio telescope in Westford, MA. As part of this project we have discovered the first two short period Mira variables that are associated with water maser emission (Little-Marenin, Benson and Dickinson 1987).¹⁷

2.2 Summer Students

During the summer of 1986 Mary Elizabeth Ramsay, a Wellesley College undergraduate, was working with me on a Dana Foundation Fellowship from Wellesley college on the analysis of objects characterized as 4n but not previously classified as carbon stars. We were able to classify 176 new carbon stars on the basis of their SiC feature. Also, we have shown that approximately 80 out of 540 4n stars were incorrectly characterized as having an SiC emission feature (Little-Marenin, Ramsay, Stephenson, Little and Price 1987).⁵

During the summer of 1987 Todd Strohmayer, a graduate student at the University of Rochester, was working with me under the USAF-UES Summer Graduate Research program. He analyzed the 1n spectra and I have summarized many of his results. He also developed programs to calculate the color correction factor for the 12, 25, 50 and 100 μ m IRAS bands and modified Fortran programs to calculate the combined emission from the photosphere and their circumstellar dust shells assuming the shell is optically thin.

2.3 Conferences

During my tenure at AFGL/OPC I attended the following conferences and presented our research results:

1) The 168th meeting of the American Astronomical Society held 22-26 June 1986 in Ames, Iowa (three papers).^{18, 19, 20}

¹⁶Little-Marenin, I.R. and Little, S.J. 1987, "A Search for Technetium (TcII) in Barium Stars," *Astron. J.*, **93**, 1539-1541.

¹⁷Little-Marenin, I.R., Benson, P.J., and Dickinson, D.F. 1987, "Water Masers Around Two Short Period Miras: R Ceti and RZ Scorpii," *Interstellar Matter, Second Haystack Observatory Conference*, 1987, June 10-12 (in press).

¹⁸Little-Marenin, I.R., Stephenson, C.B., and Little, S.J. 1986, "New Carbon Stars Classified from IRAS Low Resolution Spectra," *Bull. Am. Astron. Soc.*, **18**, 669.

¹⁹Little, S.J., Little-Marenin, I.R., Hagen, W., and Lewis, L. 1986, "New Late-Type Stars with Technetium," *Bull. Am. Astron. Soc.*, **18**, 669.

²⁰Culver, R.B., Little-Marenin, I.R., Little, S.J., and Craine, E.R. 1986, "Missing LRS Spectra of IRAS C and S Stars," *Bull. Am. Astron. Soc.*, **18**, 669.

2) The Summer School on *INTERSTELLAR PROCESSES* held 3-7 July 1986 at Grand Teton National Park, Wyoming.³

3) The Second Haystack Observatory meeting on *INTERSTELLAR MATTER* held in Honor of Alan H. Barrett on 10-12 June 1987 at MIT, Cambridge, MA.¹⁷

4) The Fifth Cambridge Workshop on *COOL STARS, STELLAR SYSTEMS AND THE SUN*, held 7-11 July 1987 at Boulder, CO.^{10, 13}

3. PUBLICATIONS

The following is a list of publications produced or published during my two years of tenure at AFGL.

PAPERS PUBLISHED, ACCEPTED OR SUBMITTED FOR PUBLICATION TO REFERREED JOURNALS

Little-Marenin, I.R., Simon, T., Ayres, T.R., Cohen, N.L., Feldman, P., Linsky, J.L., Little, S.J., and Lyons, R. 1986, "Ultraviolet, Optical Infrared, and Microwave Observations of HR 5110," *Ap. J.*, **303**, 780-790.

Little-Marenin, I.R. 1986, "Carbon Stars with Silicate Dust in Their Circumstellar Shells," *Ap. J. (Letters)*, **307**, L15-L19.

Little-Marenin, I.R., Ramsay, M.E., Stephenson, C.B., Little, S.J. and Price, S.D. 1987, "New Carbon Stars Classified from IRAS Low Resolution Spectra," *Astron. J.*, **93**, 663-668.

Benson, P.J. and Little-Marenin, I.R. 1987, "A Water Maser Associated with EU Andromedae: A Carbon Star Near an Oxygen-Rich Circumstellar Shell," *Ap. J. (Letters)*, **316**, L37-L40.

Little-Marenin, I.R. and Little, S.J. 1987, "A Search for Technetium (TcII) in Barium Stars," *Astron. J.*, **93**, 1539-1541.

Little, S.J., Little-Marenin, I.R., and Bauer, W.H. 1987, "Additional Late Type Stars with Technetium," *Astron. J.*, **94**, 981-995.

Little-Marenin, I.R., Benson, P.J., and Dickinson, D.F. 1988, "Masers Associated with two Carbon Stars: V778 Cygni and EU Andromedae," (in press the *Astrophysical Journal*, 1988, July 15).

Little-Marenin, I.R. and Little, S.J. 1988, "Emission Features in IRAS LRS Spectra of MS, S and SC Stars," (submitted to the *Astrophysical Journal*).

PAPERS GIVEN AT CONFERENCES AND PUBLISHED AS CONFERENCE PROCEEDINGS

Little-Marenin, I.R., and Wilton, C., 1986, "Analysis of IRAS Low Resolution Spectra (LRS) of Carbon and M Variable Stars," *Cool Stars, Stellar Systems and the Sun*, Lecture Notes in Physics No. 254, eds. M. Zeilik and D.M. Gibson, (Springer-Verlag: Berlin), p. 420-422.

Little, S.J. and Little-Marenin, I.R. 1986, "An Analysis of IRAS Low-Resolution Spectra of S Stars," *Cool Stars, Stellar Systems and the Sun*, Lecture Notes in Physics, eds. M. Zeilik and D.M. Gibson, (Springer-Verlag: Berlin), p. 423-425.

Little-Marenin, I.R., Linsky, J.L., and Simon, T. 1986, "HR 5110: An Algol System with RS CVn Characteristics," *Cool Stars, Stellar Systems and the Sun*, Lecture Notes in Physics, No. 254, eds. M. Zeilik and D.M. Gibson, (Springer-Verlag: Berlin), p. 247-249.

Little-Marenin, I.R. and Price, S.D. 1986, "The Shapes of the Circumstellar Silicate Feature," *Summer School on Interstellar Processes*, Grand Teton National Park, July 2-7, 1986, NASA Technical Memorandum

88342, p. 137-138.

Little-Marenin, I.R., Benson, P.J., and Dickinson, D.F. 1987, "Water Masers Around Two Short Period Miras: R Ceti and RZ Scorpii," *Interstellar Matter*, Second Haystack Observatory Conference, 1987, June 10-12 (in press).

Little-Marenin, I.R., Benson, P.J., and Little, S.J. 1987, "Water Masers Associated with Two Carbon Stars: EU Andromedae and V778 Cygni," *Cool Stars, Stellar Systems and the Sun*, Fifth Cambridge Workshop, 1987, July 7-10, Boulder, CO, eds J.L. Linsky and R. Stencel (Heidelberg: Springer Verlag) p. 396.

Little, S.J., Little-Marenin, I.R., and Price, S.D. 1987, "Emission Features in IRAS LRS Spectra of MS, S and SC Stars," *Cool Stars, Stellar Systems and the Sun*, Fifth Cambridge Workshop 1987, July 7-10, Boulder, CO, eds J.L. Linsky and R. Stencel (Heidelberg: Springer Verlag) p. 377.

PAPERS PRESENTED AT MEETINGS WITH PUBLISHED ABSTRACTS

Little-Marenin, I.R., Stephenson, C.B., and Little, S.J. 1986, "New Carbon stars Classified from IRAS Low Resolution Spectra," *Bull. Am. Astron. Soc.*, **18**, 669.

Little, S.J., Little-Marenin, I.R., Hagen, W. and Lewis, L. 1986, "New Late-Type Stars with Technetium," *Bull. Am. Astron. Soc.*, **18**, 669.

Culver, R.B., Little-Marenin, I.R., Little, S.J., and Craine, E.R. 1986, "Missing LRS Spectra of IRAS C and S Stars," *Bull. Am. Astron. Soc.*, **18**, 669.

Appendix A

Ultraviolet, Optical, Infrared, and Microwave
Observations of HR 5110

ULTRAVIOLET, OPTICAL, INFRARED, AND MICROWAVE OBSERVATIONS OF HR 5110

I. R. LITTLE-MARENIN¹

Joint Institute for Laboratory Astrophysics, University of Colorado and National Bureau of Standards

THEODORE SIMON^{2,3}

Institute for Astronomy, University of Hawaii

T. R. AYRES²

Laboratory for Atmospheric and Space Physics, University of Colorado

N. L. COHEN

Department of Earth and Planetary Sciences, MIT; Astronomy Department, Cornell University; Astronomy Department, Harvard University

P. A. FELDMAN

Herzberg Institute of Astrophysics, National Research Council of Canada

J. L. LINSKY^{2,4}

Joint Institute for Laboratory Astrophysics, National Bureau of Standards and University of Colorado

S. J. LITTLE

Department of Natural Sciences, Bentley College

AND

R. LYONS

David Dunlap Observatory, University of Toronto

Received 1985 June 10; accepted 1985 October 10

ABSTRACT

HR 5110 is a close binary system ($P = 2^d6$) which is viewed nearly pole-on ($i = 13^\circ$). A comparison of the characteristics of Algol and RS CVn systems to those of HR 5110 shows that HR 5110 can also be considered an Algol system. Because the primary star is relatively cool (F2 IV) and there is no apparent emission from an accretion disk, we are able to detect in *IUE* spectra the emission of an active chromosphere and transition region of the cooler (K0 IV) secondary. HR 5110 is important because it is the only known Algol system for which the properties of the secondary star can be studied in detail. Velocity shifts of the ultraviolet emission lines relative to the absorption lines formed in the F2 IV star photosphere, which are measured in a short-wavelength high-dispersion spectrum obtained near quadrature, show unambiguously that the active chromosphere and transition region are located on the K0 IV star and not the F2 IV or an accretion disk around the F2 IV star. The surface fluxes of the UV emission lines of the K star are similar to those of active RS CVn binaries (HR 1099, UX Ari). The line fluxes appear to vary with orbital phase and are interpreted as emission from an active region on the K star moving across the line of sight. Two large radio flares were detected, but coordinated observations of the second flare in the UV and at the Ca II and H α lines showed no detectable effect of the flare in these spectral regions 26 hr after the flare onset, during a time of continuing activity at radio wavelengths. VLBI observations during one of these flares indicated that half the emission came from a region more than 4 times the binary separation. The visual and near-infrared broad-band colors of HR 5110 are best matched with an F2 IV primary and a spotted K0 IV secondary.

Subject headings: stars: binaries — stars: individual — stars: radio radiation — ultraviolet: spectra

1. INTRODUCTION

The short-period spectroscopic binary HR 5110 (HD 118216 = BH CVn) presents a unique opportunity to study the similarities and differences between Algol and RS CVn variable stars. RS CVn binaries are detached systems having orbital and rotational periods generally less than 20 days and mass ratios close to unity (Hall 1981). They were first recognized as a (separate) class of objects distinct from Algols and other close binaries by Hall (1976) and are noted for unusually strong Ca II H and K emission, which arises in the active chromosphere of

the cooler component. This intense activity is also observed in UV spectra taken with the *International Ultraviolet Explorer* (*IUE*) satellite in strong emission lines of ions from Mg II through N V; these lines are diagnostic of chromospheric and transition region (TR) plasmas ranging in temperature from about 10^4 K to 2×10^5 K. This enhanced activity is thought to be due to the rapid rotation of the cooler component (Ayres and Linsky 1980; Dupree 1981). Evidence for dark starspots on RS CVn stars is found in the wavelike distortion of their optical light curves (Eaton and Hall 1979; Rodonó 1983). They are also strong coronal X-ray emitters (Walter and Bowyer 1981) and undergo large radio and UV flares (Feldman *et al.* 1978).

Algol binaries, on the other hand, are semidetached systems whose mass ratios average about 0.2. Their more

¹ JILA Research Fellow 1983-1984, on leave from Wellesley College.

² Guest Observer, *International Ultraviolet Explorer*.

³ Guest Observer, Kitt Peak National Observatory.

⁴ Staff Member, Quantum Physics Division, National Bureau of Standards.

evolved but less massive member fills its Roche lobe. The general properties of 101 eclipsing Algol systems are summarized by Giuricin, Mardirossian, and Mezzetti (1983). Over 50% of the primary spectra are early A but do range from B through K. Relatively little is known about the secondaries except that the spectral classes in over two-thirds of the systems range from late G to early K. Spectra of the secondaries can be obtained during primary eclipse but emission from accretion disks or gas streams often dominates the stellar flux (Plavec 1983; Plavec, Weiland, and Koch 1982). These eclipse spectra show strong emission lines of C IV, N V, C II, Si IV-II, Al II-III, and Fe III and are qualitatively similar to spectra of RS CVn stars (except for the lack of He II emission). This emission has been attributed to accretion disks around the hotter stars based primarily on the decreasing strengths of the emission lines as the system proceeds toward totality during primary eclipse (Plavec 1983; Plavec, Weiland, and Koch 1982). Plavec argues that the absence of observed He II emission in Algol systems is consistent with a recombination spectrum formed at 10^5 K. In the case of AW Peg, H α emission from the cooler K component has been attributed to an extended chromosphere (Plavec and Polidan 1976). Algols are soft X-ray sources with the emission appearing to come from a corona around the cooler component, but at flux levels 3 times lower (for a given rotation period) than RS CVn systems (White and Marshall 1983). Algols show sporadic radio outbursts (Hjellming, Webster, and Balick 1972) with characteristics similar to RS CVn binaries. The radio emission is probably associated with the secondary (Gibson 1980; Feldman and Kwok 1979). VLBI observations by Mutel *et al.* (1985) when HR 5110 was quite active indicated a source with angular diameter 0".0010 (FWHM), which is about twice the inferred angular diameter of the secondary (see below).

The most relevant characteristics of Algols and RS CVn systems are summarized in Table 1. The principal distinction between the two systems appears to be that the secondaries of Algols fill their Roche lobe whereas the RS CVn secondaries are detached. Many of the other differences may be outgrowths of this: in Algols, mass flow through the inner Lagrangian point produces the observed gas streams and accretion disks around the primary; eventually mass transfer to the less evolved component makes it the more massive member of the system (by a factor of 5 on the average) and produces under-massive K subgiant secondaries. As Popper and Ulrich (1977)

pointed out, RS CVn stars appear to evolve from ordinary nonemission close binaries that develop their characteristics when the more massive star enters the Hertzsprung gap. With time, this primary swells and may fill its Roche lobe as it evolves across the H-R diagram. The second major distinction between Algol and RS CVn binaries is the fact that in RS CVn systems we are able to observe chromospheric and TR emission produced by the rapidly rotating, cooler, larger component. Spin-orbit synchronization does not allow these stars to dissipate their rotational angular momentum as they cross the Hertzsprung gap for the first time as is seen in single stars (Simon 1984).

The secondaries of short-period Algol systems are also in synchronous orbits and should, like RS CVn binaries, exhibit enhanced chromospheric and TR emission. This emission is best studied in the UV with *IUE*. However, in Algols, the UV spectrum is usually dominated by either the hot primary, an accretion source, or hot gas streams. Only when the primary is relatively cool and has a faint accretion disk, will we be able to study UV emission from an Algol secondary. This is the situation we observe for the nearby HR 5110 system but for no other known bright Algol system. According to Conti's (1967) analysis HR 5110 consists of an F2 IV primary and an evolved late-type secondary in a nearly pole-on ($i = 13^\circ$) circular orbit (Lucy and Sweeney 1971) with a period of 2.61 days, a mean separation of 0.05 AU (about $10 R_\odot$), and a mass ratio of 0.28. If we assume a mass of $1.5 M_\odot$ for the F2 IV star, then the mass of the secondary is $0.43 M_\odot$. Based on the separation of the components and the estimated spectral and luminosity class of the secondary (as long as it is not a dwarf), the secondary fills its Roche lobe of $2.6 R_\odot$. Hence mass loss or transfer is the likely reason for making the current secondary the less massive component. From the statistics of Algol systems we find that F star primaries have early K secondaries with a mass in the range 0.2–0.4 M_\odot as is found for HR 5110. This system was included by Hall (1976) in his list of RS CVn binaries based on the fact that strong Ca II emission is associated with the K secondary (Conti 1967), but it can also be described as an Algol system as a comparison of the characteristics of Table 1 show. Hence HR 5110 gives us the unusual opportunity of studying an Algol system in a nearby pole-on configuration. (Many nonclipping Algols should exist, but they are difficult to detect.) HR 5110 does show a slight periodic photometric variation of 0.01 mag but no pronounced photometric wave

TABLE 1
COMPARISON OF RS CANIS VENATICORUM BINARIES,
ALGOL SYSTEMS, AND HR 5110

Parameter	RS CVn	Algol	HR 5110
Mass ratio (secondary/primary)	≈ 1.0	≈ 0.2	0.28
Secondary fills Roche lobe	No	Yes	Yes
Typical inclination of orbit (degrees)	~ 60	~ 90	13
Evidence for mass streams	No	Yes	Maybe
Evidence for accretion disks	No	Yes	No
Evidence for active regions	Yes	No	Yes
Photometric wave	Yes	No	No
Typical spectral type of secondary stars	K0 IV	Early K	K0 IV
Typical mass of secondary (M_\odot)	~ 1	0.2–0.4	0.42
Typical spectral type of primary stars	G V	Early A	F2 IV
Flaring	Yes	Yes	Yes
Radio, X-ray emission	Yes	Yes	Yes
Ca II H + K emission	Yes	No	Yes
UV surface fluxes	High	High	High

(Hall *et al.* 1978). Since the decrease in magnitude coincides with conjunction at phase 0.0 (cooler star in front), Dorren and Guinan (1980) interpreted the variability as a reflection effect rather than rotational modulation due to dark starspots.

The ultraviolet spectrum (1200–2000 Å) of HR 5110 observed with *IUE* shows the strong emission lines typical of RS CVn binaries (interpreted as coming from chromospheres and TR around the cooler secondary) (Simon, Linsky, and Schiffer 1980a, b); but the spectrum also resembles spectra observed during the primary eclipse of Algol (W Serpentis) systems (interpreted as coming from accretion disks around the hotter primary) (Plavec 1983; Plavec, Weiland, and Koch 1982). Hence it is essential to pinpoint the location of the UV emission of HR 5110 in order to interpret the system correctly. HR 5110 is also a soft X-ray source with an X-ray luminosity of 1.3×10^{31} ergs $\text{cm}^{-2} \text{s}^{-1}$ (Walter and Bowyer 1981), which is more typical of the higher X-ray luminosity of RS CVn stars rather than Algols (White and Marshall 1983). HR 5110 has also been detected as a flaring and nonflaring radio source. A recent reanalysis of the orbit (Bonsack and Simon 1983; Lyons, Bolton, and Fraquelli 1984) indicates a slight period change and/or a phase shift of about 0.1 phase relative to the previous analysis of Conti (1967). We found a similar shift in analyzing Ca II K line region from CCD spectral data kindly made available to us by F. Walter.

II. INFRARED OBSERVATIONS

An interpretation of HR 5110 depends critically on knowing the spectral type and luminosity class of the two stars in the system. Line surface fluxes (to be compared to RS CVn binaries) can be calculated if the sizes of the components (as estimated from the spectral information) are known. The primary was classified as F2 IV by Slettebak (1955) and F5 III by Cowley (1976). From the visual colors of the system, Conti (1967) estimated that the secondary is an evolved K star and that the difference in V magnitude between the components is 2.5 mag. Dickens and Penny (1971) determined $\theta (=5040/T) = 0.76$ and $\log g = 3.8$ from fitting model atmospheres to the continuum energy distribution of HR 5110. Their surface gravity would be more in line with a luminosity classification of IV or III–IV rather than Cowley's luminosity classification.

To estimate the spectral type and luminosity class of the secondary we obtained near-infrared *JHKLM* photometry of HR 5110 on the 1.3 m telescope of the Kitt Peak National Observatory in 1980 February and June and also 1981 May. HR 5110 was measured with respect to the standard stars used by Castor and Simon (1983), on magnitude scales whose zero points were defined by the primary standard α Lyrae. There was no clear evidence, even at the longest wavelength, for any photometric wave above observational uncertainties (e.g., ± 0.03 mag at *M*). An infrared photometric wave has been observed by M. Zeilik (private communication). We have derived a best fit of the combined colors for different types of primaries (F2 V, F2 IV, F5 IV, F5 III, G0 V) and secondaries (G5 IV, G8 IV, K0 IV, K1 IV) to the observed colors of HR 5110. Our photometry is listed in Table 2A.

Line doubling is present at Li I 6707 Å (M. Tripicco and F. Fekel, private communication), so the model derived from fitting the colors should give a reasonable small V magnitude difference for the primary and secondary components, i.e., $V_s - V_p \lesssim 2.5$ mag. Following Conti (1967, eq. [2]) we calculate the flux f (normalized to V) of the system at any wavelength according to $f = \alpha f_p + (1 - \alpha) f_s$, where $f_{p,s}$ is the normalized

flux of the primary and secondary, respectively. The factor α is given by $\alpha = r(r + 1)^{-1}$, where r is the ratio of the brightness in the V band of the primary to the secondary. The value of α , or equivalently r , is not known *a priori* but is calculated from spectral fitting. The value of α is obtained from a least-squares fit to the observed flux f of HR 5110, starting from the assumed colors and hence normalized fluxes f_p and f_s at each wavelength. That is, we take

$$\alpha = \frac{\sum_i (f - f_s)(f_p - f_s)_i}{\sum_i (f_p - f_s)_i^2},$$

where the sum is carried out over filter bands other than V . In practice we usually summed over (1) R and I , or (2) J , H , K , and L in order to derive a best fit to these particular wavelength regions. Tables 2A and 2B summarize the derived colors for HR 5110, for several primaries and secondaries, and for the most relevant models. For each model we list the value of α (and the filters used for its derivation), the standard deviation σ of the fit, and the V magnitude difference between the secondary and primary, $V_s - V_p$.

Our final models were calculated with σ Boo (F2 V) as primary. Its IR photometry is better established than that of the standard F2 IV star of Johnson *et al.* (1966) and the fit to the IR region is most critical for determining the characteristics of the secondary. As can be seen (Table 2A), σ Boo is photometrically similar to an F2 IV star. The best fit to the photometry of HR 5110 is obtained for an F2 IV (σ Boo) + K0 IV model. Fitting the R and I colors gives an IR excess of ~ 0.2 mag at both L and M' . On the other hand, fitting the $J-L$ colors produces a deficit of $\sim 0.05-0.1$ mag at I , which seems large considering the small statistical errors of the photometry. Figure 1 shows the residuals ($O - C$) of these models as open circles (to fit R and I) and as triangles (to fit $J-L$). The range of residuals produced by combining different secondaries (G5 IV, G8 IV, K1 IV, as listed in Table 2B) with σ Boo as primary is indicated by the hatched areas. The $J-L$ colors cannot be fitted with a G5 IV secondary. Using an F5 IV or F5 III primary gave the same general trends except that the residuals were larger. The result of our spectral synthesis is in agreement with the statistics found for Algol systems by Guiricir, Mardirossian, and Mezzetti (1983): every F primary has a K secondary.

According to our first solution (col. [2] of Table 2B), HR 5110 has an IR excess which could be due to intrasystem material. To interpret the IR excess, we assume an absolute flux calibration and plot this excess against λ . The excess from J to M' is fairly well matched with a blackbody curve of 3100 K and therefore is too hot to be produced by dust and has the wrong wavelength dependence to be produced by free-free emission. We believe the IR excess can be explained if the colors of the secondary itself are composite because it is heavily spotted. Assuming a weighting factor A for the spot coverage on the secondary, and a temperature of about 3100 K for the spots (Vogt 1983), we recalculated the combined flux f of the system for an F2 IV primary and spotted K0 IV secondary from $f = \alpha f_p + (1 - \alpha)[(1 - A)f_{sq} + Af_{ss}]$, where $f_{sq,ss}$ is the normalized flux of the quiet photosphere and the spotted area of the secondary, respectively. For f_{sq} we used the colors corresponding to K0 IV and for f_{ss} we used the average of the colors of the M3 III and M5 V standard stars (Johnson *et al.* 1966). However, the colors of the M filter are not very reliable. The best fit to the observed flux for $\alpha = 0.85$ is produced with

TABLE 2A
SPECTRAL SYNTHESIS FOR HR 5110

Color	HR 5110 Observed	F2 IV Standard	σ Boo F2 V	48 Gem F5 IV	β Com G0 V	μ Her A G5 IV	β Aql G8 IV	η Ser K0 IV	κ CrB K1 IV
$U-V$	0.45 ^a	0.39 ^a	0.29 ^b	0.45 ^a	0.66 ^a	1.14 ^a	1.35 ^a	1.59 ^a	1.87 ^a
$B-V$	0.41 ^b	0.29 ^a	0.36 ^b	0.36 ^a	0.58 ^b	0.74 ^b	0.86 ^a	0.94 ^a	1.00 ^a
V	4.96 ^b	0.00	4.48 ^b	5.85 ^a	4.25 ^b	3.42 ^b	3.71 ^a	3.25 ^a	4.82 ^a
$V-R$	0.41 ^b	0.35 ^a	0.34 ^b	0.43 ^a	0.45 ^b	0.55 ^b	0.66 ^a	0.70 ^a	0.76 ^a
$V-I$	0.69 ^b	0.55 ^a	0.57 ^b	0.68 ^a	0.76 ^b	0.90 ^b	1.15 ^a	1.20 ^a	1.25 ^a
$V-J$	1.03	0.68 ^a	0.76	0.77	1.09	1.28	1.53	1.68	1.75
$V-H$	1.35	0.83 ^c	0.95	0.94	1.36	1.60	1.99	2.17	2.24
$V-K$	1.43	0.93 ^a	0.98	1.00	1.40	1.67	2.07	2.25	2.33
$V-L$	1.49	1.07 ^a	1.00	1.02	1.44	1.66	2.06	2.29	2.38
$V-M'$	1.52	0.93 ^a	1.05	1.12	1.43	1.61	1.99	2.19	2.27

NOTE.—Colors from this paper unless otherwise indicated; units are mag throughout.

^a Johnson *et al.* 1966; Johnson 1966.

^b Moffett and Barnes 1979.

^c Calibration for H taken from Koornneef 1983.

TABLE 2B
SPECTRAL SYNTHESIS FOR HR 5110

Parameter (1)	σ Boo + η Ser (F2 V + K0 IV) (2)	σ Boo + η Ser (F2 V + K0 IV) (3)	48 Gem + η Ser (F5 IV + K0 IV) (4)	48 Gem + β Com (F5 IV + G0 V) (5)	σ Boo + η Ser + spot (F2 V + K0 IV + spot) (6)
$U-V$	0.41	0.47	0.63	0.48	0.41
$B-V$	0.43	0.46	0.47	0.39	0.43
V	0.00	0.00	0.00	0.00	0.00
$V-R$	0.40	0.43	0.50	0.43	0.41
$V-I$	0.69	0.75	0.82	0.70	0.74
$V-J$	0.96	1.04	1.06	0.84	1.03
$V-H$	1.25	1.36	1.37	1.02	...
$V-K$	1.29	1.41	1.44	1.08	1.42
$V-L$	1.32	1.44	1.47	1.11	1.49
$V-M'$	1.32	1.42	1.48	1.17	1.44
α	0.84	0.78	0.77	0.83	0.85
Filters ^a	R, I	J, H, K, L	J, H, K, L, M	B, I	R, I
σ	0.11	0.05	0.09	0.24	0.04
$V_s - V_p$ (mag)	1.80	1.37	1.31	1.67	1.88
a_s	0.35-0.40

^a The value of α is derived by fitting the predicted and observed fluxes of the listed filter bands.

$A = 0.025$ (see Fig. 1 and Table 2B), but there remains a flux deficit at I of ~ 0.05 mag. The weighting factor A of 0.025 corresponds to a spot filling factor a_s of 0.35-0.40 for an estimated flux contrast ratio c_s between spot and quiet photosphere of 20-25. The contrast ratio is estimated from the assumed spot and photospheric temperatures; then $a_s = Ac_s(\bar{i} - A + Ac_s)^{-1}$.

It is important to match the absolute magnitudes (M_v) deduced for the components with what is expected from evolutionary considerations. We derived M_v 's for two assumed values of the parallax π considered by Conti (1967), 0".019 and 0".027. The π of 0".027 forces the primary onto the post-main-sequence evolutionary track for a 1.5 M_\odot star, while a π of 0".019 places HR 5110 closer to the 2 M_\odot track. The locus of possible secondaries is close to the 1.0 M_\odot track for $\pi = 0".027$. Thus if $M_s = 0.4 M_\odot$, the secondary is overluminous for its mass.

Shore and Adelman (1984) have suggested that the components of HR 5110 are F5 IV + G0 V, based on a comparison with the composite spectral energy distribution between 4000 Å and 11000 Å of β Com (G0 V) and 48 Gem (F5 IV). We disagree with their conclusion. First, their model is incompatible with the observed near-IR infrared colors of the system

(Table 2B). A least-squares fit to the B , V , R , and I data gives an IR excess of ~ 0.4 mag at L and M' and a V magnitude difference of 1.67. This is less than the V magnitude difference between a G0 V and a F5 IV star of 2.1 star cited by Allen (1981). Second, if we assume a mass of 1.1 M_\odot for their G0 V secondary, then the known mass ratio would imply a mass of $\sim 4 M_\odot$ for their F5 IV primary, which is larger by a factor of ~ 2 than expected for a typical F5 IV star. In conclusion, an F2 IV + K0 IV system is a better match to the observed broadband colors of HR 5110 than Shore's and Adelman's choice of F5 IV + G0 V. In fact, except for the U and B colors, the colors of β Com itself match those of HR 5110 quite well, but no combination of a G0 V secondary with any F primary matches HR 5110 over the entire spectral range. The observed line doubling near 6700 Å eliminates any dwarf cooler than G2 as a candidate for the secondary of HR 5110.

Adopting a spotted K0 IV star for the secondary, we obtain from the Barnes-Evans relationship (Barnes and Evans 1976) between color, visual magnitude, and angular diameter, an angular diameter of 0.47 mag if $V-R = 0.70$ (see Table 2A) and $V_s = 7.1$, corresponding to $V_s - V_p = 1.88$. This diameter yields a radius of 1.9-2.7 R_\odot for a parallax of 0".027 $\geq \pi \geq$ 0".019. Hence, we conclude that the secondary fills its Roche

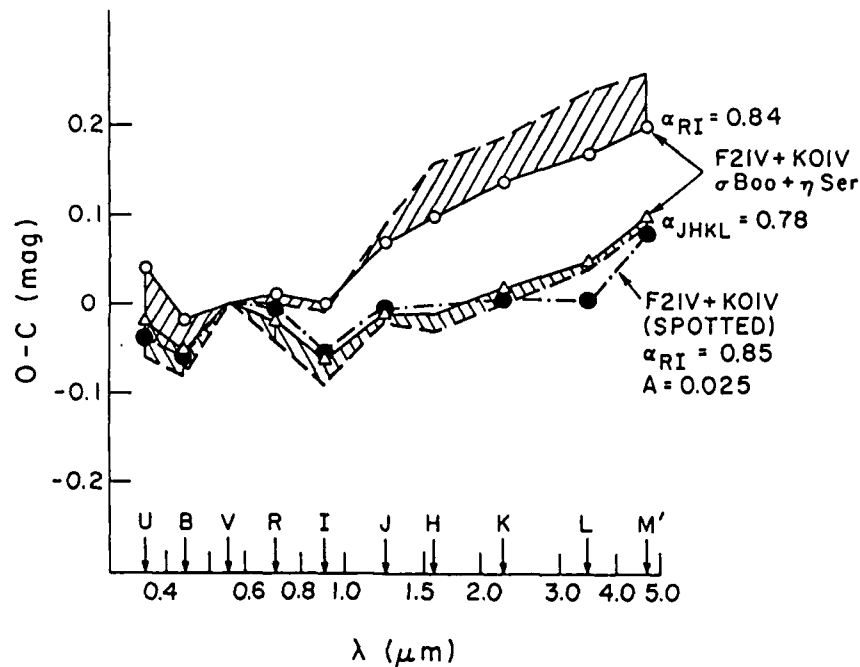


FIG. 1.—The residuals (observed — computed colors) of HR 5110 as compared to an F2 IV + K0 IV system. Open circles show the fit if the R and I colors are matched; triangles show the fit to J, H, K, and L colors, and filled circles show the fit for an F2 IV + spotted K0 IV secondary with a filling factor $\alpha_s = 0.25$. The hatched areas indicate the range in residuals for F2 IV + (G5 IV or G8 IV or K IV secondary).

lobe radius of $2.6 R_\odot$ calculated from the mass ratio and the separation of the stars, as originally suggested by Conti (1967).

III. RADIO OBSERVATIONS

HR 5110 was detected during two major radio flaring events, and also detected by VLBI techniques. The first major flare was observed from the Algonquin Observatory (Feldman 1979) on 1979 May 29 (8:26 UT) with a measured flux at 10.46 GHz of 425 mJy. Flaring continued over the next 2 days at the 200–350 mJy level. The second flare (Feldman 1981) was similar to the first. On 1981 April 4 the system was observed at a flux level of 240 mJy. A larger outburst at the 350–410 mJy level occurred on 1981 April 5 starting at 6:30 UT and lasted for about 4 hr. Flaring continued at the 150–200 mJy level for the next several days (Feldman 1983). These radio outbursts are probably due to gyrosynchrotron emission from mildly relativistic electrons (Owen, Jones, and Gibson 1976; Lestrade *et al.* 1984). Figure 2 shows the radio light curve for the second flare together with the times of coordinated VLBI, IUE, Ca II, and H α observations. While these other observations were made 1–2 days after the major outburst, radio activity continued at the time of these observations.

On 1981 April 6 we observed HR 5110 at 5.0 GHz (6 cm) in left-hand circular polarization using the Mark III VLBI System with 56 MHz bandwidth. The stations used were the OVRO 130 foot (40 m) and the NRAO 140 foot (43 m) telescopes. At 03:50 UT we obtained a 10 minute correlated scan for HR 5110, followed by a 3 minute scan on the unresolved (D. Shaffer, private communication) VLBI calibration source 0552 + 398. Reductions of this one-baseline VLBI "snapshot" indicate that the fringe-visibility amplitude was 0.53 ± 0.05 at fringe spacing of 3.7 mas. This implies that during the later (plateau) phase of the outburst about half of the radio emission arose from a region greater than 3.7 mas in size ($= 2.7 \times 10^{12}$

cm = 0.17 AU = $40 R_\odot$ for an assumed distance of 45 pc) which was characterized by a brightness temperature $T_b > 3 \times 10^8$ K. This source region is at least 4 times the separation of the components and accordingly, at this stage in the evolution of the flare, gyrosynchrotron emission comes from a region which is not limited to the confines of either stellar component or to the binary as a whole. During a smaller flare (1982 December 19) Lestrade *et al.* (1984) detected a source of maximum size 1.4 mas using a four-element Mark III VLBI network at 8.4 GHz, and during another smaller flare (1983 July 26/27) Mutel *et al.* (1985) detected a source of size 1.0 mas using a six-element Mark III VLBI network at 5.0 GHz. In these cases the flare region was comparable to or smaller than the size of the binary system and $T_b \approx 2 \times 10^{10}$ K. These VLBI observations of three flares on HR 5110 are consistent with the hypothesis that the flux tubes responsible for the flare emission expand and the electrons lose energy with time.

IV. Ca II AND H α EMISSION

After being notified by P. Feldman of the occurrence of the 1981 April flare, we obtained 6.5 \AA mm^{-1} (taken at DAO) and 8 \AA mm^{-1} (taken at DDO) spectra of the Ca II region starting about 21 hr and 47 hr, respectively, after the onset of the major radio burst and continuing for the next two weeks at DDO. The Ca II emission at this later (plateau) stage of the flare does not show any evidence of flare induced activity. The intensity of the Ca II emission at other times is known to vary by a factor of 3–4 (Conti 1967) and was confirmed by visual inspection of other spectra kindly loaned to us by P. Conti. Whether or not these variations are accompanied by other (unobserved) radio flares is unknown. H α spectra obtained at DDO at 16 \AA mm^{-1} , starting at about 5 UT on April 7 and continuing for the next two weeks, also showed normal, variable, weak emission in the H α profile. The H α emission is variable in both

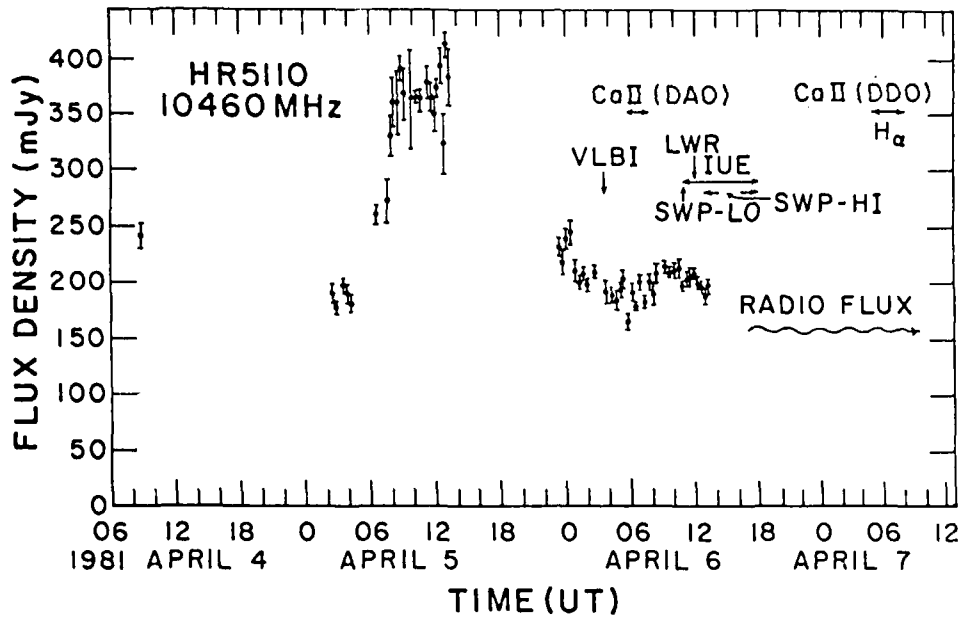


FIG. 2.—The radio light curve of HR 5110 during and immediately following the 1981 April 5 flare (Feldman 1983). The time line of spectroscopy of the Ca II region at DAO and DDO, of the H α region at DDO, of the UV region with IUE, and the time of the VLBI observation are indicated during the later "plateau" phase of the flare.

mean wavelength and intensity but does not appear to be well correlated in velocity with either binary component or to show any effect from flaring. The emission may be due to permanent intrasystem material (Fraquelli 1981; Bopp 1983), but the large mass motions deduced from H α observations in Algol-type systems are not evident in HR 5110.

In conclusion, we find no increase in emission in H α , Ca II H and K, and the UV (see § V) from enhanced chromospheric and TR activity about 20 hr after the onset of a major radio outburst, although the radio emission was still greatly enhanced.

V. IUE OBSERVATIONS

We obtained IUE spectra during the latter (plateau) phases of both radio outbursts, roughly 56 hr after the first major event and 26 hr after the second. We also observed HR 5110 in 1980 February and in 1983 August. An analysis of the data

associated with the first flare was reported by Simon, Linsky, and Schiffer (1980b). A search through the IUE archives yielded two additional spectra presumably taken when the system was quiescent. The observational data for the four SWP low-dispersion spectrum (1200–2000 Å at ~6 Å resolution), the five LWR high-dispersion spectra (2000–3200 Å at ~0.2 Å resolution) and one SWP high-dispersion spectrum (1200–2000 Å at ~0.2 Å resolution) are summarized in Table 3. The phases were calculated from an ephemeris having an epoch of JD 2,445,079.478 and period of 2.61328 days, obtained from the reanalysis of the orbit by Lyons, Bolton and Fraquelli (1984); we have adjusted the epoch so that an orbital phase of 0.0 corresponds to conjunction (K0 star in front) rather than to quadrature (with the secondary at maximum velocity of approach) as in their analysis.

The spectra were calibrated in absolute flux units at Earth using standard IUE calibration factors. The latest Intensity

TABLE 3
IUE OBSERVATIONAL DATA FOR HR 5110

Image Number	Dispersion	Date	Time (UT) (hr/minutes/s)	Orbital Phase ^a ϕ	Exposure Time (minutes)	Comment ^b
SWP 5415	Low	1979 May 31	15:56:21	0.56	30	1
LWR 4652	High	1979 May 31	17:47:25	0.58	10	1
LWR 6333	High	1979 Dec 7	17:17:32	0.67	15	
SWP 7344	Low	1979 Dec 7	17:49:40	0.68	35	
LWR 6838	High	1980 Feb 1	5:31:01	0.52	10	
SWP 7834	Low	1980 Feb 1	5:53:48	0.53	25	
LWR 10297	High	1981 Apr 6	11:40:31	0.17	10	2
SWP 13668	Low	1981 Apr 6	11:06:07	0.16	25	2
SWP 13669	High	1981 Apr 6	17:53:33	0.27	378	2
LWP 16548	High	1983 Aug 8	8:36:00	0.91	10	

^a Based on ephemeris JD = 2,445,079.478 + 2.61328 ϕ , where ϕ = 0.0 corresponds to conjunction with the K0 IV star in front.

^b COMMENTS.—(1) Flare: 1979 May 29, 8:26 UT. (2) Flare: 1981 Apr 5, 6:30 UT.

TABLE 4
INTEGRATED EMISSION-LINE FLUX FOR HR 5110 AT EARTH ($\times 10^{-12}$ ergs cm^{-2} s^{-1})

Image Number	Phase	N v $\lambda 1240$	O I $\lambda 1305$	C II $\lambda 1335$	Si IV $\lambda 1400$	C IV $\lambda 1549$	He II $\lambda 1640$	Continuum ^a 1560-1630 Å	Mg II k $\lambda 2796$	Comments
SWP 13668	0.16	0.32	0.69	0.87	0.79	1.87	0.57	0.19	...	Flare
LWR 10297	0.17	13.0	Flare
LWR 6838	0.52	17.1	
SWP 7834	0.53	0.75	1.75	1.67	1.23	2.63	1.30	0.20	...	
SWP 5415	0.56	0.35	1.61	1.53	1.15	2.56	1.17	0.25	...	Flare
LWR 4652	0.58	15.3	Flare
LWR 6333	0.67	13.7	
SWP 7344	0.68	0.30	0.81	0.83	0.61	1.23	0.66	0.19	...	
LWR 16548	0.91	12.4	
SWP 7834	0.53	2.3	2.5	1.9	1.6	1.4	2.3	1.09	...	To show flux variation at different phases
SWP 13668	0.16									
LWR 6838	0.52									
LWR 10297	0.17									

^a Average continuum flux level in units of 10^{-12} ergs cm^{-2} s^{-1} Å^{-1} .

Transfer Function was applied to SWP 5415 with computer programs at the *IUE* Regional Data Analysis Facility at the University of Colorado. The SWP spectra are saturated longward of 1700 Å due to the rapidly rising photospheric continuum of the F2 IV primary. We measured the integrated flux at Earth of the emission lines of N v, C IV, Si IV, He II, C II, and O I in the low-dispersion spectra. The integrated flux of the Mg II lines was also measured in the LWR high-dispersion spectra. No other emission lines could be identified in the LWR spectra. The Fe II (multiplet UV1) lines near 2600 Å as well as Si II (1804 Å), Si I (1903 Å), and C III (1909 Å) appear in absorption, indicating that the F primary dominates the spectrum in these regions. We also measured the mean continuum level of the primary between 1560 Å and 1620 Å. These fluxes are summarized in Table 4 and are plotted as a function of time in Figure 3.

The fluxes vary by about a factor of 2 in unison during this time interval, but maximum flux in the lines does not uniquely correspond to the times of flares unless an unobserved flare also occurred on 1980 February 1. Although the continuum was brighter after the first flare than at other times, the continuum was not enhanced after the second flare, when the *IUE* observations were made a day closer to the peak of the radio outburst.

Figure 4 compares the two SWP spectra taken after these two flares. The increase in brightness of the continuum in SWP 5415 is clearly evident. Since the continuum arises from the F star, it is likely that this new emission also arises from the primary. It is unclear why excess emission is visible after the first flare but not after the second. Since the two spectra were taken at different phases, the excess may be unrelated to the flare mechanism. We conclude that the radio flares produced no discernible effect on the intensity of the lines and that the changes we observe are normal variations in the activity of the system. A similar conclusion was reached by Simon, Linsky, and Schiffer (1980b) from their earlier analysis of the data associated with the first flare.

By contrast, *IUE* spectra of a flare on UX Ari also taken 26 hr after the initial detection of radio flaring showed a factor of 5.5 enhancement of the UV line strengths (Simon, Linsky, and Schiffer 1980a). Simon, Linsky, and Schiffer suggested that the mechanism for producing flares in these two systems might be quite different. Magnetic field annihilation of interacting coronal loops may be the energy source for the UX Ari flare, whereas the flare on HR 5110 may be produced by mass trans-

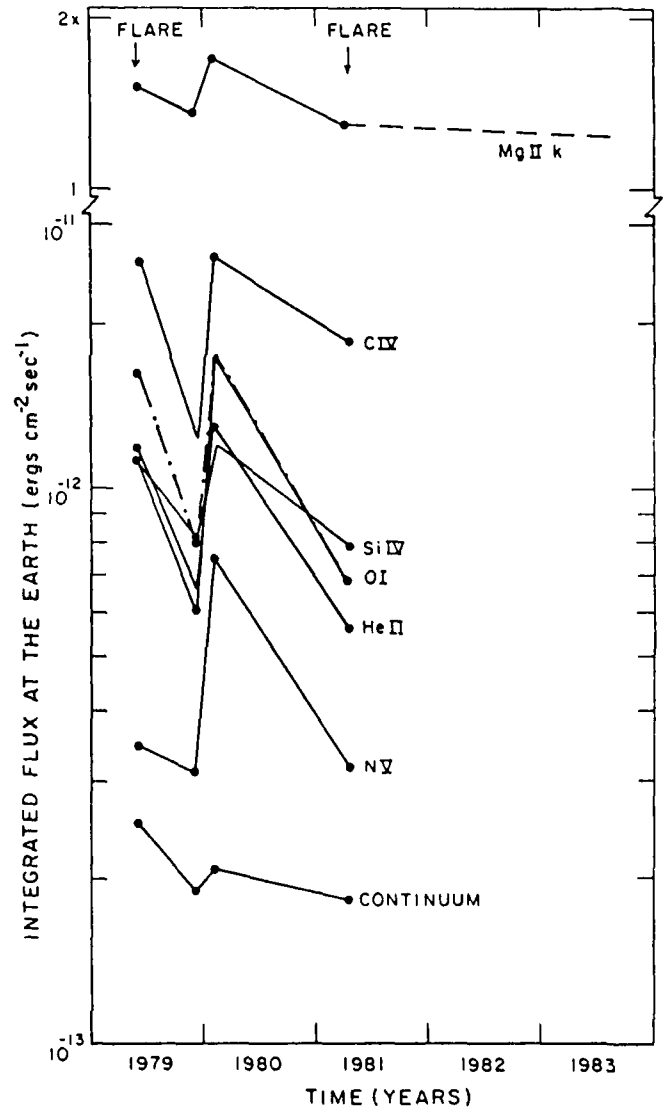


FIG. 3.—The integrated UV emission line flux received at Earth from HR 5110 as a function of time. The occurrences of the two radio flares are indicated with arrows. The continuum flux is the average flux measured in the region 1560-1620 Å.

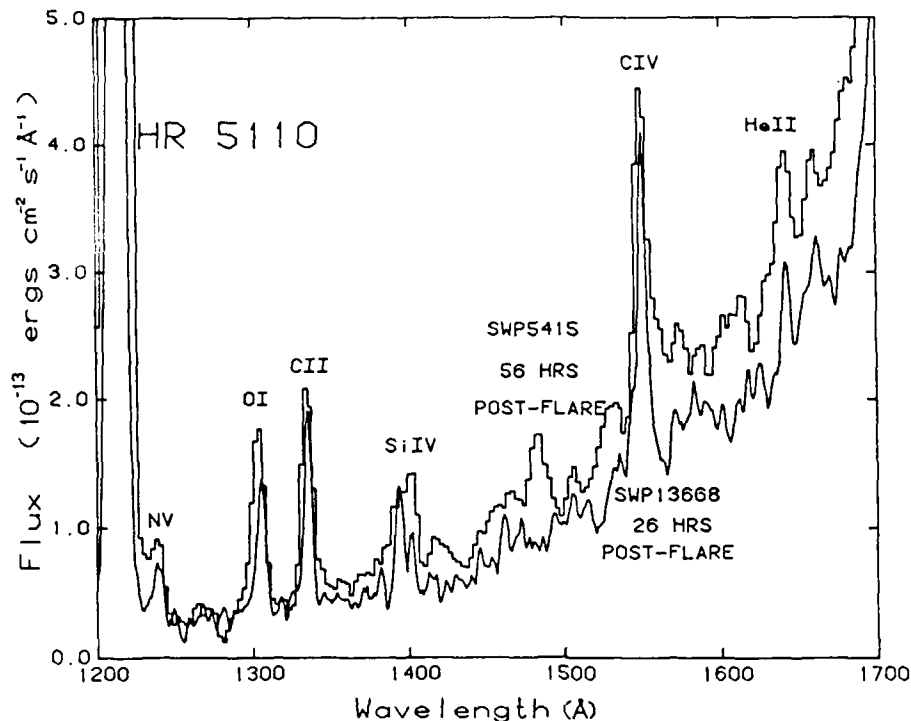


FIG. 4.—A comparison of short-wavelength, low-dispersion spectra of HR 5110 taken within 56 hr after the 1979 flare (SWP 5415 plotted as a histogram) and within 26 hr after the 1981 flare (SWP 13668). The much higher level of the continuum after the 1979 flare is clearly visible.

er from the secondary to the primary star through the inner Lagrangian point. The expected asymmetry of the ultraviolet lines due to mass motions was not observed in HR 5110 during the second flare, but this flare occurred near quadrature when mass flow through the inner Lagrangian point would be primarily across our line of sight.

VI. DISCUSSION

a) Modulation of the UV Emission

Unless an unobserved flare occurred in 1981 February, our *UE* data do appear to show correlations with phase (Fig. 5) with maximum flux occurring near phase of 0.5, i.e., when we observed the side of the secondary star that faces the F star in his nearly pole-on system. This result is very tentative as it is based on four sets of spectra taken over a time period of 4 yr. The fluxes in all the lines vary in unison by roughly a factor of 2 except for the Mg II *k* lines which varies by a factor of about 1.3.

To understand and model the variations in the emission correctly we must determine which star has the activity associated with it. Conti (1967) showed that the radial velocity variations of the Ca II emission are out of phase with those of the F star. This emission therefore defines the orbit of the secondary star. To establish from which star the upper chromospheric and TR emission originate, we analyzed a high-dispersion short-wavelength spectrum SWP 13669 taken near quadrature centered on phase 0.27. Although this spectrum is underexposed shortward of 1600 Å, it does show the He II, C IV, C II lines and, very weakly, the O I and Si IV lines in emission. Since the absolute wavelength calibration of the spectrum is uncertain owing to possible thermal flexing of the spectrograph (Leckrone 1980; Turnrose, Thompson and Bohlin 1982) and

no platinum lamp spectrum was taken for wavelength calibration at the time, we determined the shift in wavelength of the emission lines relative to the photospheric absorption lines of the F star by aligning the absorption lines of HR 5110 with those of Procyon (F5 IV-V). The two photospheric spectra match very well. Measuring next the wavelengths of the emission lines of HR 5110 relative to those of Procyon as a template, we determined an average velocity difference of $+40 \pm 10 \text{ km s}^{-1}$. At phase 0.27 the difference in radial velocity between the secondary and primary in HR 5110 is about $+45 \text{ km s}^{-1}$, in agreement with the velocity of the emission lines. We therefore conclude that the TR and chromospheric plasmas observed in the UV are located on the secondary star. The measured absolute velocity shifts of the emission lines, corrected for orbital motion of Earth and the spacecraft gave similar results. Hence this analysis shows unambiguously that the active chromosphere and TR phenomena in HR 5110 are located on the cooler K0 IV star and are not associated with the F star or with an accretion disk around the F star as in Algol systems. No emission lines are at the velocity of the F star.

Ayres, Marstad, and Linsky (1981) estimated the difference in the flux in the UV emission lines between a "moderately active" Sun and a quiet Sun to be about a factor of 2. We interpret the variation in intensity of the lines of HR 5110 as being due to the rotation of a near equatorial ($< \pm 13^\circ$) magnetic active region (plage) into and out of our line of sight. The latest Mg II spectrum (LWP 16548 obtained at phase 0.91) gives a flux slightly lower than that observed three years earlier at phase 0.67. This point would not add significantly to Figure 5 and has not been included. Complete phase coverage during one or more cycles would be needed to develop a definitive model of the active longitude and latitude. The reflection effect

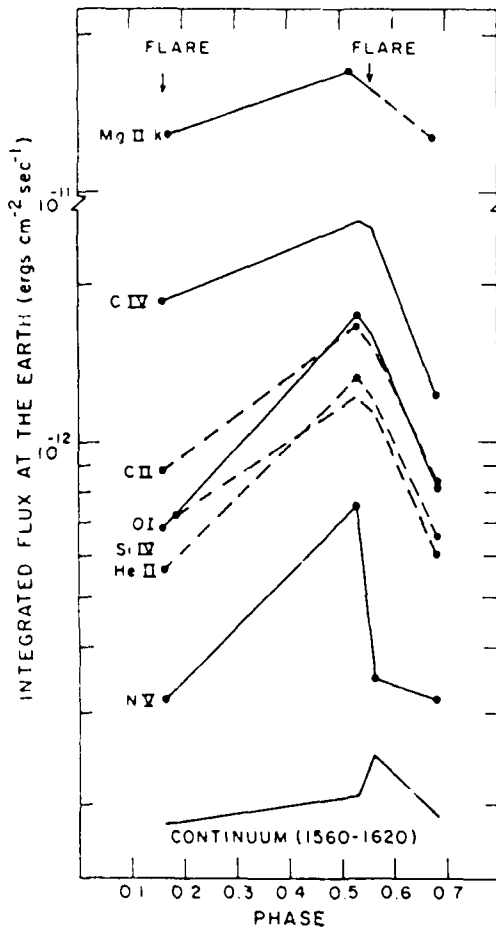


FIG. 5—The integrated emission-line fluxes of various lines received at Earth from HR 5110 as a function of phase. All lines (except Mg II) vary in emission by roughly the same factor with maximum emission occurring at phase 0.52.

(Hall *et al.* 1978) increases the photospheric temperature on the side of the K star that is facing the F star but should not increase the amount of flux emitted by the chromospheric and TR lines.

The variation of the UV continuum presents an enigma. It shows a 40% increase at phase 0.56 after the first flare relative to phase 0.17 or 0.67, but no increase after the second flare. Only a moderate increase of about 15% was observed at phase 0.52 when the emission lines reached peak brightness. Thus more data are needed in order to disentangle possible phase-from flare-related variations of the continuum.

The behavior of the Mg II *h* and *k* emission lines is more difficult to interpret. Figure 6 shows the Mg II *h* and *k* emission line profiles arranged in order of increasing phase. The shape of both Mg II lines changes dramatically with phase from emission primarily on the red side (red asymmetry) at phase 0.17 to emission primarily on the blue side (blue asymmetry) at phases 0.66 and 0.67. We interpret this as the effect of the relative motion of the stellar Mg II emission line across a stationary interstellar absorption line. Similar changes have been seen in the Mg II profiles of Capella (Ayres, Schiifer, and Linsky 1983). The velocities of the HR 5110 emission peaks relative to the interstellar feature are roughly in agreement with an orbital velocity variation of 50 km s^{-1} expected for the secondary between phase 0.17 and 0.67 (the velocity variation predicted from Conti's orbit is about 70 km s^{-1}). Therefore, like the Ca II lines, the Mg II emission appears to be formed on the secondary star. The Mg II flux varies by a factor of 1.3 between phases close to quadrature and conjunction. On the other hand, the velocity variation of the center of emission (the midpoint at Γ WHM) relative to the interstellar line is only about $15 \pm 10 \text{ km s}^{-1}$, i.e., about one-third of the variation of the emission peak, but in the same sense as the peak variations. We interpret this as an interaction of three phenomena: (a) the orbital variation of about 70 km s^{-1} of a relatively narrow Mg II emission peak arising from the secondary star, (b) the orbital variation of about 18 km s^{-1} of a broader Mg II emission peak arising

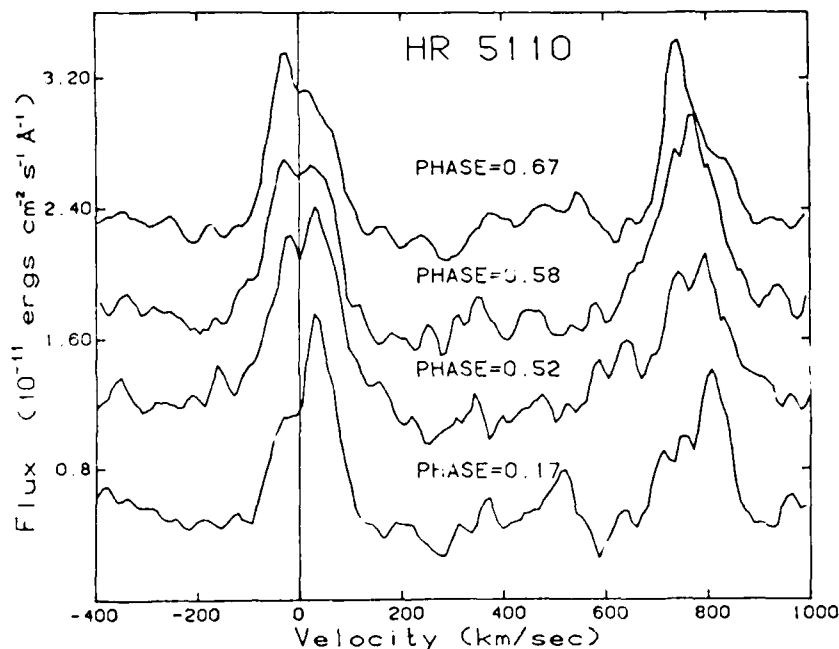


FIG. 6—The Mg II *h* and *k* profiles at different phases. The profiles have been aligned on the interstellar absorption feature of Mg II *k*. Each profile except for phase 0.17 has been shifted vertically by 6×10^{-12} flux units.

from the primary, and (c) the interstellar absorption feature with which these two emission peaks are blended. The width of the Mg II emission from the primary star must be roughly 3 times the width of the secondary's line in order not to produce asymmetry in the base of the blended line profile near quadrature. The analysis of the Mg II lines is further complicated by the fact that the widths of the lines (defined as the full width at one-fourths maximum flux) vary from 1.4 Å at quadrature to 2.0 Å near conjunction. This cannot be due to the orbital velocity variation, since that would produce the greatest width at quadrature. A possible interpretation is that this larger width is used by streaming of material from the secondary to the primary star through the inner Lagrangian point. At quadrature this flow would be primarily across our line of sight and hence would produce no additional broadening, whereas near conjunction the motion is partly along the line of sight. The minimum velocity along the line of sight inferred from the increase in width is about 65 km s⁻¹, which corresponds to a stream velocity of 300 km s⁻¹ (assuming *i* = 13°). The lines seen near conjunction are fairly symmetric implying that the stream has a relatively large angular size.

b) Activity Levels

Table 5 lists the average surface line fluxes for the quiet Sun, HR 5110, UX Ari, and HR 1099 on the assumption that all the flux in the binaries originates on their cooler components. UX Ari (*P* = 6^d4; K0 IV + G5 V) and HR 1099 (*P* = 2^d8; K0 V + G5 IV) are both known as very active RS CVn binaries in which several major radio and UV flares have been observed. The surface fluxes for HR 5110 and the two RS CVn stars are comparable and are about 100 times larger than the corresponding fluxes for the quiet Sun, except chromospheric Mg II which is enhanced by only a factor of ~10. It seems plausible to attribute the large surface fluxes for the secondary star in the HR 5110 system, like those for UX Ari and HR 1099, to rapid rotation. From the data presented by Vilhu and Tuomi (1983, their Table 3), we estimate that for stars with rotation periods of ~3 days the difference in UV line flux between an F8 star (*θ* Dra) and a K star (HR 1099) is about a factor of 10. This difference at a given rotational velocity in the length of chromospheric and TR emission must be related to another parameter, e.g., the shallower depth of the convection zone in the F stars, and hence it is not surprising that in HR 5110 we find no evidence of emission from an active TR associated with the F2 IV primary (at the 10%–20% level). This is despite the fact that the radii of both components are nearly the same so that their rotational velocities are nearly identical even synchronous rotation.

Our observations of HR 5110 has given us the unique opportunity of studying the chromosphere and TR of the secondary of an Algol system. We have shown that the behavior we observe is similar to that of rapidly rotating spotted RS CVn systems and hence must be determined primarily by the large rotational velocity of the K0 star and dynamo action rather than being related to an accretion disk. Whether other secondaries of Algol systems have magnetic active regions is not yet known, since the UV spectra of the few systems that have been observed during primary eclipse (cooler star in front) appear to be dominated by an accretion disk around the primary.

We have analyzed the SWP 17707 spectrum of one other Algol system, AS Eri, which has a period (2.67 days), secondary (K0), and mass ratio (0.11) similar to those of HR 5110. The radiation of the hot A3 primary dominates the 1200–2000 Å region, making the detection of any chromospheric emission from the secondary of AS Eri impossible. The absence of a strong C IV absorption line in this spectrum may indicate that AS Eri lacks a high temperature accretion region (Peters and Polidan 1984). Unfortunately, this system undergoes only a partial eclipse, and it would be difficult to distinguish the effects of an active chromosphere from mass transfer processes. A search through the Giuricin, Mardirossian, and Mezzetti (1983) list of Algol systems revealed only three additional short-period Algol systems composed of an F primary and K secondary, QY Aql, AL Gem, and RT UMi. All three are too faint to be studied with *IUE*. Until more bright Algol systems like HR 5110 are discovered, it appears to be the only one to which this type of analysis can be applied and for which we are able to establish the probable presence of active regions and active chromospheres and TRs on the secondary.

VII. SUMMARY

The broad-band colors of HR 5110 are best matched with an F2 IV primary and a spotted K0 IV secondary. This system is important because it is a nearly pole-on close binary in which the less massive but more evolved K secondary fills its Roche lobe, and the system can be observed in the ultraviolet. HR 5110 can be classified as an Algol system since it shows many of the common characteristics with Algols as Table 1 illustrates. Many systems like this should exist, but they are easily detected only when *i* ≈ 90° through eclipse observations. Through precisely measured wavelength shifts of the UV emission lines of HR 5110 relative to the photospheric absorption lines on a high-dispersion short-wavelength *IUE* spectrum, we can uniquely assign the active chromosphere and TR to the cooler component. This emission is most likely associated with

TABLE 5
INTEGRATED LINE SURFACE FLUXES OF THE SECONDARY COMPONENTS OF HR 5110 AND TWO RS CANIS VENATICORUM STARS (× 10⁵ ergs cm⁻² s⁻¹)

Star, State	Phase	$\frac{F(\Delta\lambda)^a}{f(\Delta\lambda)}$ (× 10 ⁻¹⁷)	N v λ1240	O I λ1305	C II λ1335	Si IV λ1400	C IV λ1549	He II λ1640	Mg II k λ2796
HR 5110 ^b	0.68–0.52	7.85	1.2–3.1	3.4–7.3	3.5–6.9	2.5–5.1	5.1–10.9	2.7–5.4	52–71
HR 1099 ^b quiescent	0.73	3.2	2.1	...	6.1	3.0	9.7	...	110
UX Ari ^b quiescent	0.61	4.6	1.9	4.4 ^c	4.4	2.5	6.5	3.5	68 ^c
Sun ^d quiet	0.0086	0.04	0.046	0.025	0.058	0.031	6.8

^a $F(\Delta\lambda) = [(4.125 \times 10^8) / \phi] f(\Delta\lambda)$, where ϕ is the stellar angular diameter in mas.

^b Simon and Linsky 1980.

^c Simon, Linsky, and Schiffer 1980b.

^d Quiet Sun surface fluxes from Ayres and Linsky 1980.

a plage facing the primary star. This system also flares at radio wavelengths, but any effects produced in other parts of the spectrum are short-lived, since within 21 hr after a flare no effects were detected either in the UV or optical region. As in other Algol systems, mass transfer from the primary to the secondary through the inner Lagrangian point may be occurring as indicated by the increased width of the Mg II lines near phase 0.5. Large amounts of intrasystem material do not appear to be present, however, as only very weak H α emission is observed and the infrared excess is too hot to be dust.

We wish to acknowledge many fruitful discussions with F. Walter as well as the use of his Ca II data to check the ephemeris of this system and the help of C. Aikman and P. Massey

while at DAO. We wish to thank the staff of the *IUE Observatory* for their help in acquiring the stellar spectra and the staff (especially T. Armitage) of the *IUE Regional Data Analysis Facility* at the University of Colorado, operated under grant NAG5-26409, for their help with the data reductions. This work is supported in part through grants NAG5-82 to the University of Colorado and grant NAG5-146 to the University of Hawaii. I. L.-M. wishes to thank JILA for its generous support, helpful discussions and good fellowship given to her during her year as a Visiting Fellow. N. L. C. acknowledges the support of a Visiting Scholarship at MIT. Mark III analysis of the Haystack Observatory and VLBI observing at OVRO and NRAO were supported by the National Science Foundation.

REFERENCES

- Allen, C. W. 1981, *Astrophysical Quantities* (3d ed.; London: Athlone).
- Ayres, T. R., and Linsky, J. L. 1980, *Ap. J.*, **235**, 76.
- Ayres, T. R., Marstad, N. C., and Linsky, J. L. 1981, *Ap. J.*, **247**, 545.
- Ayres, T. R., Schiffer, F. H., III, and Linsky, J. L. 1983, *Ap. J.*, **272**, 223.
- Barnes, T. G., and Evans, D. S. 1976, *M.N.R.A.S.*, **174**, 489.
- Bonsack, W. K., and Simon, T. 1983, in *IAU Symposium 102, Solar and Stellar Magnetic Fields*, ed. J. O. Stenflo (Dordrecht: Reidel), p. 35.
- Bopp, B. W. 1983, in *IAU Colloquium 71, Activity in Red Dwarf Stars*, ed. P. B. Byrne and M. Rodonó (Dordrecht: Reidel), p. 363.
- Castor, J., and Simon, T. 1983, *Ap. J.*, **265**, 84.
- Conti, P. S. 1967, *Ap. J.*, **149**, 629.
- Cowley, A. P. 1976, *Pub. A.S.P.*, **88**, 95.
- Dickens, R. J., and Penny, A. J. 1971, *M.N.R.A.S.*, **153**, 287.
- Dorren, J. D., and Guinan, E. F. 1980, *A.J.*, **85**, 1082.
- Dupree, A. K. 1981, in *Solar Phenomena in Stars and Stellar Systems*, ed. R. Bonnett and A. K. Dupree (Dordrecht: Reidel), p. 407.
- Eaton, J. A., and Hall, D. S. 1979, *Ap. J.*, **227**, 907.
- Feldman, P. A. 1979, *IAU Circular*, 3366.
- . 1981, *IAU Circular*, 3591.
- . 1983, in *IAU Colloquium 71, Activity in Red-Dwarf Stars*, ed. P. B. Byrne and M. Rodonó (Dordrecht: Reidel), p. 429.
- Feldman, P. A., and Kwok, S. 1979, *Workshop on Radio Stars* (Ottawa: National Research Council of Canada), p. 41.
- Feldman, P. A., Taylor, A. R., Gregory, P. C., Seaquist, E. R., Balonek, T. J., and Cohen, N. L. 1978, *A.J.*, **83**, 1471.
- Fraquelli, D. A. 1981, Ph.D. thesis, University of Toronto.
- Gibson, D. M. 1980, in *IAU Symposium 88, Close Binary Stars: Observations and Interpretation*, ed. M. J. Plavec, D. M. Popper, and R. K. Ulrich (Dordrecht: Reidel), p. 31.
- Giuricin, G., Mardirossian, F., and Mezzetti, M. 1983, *Ap. J. Suppl.*, **52**, 35.
- Hall, D. S. 1976, in *Multiple Periodic Variables*, ed. W. S. Fitch (Dordrecht: Reidel), p. 287.
- . 1981, in *Solar Phenomena in Stars and Stellar Systems*, ed. R. Bonnett and A. K. Dupree (Dordrecht: Reidel), p. 431.
- Hall, D. S., et al. 1978, *Inf. Bull. Var. Stars*, No. 1459.
- Hjellming, R. M., Webster, E., and Balick, B. 1972, *Ap. J. (Letters)*, **178**, L139.
- Johnson, H. L. 1966, *Ann. Rev. Astr. Ap.*, **4**, 193.
- Johnson, H. L., Mitchell, R. I., Iriarte, B., and Wisniewski, W. Z. 1966, *Comm. Lunar Planet. Lab.*, **4**, 99.
- Koorneef, J. 1983, *Astr. Ap.*, **128**, 84.
- Leckrone, D. S. 1980, *NASA IUE Newsletter*, No. 10, p. 25.
- Lestrade, J., Mutel, R. L., Preston, R. A., Scheid, J. A., and Phillips, R. B. 1984, *Ap. J.*, **279**, 184.
- Lucy, L. B., and Sweeney, M. A. 1971, *A.J.*, **76**, 544.
- Lyons, R. W., Bolton, C. T., and Fraquelli, D. A. 1984, preprint.
- Moffett, T. J., and Barnes, T. G., III. 1979, *Pub. A.S.P.*, **91**, 180.
- Mutel, R. L., Lastrade, J. F., Preston, R. A., and Phillips, R. B. 1985, *Ap. J.*, **289**, 262.
- Owen, F. N., Jones, T. W., and Gibson, D. M. 1976, *Ap. J.*, **210**, L27.
- Peters, G., and Polidan, R. S. 1984, *Ap. J.*, **283**, 745.
- Plavec, M. J. 1983, *Ap. J.*, **275**, 251.
- Plavec, M. J., and Polidan, R. S. 1976, in *IAU Symposium 73, Structure and Evolution of Close Binary Systems*, ed. P. Eggleton, S. Mitton, and J. Whelan (Dordrecht: Reidel), p. 298.
- Plavec, M. J., Weiland, J. L., and Koch, R. H. 1982, *Ap. J.*, **256**, 206.
- Popper, D. M., and Ulrich, R. K. 1977, *Ap. J.*, **212**, L131.
- Rodonó, M. 1983, *Adv. Space Res.*, **2**, 225.
- Shore, S. N., and Adelman, S. J. 1984, *Ap. J. Suppl.*, **54**, 151.
- Simon, T. 1984, *Ap. J.*, **279**, 738.
- Simon, T., and Linsky, J. L. 1980, *Ap. J.*, **241**, 759.
- Simon, T., Linsky, J. L., and Schiffer, F. H., III. 1980a, *Ap. J.*, **239**, 911.
- . 1980b, in *The Universe at Ultraviolet Wavelengths*, ed. R. D. Chapman (NASA CP-2171), p. 435.
- Slettebak, A. 1955, *Ap. J.*, **121**, 653.
- Turnrose, B. E., Thompson, R., and Bohlin, R. 1982, *NASA IUE Newsletter*, No. 18, p. 21.
- Vilhu, O., and Rucinski, S. M. 1983, *Astr. Ap.*, **127**, 5.
- Vogt, S. S. 1983, in *IAU Colloquium 71, Activity in Red-Dwarf Stars*, ed. P. B. Byrne and M. Rodonó (Dordrecht: Reidel), p. 137.
- Walter, F. M., and Bowyer, S. 1981, *Ap. J.*, **245**, 671.
- White, N. E., and Marshall, F. E. 1983, *Ap. J. (Letters)*, **268**, L117.

T. R. AYRES: Center for Astrophysics and Space Physics, Campus Box 391, University of Colorado, Boulder, CO 80309

N. L. COHEN: Boston Research Group, Suite 2714, 1 Longfellow Place, Boston, MA 02114

P. A. FELDMAN: Herzberg Institute of Astrophysics, National Research Council of Canada, 100 Sussex Drive, Ottawa ON, K1A 0R6, Canada

J. L. LINSKY: Joint Institute for Laboratory Astrophysics, Campus Box 440, University of Colorado, Boulder, CO 80309

S. J. LITTLE: Department of Natural Sciences, Bentley College, Waltham, MA 02154

I. R. LITTLE-MARENIN: Astronomy Department, Wellesley College, Wellesley, MA 02181

R. LYONS: David Dunlap Observatory, University of Toronto, Box 360, Richmond Hill ON, L4C 4Y6, Canada

THEODORE SIMON: Institute for Astronomy, University of Hawaii, 2680 Woodlawn Drive, Honolulu, HI 96822

Appendix B

Carbon Stars with Silicate Dust in Their Circumstellar Shells

CARBON STARS WITH SILICATE DUST IN THEIR CIRCUMSTELLAR SHELLS

IRENE R. LITTLE-MARENIN

Whitin Observatory, Wellesley College; and Air Force Geophysics Laboratory, Hanscom AFB, Mass.¹

Received 1986 March 10; accepted 1986 May 14

ABSTRACT

Almost all carbon stars having LRS spectra obtained with *IRAS* are surrounded by circumstellar dust shells usually characterized by a very uniform $11.15 \mu\text{m}$ SiC grain emission feature. About 4% of the C stars show a feature that is shifted to $\sim 11.6 \mu\text{m}$. Extraordinarily, three C stars (BM Gem, V778 Cyg, and C1003) are apparently surrounded by oxygen-rich dust shells characterized by strong silicate emission.

Subject headings: infrared: spectra — interstellar: grains — stars: carbon — stars: circumstellar shells

Many $8\text{--}22 \mu\text{m}$ low-resolution spectra (LRS) with $\lambda/\Delta\lambda \approx 50$ obtained with *IRAS* show dust grain features of silicates at $9.8 \mu\text{m}$ and of silicon carbide (SiC) at $11.2 \mu\text{m}$ which will distinguish between materials with $C < O$ or $C > O$, respectively. Circumstellar shells have dust features in emission if the shells are optically thin and relatively hot. The spectrograph and calibrations are discussed by Raimond, Beintema, and Olon (1985).

I. CARBON AND M STARS

Carbon stars have photospheric compositions with $C > O$ and their circumstellar shells are known to contain SiC dust grains (Forrest, Gillett, and Stein 1975). Almost all of the 130 high-quality LRS of C stars show evidence of circumstellar dust shells usually characterized by the SiC emission feature. Extraordinarily, three C stars with LRS show a very strong $9.8 \mu\text{m}$ emission feature (Little-Marenin and Wilton 1985) (see § II, below). Figure 1 shows the spectrum of a typical C star V Cyg matched to a 2000 K and 500 K blackbody energy distribution. The 2000 K blackbody continuum matches best the $8\text{--}13 \mu\text{m}$ region, whereas the 500 K blackbody continuum matches the $13\text{--}23 \mu\text{m}$ region better. In order to study the wavelength dependence of the SiC and silicate features, I have assumed that the $8\text{--}22 \mu\text{m}$ emission is produced by (a) the stellar photosphere, (b) a continuum dust emission, and (c) a strongly wavelength-dependent dust grain emission. Assuming that the first two terms can be represented by blackbody energy distributions, I subtracted them from the observed spectrum. I call the remaining strongly wavelength-dependent dust grain emission term the excess SiC or silicate emission. This method does not measure the total infrared excess of a star usually defined as all the emission above the photospheric continuum. The excess SiC emission of V Cyg is plotted along the bottom axis of Figure 1. An overplot of the normalized excess SiC emission of many C stars shows that the shape of the SiC feature does not depend on the strength of the feature and is quite uniform among these stars; however, for the sake of clarity only five stars are plotted in Figure 2a. The maxi-

mum of the feature is found at $11.15 \pm 0.10 \mu\text{m}$ with a FWHM of $1.6 \pm 0.15 \mu\text{m}$. The shape and the maximum of the excess emission presented in this Letter differ somewhat from the average excess emission shown by Forrest, Gillett, and Stein (1975) from ground-based observations of C stars. A few stars (Y CVn, UU Aur, RY Dra, V Aql, and IRC +10216) show an emission feature shifted to $11.6 \mu\text{m}$ (Fig. 2a). This feature was first seen in the spectrum of Y CVn by Goebel *et al.* (1980). Whether this feature is also due to SiC is not known. The graphite resonance feature predicted by Draine (1984) at $11.52 \mu\text{m}$ is too narrow to be the feature seen in these spectra. A downturn in the flux seen in many of the C star spectra (Fig. 2a) at wavelengths $< 8.2 \mu\text{m}$ is most likely due to the presence of a strong HCN and C_2H_2 absorption feature at $7.1 \mu\text{m}$ first identified in the spectrum of the C star V CrB by Goebel *et al.* (1981).

In order to identify the carrier of the $9.8 \mu\text{m}$ feature seen in the three C stars mentioned above, I analyzed high-quality LRS of M stars. Figure 3 shows the spectrum of the typical M star TY Cas together with a 640 K blackbody energy distribution and the resulting excess silicate emission feature. Figure 2b shows an overplot of the normalized silicate emission excess of eight M stars after subtracting a local blackbody continuum matched to either side of the feature. The shape of the excess is not as uniform as that due to SiC. The maximum of the average silicate feature occurs at $9.8 \pm 0.2 \mu\text{m}$, but the exact shape of the feature, the width, and the shortest wavelength of notable excess vary significantly from star to star with the FWHM varying between 2 and $3 \mu\text{m}$. In general I find that the stronger the silicate feature the greater its width and the shorter the beginning wavelength of the emission feature.

II. CARBON STARS WITH STRONG SILICATE EMISSION FEATURES

Three stars classified as C stars (see Stephenson 1973) are found here to have the same $9.8 \mu\text{m}$ and $18 \mu\text{m}$ feature as M stars. These are BM Gem = IRC +30182 = C716 (C5,4J Lb), V778 Cyg = C2919 (C5-, 5 Lb) and C1003 (the C + number = number in the Stephenson [1973] carbon star catalog). The observed spectra of these three stars and their respective

¹University Resident Research Fellow.

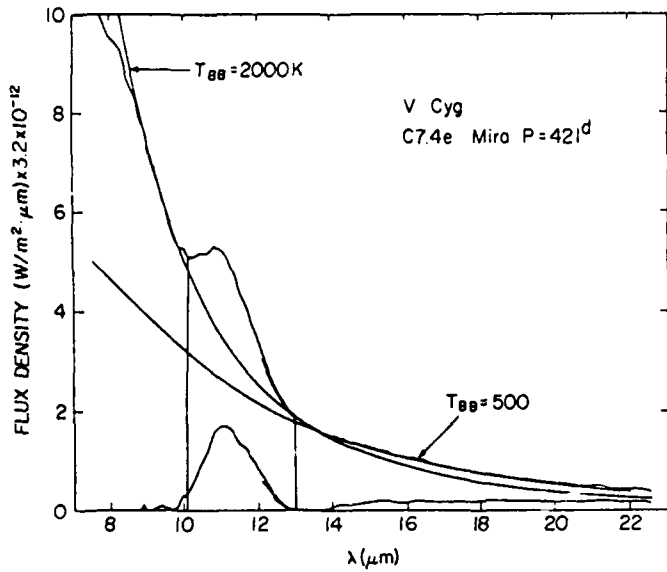


FIG. 1

FIG. 1.—The LRS spectrum of V Cyg, a Mira variable carbon star, is matched to that of a 2000 K blackbody energy distribution in the 9–13 μm region (normalized at: 9.8 μm) and to a 500 K blackbody energy distribution in the 13–22 μm region (normalized at 13.9 μm). The SiC emission excess at 11.15 μm is clearly evident, and it is plotted as the observed spectrum minus the 2000 K blackbody energy distribution along the wavelength axis.

FIG. 3.—The LRS spectrum of TY Cas, a Mira variable M star, is matched to a 640 K blackbody energy distribution normalized at 7.8 μm . The silicate emission excess at 9.8 μm is quite strong and is plotted as the observed spectrum minus the 640 K blackbody energy distribution along the wavelength axis.

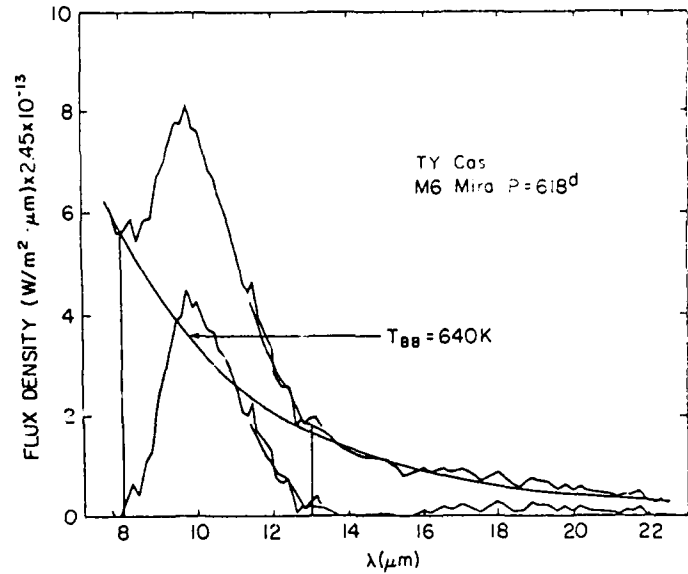


FIG. 3

blackbody energy distributions are shown in Figure 4a, 4b, and 4c. The 9.8 μm emission excess is plotted along the wavelength axis for each star. The normalized emission excess of the three stars is plotted in Figure 5 as solid lines along with the silicate feature of the M star TY Cas (*dotted line*) and the SiC feature of the C star V Cyg (*dashed line*). Since the features of the three C stars agree well with the silicate

feature of TY Cas but not with the SiC feature, I conclude that these three C stars are surrounded by material rich in silicate dust.

It is difficult to interpret these observations. The circumstellar shell is assumed to be produced by mass loss from the central carbon star and should reflect the carbon-rich material of its photosphere. The transit time of material through the

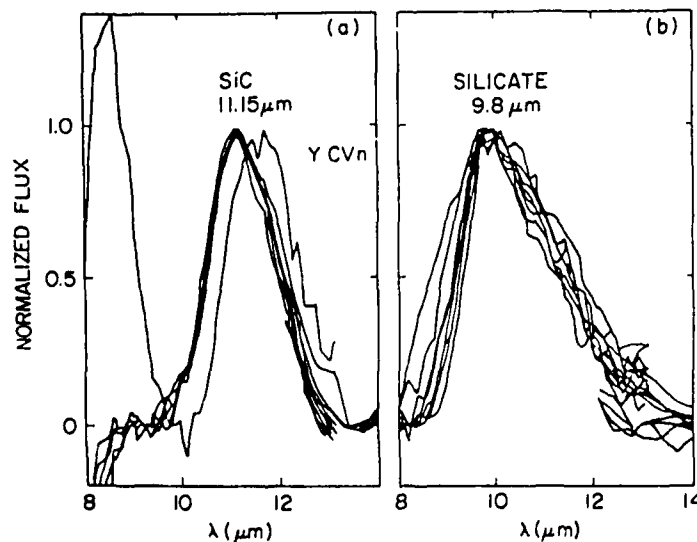


FIG. 2.—(a) The SiC emission excess of five carbon stars is overplotted (RV Aqr, V Cyg, T Dra, R Vol, C142). Each excess was normalized to 1.0 after subtracting a local blackbody continuum from each LRS spectrum. A few stars such as Y CVn have an emission excess that is shifted to longer wavelengths. A second emission feature at 8.4 μm is also visible in the spectrum of Y CVn. (b) The normalized silicate emission excess of eight M stars is overplotted (TY Cas, Z Eri, R Hor, U Men, SY Men, S Per, W Per, TV Per). The silicate excess shows much greater star to star variation than does the SiC feature.

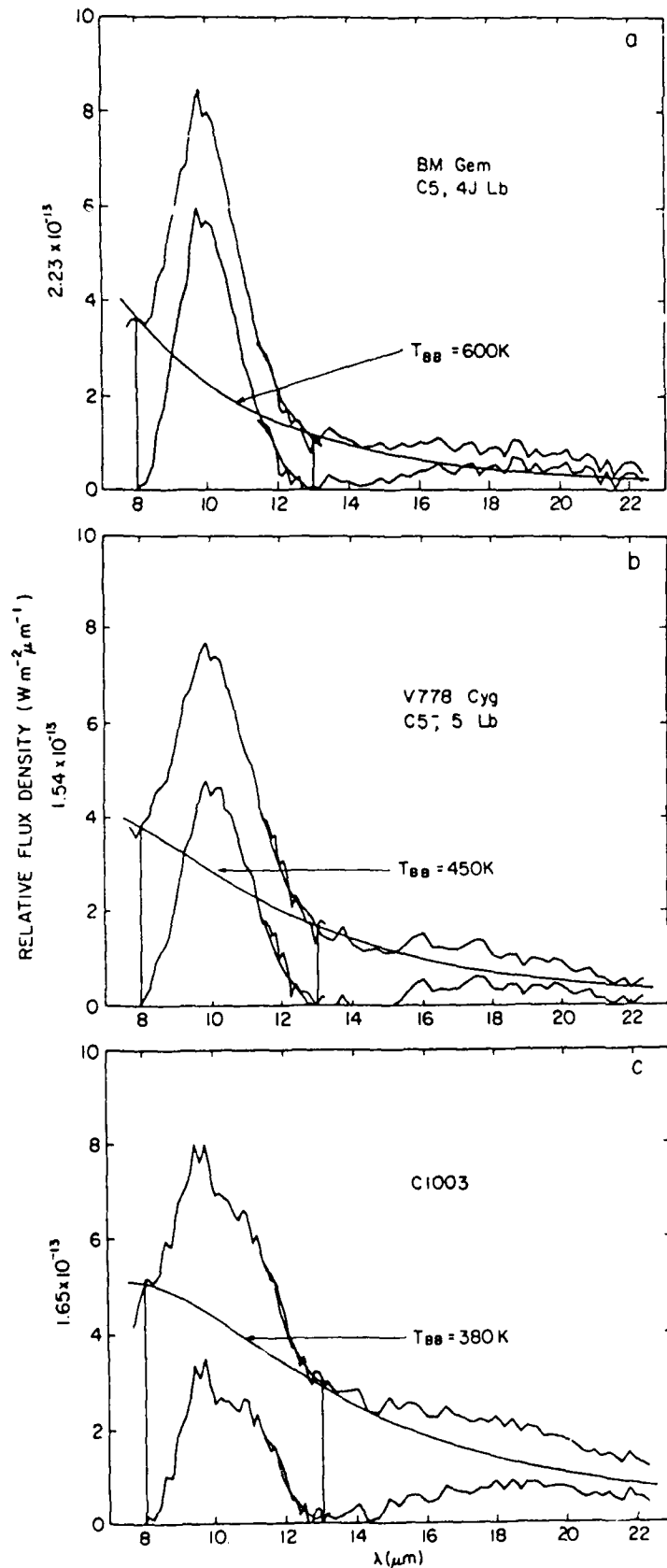


FIG. 4.—The LRS spectra for the three carbon stars with strong 9.8 μm emission features are plotted. The excess emission (observed spectrum minus a local blackbody continuum) is plotted along the wavelength axis for each star: (a) BM Gem is matched to a 600K blackbody energy distribution; (b) V778 Cyg to a 450K blackbody energy distribution; (c) C1003 to a 380 K blackbody energy distribution. All three blackbody continua are normalized at 7.9 μm . A weak 18 μm emission feature also appears to be present.

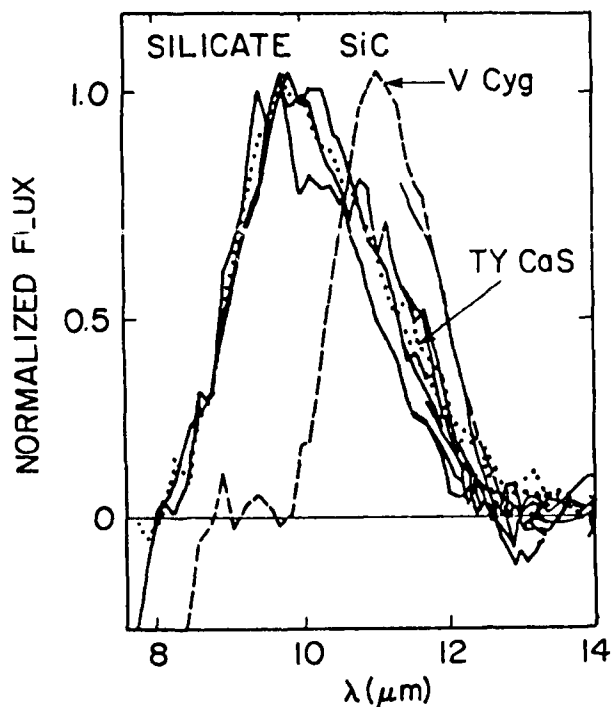


FIG. 5.—The normalized 9.8 μm emission excess of BM Gem, V778 Cyg, and C1003 are compared to the silicate excess of the M star TY Cas (dashed line) and the SiC excess of C star V Cyg (dotted line). The agreement of the 9.8 μm excess with the silicate excess is excellent.

circumstellar shell is only on the order of years to decades assuming that the grains form at distances $< 10^{15}$ cm < 70 AU (Rowan-Robinson and Harris 1983; Dyck *et al.* 1984) and have outflow velocities of > 5 km s^{-1} . Outflow velocities for C stars are typically ~ 15 km s^{-1} (Knapp and Morris 1985). V778 Cyg was classified as a carbon star over 40 yr ago.

Yamashita (1972) classified BM Gem as C4,5J with strong C_2 and CN features, and eight-color photometry by Baumert (1972) in the 0.7–1.1 μm region shows that both BM Gem and V778 Cyg have the strong CN absorption features typical of Lb variable C stars. Hence it is unlikely that these two stars are misclassified.

It is unlikely that we are observing very recently produced circumstellar material from a progenitor M star. The transformation from $\text{M} \rightarrow \text{S} \rightarrow \text{C}$ occurs on a time scale of 10^5 yr (Iben 1978; Iben and Renzini 1983) which is much longer than the transit time of material through the circumstellar shell.

We may be observing an unusual chemical equilibrium in the circumstellar shell. Thronson and Bally (1986) find that the dust/CO ratio in the carbon-rich planetary NGC 7027 is the same as that found in the oxygen-rich interstellar medium. They speculate that it may be possible to produce an oxygen-rich environment out of carbon-rich gas if the region of graphite and SiC grain formation overlaps that of CO. Graphite may remove so much carbon from the gas that after the shell becomes too cool to form CO, the remaining material may actually be oxygen-rich. I suggest that the chemical reactions in the cooler regions of the shell may form silicates.

This scenario may be able to explain the emission features of many of the S stars which appear to be a combination of relatively weak SiC and silicate emission (Little and Little-Marenin 1985). However, a different mechanism may be necessary to explain the very strong silicate features of BM Gem, V778 Cyg, and C1003, since no C star appears to have weak (or intermediate strength) silicate as well as SiC emission.

Perhaps we are actually observing a binary system with an M and a C star component. This scenario assumes that the visual and near-infrared light of the M star is absorbed by its circumstellar shell (hence we were seeing the C star at these wavelengths), whereas the flux in the 8–22 μm region is dominated by the emission from the oxygen-rich shell. A small contribution (less than 15%) of SiC to the emission feature would not be distinguishable in the LRS suggesting that at 10 μm the circumstellar shell is at least 2 mag brighter than the C star. In fact, on the average C stars are ~ 1 mag brighter than M stars of the same mass (Iben 1978). Therefore the 1 μm extinction by the circumstellar silicate shell must be at least 3 mag in order for the M star not to be observable at < 1 μm . To check for a binary companion, I suggest (a) looking for orbital radial velocity variations (which may be very difficult to disentangle from velocity variations related to their light variability), (b) searching for spectral lines from both stars in the 2–10 μm region, and (c) observing the system at various phases to see if the M star is visible when the C star is at minimum light; however, the difference in maximum and minimum light of BM Gem is only ~ 0.6 mag. Both components of a visual binary system with an S (or M) and a C star component (V633 Mon = IRC 00162; Bidelman 1980) have been observed photometrically (eight-color photometry) by R. F. Wing (private communication). The C star is about ~ 1 mag brighter in the red than the S or M star component. The LRS spectrum of V633 Mon shows only weak SiC emission and no evidence of any silicate emission. Therefore the circumstellar material associated with V633 Mon is quite different from that found near the three C stars discussed here. The probability of finding three out of 130 stars (i.e., almost 2.5%) on the AGB as binaries with very similar mass components is low.

It is also possible, but not likely, that the oxygen-rich dust is part of the interstellar medium that finds itself close to the carbon star (within about 10 stellar radii (!)) in order to be at a temperature of about 350–600 K. No nebulosity near the C stars is evident on the Palomar Sky Survey prints. Also, no bright IRAS point sources (> 3 Jy at 12 μm —1/10 the flux of these three stars) are found within the field of view of the spectrograph.

III. CONCLUSIONS

The IRAS low-resolution spectra of identified carbon stars show that almost all are surrounded by circumstellar shells usually characterized by the SiC dust emission feature. In general the spectral shape of SiC at 11.15 μm is quite uniform from star to star irrespective of the strength of the emission. Most variable M stars are surrounded by dust shells characterized by silicate emission. However, the spectral shape shows considerable variation from star to star.

The three C stars BM Gem, V788 Cyg, and C1003 appear to be surrounded by oxygen-rich shells characterized by strong silicate emission. These observations are difficult to interpret as these stars do not appear to be misclassified. They are unlikely to be brand-new C stars since the transit time of material through the circumstellar shell is only on the order of years to decades, very short compared to the transition time of an M star to a C star. It may be possible that the temperature gradient in the shell allows for different chemical equilibria to exist at different distances from the star. The most likely explanation is that we are observing a binary system with an M and a C star component. No corroborating evidence for this exists, and I suggest searching for it. In conclusion, the observations indicate the presence of rela-

tively hot, oxygen-rich, optically thin silicate dust around, or in very close proximity to, three C stars. How this particular combination of star and circumstellar dust shell has been produced is not clear.

I would like to thank L. Marcotte and C. Wilton for writing the computer programs used in this analysis and S. Price, P. LeVan, and especially S. J. Little for many stimulating and informative discussions. This research is supported by a University Resident Research Fellowship from the AFOSR to AFGL and by the 1985 USAF-UES Summer Faculty Research Program/Graduate Student Summer Support Program sponsored by the AFOSR and conducted by UES, Inc.

REFERENCES

- Baumert, J. H. 1972, Ph.D. thesis, Ohio State University.
 Bidelman, W. P. 1980, *Pub. Warner and Swasey Obs.*, Vol. 2, No. 6, p. 185.
 Draine, B. T. 1984, *Ap. J. (Letters)*, 277, L71.
 Dyck, H. M., Zuckerman, B., Leinert, Ch., and Beckwith, S. 1984, *Ap. J.*, 287, 801.
 Forrest, W. J., Gillett, F. C., and Stein, W. A. 1975, *Ap. J.*, 195, 423.
 Goebel, J. H., et al. 1980, *Ap. J.*, 235, 104.
 Goebel, J. H., Bregman, J. D., Witteborn, F. C., Taylor, B. J., and Willner, S. P. 1981, *Ap. J.*, 246, 455.
 Iben, I. Jr. 1978, *Ap. J.*, 220, 980.
 Iben, I. Jr., and Renzini, A. 1983, *Ann. Rev. Astr. Ap.*, 21, 271.
 Knapp, G. R., and Morris, M. 1985, *Ap. J.*, 292, 640.
 Little S. J., and Little-Marenin, I. R. 1985, in *Proc. Fourth Cambridge Stellar Systems Workshop on Cool Stars and the Sun*, in press.
 Little-Marenin, I. R., and Wilton, C. 1985, in *Proc. Fourth Cambridge Stellar Systems Workshop on Cool Stars and the Sun*, in press.
 Raimond, E., Beintema, D. A., and Olmon, F. M. 1985, in *Infrared Astronomical Satellite (IRAS)—Catalogs and Atlases—Explanatory Supplement*, ed. C. A. Beichman, G. Neugebauer, H. J. Habing, P. E. Clegg, and T. J. Chester (Washington: US Government Printing Office) chap. 9.
 Rowan-Robinson, M., and Harris, S. 1983, *M.N.R.A.S.*, 202, 797.
 Stephenson, C. B. 1973, *Pub. Warner and Swasey Obs.*, Vol. 1, No. 4.
 Thronson, H. A., and Bally, J. 1986, *Ap. J.*, 300, 749.
 Yamashita, Y. 1972, *Tokyo Astr. Obs. Ann.*, 13, 169.

IRENE R. LITTLE-MARENIN: AFGL/OPI, Hanscom AFB, MA 01731

Appendix C

A Water Maser Associated with EU Andromedae: A Carbon
Star Near an Oxygen-Rich Circumstellar Shell

A WATER MASER ASSOCIATED WITH EU ANDROMEDAE: A CARBON STAR NEAR AN OXYGEN-RICH CIRCUMSTELLAR SHELL

PRISCILLA J. BENSON
Whitin Observatory, Wellesley College

AND

IRENE R. LITTLE-MARENIN¹
Whitin Observatory, Wellesley College; and Air Force Geophysics Laboratory, Hanscom AFB
Received 1987 January 22; accepted 1987 February 13

ABSTRACT

An H₂O maser emission line at 22.2 GHz has been detected toward the carbon star EU And, confirming the conclusion based on analysis of LRS *IRAS* spectra that this star is in the vicinity of an oxygen-rich circumstellar shell. We interpret the 24 km s⁻¹ velocity difference between the H₂O maser, measured at -29.4 km s⁻¹, and the carbon star absorption line velocity of -53 km s⁻¹ to be due to the orbital motion of the C star about an M star with a relatively thick circumstellar shell.

Subject headings: masers — stars: carbon — stars: circumstellar shells — stars: individual (EU And)

I. INTRODUCTION

Recently, Little-Marenin (1986) and Willems and de Jong (1986) have shown that at least three reliably classified carbon stars, and three or four others with less reliable classifications, are near oxygen-rich circumstellar dust shells as deduced from the presence of the 10 μm and 18 μm silicate emission features in their *IRAS* low-resolution spectra (hereafter LRS) (*IRAS* Science Team 1986). These three stars are EU And (C4, 4; Dean 1976), BM Gem (C4, 5J with strong C₂, ¹²CN and ¹³CN features; Yamashita 1972) and V778 Cyg (C4, 5J; Yamashita 1975). The three stars were first recognized as carbon stars on the Dearborn Observatory's objective prism survey of red stars in the early 1940s. The location of the stars listed by Little-Marenin (1986) in color-color plots based on the *IRAS* point source fluxes at 12, 25, 60 and 100 μm are also indicative of oxygen-rich circumstellar (hereafter CS) shells (Zuckerman and Dyck 1986). As an independent confirmation of the oxygen nature of the dust shells, we decided to search the semiregular carbon stars EU And (R.A.[1950] = 23^h17^m41^s; decl.[1950] = +46°58'00" and BM Gem (R.A.[1950] = 7^h17^m56^s; decl.[1950] = +25°05'35") for H₂O emission, since H₂O masers are often associated with the CS shells around Mira or semiregular (hereafter SR) variable M stars (Engels 1979; Reid and Moran 1981; Dickinson and Dinger 1982).

Neither star has a well-established period. The fourth edition of the *General Catalog of Variable Stars* (Kholopov 1985) lists EU And as a SR variable with a photographic magnitude range of 12.9–14.1. The classification for BM Gem in the fourth edition was revised to SRb-286:^d from Lb. Often SR and Lb designations are indicative of less well observed Miras.

II. OBSERVATIONS

Observations of the 6₁₆-5₂₃ transition of H₂O at 22,235.080 MHz were carried out with the 37 m Haystack Observatory² telescope during 1986 December 13–15 and 1987 January 23. The system temperature averaged about 90 K. The spectra were automatically corrected by the Haystack computer for atmospheric attenuation and for variation in telescope gain with elevation. We used an autocorrelator bandwidth of 13.33 MHz with 512 channels for the 1986 December observations, resulting in a velocity window of 180 km s⁻¹ and a resolution of 0.53 km s⁻¹. In 1987 January, we used a bandwidth of 4.44 MHz with 1024 channels, resulting in a velocity resolution of 0.09 km s⁻¹. The stars were observed in a total power mode with three sets of 5 minutes on source and 5 minutes off source.

III. RESULTS

The 1986 December 15 maser detection toward EU And is shown in Figure 1. The observed line was well fitted by a Gaussian with the following parameters: $T_{\text{mb}}^* = 0.68$ (0.05) K, $V_{\text{LSR}} = -29.40$ (0.03) km s⁻¹, and $\Delta V(\text{FWHM}) = 0.67$ (0.06) km s⁻¹. The formal errors in the Gaussian fit are given in parentheses. The rms noise in the off-peak channels is 0.047 K. Although the line width is only a little greater than one resolution element, the line appears to be real since it showed up on all three runs and is typical of many other H₂O masers. The integrated area of the feature is 0.62 K km s⁻¹. Using a conversion factor of 12 Jy per K, the line intensity is 8.2 Jy. No other H₂O maser line is visible with flux > 1 Jy (3 σ).

EU And was reobserved on 1987 January 23 with better velocity resolution (0.09 km s⁻¹). The intensity appears to

¹University Resident Research Fellow.

²Radio astronomy at Haystack Observatory of the Northeast Radio Observatory Corporation is supported by the National Science Foundation under grant AST78-18227.

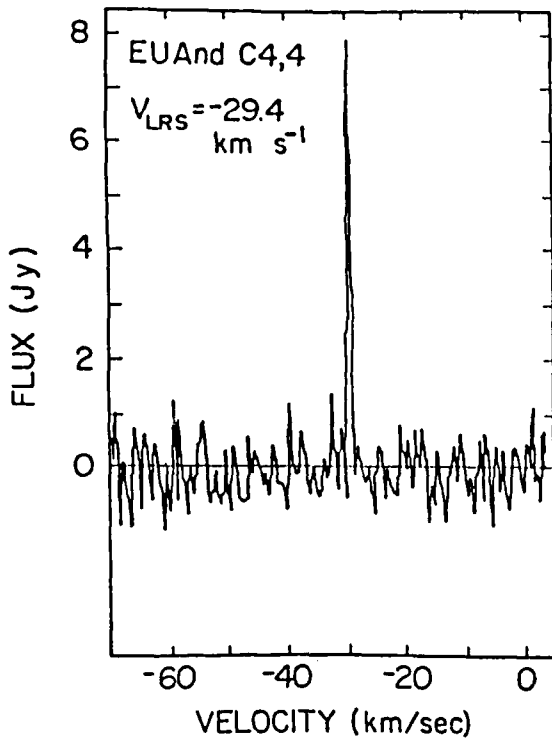


FIG. 1.—Spectrum of the H₂O maser emission in EU And

have decreased to about 5.5 Jy. The unsmoothed spectrum has rms noise equal to 0.125 K and the Gaussian fit gives values of $T_{\lambda}^* = 0.46$ (0.04) K, $V_{\text{LSR}} = -29.67$ km s⁻¹ (0.02), and $\Delta V(\text{FWHM}) = 0.52$ (0.06) km s⁻¹. The FWHM is narrow (on the order of the previous resolution), which indicates that the line probably was not fully resolved in December, and we may have underestimated its intensity. The Hanning-smoothed spectrum (with rms = 0.076) shows the possibility of a second feature with Gaussian parameters $T_{\lambda}^* = 0.16$ (0.02), $V_{\text{LSR}} = -31.21$ km s⁻¹ (0.15), and $\Delta V(\text{FWHM}) = 1.83$ (0.38) km s⁻¹. The total integrated area for both features is 1.242 K km s⁻¹.

BM Gem was observed 1986 December 14 with the velocity window centered on the optically determined radial velocity of 98 km s⁻¹ (Abt and Biggs 1972), covering velocities from 8 km s⁻¹ to 188 km s⁻¹. No H₂O lines were detected. The rms of the spectrum was 0.036 K, implying an upper limit of about 1 Jy (3 σ).

IV. DISCUSSION

The detection of the H₂O maser emission line confirms the presence of oxygen-rich material in the vicinity of EU And but leaves the physical relationship between the O-rich circumstellar shell and the C-rich photosphere unexplained. Willems and de Jong (1986) have argued that we are observing the transition from an M to a C star while the star is on the asymptotic giant branch (AGB). During helium shell flashing for AGB stars carbon-rich material can be dredged up, turning the oxygen-rich material of the M star into the carbon-rich material of a C star (Iben and Renzini 1983).

Hence, it is theoretically possible to still see the oxygen-rich material in the CS shell for a brief period after the photosphere has already turned into a C star. However, the transit time for material to move through the shell is so short that it would be very difficult to observe this transition phase (Little-Marenin 1986). Theoretical models of CS oxygen-rich shells (Rowan-Robinson and Harris 1982, 1983a) indicate that the majority of the silicate emission comes from a region around 10 R_* in agreement with observations (Dyck *et al.* 1984). Based on typical outflow velocities of about 15 km s⁻¹ obtained from CO observations of carbon stars (Knapp and Morris 1985), the material will transit through the region of strong silicate emission in 3–15 yr if a typical C star is assumed to have a radius of 1–5 AU. Even a 2 km s⁻¹ outflow velocity implies a transit time of only 15–45 yr, which is marginally compatible with the time since EU And, BM Gem, and V778 Cyg were classified as carbon stars.

Dean (1976) determined a photospheric absorption-line velocity for EU And of $V_p = -62$ km s⁻¹ ($V_{\text{LSR}} = -53$ km s⁻¹). This value is blueshifted by 24 km s⁻¹ relative to that for the H₂O maser. Theoretical models of H₂O masers around giant long-period variables (hereafter LPV) (Cooke and Elitzur 1985) show that typical outflow velocities in the H₂O masing region are about 3–6 km s⁻¹ when the terminal velocity is about 10 km s⁻¹. The H₂O emission lines may be either blueshifted or redshifted relative to the stellar lines implying that the masing region can be either in the near or the far side of the expanding envelope. Dickinson *et al.* (1978) point out that the photospheric absorption lines are often redshifted by 0–8 km s⁻¹ relative to systemic velocities determined from thermal SiO lines. The same trend seems to apply to the mean of the H₂O maser lines if two components are observed. Hence, if EU And is a usual type of LPV giant, the EU And water maser velocity would be $(-53 \pm 8) \pm 6$ km s⁻¹ or no greater than -39 km s⁻¹ compared to the observed velocity of -29.4 km s⁻¹.

Typically H₂O masers are located in an expanding gas shell between 10¹⁴–10¹⁵ cm (7–70 AU) from an exciting M star, usually a Mira or a semiregular variable giant or supergiant (Reid and Moran 1981; Bowers and Hagen 1984; Johnston, Spencer, and Bowers 1985). VLBI observations by Johnston, Spencer, and Bowers (1985) of four LPVs suggest that the H₂O masing region is located outside the silicate emission region. Although the OH emission measured by Bowers, Johnston, and Spencer (1983) appears to come from spherically symmetric envelopes, such spherical symmetry is not as well established in the H₂O data. The distribution of H₂O maser emission is quite complex and highly variable in time—both in intensity and location (Gomez Balboa and Lepine 1986; Johnston, Spencer, and Bowers 1985; Berulis *et al.* 1983). In general, the emission profiles show a greater degree of complexity around supergiants than giants. Zuckerman (1980) indicates that C stars appear to have nonspherical envelopes more often than M stars and suggests that such geometry is influenced by a companion.

We interpret the H₂O maser emission as coming from a CS envelope around an M star which has at least a 10 km s⁻¹ redshift with respect to the C star companion. We suggest that EU And is a binary system in which the visible light in the 6000–7000 Å region is dominated by the C star, while the

$10\ \mu\text{m}$ flux and H_2O emission originates in the CS shell of the M star. Thus, EU And may be the first radio spectroscopic binary (Cohen 1987).

In order to check the plausibility of this deduction, we plot in Figure 2 a CS dust shell model by Rowan-Robinson and Harris (1983*b*) for HV Cas (C4,3-C5,4; M-527^d), a C star of similar spectral class to EU And, as well as the M star model for WX Ser (M8; M-425^d), which has a $10\ \mu\text{m}$ feature similar in strength to EU And as observed by the *IRAS* LRS. A relatively thick CS shell ($\tau_{\text{uv}} = 10$) is predicted by the M star model which absorbs a large fraction of the visible light and reradiates the energy in the infrared. The Rowan-Robinson and Harris (1983*b*) C star models do not include the SiC emission which is observed at moderate strength in the LRS of HV Cas. Rowan-Robinson *et al.* (1986) have modified their models slightly in order to improve the predicted 60 and $100\ \mu\text{m}$ *IRAS* fluxes, but these differences are at wavelength $> 20\ \mu\text{m}$ and therefore will have little effect on the present analysis. We assume that the C star is at least two magnitudes brighter at $6000\text{--}7000\ \text{\AA}$ since the M star is not visible in this region. We accordingly normalize the two spectra at $0.9\ \mu\text{m}$ (*upper dashed curve for WX Ser*). The circumstellar dust shell around the M star is then approximately 5 mag brighter at $10\ \mu\text{m}$ as shown in Figure 2. Photometry of the $1.0\text{--}3.7\ \mu\text{m}$ region of BM Gem shows the typical $3\ \mu\text{m}$ HCN and C_2H_2 absorption feature of a carbon star (Noguchi *et al.* 1981). The typical spectra of M stars in the $3\ \mu\text{m}$ region show a smooth

continuum (Noguchi *et al.* 1977). Hence, if the energy distribution of EU And is similar to BM Gem in the $3\ \mu\text{m}$ region, we would expect the C component to be only about 0.5 mag or so brighter than the M star in this region. If we normalize the flux of WX Ser and HV Cas at $5\ \mu\text{m}$ (*lower dashed curve for WX Ser*), we find that the M star is still brighter at $10\ \mu\text{m}$ by about 2 mag. The shaded area on the graph therefore indicates the possible range of the M star fluxes compatible with the observations. The contribution of $11.2\ \mu\text{m}$ SiC emission to the strong $10\ \mu\text{m}$ silicate emission feature would not be observable. Therefore a model of a C star and a late M star with a circumstellar shell can explain the observed energy distribution in the $0.6\text{--}0.7\ \mu\text{m}$ region, the $8\text{--}10\ \mu\text{m}$ region, and $22\ \text{GHz}$ H_2O emission.

We expect M and C star components in a highly evolved binary system to have very similar masses and luminosities in order for both to be on the AGB. Since the more evolved C star should be slightly more luminous, we conclude that the lower curve for WX Ser, together with the solid curve for HV Cas, is a more realistic representation of the relative energy distribution for the two stars. As can be seen in Figure 2, the less luminous M star dominates the radiation in the infrared because a large fraction of its visible light is absorbed and reradiated by the CS shell.

A search through the LRS spectra shows that more than half of the LPVs with strong silicate emission like EU And are Miras with fairly long periods ($\langle P \rangle = 400^{\text{d}}$), another 25%–30% are semiregular variables, and the rest are either irregular variables or poorly observed stars. Only two short-period Miras R Cet ($P = 166^{\text{d}}$) and Sv Pup (168^{d}) show a very strong $10\ \mu\text{m}$ silicate feature. An H_2O maser has recently been detected in R Cet (Benson *et al.* 1987). Hence, by analogy the companion to EU And should be a SR or a Mira with a period around 400^{d} .

About 10% of the LPVs with strong silicate emission are classified as supergiants, with expansion velocities of around $20\text{--}50\ \text{km s}^{-1}$ in their CS shells as determined from OH, SiO, and H_2O observations. The difference between the absorption-line velocities of the carbon star and the H_2O maser velocity could then be due to the expansion of the CS shell around a single supergiant carbon star. There are several arguments which can be made against the latter interpretation. First, no supergiant C stars with large outflow velocities are known (anonymous referee 1987, private communication), in part due to the fact that no spectroscopic luminosity criteria for C stars exist. Second, the silicate and H_2O maser emission regions are predicted to be located roughly a factor of 5–10 further from a supergiant than a giant (Rowan-Robinson and Harris 1983*a*). However, the expansion velocities are larger by roughly the same factor (Bowers, Johnston, and Spencer 1983; Gomez Balboa and Lepine 1986), making the transit time of material through a supergiant silicate emission region less than about 50 yr, which is too short to be compatible with the C star classification. Third, the galactic latitude of EU And ($b = 12^\circ$) is larger than for most supergiants. Fourth, the H_2O maser line is quite narrow and shows only one component which is more typical of CS shells around giants than supergiants. Of course none of these arguments is conclusive. As a better test for distinguishing between binary giants and a single supergiant, we suggest that EU And, as

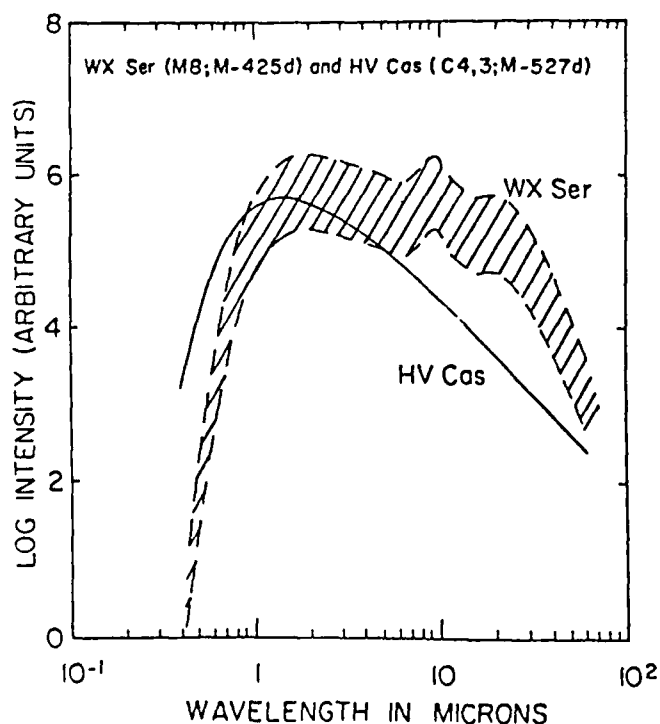


FIG. 2.—A possible model for EU And: a C star (HV Cas; *solid curve*) + an M star with a relatively thick CS shell (WX Ser; *dashed curves*). The spectra of HV Cas and WX Ser are normalized at $0.9\ \mu\text{m}$ (*upper dashed curve of WX Ser*) and at $5\ \mu\text{m}$ (*lower dashed curve of WX Ser*). The shaded area indicates the possible range of relative flux of the M star compatible with observations.

well as BM Gem and V778 Cyg, be searched for OH and SiO emission, since most CS shells with H₂O maser activity are also OH and SiO masers. Often the emission (especially in OH) is double-peaked with the mean velocity corresponding to the systemic velocity and the velocity difference between the peaks corresponding to the expansion velocity. Observations of a double-peaked maser should immediately tell us the systemic velocity.

V. CONCLUSION

We observed 22 GHz H₂O maser emission toward the C star EU And. The velocity of the line ($V_{\text{LSR}} = -29.4 \text{ km s}^{-1}$) is redshifted by about 24 km s^{-1} relative to the photospheric absorption lines of the star ($V_{\text{LSR}} = -53 \text{ km s}^{-1}$). We interpret EU And as the first detected radio spectroscopic binary system with C and M star components. The carbon star is seen and classified in the 6000–7000 Å region, whereas the O-rich CS shell around the M star is seen at $10 \mu\text{m}$ as silicate

emission and at 22 GHz as an H₂O maser line. We hypothesize that EU And, along with the other carbon stars that show strong silicate emission in their spectra (BM Gem, V778 Cyg) are H₂O, as well as OH and SiO maser sources, and we plan to search them for periodic shifts in spectral line velocities in order to establish or disprove the binary nature of these systems.

This research is in part supported by a University Resident Research fellowship from the Air Force Office of Scientific Research to the Air Force Geophysics Laboratory (IRL-M) and a Dudley Award from the Dudley Observatory, the William and Flora Hewlett Foundation Grant of the Research Corporation, and the National Science Foundation under grant AST-8610467 (P. J. B.). We would like to thank the staff of the Haystack Observatory for their assistance, the referee for very prompt and useful comments, and S. D. Price for helpful suggestions.

REFERENCES

- Abt, H. A., and Biggs, E. S. 1972, *Bibliography of Stellar Radial Velocities* (New York: Latham).
- Benson, P. J., Little-Marenin, I. R., Dickinson, D. F., Turner, B. E., and Jewell, P. R. 1987, in preparation.
- Berulis, I. I., Lekhit, E. E., Pashchenko, M. J., and Pudnitskii, G. M. 1983, *Soviet Astr.*, **97**, 179.
- Bowers, P. F., and Hagen, W. 1984, *Ap. J.*, **285**, 637.
- Bowers, P. F., Johnston, K. J., and Spencer, J. H. 1983, *Ap. J.*, **274**, 733.
- Cohen, N. L. 1987, nomenclature suggested in personal communication.
- Cooke, B., and Elitzur, M. 1985, *Ap. J.*, **295**, 175.
- Dean, Ch. A. 1976, *A.J.*, **81**, 364.
- Dickinson, D. F., and Dinger, A. S. 1982, *Ap. J.*, **234**, 136.
- Dickinson, D. R., Reid, M. J., Morris, M., and Redman, R. 1978, *Ap. J. (Letters)*, **220**, L113.
- Dyck, H. M., Zuckerman, B., Leinert, Ch., and Beckwith, S. 1984, *Ap. J.*, **287**, 801.
- Engels, D. 1979, *Astr. Ap. Suppl.*, **36**, 337.
- Gomez Balboa, A. M., and Lepine, J. R. D. 1986, *Astr. Ap.*, **159**, 166.
- Iben, I., Jr., and Renzini, A. 1983, *Ann. Rev. Astr. Ap.*, **21**, 271.
- IRAS Science Working Group. 1986, *Atlas of Low-Resolution Spectra*, *Astr. Ap. Suppl.*, **65**, 607.
- Johnston, K. J., Spencer, J. H., and Bowers, P. F. 1985, *Ap. J.*, **290**, 660.
- Little-Marenin, I. R. 1986, *Ap. J. (Letters)*, **307**, L15.
- Kholopov, P. N., ed. 1985, *General Catalogue of Variable Stars* (4th ed., Moscow: Nauka).
- Knapp, G. R., and Morris, M. 1985, *Ap. J.*, **292**, 640.
- Noguchi, K., Kawara, K., Kobayashi, Y., Okuda, H., and Sato, S. 1981, *Pub. Astr. Soc. Japan*, **33**, 373.
- Noguchi, K., Maihara, T., Okuda, H., and Sato, S. 1977, *Pub. Astr. Soc. Japan*, **29**, 511.
- Reid, M. J., and Moran, J. M. 1981, *Ann. Rev. Astr. Ap.*, **19**, 231.
- Rowan-Robinson, M., and Harris, S. 1982, *M.N.R.A.S.* **200**, 197.
- . 1983a, *M.N.R.A.S.*, **202**, 767.
- . 1983b, *M.N.R.A.S.*, **202**, 797.
- Rowan-Robinson, M., Leck, T. D., Walker, D. M., and Harris, S. 1986, *M.N.R.A.S.*, **222**, 273.
- Willems, F. J., and de Jong, T. 1986, *Ap. J. (Letters)*, **309**, L39.
- Yamashita, Y. 1972, *Ann. Tokyo Astr. Obs.*, **13**, 169.
- . 1975, *Ann. Tokyo Astr. Obs.*, **15**, 1.
- Zuckerman, B. 1980, *Ann. Rev. Astr. Ap.*, **18**, 263.
- Zuckerman, B., and Dyck, H. M. 1986, *Ap. J.*, **311**, 345.

PRISCILLA J. BENSON: Whitin Observatory, Wellesley College, Wellesley, MA 02181

IRENE R. LITTLE-MARENIN: AFGL/OPI, Hanscom AFB, MA 01731

Appendix D

New Carbon Stars Identified from Low-Resolution IRAS Spectra

NEW CARBON STARS IDENTIFIED FROM LOW-RESOLUTION *IRAS* SPECTRA

I. R. LITTLE-MARENIN

AFGL/OPI, Hanscom AFB, Massachusetts 01731

and

Whitin Observatory, Wellesley College, Wellesley, Massachusetts 02181

M. E. RAMSAY

Whitin Observatory, Wellesley College, Wellesley, Massachusetts 02181

C. B. STEPHENSON

Department of Astronomy, Case Western Reserve University, Cleveland, Ohio 44106

S. J. LITTLE

Department of Natural Sciences, Bentley College, Waltham, Massachusetts 02254

S. D. PRICE

AFGL/OPI, Hanscom AFB, Massachusetts 01731

Received 14 October 1986; revised 18 November 1986

ABSTRACT

We have classified 176 *IRAS* sources as carbon stars based on the presence of the SiC emission feature at $11.2\ \mu\text{m}$ in their low-resolution spectra.

The *Infrared Astronomical Satellite (IRAS)* obtained low-resolution spectra (LRS); $15 < \lambda / \Delta\lambda < 60$) of about 5000 *IRAS* point sources in the $8\text{--}22\ \mu\text{m}$ region (*IRAS Explanatory Supplement* 1985). This region is particularly important for the study of circumstellar shells since it contains the dust-grain signatures of both silicate dust around 10 and $18\ \mu\text{m}$ and silicon carbide (SiC) dust at $11.2\ \mu\text{m}$. The LRS have been divided into ten major classes determined by the shape of the spectra. The classification details are given in chapter 9 of the *IRAS Explanatory Supplement* (1985). Five-hundred forty-two of the LRS are characterized as belonging to class 4n. These objects have a stellar continuum energy distribution and an $11\ \mu\text{m}$ emission feature presumably due to SiC (4n: n = 1–9 is a measure of the strength of the $11\ \mu\text{m}$ feature). Eleven LRS are characterized as belonging to class 04; these LRS do not fit any of the other classes but appear to be related to the class 4n. Since three of these stars are known C stars, we have included the eight other objects in our analysis. Two-hundred twelve stars (38%) of the 4n and 04 objects can be identified with known carbon stars. Of the remainder, 41 objects are associated with known M, MS, and S stars (these particular stars have an unusual $10\text{--}11\ \mu\text{m}$ emission feature (Little and Little-Marenin 1986)) and one with a CS star. We are attempting to classify the remaining 299 objects (54%).

An analysis of the LRS of known carbon stars shows (Little-Marenin and Wilton 1986; Little-Marenin 1986) that almost all spectra contain a remarkably uniform emission feature due to SiC dust. This feature extends from about 10 to $13\ \mu\text{m}$ with a maximum at $11.2\ \mu\text{m}$. The new stars are classified by matching a blackbody energy distribution to the continuum underlying the emission feature at $11\ \mu\text{m}$ (Fig. 1) and subtracting the blackbody curve from the observed spectrum. Comparing the shape of the resulting normalized emission features of an unclassified star to that of observed SiC excesses of known carbon stars allows us to uniquely assign a given object to the stellar carbon star class (Fig. 2). We have been unable to correlate the strength of the SiC feature with the temperature or composition parameter of

the usual C spectral classification and hence cannot give a more precise subclass. Table I lists the 176 newly classified carbon stars, including five whose prior C classification is unpublished. Columns 4 and 5 list the 1950 right ascension and declination as listed in the LRS catalog and columns 2 and 3 their precessed 1900 coordinates. Column 6 gives the LRS characterization and column 7 the quality of the two halves of the LRS spectrum. The first number in column 7 refers to the $8\text{--}13\ \mu\text{m}$ region and the second to the $11\text{--}22\ \mu\text{m}$ region with 1 = good, 2 = moderate, and 3 = poor. Column 8 gives associations with other catalogs as listed in the LRS

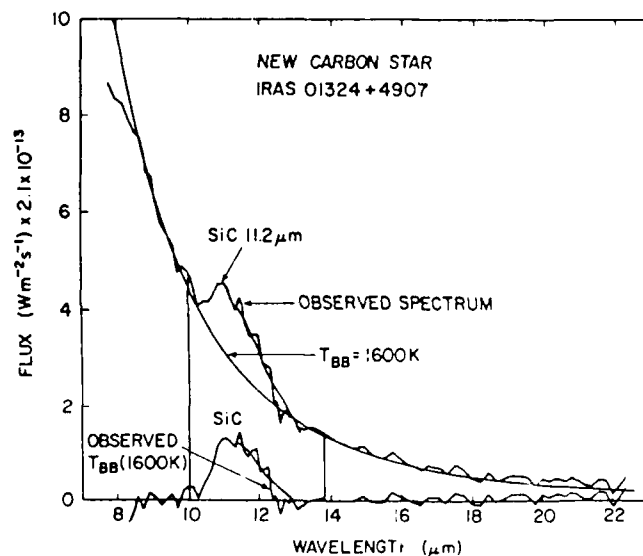


FIG. 1. The observed low-resolution spectrum of the new carbon star IRAS 01324 + 4907 is matched to a blackbody energy distribution of 1600 K. The excess emission around $11.2\ \mu\text{m}$ is clearly present. The difference spectrum (observed - 1600 K blackbody energy distribution) is plotted along the wavelength axis.

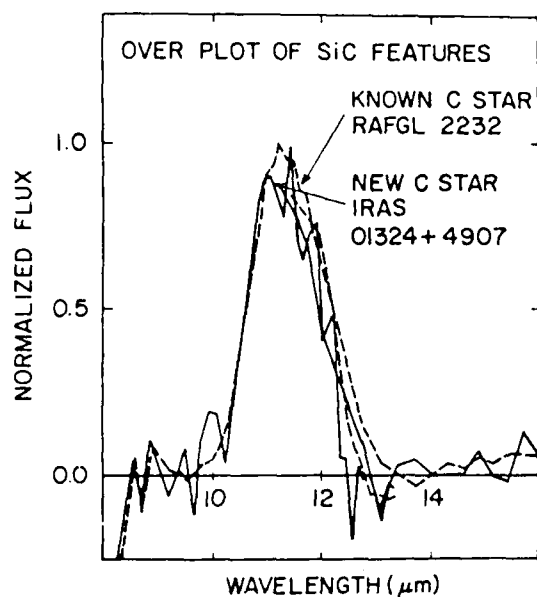


FIG. 2. The excess emission of IRAS 01324 + 4907 agrees well with the SiC features of the known carbon star RAFGL 2232. Hence this star is classified as a carbon star.

catalog. An asterisk in the Note column (9) indicates that additional information for that object is given at the end of the table. Of the 176 stars, 148 are *IRAS* sources with no catalog association, 16 are AFGL sources (Price and Murdock 1983), and 14 have an assortment of other associations. Three appear to be incorrectly classified as M stars.

It is difficult to classify the remaining 124 LRS with 4n and 04 characterizations because of their low signal-to-noise ratio or unusual spectrum. However, 42 of these appear to show a weak $10\ \mu\text{m}$ silicate absorption feature, 26 show an $18\ \mu\text{m}$ emission feature with the $10\ \mu\text{m}$ feature partly in self-absorption, and ten show the unusual $10\text{--}11\ \mu\text{m}$ emission feature found in other M, MS, or S stars with 4n characterizations. The remaining spectra are too unusual or too noisy to classify reliably.

Of the 212 *IRAS* sources which are known carbon stars, 147 were associated in the LRS catalog with stars listed in Stephenson's (1973) Catalog of Cool Carbon Stars (CCCS). For the sake of completeness, we list in Table II the remaining 65 *IRAS* sources characterized as 4n or 04 with whose C classification we agree. Coded references to their spectral classification are given in the REF column. Table II includes 12 CCCS stars with more realistic error bars for their coordinates than assumed by the *IRAS* association search program. This table does not include RAFGL 5250

TABLE I. New carbon stars.

NO. (1)	RA (1900) (2)	DEC (3)	RA (1950) (4)	DEC (5)	LRS QUAL (6) (7)	ASSOC. (8)	NOTE (9)
1	0 39 27.3	+52 53 58	0 42 16.7	+53 10 24	45 13		
2	1 11 2.1	+62 50 23	1 14 16.6	+63 6 15	42 12		
3	1 29 20.8	+48 51 57	1 32 24.1	+49 7 21	44 12		
4	1 40 46.2	+64 2 54	1 44 19.6	+64 17 58	43 12	RAFGL 248	*
5	2 55 16.1	+66 27 34	2 59 37.5	+66 39 30	44 13		
6	3 12 36.9	+32 47 36	3 15 42.9	+32 58 40	43 12		
7	3 15 23.3	+56 31 10	3 19 13.8	+56 42 3	44 12		
8	3 19 47.6	+60 23 52	3 23 52.3	+60 34 30	43 12	RAFGL 4277S	
9	3 24 5.7	+51 9 45	3 27 44.5	+51 20 9	44 12		
10	3 25 14.9	+60 28 1	3 29 21.6	+60 38 20	43 11		
11	3 26 17.0	+56 48 26	3 30 11.4	+56 58 42	43 23		
12	3 34 29.0	+59 17 43	3 38 34.1	+59 27 30	42 11		
13	3 52 13.4	+43 55 55	3 55 42.1	+44 4 39	43 12	RAFGL 5110	
14	4 9 39.5	+39 10 42	4 13 1.7	+39 18 20	43 11	RAFGL 6312S	
15	4 13 41.9	+14 12 40	4 16 30.8	+14 20 3	47 23		
16	4 13 38.8	+59 44 23	4 17 55.6	+59 51 43	42 12	RAFGL 5118	
17	4 14 30.1	+41 37 53	4 17 57.3	+41 45 11	44 23		
18	4 32 15.5	+43 17 33	4 35 47.8	+43 23 40	42 23		
19	4 31 51.5	+63 43 4	4 36 31.3	+63 49 11	45 22		
20	4 33 19.1	+44 55 41	4 36 55.0	+45 1 44	43 23		
21	4 54 7.1	+49 51 27	4 57 57.0	+49 56 3	43 23		
22	5 7 27.5	+20 52 18	5 10 26.0	+20 55 59	42 12	X0510+209B	
23	5 9 51.8	+47 9 11	5 13 36.0	+47 12 40	43 12		
24	5 28 45.0	+17 55 46	5 31 40.1	+17 57 56	45 13		
25	5 40 .4	-32 26 7	5 41 51.7	-32 24 14	43 11		
26	5 41 57.1	+13 20 23	5 44 46.6	+13 21 36	43 13		
27	5 56 4.0	+67 33 10	6 1 19.4	+67 33 16	44 23		*
28	6 5 54.1	+19 9 36	6 8 50.9	+19 9 4	43 22		
29	6 6 31.3	-27 8 43	6 10 30.7	-27 9 25	45 23		
30	6 15 28.6	+46 58 23	6 19 13.6	+46 57 7	42 12		
31	6 17 53.9	+ 9 32 59	6 20 38.7	+ 9 31 35	43 12		
32	6 19 34.1	+17 3 6	6 22 28.1	+17 1 34	44 12	GN Ori	*
33	6 21 8.7	+ 9 5 44	6 23 53.0	+ 9 4 6	43 12	RAFGL 940	
34	6 23 44.1	+20 35 4	6 26 42.7	+20 33 14	46 13		
35	6 24 7.1	+ 8 51 10	6 26 51.1	+ 8 49 19	42 11	V477 Mon	*
36	6 29 6.8	+30 17 28	6 32 19.1	+30 15 14	45 12		
37	6 31 37.1	+31 16 48	6 34 50.9	+31 14 23	42 13		
38	6 31 23.2	- 5 24 32	6 33 51.3	- 5 22 11	43 11		
39	6 46 4.4	+ 5 54 36	6 48 44.8	+ 5 51 10	43 11		
40	6 52 42.7	+28 56 57	6 55 52.2	+28 53 2	44 13		
41	6 53 9.2	+ 3 46 7	6 56 27.1	+ 3 42 8	44 12		
42	6 56 40.3	-21 34 36	6 58 48.3	-21 38 46	44 12		

TABLE I. (continued)

NO. (1)	RA (1900) (2)	DEC (3)	RA (1950) (4)	DEC (5)	LRS QUAL (6) (7)	ASSOC. (8)	NOTE (9)
43	7 5 30.1	- 1 1 39	7 8 2.5	- 1 6 27	42 12		
44	7 12 26.7	- 0 41 9	7 14 59.5	- 0 46 26	43 12		
45	7 13 33.8	- 1 5 58	7 16 6.2	- 1 11 19	42 12		*
46	7 14 22.0	+ 7 26 57	7 17 3.9	+ 7 21 32	44 12		
47	7 19 24.4	-12 40 47	7 21 43.9	-12 46 32	42 11		
48	7 19 54.4	-23 19 3	7 22 1.0	-23 24 50	42 12	RAFGL 5231	
49	7 33 48.0	-35 42 38	7 35 37.6	-35 49 20	46 23		
50	7 34 49.8	-28 26 54	7 36 50.3	-28 33 41	43 12		
51	7 45 47.3	-71 4 53	7 45 25.7	-71 12 19	43 11		
52	7 51 21.8	-53 39 16	7 52 35.1	-53 47 6	46 23		
53	7 51 26.3	+ 9 58 36	7 54 10.2	+ 9 50 42	45 23		*
54	7 52 31.9	-25 43 44	7 54 37.1	-25 51 41	44 23		
55	7 55 57.6	-40 46 51	7 57 40.8	-40 54 60	43 11		
56	7 55 59.8	-19 25 46	7 58 12.8	-19 33 56	44 11		
57	8 2 15.3	-15 16 7	8 4 33.2	-15 24 41	44 22		
58	8 3 1.0	-28 30 18	8 5 3.4	-28 38 54	43 12	RAFGL 5240	
59	8 10 3.5	-36 18 45	8 11 55.7	-36 27 47	43 12		
60	8 10 36.8	-12 27 2	8 12 58.0	-12 36 7	45 12		
61	8 17 14.1	-36 44 25	8 19 6.5	-36 53 53	42 12		
62	8 22 58.5	-25 55 49	8 25 5.8	-26 5 38	44 12		
63	8 32 6.0	-33 46 47	8 34 4.4	-33 57 8	42 11	RAFGL 5251	
64	8 33 25.3	-34 13 46	8 35 23.3	-34 24 11	44 12		
65	8 43 28.4	-38 22 12	8 45 22.0	-38 33 11	42 22		
66	8 45 49.1	-56 59 14	8 47 5.6	-57 10 20	43 13		
67	8 51 53.4	-50 44 21	8 53 27.2	-50 55 47	42 11		
68	8 51 49.6	-47 13 0	8 53 30.4	-47 24 26	42 11	MRS L 267-01/1	
69	8 54 22.5	-57 5 36	8 55 41.3	-57 17 9	44 12		
70	9 16 0.1	-51 35 3	9 17 38.5	-51 47 42	42 12		
71	9 40 53.2	-43 28 5	9 42 50.8	-43 41 51	43 12		
72	9 49 35.2	-53 10 37	9 51 20.8	-53 24 43	42 11		
73	9 51 49.1	-74 54 5	9 52 10.4	-75 8 15	43 11	RAFGL 4098	
74	9 51 14.4	-54 51 52	9 52 57.5	-55 6 2	43 12		
75	9 51 48.3	-60 6 59	9 53 20.3	-60 21 10	42 22		
76	9 53 4.4	-55 8 40	9 54 47.7	-55 22 54	45 13		
77	9 56 55.6	-50 42 36	9 58 47.6	-50 56 59	43 13		
78	10 5 19.5	-63 26 39	10 6 49.0	-63 41 20	43 12		
79	10 6 38.3	-55 58 37	10 8 25.1	-56 13 21	45 23		
80	10 21 19.5	-58 8 42	10 23 8.4	-58 23 54	43 12	EMIS -582175	
81	10 23 46.3	-40 28 46	10 25 56.8	-40 44 3	49 33		
82	10 35 25.9	-47 46 34	10 37 33.2	-48 2 10	43 12		
83	10 38 28.2	-58 10 12	10 40 24.6	-58 25 53	46 33		
84	10 53 56.7	-65 21 17	10 55 49.3	-65 37 19	44 13		*
85	11 5 16.4	-63 8 53	11 7 19.2	-63 25 8	43 13		
86	11 12 29.7	-65 18 12	11 14 33.9	-65 34 34	43 11		
87	11 24 36.5	-64 21 25	11 26 49.3	-64 37 56	44 22	EMIS HEN 658	*
88	11 25 8.7	-68 45 7	11 27 16.9	-69 1 38	43 12		
89	11 28 20.3	-10 3 53	11 30 52.4	-10 20 26	44 11		*
90	11 48 55.6	-58 25 3	11 51 24.6	-58 41 44	41 12		
91	12 16 43.4	-59 50 59	12 19 26.2	-60 7 38	42 21		
92	12 18 52.3	-62 1 34	12 21 37.1	-62 18 12	42 11		
93	12 20 1.1	-50 29 4	12 22 42.3	-50 45 42	43 13		
94	12 36 50.4	-64 30 45	12 39 47.5	-64 47 13	44 13		*
95	12 50 48.1	-68 29 24	12 54 .4	-68 45 40	42 11		
96	13 0 6.4	-57 27 12	13 3 8.0	-57 43 18	45 13		
97	13 6 8.5	-60 10 57	13 9 16.3	-60 26 56	44 23		
98	13 15 57.8	-65 12 59	13 19 19.8	-65 28 44	46 23		
99	13 31 7.7	-57 52 34	13 34 23.5	-58 7 55	43 11		
100	13 44 8.4	-65 17 9	13 47 47.2	-65 32 6	04 11	RAFGL 4183	
101	13 44 30.8	-67 1 12	13 48 15.4	-67 16 8	44 11		
102	13 47 21.2	-63 33 52	13 50 56.8	-63 48 43	42 11		
103	13 56 17.5	-52 39 50	13 59 34.4	-52 54 22	45 23		
104	13 57 32.0	-59 12 34	14 1 1.7	-59 27 3	46 23		*
105	14 27 33.1	-51 12 60	14 30 57.3	-51 26 17	44 22		
106	14 36 27.0	-63 7 53	14 40 25.1	-63 20 45	42 12		
107	14 44 29.3	-61 39 33	14 48 25.6	-61 52 2	42 11		*
108	14 48 11.4	-60 46 15	14 52 6.1	-60 58 33	44 22		
109	15 0 41.5	-54 26 44	15 4 22.2	-54 38 25	43 12		
110	15 4 45.3	-47 57 16	15 8 13.0	-48 8 44	42 11	RAFGL 4211	
111	15 15 50.2	-51 4 27	15 19 26.9	-51 15 19	04 21		
112	15 16 28.1	-55 28 15	15 20 15.9	-55 39 5	43 13		
113	16 4 15.7	-48 4 11	16 7 54.9	-48 12 9	42 11		
114	16 8 43.2	-46 47 13	16 12 20.1	-46 54 54	44 12		
115	16 13 29.4	-47 52 22	16 17 9.5	-47 59 44	43 11		
116	16 19 0.7	-46 5 7	16 22 37.5	-46 12 7	44 22		
117	16 25 54.6	-53 43 7	16 29 52.2	-53 49 39	42 12	X1629-538	
118	16 31 16.9	- 3 11 20	16 33 54.1	- 3 17 33	46 23		

TABLE I. (continued)

NO. (1)	RA (1900) (2)	DEC (3)	RA (1950) (4)	DEC (5)	LRS QUAL (6) (7)	ASSOC. (8)	NOTE (9)
119	16 50 9.6	-46 28 16	16 53 50.6	-46 33 9	45 22		
120	16 51 53.0	-44 51 40	16 55 30.5	-44 56 26	44 13		
121	16 52 20.6	-50 34 47	16 56 12.3	-50 39 50	43 12		
122	16 54 24.6	-43 33 43	16 57 59.4	-43 38 18	49 33		
123	17 1 37.2	-28 44 7	17 4 46.4	-28 48 13	42 12		
124	17 4 43.9	-32 39 37	17 7 59.3	-32 43 29	42 11	V463 SCO	
125	17 3 0.7	-65 50 37	17 7 59.3	-65 54 33	43 12		
126	17 9 38.1	-39 3 57	17 13 4.8	-39 7 28	44 22		
127	17 11 43.2	-49 14 11	17 15 32.8	-49 17 32	43 12		
128	17 18 18.4	-39 13 48	17 21 45.8	-39 16 42	42 11		
129	17 19 13.6	-23 25 18	17 22 15.8	-23 28 9	42 12		
130	17 55 16.3	-17 44 6	17 58 11.3	-17 44 20	44 11		
131	18 6 30.5	-22 29 45	18 9 31.8	-22 29 10	47 23		
132	18 7 14.6	-14 21 17	18 10 5.3	-14 20 39	43 12	X1809-143	
133	18 22 5.9	- 8 41 1	18 24 49.7	- 8 39 19	43 12		
134	18 24 9.0	-12 58 54	18 26 57.9	-12 57 2	43 12		
135	18 23 52.1	-47 19 40	18 27 37.7	-47 17 48	44 11		
136	18 39 50.8	+11 44 10	18 42 10.8	+11 47 8	44 11		
137	18 39 59.9	+ 3 43 26	18 42 29.2	+ 3 46 25	44 12		
138	18 40 28.4	- 0 35 28	18 43 2.7	- 0 32 26	45 13		
139	18 49 27.4	- 2 25 29	18 52 3.8	- 2 21 49	46 23		
140	19 8 32.9	+11 50 2	19 10 53.1	+11 55 2	44 12		
141	19 26 44.8	+19 25 34	19 28 56.5	+19 31 49	42 12		
142	19 32 18.6	+12 3 14	19 34 39.1	+12 9 52	43 12		
143	19 33 25.3	+ 9 10 33	19 35 49.0	+ 9 17 15	42 21		
144	19 40 0.7	+32 15 4	19 41 56.1	+32 22 11	44 12		
145	19 43 8.6	+ 9 13 19	19 45 32.4	+ 9 20 40	43 12	RAFGL 4253	
146	19 43 35.2	+23 39 36	19 45 42.5	+23 46 58	43 12		
147	19 50 14.8	+24 6 37	19 52 21.9	+24 14 25	43 13		
148	19 50 14.5	+21 22 49	19 52 24.9	+21 30 37	43 13		
149	19 51 37.8	+22 5 4	19 53 47.5	+22 12 57	44 11	RAFGL 2474	
150	19 53 16.2	+31 34 18	19 55 13.7	+31 42 17	42 12		
151	20 2 28.3	+35 0 5	20 4 21.7	+35 8 39	45 22		
152	20 6 15.0	+32 19 34	20 8 12.6	+32 28 22	42 12		
153	20 8 22.8	+41 14 52	20 10 6.8	+41 23 48	44 22		
154	20 8 26.8	+33 30 48	20 10 23.0	+33 39 44	47 33		
155	20 18 25.9	+29 4 28	20 20 29.0	+29 14 1	43 12		
156	20 26 17.4	+35 54 31	20 28 12.2	+36 4 31	45 22		
157	20 30 21.9	+31 43 0	20 32 22.8	+31 53 15	43 23		
158	20 31 28.6	+46 10 58	20 33 7.3	+46 21 16	42 12	MRS1 084+03/1	
159	20 41 36.8	+38 14 31	20 43 30.4	+38 25 24	42 11		
160	20 51 53.9	+55 42 41	20 53 15.8	+55 54 6	42 11		
161	20 53 43.8	+63 54 18	20 54 38.1	+64 5 48	44 13		
162	20 54 12.0	+18 45 44	20 56 29.2	+18 57 18	45 13		
163	20 57 40.5	+38 21 45	20 59 36.4	+38 33 29	42 22		
164	20 58 40.6	+47 49 16	21 0 21.8	+48 1 3	44 11	LDN 0962	
165	20 58 57.5	+47 8 24	21 0 40.0	+47 20 12	43 12		
166	21 20 40.9	+51 1 13	21 22 21.7	+51 14 5	42 12		
167	21 30 49.7	+55 24 36	21 32 24.7	+55 37 55	42 12	DO 39779	*
168	21 35 24.8	+45 27 19	21 37 18.5	+45 40 51	43 11		
169	21 40 52.4	+58 8 12	21 42 24.7	+58 21 57	44 13		
170	21 43 6.6	+49 36 17	21 44 56.2	+49 50 8	42 11		
171	22 33 31.0	+58 56 7	22 35 24.0	+59 11 40	44 12	LDN 1198	
172	23 15 16.7	+59 25 29	23 17 28.8	+59 41 53	44 12		
173	23 15 27.5	+67 53 50	23 17 29.9	+68 10 14	44 22		
174	23 25 35.9	+53 20 2	23 27 56.5	+53 36 34	43 12		
175	23 46 42.2	+62 27 16	23 49 9.1	+62 43 57	43 11	EMIS 1+62 36	
176	23 46 55.1	+62 14 9	23 49 22.1	+62 30 50	44 23	DO 43734	

Notes to TABLE I

- 4 RAFGL 248=DO 16793 (not M4; Price and Murdock 1983)
 27 independently confirmed as C by C.B. Stephenson (CBS hereafter)
 32 GN Ori=RAFGL 5192 (not M7)
 35 V477 Mon=RAFGL 5196=EIC 135 (not M1)
 45 C by MacConnell, Baker and Landis (unpublished) (MBL hereafter)
 53 independently confirmed as C by CBS
 84 C by MBL (unpublished)
 87 C by MBL (unpublished)
 89 11 micron emission characteristic of carbon stars (Hacking et al 1985)
 94 prob. CCCS 2026 (12:36:53, -64:27.3 (1900))
 104 C by MBL (unpublished)
 107 C by MBL (unpublished)
 167 DO 39779=LDN 1083

Notes to TABLE I (continued)

References to the catalogs used for the association with IRAS sources:
 CCCS =Catalog of Cool Carbon Stars (Stephenson 1973)
 DO =Dearborn Observatory (Lee et al 1947)
 EIC =Equatorial Infrared Catalog (Sweeney et al 1979)
 GLOB =Globule List (Wesselius 1979 (unpublished))
 IRC =Two Micron Sky Survey (Neugebauer and Leighton 1969)
 LDN =Lynds (1962)
 MRSL =Marsalkova (1974)
 RAFGL = Revised Air Force Geophysics Lab (Price and Murdock 1973)
 X = IRAS Small Scale Structure Catalog (1986).

TABLE II. Previously known carbon stars.

NO.	RA (1900)	DEC	RA (1950)	DEC	LRS	Q	REF	ASSOCIATIONS
1	0 21 55.6	+69 5 37	0 24 47.2	+69 22 14	43	11	5	RAFGL 67
2	1 5 3.0	+53 11 38	1 8 2.3	+53 27 38	44	12	2	HV Cas=RAFGL 167=IRC +50030=DO 24107
3	1 54 34.5	+57 49 4	1 58 0.0	+58 3 40	44	22	7	CCCS 90=EMIS IG 139 (Independently confirmed by CBS)
4	2 12 19.1	+28 9 3	2 15 12.5	+28 22 59	43	11	8	
5	2 16 46.2	+48 16 16	2 20 2.6	+48 30 1	47	13	7	CCCS 97=DO 25649
6	2 25 43.9	+57 35 29	2 29 21.0	+57 48 51	42	11	5	RAFGL 341
7	3 13 44.8	+70 5 23	3 18 38.5	+70 18 20	42	11	5	RAFGL 482
8	3 41 21.3	+44 23 27	3 44 49.2	+44 32 51	42	12	8	RAFGL 5102
9	3 45 33.6	+39 34 45	3 48 53.6	+39 43 54	42	11	2	V414 Per=RAFGL 527=IRC +40070
10	4 26 16.0	+62 3 42	4 30 46.0	+62 10 11	45	11	10	RAFGL 595=IRC +60144=DO 28389
11	4 49 29.7	+44 23 3	4 53 5.9	+44 27 59	42	11	10	
12	5 34 54.3	- 8 12 26	5 37 18.4	- 8 10 42	42	12	2	RAFGL 796=IRC -10095=SVS 6369 (Independently confirmed by CBS)
13	5 34 57.5	+13 45 10	5 37 47.4	+13 46 53	44	12	5	RAFGL 799
14	5 35 35.4	+12 14 49	5 38 23.5	+12 16 29	44	13	7	CCCS 381=RAFGL 801=IRC +10094=SVS 2557=DO 1241
15	5 37 16.8	+32 39 16	5 40 32.1	+32 40 48	42	11	5	RAFGL 809=GLOB BARNARD 34
16	5 40 25.5	+43 10 31	5 44 1.7	+43 11 49	44	11	2	RAFGL 815=IRC +40140=SVS 2629
17	6 20 15.6	- 9 3 58	6 22 38.6	- 9 5 32	43	11	2	V638 Mon=RAFGL 933=IRC -10122
18	6 20 42.3	- 9 28 43	6 23 4.8	- 9 30 19	44	21	5	RAFGL 935
19	6 25 29.8	+43 21 27	6 29 6.0	+43 19 28	43	11	5	RAFGL 954
20	6 31 38.7	+ 3 30 29	6 34 16.4	+ 3 28 5	43	11	5	RAFGL 971
21	7 0 32.8	-14 51 55	7 2 49.3	-14 56 21	43	12	5	RAFGL 1062 (confirmed by MBL)
22	7 7 43.5	-20 7 21	7 9 53.7	-20 12 17	43	11	5	RAFGL 1085
23	7 52 36.9	+ 0 24 59	7 55 10.0	+ 0 32 57	44	23	7	CCCS 981
24	9 9 27.9	-24 26 40	9 11 41.0	-24 39 1	42	11	8	RAFGL 5254
25	9 42 31.5	+13 44 31	9 45 14.2	+13 30 40	43	11	2	CW Leo=RAFGL1381=IRC +10216=X 0945+135
26	16 25 26.0	-44 57 21	16 29 1.1	-45 3 56	45	12	6	
27	17 1 51.6	-24 36 36	17 4 55.0	-24 40 41	42	11	5	RAFGL 1922
28	17 36 50.9	-78 8 28	17 44 41.9	-78 9 52	43	11	7	CCCS 2476 (at 17:36:38.9, -78:07:0 (1900))
29	18 1 20.0	- 9 41 52	18 4 5.1	- 9 41 40	44	11	9	FX Ser=RAFGL 2067=IRC -10398
30	18 0 52.7	-33 17 11	18 4 10.2	-33 17 0	45	11	4	
31	18 1 40.2	-15 25 46	18 4 32.3	-15 25 32	45	12	6	LDN 0347
32	18 4 55.3	-20 23 17	18 7 53.8	-20 22 49	43	12	5	RAFGL 2085
33	18 12 55.3	- 6 54 8	18 15 37.0	- 6 53 6	45	11	5	RAFGL 2118
34	18 16 18.6	-27 9 19	18 19 26.4	-27 8 1	43	21	3	RAFGL 2135
35	18 20 34.8	+ 5 42 43	18 23 1.8	+ 5 44 18	44	11	5	RAFGL 2150=EIC 652
36	18 20 27.0	-22 7 43	18 23 27.7	-22 6 7	45	21	2	V2548 Spr=RAFGL 2151=IRC -20482
37	18 21 15.6	- 6 57 33	18 23 57.3	- 6 55 54	43	11	5	RAFGL 2154
38	18 21 56.3	+23 25 13	18 24 1.1	+23 26 53	42	11	5	RAFGL 2155
39	18 37 29.3	+17 35 22	18 39 42.0	+17 38 10	43	11	2	RAFGL 2232=IRC +20370=SVS 11225
40	18 45 8.9	+ 9 23 13	18 47 31.7	+ 9 26 34	42	11	5	RAFGL 2259
41	19 0 47.4	+20 12 59	19 2 57.3	+20 17 26	43	12	5	RAFGL 2318
42	19 14 52.3	- 8 13 20	19 17 35.0	- 8 7 53	43	21	2	RAFGL 2368=IRC -10502=EIC 759=SVS 11912
43	19 22 22.3	+ 6 52 6	19 24 48.4	+ 6 58 3	45	12	5	RAFGL 2392=EIC 768
44	19 30 7.6	+27 50 60	19 32 8.6	+27 57 28	43	11	2	V1129 Cyg=RAFGL 2417=IRC +30374=SVS 12165
45	19 36 13.0	+33 8 31	19 38 6.8	+33 15 23	44	12	5	RAFGL 2428
46	19 45 12.4	+29 16 30	19 47 12.4	+29 23 58	49	23	7	CCCS 2806
47	19 57 41.4	+40 38 58	19 59 25.1	+40 47 14	42	11	5	RAFGL 2494
48	20 5 16.0	-31 8 8	20 7 15.2	-31 16 53	43	11	5	RAFGL 2513
49	20 8 33.2	+39 18 48	20 10 20.5	+39 27 44	45	23	1	Baldone 58
50	20 22 10.0	+69 25 19	20 22 18.2	+69 35 2	44	13	7	CCCS 2903 (Independently confirmed by Dean (thesis) and CBS)
51	20 24 37.9	+42 35 11	20 26 22.0	+42 45 5	49	33	7	CCCS 2905 (at 20:24:9, +42:30 (1900))
52	20 32 42.6	+53 28 32	20 34 5.3	+53 38 54	42	11	5	RAFGL 2613
53	20 54 51.4	+27 3 19	20 57 4	+27 14 55	42	11	5	RAFGL 2686
54	21 1 11.9	+52 57 9	21 2 43.3	+53 9 4	44	12	5	RAFGL 2699 (Independently confirmed by CBS)
55	21 14 36.7	+55 34 23	21 16 5.9	+55 46 57	43	12	7	CCCS 3017 (Independently confirmed by CBS)
56	21 25 35.1	+69 47 7	21 26 15.1	+70 0 11	45	12	2	AX Cap=RAFGL 2768=IRC +70170=DO 39655 (confirmed by CBS)
57	21 36 24.0	-45 0 6	21 38 18.5	+45 13 40	44	11	2	V844 Cyg=CCCS 3054=IRC +50388
58	21 47 13.7	+52 47 22	21 48 59.2	+53 1 23	42	11	8	
59	22 10 44.8	+55 53 25	22 12 33.3	+56 8 17	43	13	7	CCCS 3121
60	22 14 28.2	+43 18 39	22 16 32.0	+43 31 39	42	11	7	CCCS 3125=RAFGL 2881
61	22 22 20.8	+59 50 17	22 24 7.1	+60 5 31	41	11	5	RAFGL 2901
62	22 41 12.3	+74 16 8	22 42 25.9	+74 31 50	45	12	7	CCCS 3157=RAFGL 2949=DO 41941
63	22 50 2.9	+65 44 57	22 51 52.3	+66 0 54	44	11	5	RAFGL 2985
64	22 56 35.1	+63 46 29	22 59 32.0	+64 2 34	43	11	5	RAFGL 3011
65	23 29 35.9	+42 59 53	23 32 1.6	+43 18 27	42	11	10	RAFGL 3116=IRC +40540 (not MB)

References:

1. Aikine and Ozolina (1974)
2. Bidelman (1980)
3. Deguchi, Claussen, and Goldsmith (1986)
4. Fuenmayor (1981)
5. Kleinman, Gillett, and Joyce (1981)
6. MacConnell (1979)
7. Stephenson (1973)
8. Zuckerman and Dyck (1986a)
9. Zuckerman and Dyck (1986b)
10. Zuckerman, Dyck and Claussen (1986)

and RAFGL 2102. These two stars are classified as C stars by Zuckerman and Dyck (1986a, b) based on their location in an *IRAS* color-color plot and the presence of a strong HCN line in the spectrum of RAFGL 5250. The LRS of RAFGL 5250 shows an unusual emission or absorption feature which is neither due to SiC nor to silicate, and RAFGL 2102 may show the 10 μm feature partly in self-absorption.

We would like to thank P. LeVan for helpful and stimulating discussions. This work has been supported by a University Resident Research Fellowship from the AFOSR to the Air Force Geophysics Laboratory. One of us (M.E.R.) was supported by Wellesley College as a Dana Foundation Summer Research Fellow.

REFERENCES

- Alksne, Z., and Olina, V. (1976). *Investigations of the Sun and Red Stars*, edited by A. Balklavs (Zinatne, Riga), Vol. 4, p. 5.
- Beichman, C.A., Neugebauer, G., Habing, H. J., Clegg, P. E., and Chester, T. T., editors (1985). *IRAS Catalog and References, Explanatory Supplement* (U.S. GPO, Washington, DC).
- Bidelman, W. P. (1980). *Publ. Warner and Swasey Obs.* **2**, No. 6.
- Deguchi, S., Claussen, M. J., and Goldsmith, P. F. (1986). *Astrophys. J.* **303**, 810.
- Fuenmayor, F. J. (1981). *Rev. Mex. Astron. Astrofis.* **6**, 83.
- Hacking, P., *et al.* (1985). *Publ. Astron. Soc. Pac.* **97**, 616.
- Helou, G., and Walker, D., preparers (1986). *IRAS Small Scale Structure Catalog* (U.S. GPO, Washington, DC).
- Kleinman, S. G., Gillett, F. C., and Joyce, R. R. (1981). *Annu. Rev. Astron. Astrophys.* **19**, 411.
- Lee, O. J., Gore, G. D., and Bartlett, T. J. (1947). *Ann. Dearborn Obs.* **V**, part 1C.
- Little, S. J., and Little-Marenin, I. R. (1986). *Lect. Not. in Phys.* **254**, 423.
- Little-Marenin, I. R. (1986). *Astrophys. J. Lett.* **307**, L15.
- Little-Marenin, I. R., and Wilton, C. (1986). *Lect. Not. Phys.* **254**, 420.
- Lynds, B. T. (1960). *Astrophys. J. Suppl.* **7**, 1.
- MacConnell, D. J. (1982). *Astron. Astrophys. Suppl.* **38**, 335.
- Marsalkova, P. (1974). *Astrophys. Space Sci.* **27**, 3.
- Neugebauer, G., and Leighton, R. B. (1969). *Two-Micron Sky Survey*. NASA SP-3047 (NASA, Washington, DC).
- Price, S. D., and Murdock, T. L. (1983). *The Revised AFGL Infrared Sky Survey Catalog*. AFGL-TR-0208 (Air Force Geophysics Laboratory, Hanscom AFB, MA).
- Stephenson, C. B. (1973). *Publ. Warner and Swasey Obs.* **1**, No. 4.
- Sweeney, L. H., Heinsheimer, T. F., Yates, F. F., Maran, S. P., Lesh, J. R., and Nagy, T. A. (1978). *Interim Equatorial Infrared Catalogue*, TR-0078(3409-20)-1 (The Aerospace Corporation, Los Angeles).
- Wackerling, L. R. (1970). *Mem. R. Astron. Soc.* **73**, 153.
- Wesselius, R. P. (1979). Unpublished.
- Zuckerman, B., and Dyck, H. M. (1986). *Astrophys. J.* **304**, 394.
- Zuckerman, B., and Dyck, H. M. (1986). *Astrophys. J.* **311**, 345.
- Zuckerman, B., Dyck, H. M., and Claussen, M. J. (1986). *Astrophys. J.* **304**, 401.

Appendix E

A Search for Technetium (Tc II) in Barium Stars

A SEARCH FOR TECHNETIUM (Tc II) IN BARIUM STARS

IRENE R. LITTLE-MARENIN¹⁾

AFGL/OPC, Hanscom AFB, Massachusetts 01731

and

Whitin Observatory, Wellesley College, Wellesley, Massachusetts 02181

STEPHEN J. LITTLE

Department of Natural Sciences, Bentley College, Waltham, Massachusetts 02754

Received 14 January 1987; revised 3 March 1987

ABSTRACT

We searched without success for the lines of Tc II at 2647.02, 2610.00 and 2543.24 Å in *IUE* spectra of the barium stars HR 5058, α Vir, and ζ Cap. The lack of Tc II implies that the observed *s*-process enhancements were produced more than half a million years ago and supports the suggestion that the spectral peculiarities of barium stars are probably related to the binary nature of the stars.

I. INTRODUCTION

Barium stars are, in general, old disk giants or bright giants that have enhanced spectral lines of the *s*-process elements Ba II and Sr II, as well as enhanced features of CH, CN, and sometimes C₂. On the strength of the Ba II line at 4554 Å, astronomers divide the barium stars into classical (Ba2–Ba5) and mild (Ba1) barium stars. For recent reviews, see McClure (1984) and Lambert (1985). Recent abundance analyses of barium stars (Tomkin and Lambert 1986; Lambert 1985; Smith and Lambert 1984; Smith 1984; Pinsonneault, Sneden, and Lambert 1984; Kovacs 1983; Tomkin and Lambert 1983; Sneden, Lambert, and Pilachowski 1981; Smith, Sneden, and Pilachowski 1980) have shown that for classical barium stars the enhancements of *s*-process elements (Y, Zr, Ba, La, etc.) are typically about 4–10 times solar, with a C/O ratio ranging from 0.6 to 1.02. In mild barium stars, on the other hand, *s*-process enhancements are typically only about 2 times solar, and their C/O ratios are similar to those of normal G and K giants (about 0.3). Our understanding of stellar evolution is such that the mixing of *s*-processed material with surface layers is only expected to occur during the helium shell flashing phase while the stars are on the asymptotic giant branch (AGB). However, barium stars are too hot and have too low a luminosity to be at the AGB stage of evolution.

A clue to our understanding of the observed abundance anomalies comes from the discovery that all classical and probably all mild barium stars are members of a binary system (McClure, Fletcher, and Nemeč 1980; McClure 1983; Böhm-Vitense, Nemeč, and Proffitt 1984; McClure 1985). Orbital solutions give separations that are typically about 2 AU, with low-mass secondaries. Several low-mass companions (white dwarfs) have been observed directly with *IUE* (Böhm-Vitense 1980; Schindler *et al.* 1983; Böhm-Vitense, Nemeč, and Proffitt 1984; Böhm-Vitense and Johnson 1985). Radial-velocity measurements of other late-type giants with peculiar abundances, such as R, CN, CH, subgiant CH and semibarium stars, appear to show a positive correlation between the amount of *s*-process enhancement and the

percent of duplicity (McClure 1985). Hence it is assumed that the varying amount of *s*-process enhancement of all these stars is related to their binary nature, even though the mechanism for producing the excesses is not agreed upon.

A number of scenarios have been suggested to explain the abundance anomalies (McClure 1984; Böhm-Vitense, Nemeč and Proffitt 1984; Lambert 1985). The most common scenario assumes that mass was transferred from the present-day low-mass companion (white dwarf) when it was an AGB star. Lambert (1985) has pointed out that the trend from mild to classical barium star can be explained by assuming that an increasing amount of material from a "typical" cool carbon star is mixed with the atmosphere of a normal G and K giant. Cool carbon stars are produced from M stars while on the AGB (Iben and Renzini 1983) and have C/O ratios usually between 1.05 and 1.1 (Lambert *et al.* 1986). However, the assumption that barium stars are produced by mass transfer does not account for the absence of the lithium line in most mild barium stars and its presence in classical barium stars with strength similar to that found among K giants (Pinsonneault, Sneden, and Lambert 1985).

It has also been suggested that the companion is and/or has produced mixing in the barium star due to tidal interactions. If the *s*-process enhancements are indigenous to the barium star and are still increasing, then we might detect the signature of this process in the outer layers. Nature has provided us with a unique tracer of recent *s*-processing in the isotopes of technetium (Tc). All its isotopes are radioactive, with ⁹⁹Tc, the isotope produced in the *s*-process, having a half-life of about 2×10^5 yr below 10^8 K. However, at the temperatures found in the intershell region of high mass ($> 3 M_{\odot}$) AGB stars ($T > 2 \times 10^8$ K), the half-life falls to about 40 yr (Cosner and Truran 1981; Schatz 1983). The mere detection of Tc is enough to establish unambiguously those stars in which *s*-processing and mixing has occurred recently. The detection of neutral Tc in S, some C, MS, and M long-period variables has shown that *s*-processing and mixing does indeed occur (see Little-Marenin and Little 1978; and Little *et al.* 1987 for a complete list of references).

In order to distinguish between continuing (or recently stopped) *s*-processing and some other mechanism for enhancing the abundances, we have analyzed *IUE* spectra of three different kinds of barium stars: (a) the classical bari-

¹⁾ Research Fellow, Joint Institute for Laboratory Astrophysics (1983–1984), *IUE* Guest Observer, University Resident Research Fellow, AFGL (1986–1987).

um star HR 5058 (HD 116713; K0.5 III-Ba3) with *s*-process enhancements of about 4 and $C/O = 0.74$ (Snedden, Smith, and Pilachowski 1981); (b) the mild barium star *o* Vir (HR 4608 = HD 104979; G8 IIIaCN-1Ba1CH1) with $C/O = 0.34$, typical of G and K giants (Snedden, Smith, and Pilachowski 1981), but with an *s*-process enhancement of about 5 (Tomkin and Lambert 1986), similar to HR 5058; and (c) the classical supergiant barium star ζ Cap (HR 8204 = HD 204075; G4 Ib (K0-Ba3)) with $C/O = 1.02$ (the largest value determined for a barium star) and *s*-process enhancements of about 6 (Smith, Sneden, and Pilachowski 1980). ζ Cap is the most luminous and hence the most massive ($3\text{--}5 M_{\odot}$) of the known barium stars.

II. OBSERVATIONS AND REDUCTIONS

A number of searches for Tc I and Tc II lines have been made in the visible wavelength region, primarily by Warner (1965), but also by Burbidge and Burbidge (1957), Tech (1971), Boesgaard and Fesen (1974), and Smith (1984) with negative results. However, Tc, with an ionization potential of 7.3 eV, is primarily in its ionized form in barium stars ($5200 > T > 4500$ and $3.0 > \log g > 1.5$), and its strongest lines at 2647.02, 2610.00, and 2543.24 Å are not observable with ground-based equipment. We obtained high-dispersion LWP spectra of HR 5058 and *o* Vir with *IUE* (*International Ultraviolet Explorer* satellite) on 1984 July 6 and 7. The LWP camera covers the 2000–3000 Å region with a resolution of about 0.2 Å. For details of the *IUE* satellite, see Boggess *et al.* (1978). We also analyzed five LWR spectra of ζ Cap from the *IUE* archives. The LWR and LWP cameras have very similar spectral characteristics but different intensity transfer functions. The observational data are summarized in Table I. The spectra were calibrated in absolute-flux units at Earth using the standard *IUE* calibration factors and were analyzed at the *IUE* Regional Data Analysis Facility (RDAF) at the University of Colorado. Since the absolute-wavelength calibration for the earlier (ζ Cap) spectra are uncertain due to possible thermal flexing of the spectrograph (Leckrone 1980; Turnrose, Thompson, and Bohlin 1982), we measured the wavelength of all the Tc II lines relative to other photospheric absorption lines. However, we obtained radial velocities of $+64 \pm 10$ km/s and

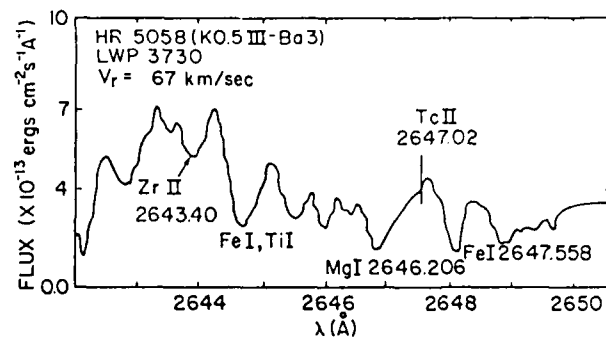


FIG. 1. The 2647 Å region of HR 5058 (LWP 3730). Several photospheric absorption lines are indicated, as well as the position of the Tc II line at 2647.02 Å. The radial velocity for the star is +67 km/s.

-24 ± 10 km/s for *o* Vir and HR 5058, respectively, using the *IUE* absolute-wavelength calibration. These values agree well with the published values of +67 km/s and -30 km/s (*Bright Star Catalog*, Hoffleit and Jaschek 1982). We were unable to identify any Tc II lines in any of the spectra, and estimate the equivalent widths of the 2647 Tc II line to be < 30 mÅ (ζ Cap), < 25 mÅ (HR 5058), and < 20 mÅ (*o* Vir). The absence of the Tc II lines in the spectrum of ζ Cap confirms our earlier analysis based on the LWR 4602 and LWR 4618 spectra (Little-Marenin *et al.* 1980). Even though all three Tc II lines lie close to other photospheric absorption lines (Fe I (6): 2647.558 Å; Mn II (19): 2610.202 Å and Fe II (204) 2609.859 Å; Fe II (159): 2543.382 Å), the Tc II lines should be displaced enough to be detectable. Figure 1 shows the 2647 Å region of the spectrum of HR 5058. The positions and wavelengths of several photospheric lines are indicated, as well as the predicted position for the Tc II 2647.02 line. The lack of evidence for the two other Tc II lines at 2610.00 and 2543.24 Å is very similar.

III. DISCUSSION

The fact that technetium is not observed in two classical barium stars and one mild one implies that the episode that produced the enhancement of the other *s*-process elements occurred at least half a million years ago. Smith and Lambert

TABLE I. *IUE* observational data.

Image No.	Star	Spectral Class	Year/Day	Expos (min)	V_r	Comments
LWP 3727	<i>o</i> Vir	G8IIIaCN-1Ba1CH1	1984/189	133	-30	ux < 2500 Å
LWP 3730	HR 5058	K0.5III-Ba3	1984/190	420	+67	ux < 2600 Å
LWR 4602	ζ Cap	G4Ib (K0-Ba3)	1979/146	120	+3	ox > 2600 Å
LWR 4604	"	"	1979/146	40	"	
LWR 4618	"	"	1979/148	40	"	
LWR 6282	"	"	1979/340	30	"	
LWR 7559	"	"	1980/112	30	"	

(1984) reached a similar conclusion for ζ Cap based on the abundance of ^{93}Nb , which is produced from the decay of ^{93}Zr after the s -process ceased. The abundance of Nb implies that the s -process stopped more than 3×10^6 yr ago. Hence the observed abundance anomalies were not produced recently in either the supergiant, classical, or mild barium stars. The lack of Tc I and Tc II lines lends support to the suggestion that all barium stars (supergiant, classical, and mild) are produced by the same mechanism, such as mass transfer from the companion when it was an AGB star or some other mechanism which produced the enhancements in the distant past.

We would like to thank the staff of the *IUE* Observatory and the staff (especially T. Armitage) of the RDAF at the University of Colorado, which is operated under grant NAG 5-26409, for their greatly appreciated help. I.R.L.-M. would like to thank J. Linsky and the Joint Institute of Laboratory Astrophysics for their support and hospitality during her year as a Research Fellow. This work is in part supported by Grant NAG 5-438 and by a University Resident Research Fellowship from the AFOSR to the Air Force Geophysics Laboratory.

REFERENCES

- Boesgaard, A. M. and Fesen, R. A. (1974). *Publ. Astron. Soc. Pac.* **86**, 76.
 Boggess, A., *et al.* (1978). *Nature* **275**, 7.
 Böhm-Vitense, E. (1980). *Astrophys. J. Lett.* **239**, L79.
 Böhm-Vitense, E., Nemeč J., and Proffitt, C. (1984). *Astrophys. J.* **278**, 726.
 Böhm-Vitense, E., and Johnson, H. R. (1985). *Astrophys. J.* **293**, 288.
 Burbidge, E. M., and Burbidge, G. R. (1957). *Astrophys. J.* **126**, 357.
 Cosner, K., and Truran, W. (1981). *Astrophys. Space Sci.* **78**, 85.
 Hoffleit, D., and Jaschek, C. (1982). *The Bright Star Catalog* (Yale University, New Haven).
 Iben, I., and Renzini, A. (1983). *Annu. Rev. Astron. Astrophys.* **21**, 271.
 Kovacs, N. (1983). *Astron. Astrophys.* **124**, 63.
 Lambert, D. L. (1985). In *Cool Stars with Excesses of Heavy Elements*, edited by M. Jaschek and P. C. Keenan (Reidel, Dordrecht), p. 191.
 Lambert, D. L., Gustafsson, B., Eriksson, K., and Hinkle, K. H. (1986). *Astrophys. J. Suppl.* **62**, 373.
 Leckrone, D. S. (1980). *NASA IUE Newsl. No. 10*, p. 25.
 Little, S. J., Little-Marenin, I., Hagen, W., and Lewis, L. (1986). *Bull. Am. Astron. Soc.* **18**, 669.
 Little-Marenin, I. R., and Little, S. J. (1978). *Astron. J.* **84**, 1374.
 Little-Marenin, I. R., Little, S. J., Wing, R. F., Carpenter, K. G., and Walsterstein, G. (1980). *Bull. Am. Astron. Soc.* **12**, 827.
 McClure, R. D. (1983). *Astrophys. J.* **268**, 264.
 McClure, R. D. (1984). *Publ. Astron. Soc. Pac.* **96**, 117.
 McClure, R. D. (1985). In *Cool Stars with Excesses of Heavy Elements*, edited by M. Jaschek and P. C. Keenan (Reidel, Dordrecht), p. 215.
 McClure, R. D., Fletcher, J. M., and Nemeč, J. M. (1980). *Astrophys. J. Lett.* **238**, L35.
 Pinsonneault, M. H., Sneden, C., and Smith, V. V. (1984). *Publ. Astron. Soc. Pac.* **96**, 239.
 Schatz, G. (1983). *Astron. Astrophys.* **122**, 327.
 Schindler, M., Stencel, R. E., Basri, E., and Helfand, D. J. (1981). *Astrophys. J.* **263**, 269.
 Smith, V. V. (1984). *Astron. Astrophys.* **132**, 326.
 Smith, V. V., and Lambert, D. L. (1984). *Publ. Astron. Soc. Pac.* **96**, 326.
 Smith, V. V., Sneden, C., and Pilachowski, C. A. (1980). *Publ. Astron. Soc. Pac.* **92**, 809.
 Sneden, C., Smith, V. V., and Pilachowski, C. A. (1981). *Astrophys. J.* **247**, 1052.
 Tech, J. (1971). *Natl. Bur. Stand. Monogr. No. 119*.
 Tomkin, J., and Lambert, D. L. (1983). *Astrophys. J.* **273**, 722.
 Tomkin, J., and Lambert, D. L. (1986). *Astrophys. J.* **311**, 819.
 Turnrose, B. E., Thompson, R., and Bohlin, R. (1982). *NASA IUE Newsl. No. 18*, p. 21.
 Warner, B. (1985). *Mon. Not. R. Astron. Soc.* **129**, 263.

Appendix F

Additional Late-Type Stars with Technetium

ADDITIONAL LATE-TYPE STARS WITH TECHNETIUM

STEPHEN J. LITTLE^{a)}

Department of Natural Sciences, Bentley College, Waltham, Massachusetts 02254

IRENE R. LITTLE-MARENIN^{a), b)}

AFGL/OPC, Hanscom AFB, Massachusetts 01731

and

Whitin Observatory, Wellesley College, Wellesley, Massachusetts 02181

WENDY HAGEN BAUER^{a), b)}

Whitin Observatory, Wellesley College, Wellesley, Massachusetts 02181

Received 22 May 1987; revised 29 June 1987

ABSTRACT

We present the results of a survey of 279 late-type giants and supergiants for the spectral lines of the radioactive element technetium (Tc I) at 4297, 4262, and 4238 Å. We reach the following conclusions: (a) the presence of Tc correlates very strongly with the existence of light variability—nonvariable, low-amplitude semiregular and irregular M stars and M supergiants do not show Tc, whereas M star Mira variables tend to show Tc if $P > 300$ days; (b) evolutionary MS stars show Tc and spectroscopic MS stars do not show Tc; (c) single S stars show Tc; (d) SC stars show Tc; (e) about 75% of the C stars show Tc; (f) Ba II stars do not show Tc. Our findings are compatible with the predictions from stellar evolution theory that Tc, along with other *s*-process elements and carbon, is mixed with the surface materials after helium shell flashing episodes even though we observe Tc in stars not predicted to experience the third dredge-up. The presence of Tc is a very sensitive indicator of the third dredge-up and can be detected in the spectrum before enhancements of other *s*-process elements are measurable.

I. INTRODUCTION

Merrill (1952) first identified the resonance lines of the radioactive element technetium (Tc) in several S stars at 4297, 4262, and 4238 Å. Since then, Tc has been discovered in other evolved stars such as cool carbon stars (N stars) (Peery 1971), and MS and M stars (Little-Marenin and Little 1979 and references therein, hereafter referred to as Paper I).

The presence of Tc in the atmospheres of late-type stars is an unambiguous tracer of recent *s*-process nuclear reactions in stellar interiors. All the isotopes of Tc are radioactive, and the isotope ⁹⁹Tc has a half-life of about 2×10^5 yr. In stars, ⁹⁹Tc is assumed to be produced by the *s*-process and mixed to the surface during the late stages of stellar evolution in asymptotic giant-branch (AGB) stars (see Iben and Renzini 1983). Theoretical evolutionary models predict that the production and mixing of *s*-process elements and helium-burning products (primarily ¹²C) into the outer envelope occurs during helium shell flashing at the end of the AGB evolution of stars (a process called the third dredge-up). At the temperatures that occur in the intershell region of these stars (about $2\text{--}3 \times 10^8$ K), it has been found that the half-life of ⁹⁹Tc decreases to < 40 yr (Schatz 1983; Cosner and Truran 1981). However, Mathews *et al.* (1986) have shown that the shorter decay rates for Tc are almost completely compensated by the larger neutron fluxes that occur at the higher temperatures, leaving the Tc abundances almost un-

affected. It has also been suggested that Tc may be produced by surface nuclear reactions, most recently by Akopyan and Melik-Alaverdyan (1983), but there is little observational and theoretical support for this process.

Stars experiencing the third dredge-up should show an increasing amount of carbon and of *s*-processed elements with successive helium flashes and should evolve from M to C stars. The location of stars on the AGB of Magellanic Cloud intermediate-age globular clusters bears out the prediction that the $M \rightarrow MS \rightarrow S \rightarrow (SC) \rightarrow C$ stars form, unambiguously, an evolutionary sequence of stars evolving to higher luminosities up the AGB (Wood 1985). The SC stars are enclosed in parentheses in order to indicate that not all stars may go through the SC phase.

Abundance analyses of galactic AGB stars also show an increase in the C/O ratio and *s*-process enhancement along the $M \rightarrow C$ sequence. M giants show only marginal, if any, *s*-process enhancements (Smith and Lambert 1985); MS stars show enhancements from about a factor of 2 to about 5 (Smith and Lambert 1985, 1986); four S stars are enhanced by a factor of 3–8 (Smith and Wallerstein 1983; Smith and Lambert 1986); in four SC stars Zr and Nb are enhanced by about a factor of 5–10 with Mo and Ru showing enhancements of about 50–100 (Dominy and Wallerstein 1983); and the cool C stars show enhancements in the 10–100 range (Utsumi 1985). The C/O ratio increases from about 0.4 in M stars, to ~ 0.64 in MS stars (Smith and Lambert 1985, 1986), to ~ 0.8 in S stars (if the C/O ratio is corrected for a likely overestimate in the O abundance) (Smith and Lambert 1986), to values very close to unity in SC stars (Keenan and Boeshaar 1980; Dominy, Wallerstein, and Suntzeff 1986), and to values in C stars ranging from about 1.01 to 1.5 with more than 40% of the stars having $C/O > 1.05$ (Lambert *et al.* 1986). The early R stars apparently do not belong to this sequence. They are not luminous enough to be on the AGB and show no *s*-process enhancements (Dominy 1984). Their carbon enrichment, in order to produce $C/O > 1$,

^{a)} Visiting Astronomer, Kitt Peak National Observatory, National Optical Astronomy Observatories, which is operated by the Association of Universities for Research in Astronomy, Inc., under contract with the National Science Foundation.

^{b)} Visiting Astronomer, Cerro Tololo Inter-American Observatory, National Optical Astronomy Observatories, which is operated by the Association of Universities for Research in Astronomy, Inc., under contract with the National Science Foundation.

must have been produced during a different evolutionary phase, possibly the He core flash (Dominy 1984).

In order to define more closely the onset and continuation of the *s*-process and dredge-up phase in stars on the AGB, we have conducted a systematic search of evolved stars, primarily variable M stars, for the presence of the neutral Tc lines. Our survey contains 227 stars, which are listed in Table I along with 52 stars analyzed by other investigators. Table I includes the stars published in Paper I.

II. OBSERVATIONS AND REDUCTIONS

The spectra for the present study were obtained over the last decade, primarily with the 0.9 m feed telescope to the coude spectrograph of the 2.1 m telescope at Kitt Peak National Observatory (KPNO). A few 4 m echelle spectra were also obtained at KPNO and CTIO (Cerro Tololo Inter-American Observatory) and from the KPNO archives. The characteristics of the echelle spectra are discussed in greater detail by Hagen, Stencil, and Dickinson (1983). At the coude feed, we have used since 1981 camera 5 with a cooled RCA two-stage S-20 image tube and grating C with the small collimator. This combination gives a dispersion of about 8 Å/mm in the blue. Spectra of stars brighter than ~ 9 mag in the blue were obtained on IIIa-J plates (baked in forming gas) or, if fainter than ~ 9 mag, on baked IIa-O plates. The stars we observed were selected to be brighter than ~ 9.5 mag in the blue, which meant that, in general, variable stars were observed near maximum light. The strongest lines of Tc I lie in the 4200–4300 Å region and are difficult to observe since these red stars emit relatively little light in the blue. Since typical exposure times are 2–4 hr, we found it impractical to try to obtain higher-dispersion spectra with the coude feed. The effective resolution for camera 5 is about 0.2 Å for the IIIa-J plates and 0.25 Å for the IIa-O plates. The spectra obtained before 1978 have been described in Paper I. We traced the spectra using the PDS microdensitometer at KPNO, reduced them with a standard H-D curve derived from spot plates, and obtained intensity tracings for each spectrum. The differences in the H-D curves of plates from different batches and with different exposure times is small so that one H-D curve for the IIIa-J and one for the IIa-O plates was deemed adequate for most of the spectra for the purpose of identifying the presence of the Tc lines.

III. ANALYSIS

The resonance lines of Tc I are located at 4297.06, 4262.27, and 4238.19 Å, with intensity ratios of 5:4:3. Due to the crowding of the lines in late-type spectra, we find the spectral resolution we used to be marginal for separating weak Tc lines from the nearby blends, except for our 4 m IIIa-J echelle plates. Each of the Tc lines is near other blending features. In particular, the strongest line (4297) tends to be blended with a combination of a Ce II line, the Raic Ultimate of Sm I and a weak Zr II line. This "blend" has an average wavelength of about 4296.7 Å. Since the *s*-process elements Ce, Sm, and Zr strengthen as Tc strengthens, we tend to find the central wavelength of the 4297 line to be shifted to approximately 4296.9 Å for a roughly equal contribution to the observed feature of the Tc line and the blend. Only in a few cases is the Tc line so strong as to dominate the feature so that only a negligible shift from the 4297.06 Å position is observed. The observed wavelength minimum of the 4297 feature is listed in column 11 of Table I. In a few of the

warmer M stars we attributed a 4297.06 Å feature to Cr I (64) after checking for the other lines of the multiplet when we observed no corresponding features at the positions of the two weaker Tc lines. Despite the blending problems, we found the 4297 line to be our best indicator of Tc since the Cr I (64) line could be eliminated as a contributor relatively easily and the 4262 line is badly blended in the cooler stars. For a complete list of blending agents that affect the Tc lines, see Table III of Paper I.

Our analysis proceeded by fitting a dispersion solution through up to 30 photospheric absorption lines in the 4150–4350 Å region. This allowed us to calculate the wavelength of any feature with a typical accuracy of ± 0.05 Å. We then calculated the line centers of features near the Tc lines, checked all possible blending contributors, checked the relative intensities of all three Tc lines, and assigned a likelihood for the presence of Tc in the spectrum, which is listed in column 12 of Table I. The definitions are the same as in Paper I, as follows.

(1) **yes**. All three Tc lines are strong, in the correct intensity ratio, and a negligible shift in the central wavelength of the features is observed.

(2) **probable** (abbreviated as prob). The 4297 Tc line is blended with an approximately equally strong feature of Sm I, Ce II (and Zr II) so that the central wavelength of the observed feature is around 4296.90 ± 0.1 Å. The 4262 and 4238 lines are also blended and/or too weak to make the identification definite. In a few cases, the observed central wavelength is around 4296.7 Å, but the observed feature is distinctly asymmetric with a contributor estimated to be at ~ 4297.06 . These cases are listed in the Remarks (column 14).

(3) **possible** (poss). The Tc lines are weak and badly blended, but features are located near all three Tc lines. In our judgment the evidence favors the presence of Tc.

(4) **doubtful** (dfl). Any lines present at the Tc I positions are too weak or too badly blended to be identified with Tc even though features are present near the Tc lines. In our judgment the evidence favors the absence of Tc.

(5) **no**. No features are present that can be attributed to Tc.

Table I summarizes the results of the present survey, of Paper I, and of other investigators. The stars are listed in alphabetical order by the abbreviated name of the constellation. Column 3 gives the spectral class as listed in the fourth edition (Kholopov 1985) of the *General Catalog of Variable Stars* (GCVS) for the constellations Andromeda through Orion, and from the third edition (Kukarkin 1969) for Pegasus through Vulpecula for which the fourth edition is not yet available. The Remarks column (14) lists the spectral class from the *Bright Star Catalogue* (BSC) (Hoffleit and Jaschek 1982) if different from the GCVS. In a few cases we list other spectral classes in the Remarks if we felt they were especially relevant to our analysis. Column 4 lists the average spectral class observed at maximum (Keenan, Garrison, and Deutsch 1974). Columns 5, 6, and 7 list the variability type, the period, and the asymmetry in the light curve (defined as time of $\{(\text{maximum} - \text{minimum})/P\} \times 100$) from the GCVS, where a value of 50 indicates a symmetric light curve. Column 8 lists the radial velocity of the stars as given by Keenan, Garrison, and Deutsch (1974), Abt and Biggs (1972), Wilson (1953), Wallerstein and Fawley (1980), or Barbier-Brossat and Petit (1986). Column 9 contains coded information about H₂O, OH, and SiO stellar

TABLE I. Stars searched for technetium.

No	Name	Sp. Class(GCVS)	<Sp.Cl>	Var	P	f	Vr	Maser	Int	Wave	Tc	Ref	Remarks
(1)	(2)	(3)	(4)	(5)	(6)	(7)	(8)	(10)	(11)	(12)	(13)	(14)	(15)
1	And	S3.5e-SB.8e(M7e)	S4.6 M		409	38	-11	XXX	4.5	97.06	yes	a,m,r	
2	And	S6.1e-S9.2e/M4-M10	S8.2 M		326	42	-29	XXS	4	96.77	yes	b	
3	And	M3e-M4.5e	M3		221	48	-7	X--		96.80	no	a	=BS 5261
4	Theta	M6.5 III	SRb		119		+10						period variable
5	R	Aq1 M5e-M9e	M6.5 M		284	42	+32	HOS		96.89	dbfl	a,b	
6	R	Aq1 M6e-M9	M7 M		395	47	+17	HOS	1	96.91	poss	b	
7	T	Aq1 M6e-M8e(S)	M7 M		327	42	-41	HOS		96.75	no	b	
8	V	Aq1 M5e-M7e	M6 M		356	37	-68	HOS		96.86	no	a	
9	915	Aq1 S5.2-S7.2	Lb						>5	97.10	yes	a	
10	Aqr	M5e-M8.5e	M7 M		387	42	-22	XXS	2	97.02	prob	b	
11	Aqr	M4e-M6e	M5.5 M		279	39	-58	X-X		96.84	dbfl	a	
12	Aqr	M2e-M5.5e	M3 M		202	48	-39	X-X		97.46	no	b	
13	Aqr	M6-M8e	M M		381	42	-15	XXS	1.5	96.89	poss	a	
14	Aqr	S6.3e:(M4e-M6.5e)	M M		312	42	+10	X-X	2	96.86	prob	a,b	shows definite blend at 97.10 Ref (b) Tc=no; Sp.Cl. prob MS Period and amplitude vary
15	Ar1	M6e-M8e	M6 SRa		317	49	+7	XXS		96.71	dbfl	b	
16	Ar1	M6.5e-M9.5e	M6.5 M		458	51	+8	XXS	3	96.92	prob	a,kk	
17	Aur	M7e-M9e	M7		408	39	+15	HXS		96.83	dbfl	a,b	
18	J	Aur C5.3-C7.4(N3)	SRb		234		+12	XXX			no	p	
19	V	Aur C6.2-C8.2(Jep(Ne))	M M		394		-6	X-		97.00	yes	a	Tc strong; C star with [NeII] and [O III] emiss; Mass > 4Msol
20	X	Aur M4e-M6	M M		322	43	+24	X--		96.8	no	l	
21	J	Aur M2S1ab	Lc				+6	X-		96.77	no	a	=BS 1939, BSC: M2IIIS =BS 2289
22	psi	Aur K5-M0 Iab-Ib	Lc				+5	X-		96.69	dbfl	a	
23	B	B00 M3e-M8e	M4.5 M		223	46	-58	HXX		96.92	nc	a,b	
24	B	B00 M3e-M6e	M5.5 M		271	44	-17	XXX		96.91	dbfl	a	
25	B	B00 M6e	M5.5 SRa		256	49	-38	XXX	1.5	96.98	prob	b	
26	r	B00 M2-4III	SRb		450		+6	X-		96.82	dbfl	a	
27	v	B00 M5e-M7e	SRb		137	50	-36	XXX		96.88	dbfl	b	=BS 5490, BSC: M3III
28	v	B00 M4-4.5III	Lb:					---		96.80	dbfl	a,tt	=BS 5299, BSC: M4III
29	F	B00 M2IIIab	Lb:				-13	---		96.75	dbfl	a	=BS 5300, BSC: M1.5III
30	F	Cam S4.7e-S8.5.8e	M5.7 M		373	47	-2	X-X	(1.5)	97.06	yes	a,b	
31	z	Cam M5(S)	Lb				-52	---	2.5	96.98	prob	a	
32	D	Cam S5.3 (M4III)	Lb				-22	---		96.86	dbfl	a,h,m,p,t	=BS 1105, BSC:S3.5/2, SB, poss. WD companion. =BS B204; BSC: G4Ib; no Tc II (2600A)
33	Beta	Cap G4Ib(K0-Ba3)	NV				+3	---			no	c,w,x	
34	E	Car K5e-M6e	M0 M		149	51	286	X-		96.74	no	a	
35	D	Car M4Ib	Lc				-1	XX-		96.71	dbfl	a	
36	E	Cas M6e-M10e	M7 M		430	40	+21	HOS	1-	96.87	poss	b,l	
37	v	Cas M6e-M9.0e	M7.5 M		445	56	-12	XXS	(2.5)	96.83	prob	b	Zr-O(.93 um), prob S. ref(vt)
38	v	Cas S3.5e-S8.6e	S4.5 M		277	44	-45	X-X	3		yes	m	line asymmetric at 97.06 has a double maximum prob. blend with CrI(64)
39	v	Cas M5e-M8.5e	M5.5 M		229	48	-31	XXX	0.5	96.83	poss	b	
40	F	Cam M4e-M8Ile	M4.5 M		54f		-24	HXX			no	a	
41	F	Cam K0:e-M4Ile	K5 SRa		90	47	+28	---		96.99	dbfl	a	
42	396	Cam M4Ia-Iab-MG	Lc:					XX-		96.68	no	a	=2 Cen=BS 5192.
43	306	Cen M5III	SRb		17		+41	---		96.84	dbfl	a	Zr-O(.93 um), prob MS, ref(t)
44	v	Cep M5.5e-M8.8e	M6.5 M		368	54	-13	XXS	(1.5)	96.95	yes	b,q,kk	=BS 8383, BSC:M2Iaep+88ve =18 Cep=BS 8416, BSC:M5IIIab
45	v	Cep M7epIa-Iab +88	SRc				-19	XX-			no	a	
46	v	Cep M5 III	Lb:				-4	---		96.97	dbfl	a	
47	v	Cep M2e Ia	SRc		73c	33	+19	XXX		96.83	no	a,b	
48	F	Cet M4e-M9	M4.5 M		73c	43	+42	HOS		96.69	no	a	
49	F	Cet M5-6S IIe	SRc		15e		+9	XXX	2+	96.89	prob	b,r	
50	F	Cet M2e-M6e	M4 M		23:	44	-27	HX-		96.95	dbfl	b	
51	F	Cet S6.3e-S9.2e	M6 M		35:	51	+13	X-X	4	97.06	yes	a	
52	F	Cet M2e(S)-M6e	M3 M		17:	49	+59	X--		96.90	dbfl	a	= BS 85; BSC: M5Ile

TABLE I. (continued)

No (1)	Name (2)	Sp. Class(GCVS) (3)	<Sp.C1> Var (4)	P (5)	F (6)	Vr (7)	Maser (8)	Int (9)	Wave (10)	Tc (11)	Ref (12)	Remarks (13)
53	AR Cet	M3III										
54	Alpha Cet	M2 III										
55	omic. Cet	M5e-M9e										
56	Delta Cha	k III										
57	Alpha Cma	A1Vm										
58	Sigma CMa	K7 Ib										
59	R CMi	C7.1Je(CSep)										
60	S CMi	M6e-M8e										
61	U CMi	M4e										
62	V CMi	M4e-M10										
63	R Cnc	M6e-M9e										
64	V Cnc	S0e-S7.9e										
65	X Cnc	C5.4(N3)										
66	RR Cnc	M3e										
67	RS Cnc	M6e Ib-II(S)										
68	R Col	M3e-M7										
69	T Col	M3e-M6e										
70	R Com	M5e-M8ep										
71	S CrB	M6e-M8e										
72	W CrB	M2e-M5e										
73	X CrB	M5e-M7e										
74	Gamma Cru	M3.5 III										
75	R Crv	M4.5e-M9:e										
76	R Crv	M5.5e-M9e										
77	V Cvn	M4e-M6e IIIa:										
78	Y Cvn	C5.4J(N3)										
79	TU Cvn	M5 III										
80	Z Cvn	M1 III + F7 V										
81	R Cyg	S2.5.9e-S6.9e(Tc)										
82	U Cyg	C7.2e-C9.2(ripe)										
83	W Cyg	M4e-M6e(Tc:III)										
84	RS Cyg	C8.2e(MQpe)										
85	RT Cyg	M2e-M8.8e Ib										
86	TW Cyg	M6e-M8e										
87	TU Cyg	M6.5-M10ep										
88	AA Cyg	S7.5-S7.5.6(MpTc)										
89	AF Cyg	M5e-M7										
90	CY Cyg	C5(M2p)										
91	V460 Cyg	C6.4(N1)										
92	V973 Cyg	M3IIIIa										
93	V1351 Cyg	M5IIIIa										
94	Chi Cyg	S6.2e-S10.4e(MSe)										
95	R Del	M5e-M6e										
96	T Del	S5.2.5e-S7.2e:										
97	Z Del	M6.4III										
98	EU Del	M6.4III										
99	R Dra	M5e-M9e III										
100	UX Dra	C7.3(NO)										
101	CL Dra	M3III										
102	T Eri	M3e-M5e										
103	U Eri	M4e										
104	Z Eri	M4 III										
105	RR Eri	M5 III										
106	OV Eri	M3 III										
107	R Gem	S2.9e-S8.9e(Tc)										
108	T Gem	S1.5.5e-S9.5e										
109	V Gem	M4(S)e-M8										

TABLE I. (continued)

No (1)	Name (2)	Sp. Class(GCVS) (3)	<Sp.Cl> (4)	Var (5)	P (6)	f (7)	Vr (8)	Maser Int (10)	Int (11)	Wave (12)	Tc (13)	Ref (14)	Remarks (15)	
110	X	Gem	M5e-M8e(Tc:)		M	264	49	+35	XXS	1.5	96.90	poss	a,b	
111	TV	Gem	K5.5-M1.3Iab		SRc	182		+17	XO-		96.70	no	a	
112	BU	Gem	M1-M2 Ia-Iab		Lc			+22	-XX		96.81	no	a	
113	NZ	Gem	M3II-III		SR			-16	---		96.97	dbf1	b	
114	Eta	Gem	M3 IIIab		SRa	233	5	+19	X--		---	no	a,tt	
115	Mu	Gem	M3.0IIIab		Lb			+55	XX-		96.84	dbf1	a,t	
116	S	Gru	M8 IIIe		M	402		+2		4+	97.03	yes	a	
117	Beta	Gru	M5 III		Lc			+2			96.81	dbf1	a	
118	Del 2	Gru	M4.5 IIIa		Lb:			+2			96.78	dbf1	a	
119	Pi 1	Gru	S5.7e		SRb:	150:		-20	---	7	97.00	yes	a,s	
120	S	Her	M4.5e-M7.5 Se		M5S	M	318	47	-10	X-X	2	97.03	dbf1	a
121	T	Her	M2.5e-M8e		M4	M	165	47	-122	X-X		96.81	dbf1	b
122	U	Her	M6.5e-M9.5e		M7	M	406	40	-28	HOS		96.86	dbf1	b
123	X	Her	M6e		SRb	95		-92	XXX		96.86	dbf1	b	
124	RU	Her	M6e-M9		M7	M	485	43	-25	XXS	1+	96.95	prob	b
125	RZ	Her	M5e-M6e		M5	M	329	44	+38	X--	2	96.86	prob	a
126	ST	Her	M6-7 IIIaS		SRb	148		-29	X--	3.5	96.92	prob	a,p	
127	SV	Her	M5e		M	239	46	-32	X--		---	no	a	
128	SV	Her	M1e-M6e		M	117	49	+33	X--		96.82	dbf1	a	
129	UV	Her	M6e-M6.5e		M6	M	342	44	+0	-XX		96.85	dbf1	b
130	CF	Her	M0		M	306	46	-25	---		96.84	dbf1	a	
131	LQ	Her	M4IIIIa		Lb:			+13	---	2	97.07	prob	a,r,t	
132	Op	Her	M5 IIb-IIIa(S)		SRb	121		-33	XXX		96.85	no	b,r	
133	Alf 1	Her	M5 Ib-II		SRc			-10	---		96.85	no	a	
134	2	Her	M3 III 8a 0.3		NV?			+3	XXX		96.75	no	b, f, r, tt	
135	9	Her	M6 III		SRb	89		+60	HOS	5	97.05	yes	a	
136	R	Her	M5e-M8e II-III		M6.5	M	408	49	-10	HOS	1.5	96.92	prob	a,b, l, m, r
137	R	Hya	M6e-M9e S (Tc)		M4	M	299	49	-3	XXX	1	97.00	prob	a
138	T	Hya	M3e-M9e		SRb	450:		-25	X-X		96.89	prob	b	
139	U	Hya	C6.5.3(K2)(Tc)		SRa	361	50	+42	HOS	2	96.89	dbf1	a	
140	W	Hya	M7.5e-M9ep		M	301	42	+42	HOS		96.89	yes	a	
141	X	Hya	M7e-M8.5e		M	343	50	+33	X--	4	97.06	yes	a	
142	RR	Hya	M3.0e-M8e		SRb	290	46	+40	XX-	(1.5)	97.06	prob	b	
143	RT	Hya	M6e-M8e		M6.5	M	332	35	+2	HOS	0.5	96.84	poss	a
144	RU	Hya	M6e-M8.8e		SRb	320:		+2		4	97.06	yes	a	
145	T	Ind	C7.2		M5.5	M	242	46	-61	X-X		96.66	no	b
146	S	Lac	M4e-M8.2e		M7	M	310	43	+13	HOS		96.81	dbf1	b, l, m, r
147	R	Leo	M6e-M9.5 IIIe		SRb			-20	X--		96.87	dbf1	a,t	
148	DE	Leo	M2IIIabS											
149	T	Lep	M6e-M9e		M	368	47	-18	HXS		96.75	dbf1	a	
150	RX	Lep	M6.2III		SRb	60:		+46	XX-		96.87	dbf1	a	
151	RR	Lfb	M4e-M8e		M4	M	277	47	-33	X--		96.81	no	b
152	RS	Lfb	M7e-M8.5e		M7	M	218	48	+9	XXS		96.83	dbf1	b
153	RT	Lfb	M2.5pe-M8.2e		M4	M	251	45	+41	-X-		---	dbf1	b
154	Sigma	Lfb	M3.5 IIIa		SRb			-4	X-X		96.88	dbf1	a,b	
155	R	LMi	M6.5e-M9.0e(Tc:)		M7	M	372	41	+10	HOS	1	96.81	poss	b
156	S	LMi	M2.0e-M8.2e		M5	M	234	42	-2	HX-		97.00	dbf1	a
157	S	Lup	Se		M	340		-41		>5	97.04	yes	a	
158	V	Lyn	M6SIIb-III		SRc	110		+7	XX-	3	96.90	prob	a	
159	R	Lyr	M5 III		SRb	46:		-28	XOX		96.90	dbf1	a,b,i	
160	V	Lyr	M7e		M	374	33	-22	XOX	1	96.93	poss	b	
161	XV	Lyr	M4-5 Ib-II		Lc			-19	XX-		62.43	no	a,r	
162	Alpha	Lyr	A0 Va		Lc			-14	---			no	e	
163	Del 2	Lyr	M4II		SRc			-26	X--		97.08	dbf1	a	
164	T	Mic	M6e		SRb	347		+18	XXX		96.81	poss	a,b	
165	V	Mon	M5e-M8e		M	341	46	+24	XXS	3.5	96.96	prob	a	
166	X	Mon	M1eII-III-M6ep		M3	SRa	156	51	+162	X-X		96.75	dbf1	a
167	U	Oct	M4e-M6 II-IIIe		M	308					96.69	no	a	

TABLE I. (continued)

No (1)	Name (2)	Sp. Class(GCVS) (3)	<Sp.Cl> Var (4)	P (5)	f (6)	Vr (7)	Maser (8)	Int (9)	Wave (10)	Tc (11)	Ref (12)	Remarks (13)
168	R	Cph	M5	M	307	45	-47	XXS	96.76	no	a,b	p variable
169	X	Oph	M6.5	M	329	53	-71	HXS	96.86	poss	a,b	=BS 7002, BSC: (K1III+M6IIe) BSC: Mass=15.9Mo+5 Mo, but typical K III star has Mass about 1 Mo
170	Z	Oph	K3p	M	349	40	-78	-XX	96.86	dbfl	b	
171	RR	Oph	M3e	M	292	46	+60	X--	97.25	dbfl	a	
172	RY	Oph	M3e	M	150	46	-56	XX	96.95	no	a	
173	S	Or1	M6.5e	M	414	48	+22	XXS	96.94	dbfl	a	
174	U	Or1	M6e	M	368	38	-21	HOS	97.02	poss	a	=BS 2063, BSC:M6.5IIe, Tc wk feature in wing of str. line at 4296.70
175	BL	Or1	C6.3(Nb,Tc)	Lb			+13	---		yes	p	
176	A1f	Or1	M1-M2Ia-Ibe	SRC	2335		+21	XXX	96.79	no	a	=BS 2061, BSC: M1-2Ia-Iab
177	o 1	Or1	M3.2IIaIaS	SRb	30:		-8	---	96.99	prob	a,b,t, kk	=BS 1556, BSC: S3.5/1-, also S4ZrIIa WD companion
178	S	Peg	M5e-M8e	M	319	47	+3	XXX	96.90	dbfl	a	
179	T	Peg	M6e-M7e	M	374	49	-24	XX-	96.97	prob	a	
180	X	Peg	M2e-M5e	M	201	49	-56	X--	62.39	no	a	no 4297 section
181	Z	Peg	M6e-M8e	M	325	50	-31	XX-	97.06	yes	b	
182	RV	Peg	M6e	M	389	38	-46	XOS	96.92	poss	a	
183	RZ	Peg	C9e:CS	M	439	44	-27	---		yes	o	
184	SW	Peg	M4e	M	396		-X-	---	96.92	prob	a	
185	TU	Peg	M7e-M8e	M	322		+9	HXS	96.86	dbfl	a	
186	TW	Peg	M6-M7	SR	956		-27	HOX	96.77	dbfl	a	
187	GZ	Peg	M4IIIS + A2V	Lb?			+14	X--	97.07	dbfl	a	Small oscil. with P of 90d on P of 956d
188	HR	Peg	S4+/1+		50:		+11	X--	96.96	prob	b,p,t	=BS 8714, Ref(P):Tc=no
189	Beta	Peg	M2.5II-III	Lb			+9	---	96.80	no	b,h,i,tt	=BS 8775, Sp.Cl from BSC
190	U	Per	M6e-M7e	M	321	46	+19	XXX	96.98	prob	b,h	
191	RR	Per	M6e-M7e	M	390	45	+9	XOX	96.85	poss	a	
192	SU	Per	M3.5 Iab	SRC	470		-39	XXX	96.85	dbfl	a	
193	AD	Per	M2-M3Iab	SRC	320		-45	-X-	97.03	dbfl	a	
194	FZ	Per	M1VIab	Lc	184		-48	-X-	96.74	dbfl	a	
195	KK	Per	M1.0-M3.5Ib	Lc			-42	-X-	96.78	dbfl	a	
196	PR	Per	K5eIb-M2Ib	Lc			-39	---	96.81	dbfl	a	
197	Rho	Per	M4 I Ib-IIIa	SRb	50:		+28	XXX	96.74	dbfl	b,pp,t	=BS 921, BSC:M4II, asym. at 97.03 prob. Cr I(64)
198	R	Psc	M3e-M6e	M	344	44	-48	XX-	96.86	prob	a	
199	TV	Psc	M3 III	SR	49	49	+6	XXX	96.91	dbfl	b	=BS 103, BSC:M3IIIv, Hyades group
200	TX	Psc	C6.2(N0)	Lb			+11	X-X	2-3	yes	p	=19 Psc=BS 9004, BSC: C5 II
201	Z	Pup	M4e-M9e	M	510	38	+26	HOS	96.87	dbfl	a	
202	KQ	Pup	M2eIab +B2V	M			+22	-X-	96.77	dbfl	a	=BS 2902, VV Cep or symbiotic, shell spectrum
203	L 2	Pup	M5e-M6e	SRb	140	40	+53	HOS		prob	a	=BS 2748, BSC: M5IIe
204	S	Sc1	M3e-M8e	M	365	48	+35	HXX	96.83	prob	b,g	
205	RR	Sc0	M6II-IIIe-M8IIe	M	280	47	-36	XXS	96.79	no	a,b	
206	RZ	Sc0	M3e-M4e	M	160	45	-174	H--	---	no	a	
207	AH	Sc0	M5Ia-Iab	SRa	714	46	-14	HOS	96.97	dbfl	b	Sp. Cl. from Humphreys and Ney(1974)
208	A1f	Sc0	M1.5Iab-Ib + B4Ve	SRa	1733		-3	-XX	96.87	dbfl	b	=BS 6134, Sp. Cl. from BSC
209	R	Ser	M5e-M9e	M	356	41	+24	HXS	97.02	yes	a,b,i	=BS 5894, BSC: M7IIe prob ZrO (.93 um), ref (vv)
210	U	Ser	M4e-M6e	M	238	47	-31	-X-	96.89	poss	a,b	=47 Ser=BS 6010; amp =0.04V
211	FS	Ser	M3.5IIa	Lb			-22	---	96.83	dbfl	a	
212	Tau 4	Ser	M5 I Ib-IIIa	Lb			+4	X-X	96.82	dbfl	a,r	
213	16	Ser	K1-Ba1	NV			+8	---		no	x	=BS 5802, BSC: K0III:CNIBa0.7Sr2
214	Delta	Sge	M2 II + A0 V	var			+3	---	96.74	no	a	=BS 7536, S80
215	R	Sgr	M4e-M6e	M	269	46	-45	XXX	96.82	no	b	
216	T	Sgr	S4.5.8e-S5.5.8e	M	392	47	+3	-X	3	yes	m	
217	Z	Sgr	M4e-M5(Se)	M	450	47	-21	XXX	96.96	prob	a	
218	RR	Sgr	M5e-M6e	M	334	43	+85	HOS	97.01	prob	a	
219	RT	Sgr	M5e-M7e	M	305	47	+35	XX-	96.84	dbfl	a	misprinted as Vr=-21 (Ap.J. Supp., 28, 271)
220	RV	Sgr	M5e	M	318	47	+24	XX-	97.02	yes	a,b	

TABLE I. (continued)

NO (1)	Name (2)	Sp. Class(GCVS) (3)	<Sp.Cl> (4)	Var (5)	P (6)	f (7)	Vr (8)	Maser (10)	Int (11)	Wave (12)	Tc (13)	Ref (14)	Remarks (15)
221	RX	Sgr M5e		M	334	49	-37	---	2	97.05	yes	a	
222	SZ	Sgr C5.2		SRb	100?		-34			97.06	prob	a	
223	TV	Sgr M3e		M	326	44		---	2	97.03	prob	a	
224	VX	Sgr M4e Ia-M8		SRb	732	44	0	HOS		---	dbfl	a	Sp. Cl. from Humphreys (1974)
225	R	Tau M5e-M9e	M6	M	324	41	+32	HOS	2	96.96	prob	a,b	
226	CE	Tau M2Ib		SRc	165		+23	XXX		96.71	dbfl	a	=119 Tau= BS 1845, BSC: M2Iab-Ib
227	X	TrA C5.5		Lb			-4			96.96	prob	a	=BS 5644
228	R	TrI M3e-M8.5e	M4	M	266	44	+67	HX5		96.80	no	b, l, kk	Maehara (1971), Tc=yes
229	V1 47	Tuc M4e		M	212		-8			96.92	no	a	Vr=-17 emission
230	BQ	Tuc M4 III		Lb?			-10	---		96.80	no	a	=BS 257
231	Nu	Tuc Me III		var			-3			96.80	no	a	=BS 8582
232	S	UMA S0.5.9e-S5.9e		50.5 M	226	47	+8	--X	1		yes	m, u	
233	T	UMA M4e-M7e	M4	M	257	41	-91	HXX		96.82	no	b, l	Maehara (1971): Tc=yes
234	Z	UMA M5e III		SRb	196		-53	XXX		---	no	r	
235	RR	UMA M4e		M	231	43:	-49	X--		---	no	a	
236	RV	UMA M2-3e III		SRa	311		-12	---		---	no	r	
237	VY	UMA C5.3(NO)		Lb			-5	X--		96.83	yes	p, kk	=BS 4195, BSC: C5II
238	B3	UMA M2IIiab Ba 0.7:		NV?			-17	---		96.82	no	a	
239	S	UMi M7e-M9e	M7	M	326	50	-40	XXS		96.81	dbfl	b	
240	RR	UMi M5III		SR?	40?		+7	X--		96.67	no	a	=BS 5589, Hyades group
241	Lam	Vel K4 Ib-II		Lc			+18	---		---	no	a	
242	R	Vir M3.5e-M8.5e		M4.5 M	146	50	-26	XXX		96.79	no	b	
243	S	Vir M6e-M9.5e	M6.5 M	M	377	45	+10	HXS	1.5	97.01	prob	b	
244	U	Vir M2e-M5.5e	M3.5 M	M	207	47	-6	XXX		96.8	dbfl	a	
245	RS	Vir M6e-M7e		M	353	37	-26	HOS		96.64	no	b	
246	SS	Vir Ne(C5.3e)		M	355	48	+4	X--		96.86	dbfl	a	
247	ET	Vir M2III-IIIa		SRb	80		+18	---		96.86	dbfl	a	=BS 5301, GCVS:gm3
248	R	Vul M3e-M7e	M4	M	136	49	-12	X--		96.80	no	b	
249	BS	363 S3+/2-		NV?			+2	---		96.80	no	a, b, cc, p, t	BSC: S3ZrTi13; SB
250	BS	774 G8-Ba3		NV			+18			96.81	no	v	BSC: G8p Ba.
251	BS	2508 M1 Ib-IIa		NV?			+24	---		96.81	dbfl	a	
252	BS	3842 K0-Ba1		NV			+3	---			no	x	BSC: G8II
253	BS	5058 K1-Ba3		NV			+67	---			no	x	BSC: K0.5III:Ba3; no TcII(2600A)
254	BS	7442 M4.5IIIIaS		Var			-10	---		96.83	dbfl	a, t	
255	BS	8062 S4/1		NV			+1	---			yes	t	
256	HD	26 G8-Ba3p		NV			-211	---			no	x	
257	HD	16458 G8-Ba3		NV			+18	---			no	x	
258	HD	31487 K0-Ba2		NV				---			no	x	
259	HD	35155 S4.1		NV			+75	---			no	p	poss underluminous companion
260	HD	44986 K4-Ba8		NV			+51	---			no	v	
261	HD	46407 K0-Ba3		NV			-14	---			no	f, x	
262	HD	60197 K2IV-Ba4		NV			+51	---			no	v	
263	HD	77247 G8-Ba2		NV				---			no	x	
264	HD	84678 K2-Ba4		NV				---			no	x	
265	HD	92626 K0-Ba5		NV			+11	---			no	x	
266	HD	100503 M1-Ba9		NV			-4	---			no	v	
267	HD	101013 K1-Ba3		NV			-4	---			no	x	
268	HD	121447 K7-Ba5		NV			-14	---			no	v, x	
269	HD	165774 S4.6		NV				---		96.74	no	a	
270	HD	175674 K5-Ba1		NV			+9	---			no	x	
271	HD	176021 CH-subgiant		NV			+115	---			no	d	
272	HD	178717 K3II-Ba5		NV			+13	---			no	u, v, x	
273	HD	183915 K1-Ba2		NV			-45	---			no	b	
274	HD	191226 M2III		NV			-24	---			no	x	
275	HD	196673 K0-Ba2		NV			-27	---		96.81	no	x	SB, Sp.Cl. Mikami (1978)
276	HD	199394 G8-Ba1		NV			0	---			no	x	
277	HD	199939 K0-Ba4		NV			-33	---			no	x	
278	HD	211594 G8-Ba3p		NV			-7	---			no	x	
279	CPD-64 4333	K0-Ba7.5		NV			+23	---			no	v	

Notes to TABLE I—Key to the references

- | | | | |
|-------------------------------------|--------------------------------------|----------------------------------|------------------|
| a) present study | i) Dominy and Wallerstein (1986) | q) Sanner (1977) | x) Warner (1965) |
| b) Little-Marenin and Little (1979) | k) Hackos (1974) | r) Sanner (1978) | |
| c) Boesgaard and Fesen (1974) | kk) Kipper and Kipper (1984) | s) Scalo (private communication) | |
| cc) Boesgaard (1969) | l) Maehara (1971) | tt) Smith and Lambert (1985) | |
| d) Bond (1974) | m) Merrill (1952) | t) Smith and Lambert (1986) | |
| e) Boyarchuk and Snow (1978) | n) Merrill (1956) | u) Smith and Wallerstein (1983) | |
| f) Burbidge and Burbidge (1957) | o) Peery, Keenan, and Marenin (1971) | v) Smith (1984) | |
| g) Cohen (1973) | p) Peery (1971) | vv) Spinrad and Newburn (1965) | |
| h) Davis (1968) | pp) Peery (1985) | vt) Spinrad et al. (1966) | |
| | | w) Tech (1971) | |

abundance analyses available for the stars listed under reference i, kk, t, tt, u, v

masers found in the literature. A number of our stars were searched for H₂O emission by Benson *et al.* (1987). A positive detection of a maser is indicated as H (first position) for water, O (second position) for OH, and S (third position) for SiO. A dash (—) in the appropriate position means the star has not been searched, and X indicates that the star has been searched but has not been detected. A positive detection is listed in preference to a negative result if both cases are found in the literature. Column 10 lists our estimate of the depth of the 4297 line relative to the local continuum on a scale of 1 to 10. This is a very crude estimate of the intensity and should be interpreted with caution. Estimates in parentheses are from density tracings and do not have the same quality as those from intensity tracings. Column 11 gives the central wavelength of the observed 4297 feature. For XY Lyr and X Peg we list the wavelength of the 4262 feature as measured on 4 m archival echelle plates since the 4297 Å line was off the end of the order. Column 12 gives the likelihood for the presence of Tc. Column 13 gives references to Tc searches: (a) refers to stars analyzed for the present study, (b) to Paper I. Other references are keyed to a list at the end of the table. In the Remarks (column 14) we give the BS number (Hoffleit and Jaschek 1982) and the spectral class if different from the GCVS and other comments; SB indicates a spectroscopic binary and VB a visual binary as listed in the BSC. Since the variable star designation for a number of low-amplitude variables is not yet well established in the literature, we have listed in Table II all the stars with BS numbers and their corresponding variable star names.

IV. DISCUSSION

Table I lists the 279 stars that have been searched for Tc. The Ba II stars (25) show *s*-process enhancements that appear to be derived from the binary nature of the stars (McClure 1984). No Tc I lines have been detected in any Ba II star. However, Tc is expected to be primarily ionized in these higher-temperature stars. A search for the resonance lines of Tc II (2647, 2610, and 2543 Å) in ζ Cap, o Vir, and BS 5058 in *IUE* (*International Ultraviolet Explorer* satellite) spectra has also proved negative (Little-Marenin and Little 1987), implying that the *s*-process episode producing the observed enhancements occurred more than 10⁶ yr ago, most likely by mass transfer from a companion. A subgiant, two A stars, and three K stars are excluded from the rest of the discussion since they do not show Tc lines and are not AGB stars. The remaining stars include 190 M stars (108 are Mira variables), 17 MS stars (five Miras), 24 S stars (15 Miras), three SC stars (two Miras), and 16 C stars (five Miras). We reach the following 12 general conclusions (exceptions will be discussed in subsec c).

a) General Conclusions

1) M stars

- (1) Nonvariable (NV) M stars do not show Tc.
- (2) M supergiants do not show Tc.
- (3) Irregular variable (Lb) M giants do not show Tc. In general, these are low-amplitude variables (mean Δ*m* ~ 0.2 mag).
- (4) M star Mira variables tend to show the Tc I lines if their period is longer than 300 days. This confirms the main conclusion of Paper I. Subsection b contains a longer discussion of the Mira variables and the exceptions.
- (5) The semiregular (SRb) M giants do not show Tc if

TABLE II. Cross reference between BS numbers and variable star names.

BS	Star name
85	T Cet
103	TV Psc
257	BQ Tuc
587	AR Cet
681	o Cet
868	R Hor
911	α Cet
921	ρ Per
1105	BD Cam
1451	DV Eri = 47 Eri
1556	o ¹ Ori
1693	RX Leo
1845	CE Tau = 119 Tau
1939	NO Aur
2061	α Ori
2063	U Ori
2190	TV Gem
2197	BV Gem
2216	η Gem
2286	μ Gem
2289	ψ ¹ Aur
2646	σ CMa
2748	L ² Pup
2902	KQ Pup
2967	NZ Gem
3541	X Cnc
3639	RS Cnc
3882	R Leo
4088	DE Leo = 44 Leo
4195	VY UMa
4231	δ Cha
4666	2 CVn
4763	γ Cru
5080	R Hya
5192	V806 Cen = 2 Cen
5226	CU Dra = 10 Dra
5261	θ Aps
5299	BY Boo
5300	CF Boo
5301	ET Vir
5490	W Boo
5589	RR UMi
5603	σ Lib
5644	X TrA
5802	16 Ser
5894	R Ser
5932	2 Her
6010	τ ⁴ Ser = 47 Ser
6039	LQ Her = 10 Her
6134	α Sco
6146	g Her = 30 Her
6406	α ² Her
6702	OP Her
7001	α Lyr
7002	X Oph
7009	XY Lyr
7139	δ ² Lyr
7157	R Lyr
7509	V1351 Cyg
7523	V973 Cyg
7536	δ Sge
7564	χ Cyg
7886	EU Del
8145	T Ind
8204	ζ Cap
8262	W Cyg
8292	V460 Cyg
8383	VV Cep
8416	MO Cep = 18 Cep
8521	π ¹ Gru
8560	δ ² Gru
8562	NU Tuc
8636	β Gru
8714	HR Peg
8775	β Peg
8815	GZ Peg = 57 Peg
9004	TX Psc = 19 Psc

$P < 100$ days or $P > 150$ days (except for TU CVn—50 days, RT Hya—290 days, and T Mic—347 days). Only seven SRA's have been observed. In general the longer-period SRA's show Tc and the shorter-period ones do not (see Fig. 3). SRC variables are estimated to be supergiants and do not show Tc (see discussion on MS supergiants in subsec c).

(6) M stars with Tc have spectral types later than M2.

2) MS stars

(7) Evolutionary MS stars, as defined in subsec c, show Tc.

(8) Spectroscopic MS stars, as defined in subsec c, do not show Tc.

3) S stars

(9) Single S stars show Tc (usually quite strongly). The five stars, BS 363, HD 35155, HD 165774, BD Cam (BS 1105) and V Cnc, that do not show Tc are discussed in subsec c.

4) SC stars

(10) The three SC stars listed in Table I show the resonance lines of Tc. Table I does not include the two SC stars FU Mon and GP Ori, which do not show the Tc I intercombination line at 5924 Å (Dominy and Wallerstein 1986). This line is much weaker than the resonance lines we observed, and its absence does not preclude the presence of the resonance lines. Clearly, more SC stars should be searched for the Tc I resonance lines in order to establish whether all SC stars show the Tc I lines. We are not making a distinction between SC and CS stars in this paper.

5) C stars

(11) Twelve out of the 16 C stars (75%) show Tc. All four Lb C stars show Tc. The C star Lb's have larger amplitudes ($\Delta m \sim 1$ mag) than the M star Lb's mentioned in (3). The four C stars, SS Vir, UU Aur, X Cnc, and Y CVn, that do not show Tc are discussed in subsec c.

6) Masers

(12) Maser emission from H₂O, OH, and SiO shows no correlation with the presence of Tc.

b) The M Star Miras and Semiregular Variables

The main conclusion reached from this analysis is that the onset of the third dredge-up occurs in M stars on the AGB (as predicted by theory) and is accompanied by the onset and the continuation of variability. Nonvariable stars do not show Tc (with the exception of the S star BS 8062 (S4,1)); even the small-amplitude irregular (Lb, Lc) variables do not show Tc. For Miras the third dredge-up appears to correlate very strongly with period (Fig. 1).

In Figs. 1(b) and (c) we plot histograms of the Miras listed as having Tc-no or Tc-doubtful (b) and those with Tc-yes, Tc-probable, and Tc-possible (c). The periods are binned in 15 day intervals. Usually, only Miras with $P > \sim 300$ days show Tc (Fig. 1(c)). There are three exceptions: V Cas—229 days, U Ser—238 days and X Gem—264 days (Fig. 1(c)). However, all three are listed as Tc-possible, meaning that their Tc lines tended to be weak and blended. We will assume for the rest of the discussion that $P > 300$ days is the most realistic division for Miras with Tc.

The onset of the detectability of s-process products on the surface appears to be quite sharp, and the percent of stars

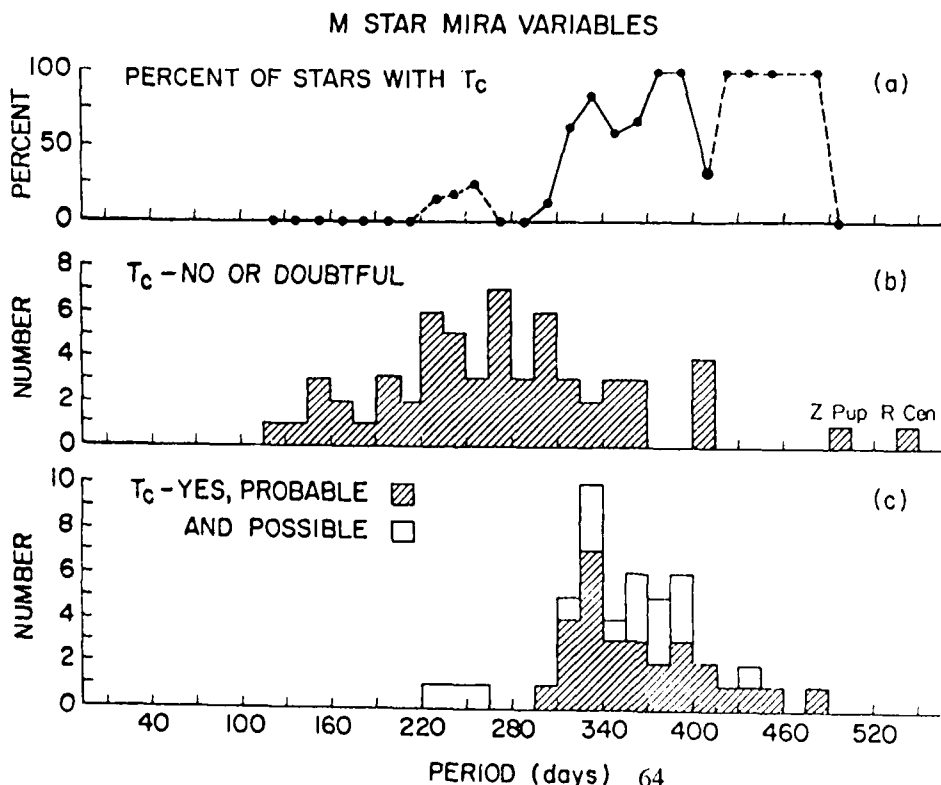


FIG. 1. Histogram of the M Mira variables versus period binned in 15 day intervals. The bottom panel (c) shows the stars with Tc present (Tc-yes or probably present) indicated as hatched areas and stars with Tc possibly present indicated as open areas. The middle panel (b) shows the stars with Tc-no or -doubtful. The top panel (a) plots the percent of stars with Tc. As can be seen, stars with Tc in general have $P > 300$ days.

with Tc rises rapidly for stars with $P > 300$ days, reaching 100% for Miras with periods between 370 and 400 days (Fig. 1(a)). We have been able to observe only 13 Miras with $P > 400$ days. Even though the statistics are poor, the trends are suggestive. Four out of the six stars with $400 < P < 415$ days (U CMi—414 days, S Ori—414 days, U Aur—408 days, U Her—406 days) *do not have* Tc, whereas the five stars with $415 < P < 490$ days (RU Her—485 days, R Aur—458 days, T Cas—445 days, R Cas—420 days, Z Sgr—420 days) *do show* Tc. The two stars with $P > 500$ days (R Cen—546 days, Z Pup—510 days) *do not show* Tc. R Cen, with alternating deep and shallow minima, may actually have a period of ~ 275 days as suggested previously. However, the light curve for Z Pup shows no such double structure (American Association of Variable Star Observers (AAVSO) 1983). If the true period of both stars were half their published value, then the lack of Tc would agree with the other stars we observed in the 260–280 day period range.

Miras form a fairly well-defined group. Kinematic studies of Miras have shown that the shorter-period Miras ($P \sim 150$ –200 days) tend to be old (Pop. II), low-mass objects with masses around $1 M_{\odot}$, whereas the longer-period Miras ($P \sim 300$ –400 days) are somewhat younger (intermediate Pop. I) with masses between 1.5 and $2.5 M_{\odot}$ (Feast 1963; Clayton and Feast 1969). The kinematic studies of C stars by Dean (1974) show that most C stars have F5 main-sequence progenitors with masses around $1.2 M_{\odot}$. This agrees with the kinematic studies of the Pop. I Miras since M type AGB stars are predicted to develop into C stars.

In a given globular cluster, Miras tend to have a very limited range of periods, and the mean period increases with metallicity. This implies that Pop. II Miras of a given period form a homogeneous set of mass, age, and composition (Feast 1980). Not enough data are available about the Pop. I Miras to establish whether these stars also form a homogeneous set for a given period. The fact that both R Hya ($P = 388$ days Tc-yes) and RR Sco ($P = 280$ days, Tc-no) probably belong to the Hyades Supercluster (i.e., relatively young), and R Leo ($P = 312$ days, Tc-dbf) and S Scl ($P = 366$ days, Tc-prob) are assigned to the old-disk moving groups Wolf 630 and 61 Cyg, respectively (Eggen 1970, 1975), argues against the same-age Pop. I stars having similar characteristics. Our data seem to indicate that Tc (and other *s*-process elements) is mixed with the outer layers, presumably during the third dredge-up in the 1.5 – $2.5 M_{\odot}$ Pop. I stars and not in older, lower-mass objects. The lack of Tc in V1 (47 Tuc) lends support to this conclusion. Our data do show that mixing occurs in higher-mass stars. For example, the carbon star UV Aur (Tc-yes) has a B8.5 V companion and hence should have a mass $> 4 M_{\odot}$. However, very few stars have individually determined masses.

Miras define a period-luminosity (P - L) relationship that is given by Glass and Lloyd Evans (1981) for the LMC Miras as

$$M_{\text{bol}} = 0.56 - 2.09 \log P.$$

Using the slope of their LMC P - L relation, Glass and Lloyd Evans fit the galactic Mira data of Robertson and Feast (1981) with

$$M_{\text{bol}} = 0.76 (\pm 0.11) - 2.09 \log P.$$

There is a difference of 0.2 mag between the two P - L relationships which may be related to differences in metallicity between the LMC and the Milky Way and/or to uncertainties in the distance modulus of the LMC (Feast 1984). Using

the galactic P - L relationship implies that Miras with observed Tc lines (i.e., P between 300 and 500 days) should have M_{bol} between -4.4 and -4.9 . Hence our data seem to indicate that stars showing Tc I are Pop. I stars ($Z = 0.01$ – 0.02) that have experienced the third dredge-up with masses in the 1.5 – $2.5 M_{\odot}$ range and luminosities in the 5 – $6 \times 10^3 L_{\odot}$ range. Current evolutionary models do not predict the third dredge-up in this mass, luminosity, and metallicity range (Iben 1983; Iben and Renzini 1983; Lattanzio 1986, 1987).

The Mira sequence can be extended to longer-period (500–1500 days) objects by including the Type II OH/IR sources. Since the mass-loss rates also increase towards the longer period, we find that these objects are heavily enshrouded in dust shells. The Type II OH/IR sources are strongly concentrated towards the galactic plane, and their masses are estimated to be $> 4 M_{\odot}$. Theory predicts that they should be experiencing the third dredge-up. Unfortunately, the thick dust shells make it impossible to observe these stars for Tc. In general, we were able to observe only stars with optically thin dust shells, as estimated from *IRAS* low-resolution spectra and *IRAS* point-source fluxes for the stars in Table I. We find no correlation between the strength of the $10 \mu\text{m}$ silicate emission observed in the *IRAS* low-resolution spectra and the presence of Tc. With a few exceptions, such as R Cet, we were able to obtain spectra only of stars with relatively weak emission features in the 8 – $22 \mu\text{m}$ region, i.e., from optically thin shells.

Theory predicts that ^{12}C is brought to the surface during the third dredge-up with an accompanying increase in the $^{12}\text{C}/^{13}\text{C}$ ratio. Comparing our Tc data for Mira variables with the $^{12}\text{C}/^{13}\text{C}$ ratios determined from the second overtone of CO (Hinkle, unpublished), we find that $^{12}\text{C}/^{13}\text{C} \sim 8$ for the Miras with Tc-doubtful or Tc-no (only three stars), ~ 13 for the Miras with Tc-yes, Tc-probable, or Tc-possible (12 stars), ~ 33 for four MS Miras and ~ 55 for two S Miras. We included T Cas, T Cep, and χ Cyg among the MS stars (see discussion in subsec c). The difference in the $^{12}\text{C}/^{13}\text{C}$ ratio between the M Miras with and without Tc is small, but appears to be real (Fig. 2). Smith and Lambert (1985, 1986) found a similar trend in the $^{12}\text{C}/^{13}\text{C}$ ratio for their non-Mira M, MS, and S stars. However, their average ratio for the M stars with no *s*-process enhancements is about 14, similar to the value Hinkle obtains for the M Miras with Tc. More $^{12}\text{C}/^{13}\text{C}$ ratios for Miras without Tc would be very useful. An exception to the trend in the $^{12}\text{C}/^{13}\text{C}$ ratios is S Ori, a 414 day M star Mira with Tc-doubtful and a $^{12}\text{C}/^{13}\text{C}$ ratio of 40, typical of the MS stars.

The intensity of the 4297 \AA Tc line does not correlate with period. Neither does the presence of Tc correlate with the asymmetry in the light curve (listed in Table I, column 7). Vardya (1985) suggests that the asymmetry is a measure of the strength of the shock and that the intensity of the 4297 \AA line as listed in Paper I (marginally) correlates with the light-curve asymmetry for S stars. If the shock strength is related to thermal shell flashing, one might expect that Tc is more likely to be observed in stars with a more asymmetric light curve. However, the marginal correlation disappears with the addition of a few new S stars. For example, T Gem has a symmetric light curve ($f = 50$) and an intensity 4 Tc I line.

Figure 3 shows the distribution of the semiregular variables with known periods as a function of Tc. Two out of the three M star SRb's with periods between 130 and 141 days

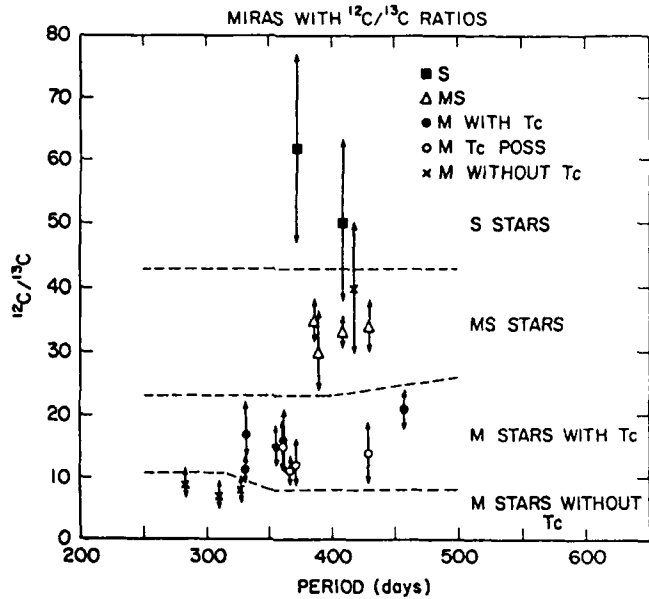


FIG. 2. The $^{12}\text{C}/^{13}\text{C}$ ratio (Hinkle, private communication) of M stars without Tc (crosses), M stars with Tc-probable and Tc-yes (dark circles), M stars with Tc-possible (light circles), MS stars (triangles), and S stars (squares).

show Tc (Fig. 3(b)). These two may be stars equivalent to Miras but pulsating in the first overtone rather than in the fundamental mode (Willson 1982). As can be seen in Fig. 3(b), the semiregular MS stars with Tc are also located in this region of the histogram and are also likely to be first-overtone pulsators. Two long-period SRb stars (RT Hya—

290 days; T Mic—347 days) show Tc and may be related to the Miras, i.e., pulsating in the fundamental mode. However, the light curve of RT Hya shows the small amplitude variations typical of the semiregular variables (AAVSO 1983) and hence it is not a misclassified Mira. No light curve of T Mic has been published by the AAVSO.

c) Exceptions

1) MS stars

Among the 17 MS stars listed in Table I, we were surprised to find seven that do not show the Tc lines: RT Aql (M—327 days); X Cet (M—177 days); DE (44) Leo (SRb— $P = ?$); NZ Gem (BS 2967) (SR— $P = ?$); GZ (57) Peg (Lb); NO Aur (Lc); and BS 7442 (var?). Smith and Lambert (1985, 1986) determined abundances for nine out of the 11 MS stars listed by Yamashita (1967) and found that four (DE Leo, BS 7442, CU (10) Dra, and BS 2508) showed no enhancements of the s-process elements whereas the five others did (RS Cnc, HR Her, OP Her, σ^1 Ori, and BS 8062). (CU Dra and BS 2508, although classified as M3 IIIaS by Yamashita (1967), are not included among our 17 MS stars since they are not listed with an MS classification in either the GCVS or BSC.)

MS stars were originally defined by Keenan (1954) as stars that show weak ZrO bands and enhanced lines of Ba II and Sr II in the blue spectral region. It appears to us that the MS stars should be divided into two classes which we shall call *evolutionary* MS stars and *spectroscopic* MS stars. We define *evolutionary* MS stars as those stars in the intermediate evolutionary phase between the M and the S stars. These *evolutionary* MS stars show the same spectroscopic characteristics as the MS stars defined by Keenan, but in addition

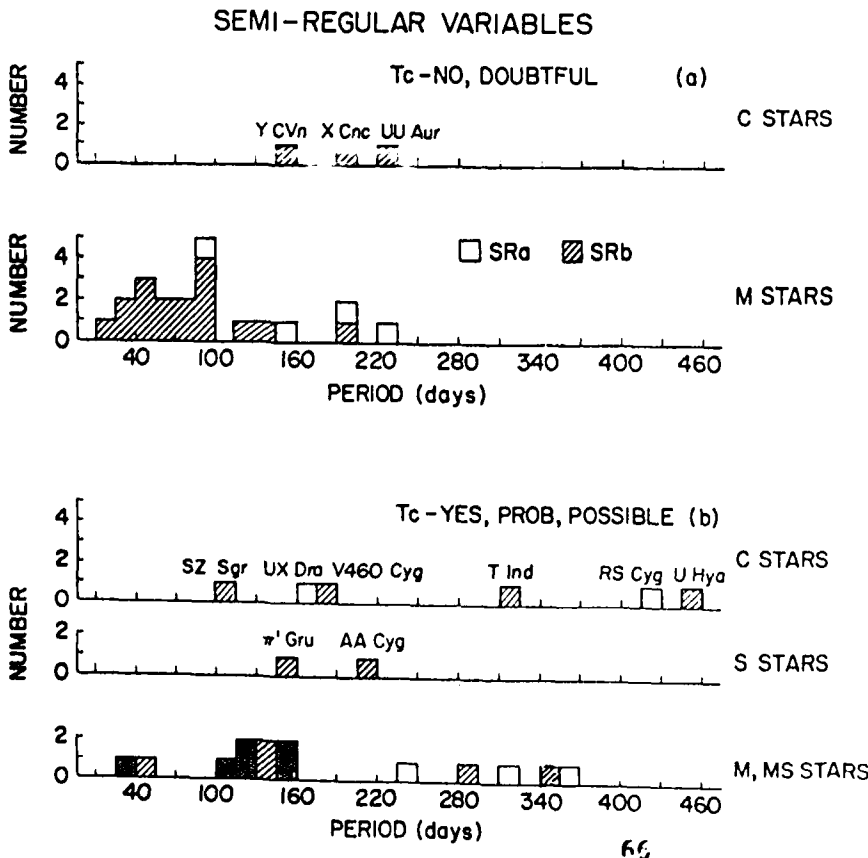


FIG. 3. (a), (b) Histograms for the semiregular variables binned in 15 day intervals. The bottom panel (b) shows the stars with Tc. The M and MS stars, C, and S stars are plotted on separate lines. SRb variables are indicated as hatched areas. SRa's as open areas and MS semiregular variables as double-cross-hatched areas. The top panel (a) shows the stars with Tc-no or -doubtful. The three SRb C stars are plotted on a separate line. No semiregular S or MS stars without Tc are known.

they have abundances of the *s*-process elements (including Tc) and C/O ratios intermediate between the M and the S stars, e.g., RS Cnc and OP Her. (Smith and Lambert (1986) call our *evolutionary* MS stars true MS stars.)

It seems that atmospheric conditions in certain stars are also able to produce enhanced strengths of Sr and Ba lines, i.e., enhancements not due to increased abundances, for example, DE Leo and CU Dra (Smith and Lambert 1985, 1986). The Smith and Lambert abundance analyses point out the difficulty in interpreting classification criteria in terms of abundances. It is also likely that some MS stars will be found with *s*-process enhancements and no Tc. A possible example is g Her, which shows mild *s*-process enhancements by about a factor of 2 but no Tc. These types of objects may be cooler analogs of barium stars whose enhancements are likely to be produced by mass transfer from a companion. We postulate the existence of these types of objects among the S and the C stars. We will refer to the MS stars with observed enhanced *s*-process lines and no Tc as *spectroscopic* MS stars. The presence of Tc will distinguish between the *evolutionary* and the *spectroscopic* MS stars, but only a complete abundance analysis will distinguish between atmospheric enhancements and real *s*-process enhancements produced in the past.

ST Her and NZ Gem (BS 2967) are listed in Table I as MS stars and are also among the MS stars of Yamashita (1967). ST Her shows strong Tc lines and Smith and Lambert (1986) did notice enhanced *s*-process lines on its spectrum (although they derived no abundances). We will consider it to be an *evolutionary* MS star. NZ Gem shows neither Tc (present study) nor enhanced *s*-process lines (Smith and Lambert 1986) and may be either a *spectroscopic* MS star or an ordinary M star.

NO Aur and GZ Peg, listed as MS stars in Table I, are low-amplitude irregular variables that do not show Tc lines. GZ Peg should be examined for *s*-process abundance enhancements. We include it among the *spectroscopic* MS stars.

NO Aur is listed as M2 Slab in the GCVS and as M2 IIIS in the BSC. However, our 4 m echelle spectrogram is more consistent with its supergiant classification. The *IRAS* low-resolution spectrum of NO Aur shows an emission feature in the 9 to 13 μ m that is typical of many S stars (Little and Little-Marenin 1986). Supergiants in general do not show the Tc lines (subsec *a*, conclusion no. 2). Red supergiants (usually irregular or semiregular variables) are estimated to be in the beginning stages of core helium burning (Stothers and Leung 1970). The lack of Tc in any M supergiants agrees with this conclusion. However, three MS stars, classified as supergiants or bright giants, *do show* strong Tc lines (RS Cnc (M6e Ib-II(S)), Y Lyn (M6S Ib-II) and T Cet (M5-6S IIe)). Their luminosity class may be suspect since luminosity criteria such as the Sr lines are also enhanced by the *s*-process and as the conflicting classification for RS Cnc shows: M6e Ib-II(S) in the GCVS and as M6 IIIaSe in the BSC. Until we are certain about the supergiant classification of these MS stars, we will believe that no supergiants show Tc. Hence we reach two contradictory conclusions for NO Aur. Its supergiant characteristics and its low amplitude are consistent with no Tc lines in its spectrum. On the other hand, its *IRAS* spectrum argues for NO Aur having S star characteristics and as such it should show Tc. An abundance analysis is needed in order to clarify its status.

The two MS Miras, RT Aql and X Cet, may be classified incorrectly as MS stars and should be considered M star

Miras. Neither shows Tc, and Keenan, Garrison, and Deutsch (1974) observe no ZrO in RT Aql. However, their spectrum of X Cet was too underexposed for ZrO to be observable. X Cet should be reobserved at classification dispersion and should be reanalyzed for Tc. Two M Miras, T Cas and T Cep, should probably be classified as *evolutionary* MS stars. They show fairly strong Tc lines and definitely show ZrO bands around 9300 Å (Spinrad *et al.* 1966). R Ser probably shows the 9300 Å ZrO bands (Spinrad and Newburn 1965) and weakly ZrO in the blue at two out of four phases (Keenan, Garrison, and Deutsch 1974) and strong Tc. However, its $^{12}\text{C}/^{13}\text{C}$ ratio of 15 ± 3 (Hinkle, unpublished) is more typical of M stars with Tc and we will not include it among the *evolutionary* MS stars until its *s*-process abundances can be determined. A comparison of the intensity of the ZrO band as listed by Keenan, Garrison, and Deutsch (1974) and our Tc data show that stars with Tc have ZrO intensities of ≥ 1 or have intensities of about 0.5 at several phases. An occasionally weakly visible ZrO band does not indicate the presence of Tc and may relate to unusual atmospheric conditions.

Summarizing, we find that *evolutionary* MS stars show Tc, whereas *spectroscopic* MS stars do not. This is a somewhat circular argument in that we have excluded from the *evolutionary* MS group those stars that do not show Tc. The value of the distinction between the two groups lies in the fact that we are able to distinguish between unusual atmospheric conditions (or possible mass transfer from a companion) and real abundance anomalies produced very recently in AGB stars. The presence of Tc establishes a star as belonging to the *evolutionary* MS category without having to perform complex abundance analyses, especially for the Mira variables for which good atmospheric models are not yet available.

2) S stars

The S stars BS 363, HD 35155, HD 165774, BD Cam (BS 1105)-Lb and V Cnc (M—272 days) that do not show Tc are of particular interest since their spectral classification implies that the other *s*-process elements are enhanced. BD Cam (= BS 1105) is a low-amplitude Lb variable in a binary system (Griffin 1984), and its *s*-process enhancements (Smith and Lambert 1986) may be due to mass transfer from a companion analogous to the enhancements observed in Ba II stars. Peery (1985) reports the possible detection of an underluminous (white dwarf?) companion to BD Cam in an *IUE* spectrum and Johnson and Ake (1984) interpret the very strong C IV and N V lines in an *IUE* spectrum of HD 35155 as possibly being produced in an interacting binary system. Hence the *s*-process enhancements in both these stars may be related to mass transfer. BS 363 may be similar since it is listed as a probable spectroscopic binary in the BSC. However, no white dwarf companion with M_v brighter than 11.1 has been detected with *IUE* (Johnson and Ake 1986). It should be searched for radial-velocity variations. No extra information on HD 165774 is available. V Cnc is the only S type Mira with no Tc lines, and it definitely needs to be reobserved. We observed it near maximum when it is quite warm (S0) and Tc is somewhat ionized. It would be most unexpected to find an S star Mira without Tc lines since this type of star is a prime candidate for the third dredge-up. V Cnc is also a visual binary; however, the secondary is too bright ($m_v = 13.5$ mag) to be a white dwarf and the separa-

tion is too large ($10''$) for the companion to have exchanged mass with V Cnc. We conclude that all *single* S stars show the products of recent *s*-processing in their atmospheres. The few S stars without Tc are nonvariable or low-amplitude binaries (V Cnc may be an exception). The only nonvariable star to show Tc is BS 8062 (S4,1). It may be temporarily in a quiet evolutionary phase since all other Tc stars are relatively large-amplitude variables. It is of interest to point out that a white dwarf companion can be present and Tc be observed in the atmosphere of a star. For example, the MS star α^1 Ori shows Tc and has a white dwarf companion (Johnson and Ake 1986).

3) Carbon stars

The four C stars that do not show the Tc lines are SS Vir (M—355 days), UU Aur (SRb—234 days), X Cnc (SRb—195 days), and Y CVn (SRb—157 days). Utsumi (1970, 1985) has found that C stars rich in ^{13}C (type J) such as Y CVn do not show *s*-process enhancements. Hence it is not surprising that Y CVn does not show Tc. No other J type stars have yet been searched for Tc. Lambert *et al.* (1986) determined a C/O ratio of 1.087 for Y CVn. Its greater-than-unity C/O ratio together with its low $^{12}\text{C}/^{13}\text{C}$ ratio of 3.5 implies a compositional change during an earlier evolutionary phase and not the third dredge-up. On the other hand, UU Aur and X Cnc show the typical *s*-process enhancements (Utsumi 1985) and C/O ratios of C stars (Lambert *et al.* 1986) (SS Vir was not analyzed by Utsumi and no C/O ratio was determined by Lambert *et al.* 1986). The lack of Tc in these two stars is difficult to understand unless the third dredge-up has ceased in these stars more than 10^6 yr ago so that Tc has had time to decay away. However, the AGB lifetime of low-mass stars is only a few times 10^6 yr (Iben 1983). The cutoff for the third dredge-up would have to be very finely tuned in order to allow for the formation of a C star and the decay of Tc before the star ends its AGB evolution with the ejection of a planetary nebula. Another possibility is that these particular stars are cooler analogs to the barium stars (*i.e.*, unidentified binary stars). More C stars should be searched for Tc and binary companions. It is, however, very difficult to observe carbon stars for the Tc I resonance lines since their ultraviolet depression makes most of them quite faint in the 4200–4300 Å region.

V. CONCLUSIONS

During the late stages of evolution, stars on the upper part of the AGB can experience helium shell flashing and the third dredge-up which mixes carbon (a product of helium burning) and *s*-process elements with the atmosphere. During this phase, M stars progressively evolve from M → MS → S → (SC) → C stars. Abundance analyses of stars along this sequence confirm an increase in the C/O ratio and in the amount of *s*-processed elements in their atmospheres. The detection of Tc in our much larger sample of stars agrees very well with the increasing amounts of *s*-process elements observed in the sequence from M → C stars. We find that all *evolutionary* MS, probably all single S stars, and all SC stars show Tc. However, among the C stars, we find a significant percentage of stars that do not show Tc even if other *s*-process elements are enhanced. Whether the decrease in the percent of C stars with Tc is related to undiscovered binary systems is not yet known.

In M stars we find that the presence of the Tc lines in the

spectrum is a very sensitive indicator of the mixing of *s*-processed elements. At times, we can detect the presence of an *s*-process product (*i.e.*, Tc) more readily than can abundance analyses of other *s*-process elements since the detection of Tc is more easily accomplished than the determination of abundance enhancements. We find a significant number of M stars with Tc even when no *s*-process enhancements have been determined by spectroscopic abundance analyses. Specifically, the pure M star α Cet (Mira) shows the Tc I lines and no apparent enhancement of Zr and Nb (Dominy and Wallerstein 1986), R Ser shows a strong Tc line but ZrO appears to be present only occasionally and then very weakly (Dominy and Wallerstein 1986; Keenan, Garrison, and Deutsch 1974; Spinrad and Newburn 1965), and no ZrO has been observed in Mira. The detection of Tc in a large number of stars allows us to delineate those stars in which *s*-process products have recently been mixed with surface materials. The percent of stars with Tc rises from 0% for nonvariable M stars to probably 100% in the MS, S, and SC stars.

The onset of the third dredge-up is accompanied by light variability in these stars. The nonvariable and low-amplitude variables do not show Tc, whereas larger-amplitude semiregular (SR) and Mira variables do show Tc. In Mira variables the presence of Tc is a very strong function of their period and Tc is not usually detected in stars with $P < 300$ days. Some of the semiregular M stars in the 130–150 day period range also show Tc and may be first-overtone pulsators corresponding to the longer-period fundamental-mode Mira pulsators.

We argue that the MS stars should be divided into two categories: (a) the *evolutionary* MS stars, which represent the intermediate evolutionary phase between M and S stars and have the intermediate abundance characteristics between the two spectral classes (including Tc); and (b) the *spectroscopic* MS stars in which unusual atmospheric conditions or possibly enhancements due to mass transfer from a companion produce enhanced Sr II and Ba II lines but no Tc I lines.

The few S stars that do not show Tc may have companions and their *s*-process enhancements may be related to a mass-transfer process as suggested for the barium stars.

Supergiants do not appear to be in a third dredge-up phase since they do not show Tc and probably are likely to be in their core-helium-burning phase. The supergiant classification of the MS stars is suspect because of the difficulty in finding luminosity criteria that are independent of *s*-process elements. Holweger and Kovacs (1984) observed several K giants and supergiants with apparent abundance enhancements of Sr and Ba which they attribute to a weak *s*-process. However, Smith and Lambert (1986) point out that the apparent enhancements are likely to be related to non-LTE effects in the Sr lines and not a weak *s*-process. The lack of Tc in our three K stars lends support to the suggestion by Smith and Lambert.

We would like to acknowledge the cheerful and helpful assistance of the staff at Kitt Peak National Observatory and Cerro Tololo Inter-American Observatory. We would like to thank K. Hinkle for the $^{12}\text{C}/^{13}\text{C}$ ratios of Mira variables prior to publication. This research has been supported in part by a University Resident Research Fellowship of the Air Force Office of Scientific Research to the Air Force Geophysics Laboratory (I.R.L.-M.). S. J. L. would like to thank Bentley College for an Assigned Time Research grant. We

would also like to thank P. Gaeta, L. Lewis, and C. Leslie for their help with the analysis of the spectra. We especially would like to thank the many members of the American

Association of Variable Star Observers without whose observations it would have been difficult to predict maximum brightness for the variables on our observing program.

REFERENCES

- Abt, H. A., and Biggs, E. S. (1972). *Bibliography of Stellar Radial Velocities* (Latham Process Corporation, New York).
- Akopyan, A. A., and Melik-Alaverdyan, Yu. K. (1983). *Sov. Astrophys.* **19**, No. 2, 273.
- American Association of Variable Star Observers (AAVSO) (1983). *Observations of Long Period Variables*, Rep. No. 38 (AAVSO, Cambridge, MA).
- Barbier-Brossat, M., and Petit, M. (1986). *Astron Astrophys. Suppl.* **65**, 59.
- Benson, P. J., Little-Marenin, I. R., Dickinson, D. F., Turner, B. E., and Jewell, P. R. (1987). In preparation.
- Boesgaard, A., and Fesen, R. (1974). *Publ. Astron. Soc. Pac.* **86**, 76.
- Boesgaard, A. M. (1969). *Publ. Astron. Soc. Pac.* **81**, 365.
- Bond, H. (1974). *Astrophys. J.* **194**, 95.
- Boyarchuk, A. A., and Snow, T. P. (1978). *Astrophys. J.* **219**, 515.
- Burbidge, E. M., and Burbidge, G. R. (1957). *Astrophys. J.* **126**, 357.
- Clayton, M. L., and Feast, M. W. (1969). *Mon. Not. R. Astron. Soc.* **146**, 411.
- Cohen, J. (1973). *Publ. Astron. Soc. Pac.* **85**, 187.
- Cosner, K., and Truran, W. (1981). *Astrophys. Space Sci.* **78**, 85.
- Davis, D. N. (1968). *Astrophys. J. Lett.* **152**, L13.
- Dean, Ch. A. (1974). *Astron. J.* **81**, 364.
- Dominy, J. F. (1984). *Astrophys. J. Suppl.* **55**, 27.
- Dominy, J. F., and Wallerstein, G. (1986). *Astrophys. J.* **310**, 371.
- Dominy, J. F., Wallerstein, G., and Suntzeff, N. B. (1986). *Astrophys. J.* **300**, 325.
- Eggen, O. J. (1970). *Astrophys. J. Suppl.* **22**, 289.
- Eggen, O. J. (1975). *Astrophys. J.* **195**, 661.
- Feast, M. W. (1963). *Mon. Not. R. Astron. Soc.* **125**, 367.
- Feast, M. W. (1980). In *Physical Processes in Red Giants*, *Astrophysics and Space Library*, Vol. 88, edited by I. Iben, Jr. and A. Renzini (Reidel, Dordrecht), p. 193.
- Feast, M. W. (1984). *Mon. Not. R. Astron. Soc.* **211**, 51p.
- Hackos, W. (1974). *Publ. Astron. Soc. Pac.* **86**, 78.
- Hagen, W., Stencel, R. E., and Dickinson, D. F. (1983). *Astrophys. J.* **274**, 286.
- Hoffleit, D., and Jaschek, C. (1982). *Bright Star Catalogue* (Yale University, New Haven).
- Holweger, H., and Kovacs, N. (1984). *Astron. Astrophys.* **132**, L5.
- Humphreys, R. M. (1974). *Astrophys. J.* **188**, 75.
- Humphreys, R. M., and Ney, E. P. (1974). *Astrophys. J.* **194**, 623.
- Glass, L. S., and Lloyd Evans, T. (1981). *Nature* **291**, 303.
- Griffin, R. F. (1984). *The Observatory* **104**, 224.
- Iben, I., Jr. (1983). *Astrophys. J. Lett.* **275**, L63.
- Iben, I., Jr., and Renzini, A. (1983). *Annu. Rev. Astron. Astrophys.* **21**, 271.
- Johnson, H. R., and Ake, T. B. (1984). In *Third Cambridge Workshop on Cool Stars, Stellar Systems, and the Sun*, edited S. L. Baliunas and L. Hartmann (Springer, New York), p. 362.
- Johnson, H. R., and Ake, T. B. (1986). In *New Insights in Astrophysics—Eight Years of UV Astronomy with IUE*, ESA-SI-263, edited by E. Rolfe (European Space Agency, Noordwijk), p. 395.
- Keenan, P. C. (1954). *Astrophys. J.* **120**, 484.
- Keenan, P. C., and Boeshaar, P. C. (1980). *Astrophys. J. Suppl.* **43**, 379.
- Keenan, P. C., Garrison, R. F., and Deutsch, A. J. (1974). *Astrophys. J. Suppl.* **28**, 271.
- Kholopov, P. N., editor (1985). *General Catalog of Variable Stars*, 4th ed. (Nauka, Moscow).
- Kipper, T. A., and Kipper M. A. (1984). *Sov. Astron. Lett.* **10**, No. 6, 363.
- Kukarkin, B. V., et al. (1969). *General Catalog of Variable Stars*, 3rd ed. (Nauka, Moscow).
- Lambert, D. L., Gustafsson, B., Eriksson K., and Hinkle, K. H. (1986). *Astrophys. J. Suppl.* **62**, 373.
- Lattanzio, J. C. (1986). *Astrophys. J.* **311**, 708.
- Lattanzio, J. C. (1987). *Astrophys. J. Lett.* **313**, L15.
- Little-Marenin, I. R., and Little, S. J. (1979). *Astron. J.* **84**, 1374.
- Little-Marenin, I. R., and Little, S. J. (1986). *Lect. Not. Phys.* **254**, 423.
- Little-Marenin, I. R., and Little, S. J. (1987). *Astron. J.* **93**, 1539.
- Maehara, H. (1971). *Publ. Astron. Soc. Jpn.* **23**, 313.
- Mathews, G. J., Takahashi, K., Ward, R. A., and Howard, W. H. (1986). *Astrophys. J.* **302**, 410.
- McClure, R. D. (1984). *Publ. Astron. Soc. Pac.* **96**, 117.
- Merrill, P. (1952). *Astrophys. J.* **116**, 21.
- Merrill, P. (1956). *Publ. Astron. Soc. Pac.* **68**, 70.
- Mikaki, T. (1978). *Ann. Tokyo Astron. Obs.* **11**, 17, 1.
- Ostlie, D. A., and Cox A. N. (1986). *Astrophys. J.* **311**, 64.
- Peery, B. F. (1971). *Publ. Astron. Soc. Pac.* **83**, 162.
- Peery, B. F. (1985). In *Cool Stars with Excesses of Heavy Elements*, *Astrophysics and Space Science Library*, Vol. 114, edited by M. Jaschek and P. C. Keenan (Reidel, Dordrecht), p. 333.
- Peery, B. F., Keenan, P. C., and Marenin, I. R. (1971). *Publ. Astron. Soc. Pac.* **83**, 496.
- Robertson, B. S. C., and Feast, M. W. (1981). *Mon. Not. R. Astron. Soc.* **196**, 111.
- Sanner, F. (1977). *Publ. Astron. Soc. Pac.* **89**, 768.
- Sanner, F. (1978). *Astrophys. J.* **219**, 538.
- Schatz, G. (1983). *Astron. Astrophys.* **122**, 327.
- Smith, V. V. (1984). *Astron. Astrophys.* **132**, 326.
- Smith, V. V., and Lambert, D. L. (1985). *Astrophys. J.* **294**, 326.
- Smith, V. V., and Lambert, D. L. (1986). *Astrophys. J.* **311**, 843.
- Smith, V. V., and Wallerstein, G. (1983). *Astrophys. J.* **273**, 742.
- Spinrad, H., and Newburn, R. L., Jr. (1965). *Astrophys. J.* **141**, 965.
- Spinrad, H., Pypser, D. M., Newburn, R. L., Jr., and Younkin, R. L. (1966). *Astrophys. J.* **143**, 291.
- Stothers, R., and Leung, K. C. (1970). *Astron. Astrophys.* **10**, 290.
- Tech, J. (1971). *Natl. Bur. Stand. Monogr. No.* 119.
- Utsumi, K. (1970). *Publ. Astron. Soc. Jpn.* **22**, 93.
- Utsumi, K. (1985). In *Cool Stars with Excesses of Heavy Elements*, *Astrophysics and Space Science Library*, Vol. 114, edited M. Jaschek and P. C. Keenan (Reidel, Dordrecht), p. 243.
- Vardya, M. S. (1985). In *Cool Stars with Excesses of Heavy Elements*, *Astrophysics and Space Science Library*, Vol. 114, edited M. Jaschek and P. C. Keenan (Reidel, Dordrecht), p. 105.
- Wallerstein, G., and Fawley, W. M. (1980). *Publ. Astron. Soc. Pac.* **92**, 183.
- Warner, B. (1965). *Mon. Not. R. Astron. Soc.* **129**, 263.
- Willson, L. A. (1982). In *Pulsations in Classical and Cataclysmic Variable Stars*, edited J. P. Cox and Carl J. Hansen (JILA, Boulder, CO), p. 269.
- Wilson, R. E. (1953). *General Catalogue of Stellar Radial Velocities* (Carnegie Institution of Washington Publ. No. 601 (Carnegie Institution of Washington, Washington, DC).
- Wood, P. R. (1985). In *Cool Stars with Excesses of Heavy Elements*, *Astrophysics and Space Science Library*, Vol. 114, edited by M. Jaschek and P. C. Keenan (Reidel, Dordrecht), p. 357.
- Yamashita, Y. (1967). *Publ. Dom. Astrophys. Obs., Victoria, B. C.* **13**, 47.

Appendix G

Maser Associated with Two Carbon Stars: V778 Cygni and EU Andromedae

accepted for publication by the
Astrophysical Journal July 15, 1988 330:828-834

MASERS ASSOCIATED WITH TWO CARBON STARS: V778 CYGNI and EU ANDROMEDAE

Irene R. LITTLE-MARENIN

AFGL/OPC, Hanscom AFB and Whitin Observatory, Wellesley College

Priscilla J. BENSON¹

Whitin Observatory, Wellesley College and
Smithsonian Astrophysical Observatory

Dale F. DICKINSON

Lockheed Palo Alto Research Laboratory

Received: November 14, 1987

¹Visiting Scientist, Smithsonian Astrophysical Observatory, Center for
Astrophysics

ABSTRACT We present several observations of the 22.2 GHz H₂O maser line from two C stars, V778 Cyg and EU And, and the 1665/67 MHz OH maser lines from V778 Cyg. For both sources the intensity of the H₂O line has varied by more than a factor of 5 over several months. We interpret the systems as being binaries, each with an M star component with a thick shell and a C star component.

Subject Headings: masers: water - masers: OH - stars: carbon - stars:
individual (EU And, V778 Cyg) -

Seven carbon stars are associated with oxygen-rich circumstellar material (Little-Marenin 1986; Willems and de Jong 1986) as deduced from the presence of strong 10 μm and 18 μm emission features in their IRAS low resolution spectra (Joint IRAS Science Working Group 1986). These stars are EU And (C4,4), V778 Cyg (C5⁻,5), BM Gem (N), IRAS 08002-3803 (=CCCS1003=star 1003 in Catalog of Cool Carbon Stars, Stephenson (1973)), IRAS 08577-6035 (=MaC79#11=star 11, Table 2, MacConnell (1979)), IRAS 18006-3213 (=FJF270=star 270 of Fuenmayor (1981), erroneously labeled FJF272 in Fig. 1 of Willems and de Jong), and IRAS 19139+5412 (=NC#83=star 83 of Stephenson (1985))). We exclude from the list two other stars mentioned by Willems and de Jong (1986). IRAS 10091-7049 =CCCS1633 maybe an S or MS star as mentioned by Stephenson (1973). Also its 10-11 μm emission feature is more typical of MS stars rather than M stars (Little, Little-Marenin and Price 1987). IRAS 13442-6109 (maybe =CCCS2123) has an uncertain C position and Stephenson (1973) could not confirm its C classification.

To better understand the unexpected phenomena of an oxygen-rich circumstellar shell near a carbon-rich photosphere, we searched the four C stars visible to the Haystack Observatory² 37 m telescope for H₂O emission.

²Radio astronomy at Haystack Observatory of the Northeast Radio Observatory Corporation is supported by the National Science Foundation under grant AST78-18227.

The 6₁₆-5₂₃ H₂O maser emission line at 22,235.080 MHz was detected towards EU And (Benson and Little-Marenin 1987) and V778 Cyg (Little-Marenin, Benson and

Little 1987; Nakada et al. 1987). We also searched EU And and V778 Cyg for OH maser emission with the NRAO³ 300'; the mainline 1665 and 1667 MHz OH maser

³The National Radio Astronomy Observatory is operated by Associated Universities, Inc., under contract with the National Science Foundation.

lines were seen towards V778 Cyg but not EU And (<0.07 Jy (3σ)).

I. OBSERVATIONS and RESULTS

Since March 1987 we have monitored EU And and V778 Cyg at Haystack Observatory for H₂O maser emission. The spectra were automatically corrected by the Haystack computer for atmospheric attenuation and for variation in telescope gain with elevation. We observed the stars in total power mode with 5 minutes on and 5 minutes off source. The first detections of EU And (12/15/86) and V778 Cyg (3/23/87) were obtained with an autocorrelator bandwidth of 16.67 MHz with 512 channels, resulting in a resolution of 0.53 km s⁻¹ which only marginally resolved the H₂O lines. Later observations were usually made with a bandwidth of 5.55 MHz with 1024 channels, resulting in a velocity resolution of 0.09 km s⁻¹. Pointing was checked twice daily with observations of 3C84 and 3C374. We used a conversion factor of 12 Jy per degree K (Haschick 1986).

H₂O maser emission from V778 Cyg (RA=20:35:07; Dec=+59:54:48 (1950)) was first detected 1987 March 23 with a flux of 1.9 (.5) Jy at $V_{LSR}=-16.8$ (.1) km s⁻¹. The formal errors of the Gaussian fits are in parenthesis. Since then the intensity of the maser has increased to a value of 11 Jy on 1987 June 9. Figure 1a displays the temporal sequence of the V778 Cyg spectra. At times the line has shown two additional components which are weaker by about a

factor of 3 to 5 at -20.5 km s^{-1} and -15.1 km s^{-1} . Figure 2a plots the peak flux and integrated area for the three components as a function of Julian date. The intensity of the weaker components tend to vary in phase with the main water line. The parameters of the Gaussian fits to the observed lines are summarized in Table 1; for weak lines we estimated the peak flux only. Upper limits to the flux are estimated as being $< 3 \sigma$. Table 1 and Figure 2a include the data from the independent detection of V778 Cyg by Nakada et al. (1987) on 1987 April 30 with a peak flux of 7 Jy.

The 1665 and 1667 MHz OH observations of V778 Cyg were made at the 300 foot NRAO Greenbank telescope on 1987 July 13. The spectra were taken simultaneously in two different polarizations for each line using the 384 channel autocorrelator split into four 92 channel sections. Standard calibrations were used and the two polarizations were averaged. The system temperature averaged about 20 K. The bandwidth of 625 kHz for each segment provided a velocity window of 113 km s^{-1} and a resolution of about 1.5 km s^{-1} . We detected the 1665 and 1667 MHz lines at about the same velocity as the H_2O line. The intensity of the 1667 line of $0.26 \text{ K}=0.195 \text{ Jy}$ at $-15.3 \pm 1 \text{ km s}^{-1}$ is almost twice as intense as the 1665 line of $0.15 \text{ K}=0.113 \text{ Jy}$ at $-16.5 \pm 1 \text{ km s}^{-1}$ see Fig. 1c.

The 22 GHz flux of EU And (RA=23:17:41; Dec=+46:58:00 (1950)) has varied by at least a factor of 8 between 1986 December and 1987 June (Figure 1b) with the main component being below the detection limit of about 1.5 Jy on 1987 March 22 and very weak ($\sim 2 \text{ Jy}$) on 1987 May 19. On 1987 May 22 Nakada et al. were unable to detect EU And at the 1.5 Jy level. At times EU And has shown at least one other component at -31 km s^{-1} , once possibly another at -26 km s^{-1} and on 1987 October 20 a possible component at -12.4 km s^{-1} . EU And shows

greater temporal variations than V778 Cyg in the intensity of the main component as can be seen in Figure 2b. The integrated flux has primarily been decreasing for EU And (Fig. 2b) and primarily been increasing for V778 Cyg (Fig. 2a) since we have been observing these sources. The water maser receiver was unavailable at Haystack Observatory from 1987 mid-June until 1987 early October. Optically, both stars are quite faint with $m_p \sim 12-13$. Their optical variability types are only poorly established with EU And being classified as SR and V778 Cyg as Lb. It is not known if their maser variability correlates with optical variability.

BM Gem (RA=07:17:56; Dec=+25:05:03 (1950)) has been searched over a velocity range of 10 to 190 km s⁻¹ three times and IRAS 19139+5412 (RA=19:13:55; Dec=+54:12:06 (1950)) over a velocity of -180 to +180 km s⁻¹ three times with negative results. Considering the variability of the H₂O emission from EU And and V778 Cyg and the fact that both were detected during our first try, we expect that both BM Gem and IRAS 19139+5412 have a very high probability of being detected as maser sources if observed often enough.

II. DISCUSSION

Stellar water masers are located in expanding circumstellar shells around M Miras or semi-regular variables (Kleinmann, Dickinson and Sargent 1978; Reid and Moran 1981; Dickinson and Dinger 1982; Bowers and Hagen 1984). H₂O emission is highly variable in intensity both in space and in time (Gomez Balboa and Lepine 1986; Johnston, Spencer and Bowers 1985) with the various velocity components of the masers being located in different parts of the circumstellar shell. Interferometric observations of the spatial distribution of H₂O maser spots indicate that the maser regions range from <9 - 100 AU

(average about 50 AU) in total extent around giants and from 300 -720 AU around supergiants and show elongated structures as well as spherical symmetry (Lane et al 1987). Assuming that the masers in V778 Cyg and EU And are located in expanding shells, then half of our observed maser velocity range of about 3 km s^{-1} should be the lower limit to the expansion velocity of the shell in the masing region. Theoretical models of H_2O masing regions around giants (Cooke and Elitzur 1985) predict expansion velocities of about 3 to 6 km s^{-1} which correspond to a terminal velocity of about 10 km s^{-1} in agreement with our observations. The relatively simple structure and small velocity difference between the H_2O maser components argues strongly for the masers being located around giants rather than supergiants. The galactic latitudes of V778 Cyg and EU And ($b=12^\circ$ and -13° , respectively) also support these stars being giants since, in general, supergiant OH/IR stars tend to be strongly concentrated towards the galactic plane with $b < 4^\circ$.

The mapping of the 1665/67 MHz OH and 22 GHz H_2O masers around the supergiant VX Sgr shows that the two maser sources are at very similar distances and have very similar outflow velocities (Chapman and Cohen 1986) unlike the 1612 MHz OH emission which is about a factor of 10 further out. Although we estimate that the H_2O and OH masers for V778 Cyg are located around a giant rather than a supergiant, we interpret the agreement between our observed H_2O and OH velocities for V778 Cyg as indicating that both types of masers are located at roughly the same distance from the central star. Other OH velocity components which correspond to the weaker H_2O components are not detectable at the OH velocity resolution of 1.17 km s^{-1} .

If V778 Cyg and EU And are giants, then the material outflowing from the central star will transit through the H_2O and OH masing region (about $50/2=25$

AU, (Lane et al. 1987)) in about 40 years if a conservative estimate of 3 km/sec for the expansion velocity in the masing region is assumed ($t(\text{yr})=D(\text{AU})*(4.74/v(\text{km s}^{-1}))$). The transit time of material through the silicate emitting region is estimated to be about 20-30 years for a similar expansion velocity since circumstellar shell (hereafter CS) models predict that the 10 μm emission comes primarily from a distance of, about 10 R_* or about 15-20 AU for M star Miras (Rowan-Robinson and Harris 1983a; Dyck et al. 1984).

There are two principle interpretations possible for the extraordinary situation of having an oxygen-rich CS associated with a carbon-rich photosphere.

A) We are observing a binary systems with a C star and an M star companion with a relatively thick CS. The CS of the M star produces the 10 and 18 μm emission, and the H_2O and OH maser lines. However, the CS absorbs the visible light of the M star so that only light from the carbon star is seen in the visible and near infrared region.

B) We are observing the transition of an M star to a C star so that we still observe the O-rich material in the CS for a brief time after the central star has already become C-rich.

We favor (A), the binary system hypothesis, since the time scales for hypothesis (B) to be correct are not compatible with the observations of the outflow velocities and of the evolutionary time scales available to transform M to C stars. First, V778 Cyg (=MSB38) and EU And (=DO42999) were first recognized as a carbon star in 1933 (Merrill, Sanford and Burwell 1933) and before 1947 (Lee, Gore and Bartlett 1947), respectively. The outflowing material at 3 km s^{-1} has traveled at least 30 AU since then and should have

passed through the silicate emission region by the time the IRAS observations were made and is likely to have passed through the H₂O and OH maser region. Only in the very unlikely situation that both stars in 1933 and 1940 were observed at the instance when the photosphere became carbon-rich without going through an S and SC phase would we still see the remnant oxygen-rich shell in the IRAS and maser data.

Second, the IRAS low resolution spectra of V778 Cyg and EU And are indistinguishable from other M star spectra which show strong silicate emission and are also H₂O and OH maser e.g. R Cet and WX Ser. On the other hand, S and SC star spectra are significantly different from M star spectra (Little, Little-Marenin and Price 1987) suggesting very strongly that we are observing the 8-22 μ m spectrum of an M star and not an S or SC star. Third, abundance analyses of S and SC stars (Dominy and Wallerstein 1983; Smith and Wallerstein 1983; Smith and Lambert 1986, Mathews et al. 1986; Winters and Macklin 1987; Wallerstein and Dominy 1988) show that the distribution of the observed s-process photospheric abundances imply several dredge-up episodes during the asymptotic giant branch (AGB) lifetime of these stars which takes on the order of 10^5 - 10^6 years. Similarly, since the observed s-process enhancements in C stars are produced during several dredge-up episodes, it would take longer than the transit time of material through the CS to produce a C star from an M star. The location in an H-R diagram of Magellanic Cloud AGB stars of intermediate-age globular clusters indicate a progression with increasing luminosities of M->MS->S->(SC)->C (Wood 1985) i.e. there is no evidence for a direct transition from M to C. Hence, we consider the scenario of an instantaneous transition from an M to C star highly unlikely. This does not mean that the scenario could not happen only that there is no evidence

that it has happened either from evolutionary considerations or transit times of material through the CS.

Fourth, Willems and de Jong (1986) argue that all C stars with strong $10\ \mu\text{m}$ emission are J type C stars. i.e. stars with low $^{12}\text{C}/^{13}\text{C}$ ratios. However, Utsumi (1985) finds that galactic C stars rich in ^{13}C show no s-process enhancements nor does the J type star Y CVn show lines of the radioactive element technetium (Peery 1971). This suggests very strongly that the carbon enrichment needed to produce J type C stars must have occurred before the stars reached their AGB phase of evolution and that it occurred more than 5×10^5 years ago so that ^{99}Tc had time to decay away. Hence, no C-rich shell should yet be observable around J type stars.

We find support for the binary star hypothesis in the observed flux of V778 Cyg at 1, 12, 25 and $60\ \mu\text{m}$. V778 Cyg shows the typical strong CN absorption features of an Lb C star in the $0.8 - 1.08\ \mu\text{m}$ region (Baumert 1972). The observed flux of about 11 Jy at $1.08\ \mu\text{m}$ and 8 Jy at $.78\ \mu\text{m}$ (triangles in Fig. 3) and the IRAS color corrected fluxes of 26 Jy at $12\ \mu\text{m}$, 14 Jy at $25\ \mu\text{m}$ and about 1.5 Jy at $60\ \mu\text{m}$ (open circles in Fig. 3) can be modeled quite well with a composite M and C star spectrum as can be seen in Figure 3. Using the Rowan-Robinson and Harris dust shell models (1983a,b) for a typical J type carbon star (Y CVn) and a typical M star Mira (WX Ser) with strong 10 and $18\ \mu\text{m}$ silicate and H_2O and OH maser emission, we find that the C star will dominate the emission shortward of about $5\ \mu\text{m}$ and the M star with its shell will dominate longward of $5\ \mu\text{m}$. The $100\ \mu\text{m}$ flux of 9.8 Jy (uncorrected) may be contaminated by infrared cirrus. No composite model can be calculated for EU And since no information on the near infrared spectrum of EU And is available.

The binary hypothesis is also supported by the observed V_{LSR} of the EU And maser emission which differs from that of the C star by 24 km s^{-1} . We interpret this as due partly to the orbital velocity of the two components. Benson and Little-Marenin (1987) estimate the minimum orbital velocity difference in the EU And system is 10 km s^{-1} . However, for V778 Cyg the water maser velocity agrees with the velocity of the C star and may indicate that the orbital plane of the system is more highly inclined and/or that the M and C star components are presently moving across our line of sight and/or that the two components are more widely separated. Deguchi et al. (1987) have confirmed that the position of the water maser source around V778 Cyg agrees with the photographic position of the C star within $0.''5$, implying that the two components of V778 Cyg could be separately seen if less than 50-500 AU apart at a distance of 10^2 - 10^3 pc. Peery's (1975) estimate of a 1.4 Kpc distance for V778 Cyg makes it even less likely that the binary components could have been separately seen. Assuming typical C and M star Mira masses of $< 3 M_{\odot}$ ($M_1+M_2 < 6 M_{\odot}$) (Willson 1982) and a separation of around 2×30 AU (so that the water masing region will be gravitationally bound to the M star), we estimate $P_{\text{orb}} > 200$ years. This value is reasonably consistent with $P_{\text{orb}} <$ about 190 years for EU And if we assume a $v_{\text{orb}} > 10/2 \text{ km s}^{-1}$ and $a=30$ AU in a circular orbit.

IRAS color-color plots separate O-rich from C-rich circumstellar material. The IRAS colors defined by Olton et al. (see Table 2) place the four C stars among those with O-rich CS; specifically they lie on the blueward extension of the newly discovered OH masers with similar colors (Lewis, Eder and Terzian 1985) close to or within the location of the optical Miras with periods usually $< 500^{\text{d}}$. This suggests that the M stars associated with the

water masers in the V778 Cyg and EU And systems are likely to be Mira variables with periods in the 400-500^d range. A similar conclusion was reached by Benson and Little-Marenin (1987) from an analysis of other stars with similar strong 10 and 18 μm emission features as V778 Cyg and EU And.

Deguchi et al. (1987) suggest that V778 Cyg is probably not a binary system because companions may perturb the CS enough to inhibit maser emission. The examples they give, α Cet and R Aqr, have (probably) hot white dwarf companions and their weak H₂O and SiO maser emission is likely to be due to their hot companions. However, we note that H₂O and OH masing regions are found around some binary M Miras e.g. X Oph, R Hya and W Hya (Proust, Ochsenbein and Pettersen 1981) and we suggest that EU And and V778 Cyg are systems more like the binary M Miras.

III. SUMMARY

The presence of H₂O maser emission and strong 10 and 18 μm silicate emission features towards EU And and V778 Cyg and 1665/67 MHz OH maser emission towards V778 Cyg indicate the presence of oxygen-rich material in the vicinity of a carbon-rich photosphere. We interpret the observations as being due to a binary system with a C star and an M star component. The CS of the M star absorbs the visible light of the star and allows the detection of the C star in the optical and near infrared region. This interpretation is aided by the observed 1, 12, 25 and 60 μm fluxes of V778 Cyg, which successfully fit a composite M and C star spectrum, and the $>10 \text{ km s}^{-1}$ difference between the radial velocity of EU And and the H₂O maser velocity. We find the suggestion that we are observing the transition from an M star to a C star to be unlikely since the time scales of material in transit through the silicate and maser emission region is too short for oxygen-rich material still to be found in

this region. This scenario also assumes that the MS, S and SC stages of stellar evolution are by-passed in these stars. Abundance analyses of these types of stars suggest the contrary.

The arguments presented above are suggestive but do not constitute a definite proof of the binary hypothesis over the M->C transition model. We suggest two observations which could help to resolve this issue: 1) The detection of SiO maser emission from any of these C stars would greatly weaken the M->C transition model because SiO masers are located in the closer warmer part of the CS shell, usually within $2 R_*$ (<10 AU). Material would transit through this region in about 10 years, which is incompatible with the 40 years since classification. SiO emission has been searched for with negative results in EU And, V778 Cyg and BM Gem by us and Nakada et al. (1987). However, considering the variability of maser emission from these sources, we suggest that they be monitored. 2) Spectroscopic observations in the 3 and 4 μm region should show evidence for the presence of an M star companion, since we estimate that the cross-over in flux between an M and a C star should occur between 2 and 5 μm (Figure 3). Around 4 μm , photospheric absorption bands of SiO are observed in oxygen-rich M stars but not in C and SC stars (Rinsland and Wing 1982) whereas absorption bands due to C_2H_2 and HCN are found around 3.1 μm in C stars and not in M stars (Noguchi et al. 1981). The detection of the 3.1 μm absorption bands e.g. in BM Gem, does not exclude the presence of an M star since in this region M stars show featureless continua. Even if an M star contributes a large amount to the total flux (say <50%), we should still detect the absorption features from the C star.

We would like to gratefully acknowledge helpful discussions with A. Haschick, the assistance of the telescope operators at Haystack Observatory

and NRAO. IRL-M would like to thank the Air Force Office of Scientific Research for a University Resident Research Fellowship to the Air Force Geophysics Laboratory. PJB thanks the Smithsonian Astrophysical Observatory for hospitality during her leave year and the NSF for support of this work under grant AST-86104.

TABLE 1
Observations of the 22 GHz H₂O maser line

Date	JD+ 2400000	V _{main} km s ⁻¹	V FWHM	Flux Jy	V _{blue} km s ⁻¹	Flux Jy	V _{red} km s ⁻¹	Flux Jy	Area W/m ² x10 ⁻²²	RMS Jy
EU And										
12/15/86 ^a	46778	-29.40	0.67	8.2	----	---	----	---	53	0.6
1/23/87	46819	-29.67	0.52	5.6	-31.2	3.0	-26.0	3.0	57	0.9
3/22/87	46877	-----	--	<1.5	-31.4	2.0	-----	--	10	0.5
4/16/87	46908	-29.79	0.49	6.4	-31.0	3.5	-----	---	23	0.8
5/ 4/87	46920	-29.82	0.45	5.5	-----	---	-----	---	24	0.8
5/19/87	46935	-29.8:	--	3.6:	-----	---	-----	---	12	0.7
5/22/87 ^b	46938	-----	--	<1.5	-----	---	-----	---	---	--
6/ 9/87	46955	-29.87	0.46	3.1	-30.9	2.2:	-----	---	7	0.6
10/20/87	47089	-29.96	0.65	2.5	-31.0	1.9	-12.4	2.6	28	0.6
V778 Cyg										
3/23/87 ^a	46878	-16.82	1.1	1.9	----	---	----	---	18	0.5
4/16/87	46908	-16.93	0.63	7.9	-20.5	1.2:	-15.1	1.2	43	0.7
4/30/87 ^b	46916	-16.9	1.0	7.0	-20.5 ^b	1.9 ^c	-15.1 ^c	2.3 ^c	---	--
5/ 4/87	46920	-17.01	.76	7.9	-20.6	2.9	-15.1	2.4	73	0.6
5/19/89	46935	-16.91	.64	7.5	-20.9:	1.6	-15:	1.6	35	1.2
6/ 9/87	46955	-16.94	.66	10.9	-20.7	3.6	-15.1	2.7:	124	0.6
									err+/-5	
no H ₂ O emission detected										
BM Gem					IRAS 19139+5412 ^d					
3/23/87	< 2.7	Jy	3/23/87 < 1.3 Jy							
4/16/87	< 2.6	Jy	4/16/87 < 1.5 Jy							
4/30/87 ^b	< 2.1	Jy (=3xRMS)	10/20/87 < 1.2 Jy							
10/20/87	< 1.5	Jy								

colons are used to indicate uncertain measurements

velocity resolution = 0.09 km s⁻¹ unless otherwise indicated

a) velocity resolution = 0.53 km s⁻¹

b) observations by Nakada et al. (1987)

c) data read from Figure 1 of Nakada et al. (1987)

d) = NC//83 (Stephenson 1985)

TABLE 2
IRAS colors

	$\log v_{S_V}(60)/\log v_{S_V}(25)$	$\log v_{S_V}(25)/\log v_{S_V}(12)$
EU And	-1.337	-0.417
V778 Cyg	-1.336	-0.543
BM Gem	-1.220	-0.571
19139+5412	-1.327	-0.560

REFERENCES

- Baumert, J.H. 1972, Ph.D. thesis (Ohio State University).
- Benson, P.J., and Little-Marenin, I.R. 1987, Ap.J. (Letters), 316, L37.
- Bowers, P.F., and Hagen, W. 1984, Ap.J., 285, 637.
- Chapman, J.M., and Cohen, R.J. 1986, M.N.R.A.S., 220, 513.
- Cooke, B., and Elitzur, M. 1985, Ap.J., 295, 175
- Deguchi, S., Kawabe, R., Ukita, N., Nakada, Y., Onaka, T., Izumiura, H., and Okamura, S. 1987 (preprint)
- Dickinson, D.F., and Dinger, St. Clair A. 1982, Ap. J., 254, 136.
- Dominy, J.F., and Wallerstein, G. 1986, Ap.J., 310, 371.
- Dyck, H.M., Zuckerman, B., Leinert, Ch., and Beckwith, S. 1984, Ap.J., 287, 801.
- Fuenmayor, F.J. 1981, Rev. Mex. Astron. Astrof., 6, 83.
- Gomez Balboa, A.M., and Lepine, J.R.D. 1986, Astr Ap., 159, 166.
- Haschick, A. D. 1986, personal communication.
- Johnston, K. J., Spencer, J. H., and Bowers, P. F. 1985, Ap. J. 290, 660.
- Joint IRAS Science Working Group, Atlas of Low Resolution Spectra, Astr. Ap. (Suppl), 65, 607.
- Kleinmann, S.G., Dickinson, D.F., and Sargent, D.G. 1978, A.J., 83, 1206.
- Lane, A.P., Johnston, K.L., Bowers, P.F., Spencer, J.H., and Diamond, P.J. 1987, (submitted to Ap.J.)
- Lee, O.J. Gore, G.D., and Bartlett, T.J. 1947, Annals Dearborn Obs., 5, pt 1c.
- Lewis, B.M., Eder, J., and Terzian, Y. 1985, Nature, 313, 200.
- Little, S.J., Little-Marenin, I.R., and Price, S.D. 1987, Cool Stars, Stellar Systems and the Sun, Fifth Cambridge Workshop (in press).

- Little-Marenin, I.R. 1986, Ap.J. (Letters), 307, L15.
- Little-Marenin, I.R., Benson, P.J., and Little, S.J. 1987, Cool Stars, Stellar Systems and the Sun, Fifth Cambridge Workshop (in press).
- MacConnell, D.J. 1979, Astr. Ap. (Suppl), 38, 335.
- Mathews, G.J., Takahashi, K., Ward, R.A., and Howard, W.H. 1986, Ap.J., 302, 410.
- Merrill, P.W., Sanford, R.F., and Burwell, C.G. 1933, Publ. A.S.P., 45, 306.
- Nakada, Y., Izumiura, H., Onaka, T., Hashimoto, O., Ukita, N., Deguchi, S., and Tanabe, T. 1987 (preprint).
- Noguchi, K., Kawara, K., Kobayashi, Y., Okuda, H., and Sato, S. 1981, Publ. Astr. Soc. Japan, 33, 373.
- Olnon, F.M., Baud, B., Habing, H.J., De Jong, D., Harris, S., Pottasch, S.R., 1984, Ap.J. (Letters), 278, L41.
- Peery, B.F. 1971, Ap.J., 163, L1.
- Peery, B.F. 1975, Ap.J., 199, 135.
- Proust, D., Ochsenbein, F., and Pettersen, B.R. 1981, Astr. Ap. (Suppl.), 44, 179.
- Reid, M. J., and Moran, J. M. 1981, Ann. Rev. Astr. Ap., 19, 231.
- Rinsland, C.P., and Wing, R.F. 1982, Ap.J., 262, 201.
- Rowan-Robinson, M., and Harris, S. 1983a, M.N.R.A.S., 202, 767.
- Rowan-Robinson, M., and Harris, S. 1983b, M.N.R.A.S., 202, 797.
- Smith, V.V. and Lambert, D.L. 1986, Ap.J., 311, 843.
- Smith, V.V., and Wallerstein, G. 1983, Ap.J., 27, 742.
- Stephenson, C.B. 1973, Pub. Warner & Swasey Obs., Vol 1, no. 4.
- 1985, A.J., 90, 784.

- Utsumi, K. 1985, Cool Stars with Excesses of Heavy Elements, Ap. Space Sc. Library, Vol 114., (eds M.Jaschek and P.C. Keenan)
(Reidel:Dordrecht), p. 243.
- Wallerstein, G., and Dominy, J.F., 1988 (in press).
- Willems, F.J., and de Jong, T. 1986, Ap.J. (Letters), 309, L39.
- Willson, L.A. 1982, in Pulsations in Classical and Cataclysmic Variable Stars, ed. J.P. Cox and Carl J. Hansen (Boulder, CO:JILA), p. 269.
- Winters, R.R., and Macklin, R.L., 1987, Ap.J., 313, 808.
- Wood, P.R. 1985, Cool Stars with Excesses of Heavy Elements, Ap. Space Sc. Library, Vol 114., (eds M.Jaschek and P.C. Keenan)
(Reidel:Dordrecht), p.357.

FIGURE CAPTIONS

Figure 1. The temporal sequence of maser spectra. 1a) The 22 GHz spectra of V778 Cyg between 23 March and 9 June 1987. 1b) The 22 GHz spectra of EU And between 15 December 1986 and 9 June 1987. 1c) The 1665 and 1667 MHz OH spectra of V778 Cyg.

Figure 2. The variation of the 22 GHz maser flux as a function of Julian Date. 2a) (top panel) The integrated area of the V778 Cyg 22 GHz line from 3/23/87-6/9/87. (bottom panel) Solid circle - peak flux of main component at -16.9 km s^{-1} (solid line). Open Circles - the peak flux of the blueshifted component at -20.5 km s^{-1} (dotted line). Triangles - peak flux of the redshifted component at -15.1 km s^{-1} . 2b) (top panel) The integrated area of the EU And 22 GHz lines from 12/15/86-10/20/87. (bottom panel) Solid circle -peak flux at -29.7 km s^{-1} . Open circle-blueshifted component at -31.1 km s^{-1} . Triangle - redshifted component at -26.0 km s^{-1} .

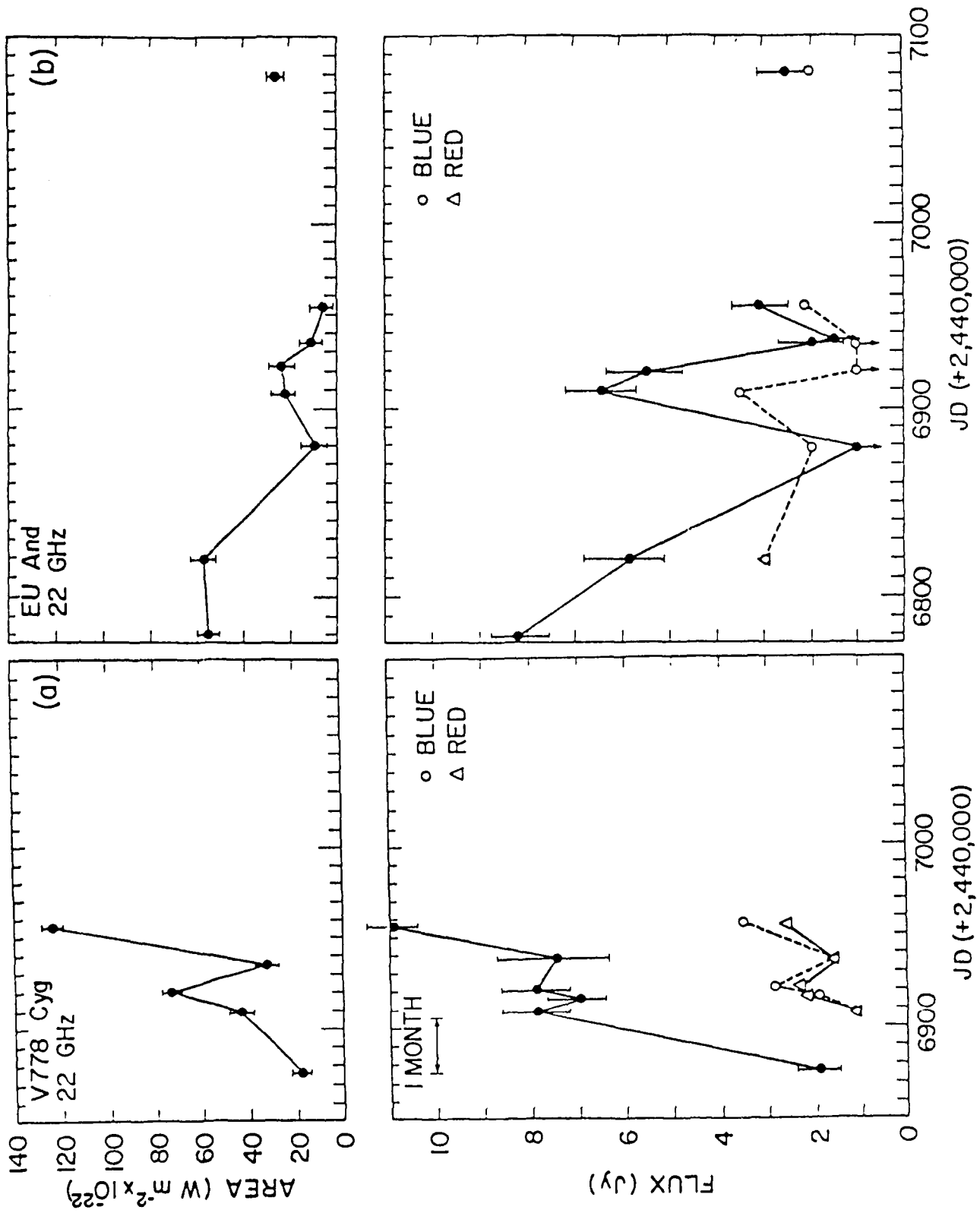
Figure 3. Composite flux calculated from the dustshell models for Y CVn and WX Ser. Triangles -- the observed $0.78 \mu\text{m}$ and $1.08 \mu\text{m}$ flux (Baumert 1972); Solid Circles -- the IRAS fluxes at 12, 25 and $60 \mu\text{m}$ of V778 Cyg.

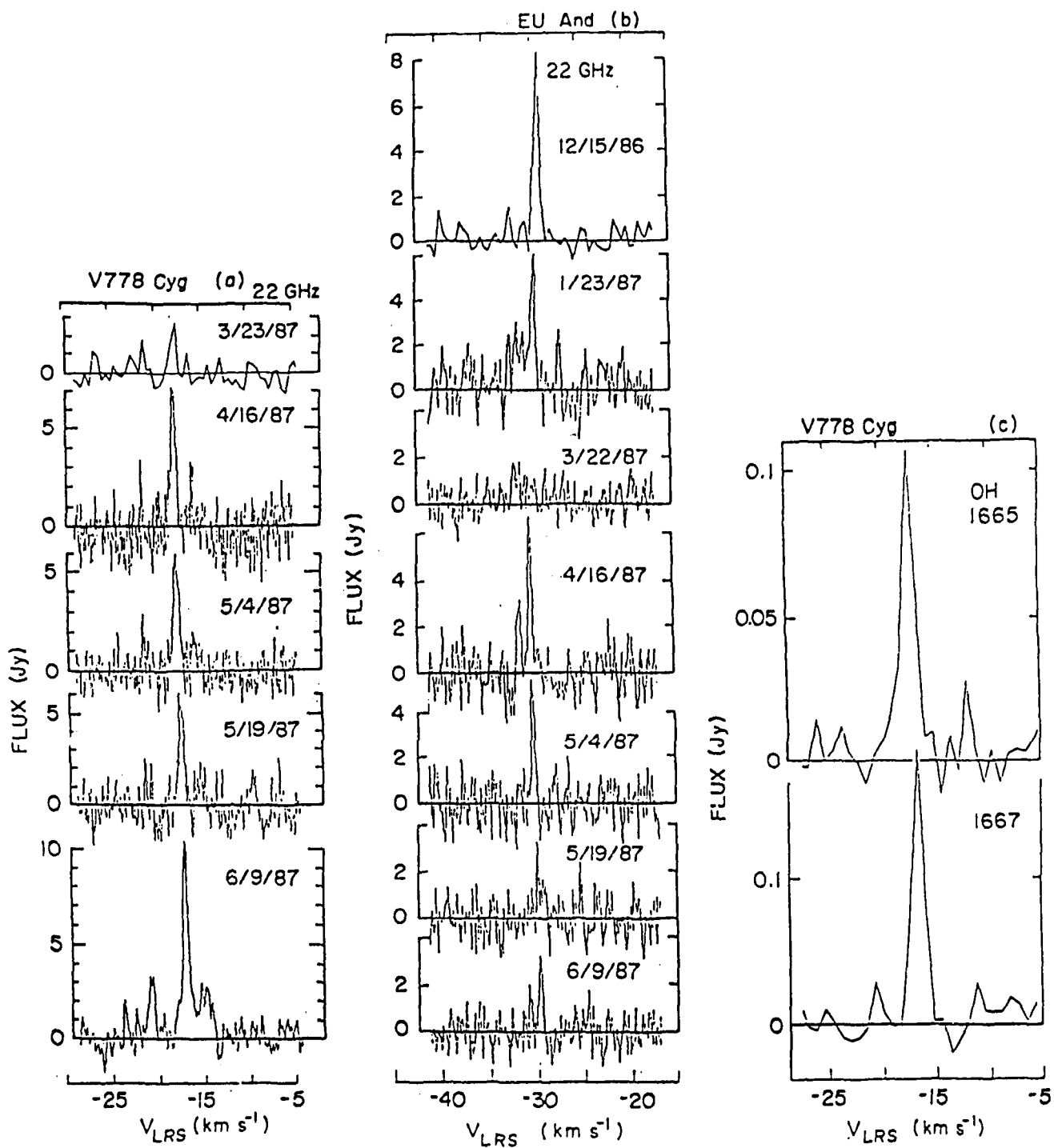
ADDRESSES:

Dr. Priscilla J. Benson, Whitin Observatory, Wellesley College, Wellesley, MA
02181

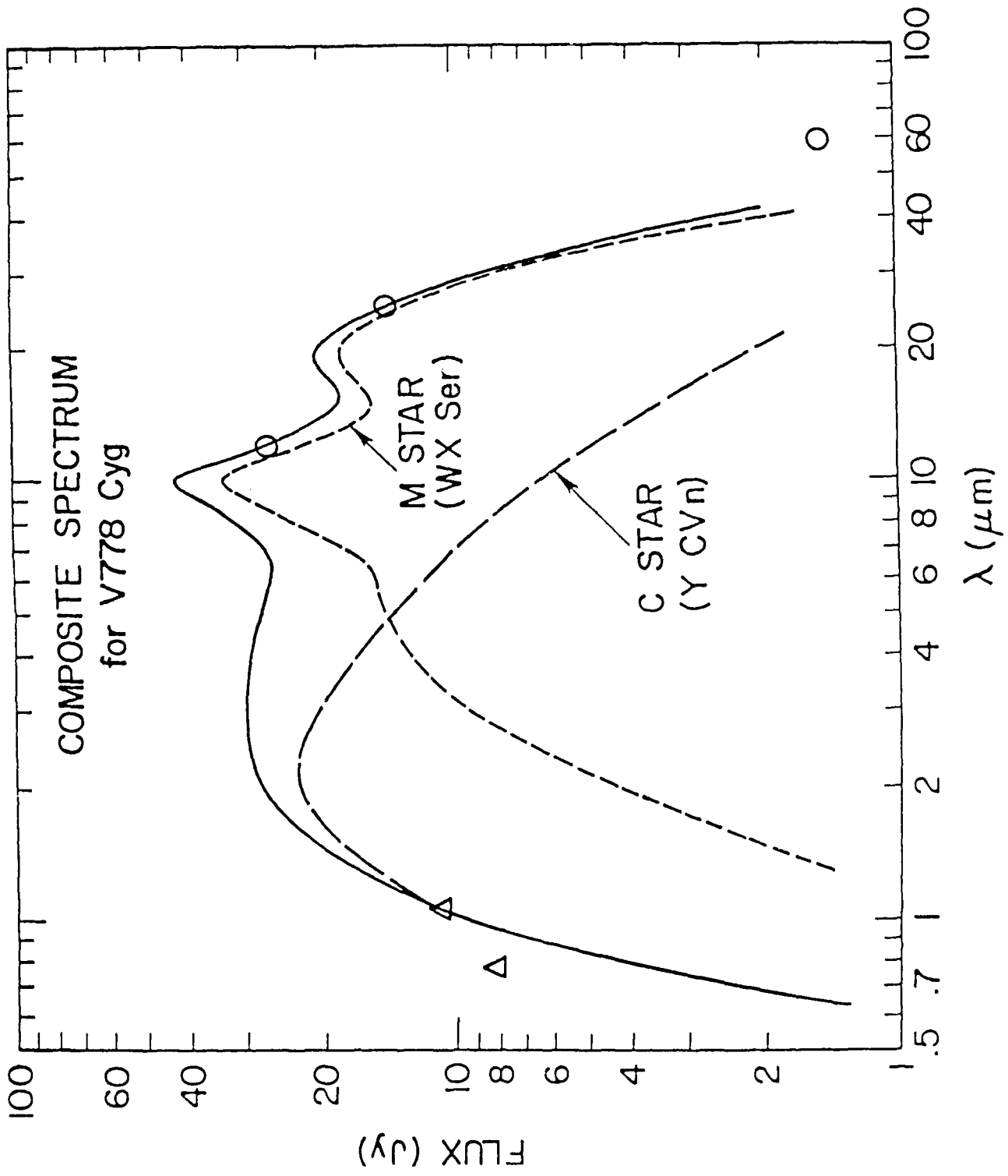
Dr. Dale F. Dickinson, Org. 92-20-205, Lockheed Palo Alto Research Lab., 3251
Hanover St, Palo Alto, CA 94304

Dr. Irene R. Little-Marenin, Whitin Observatory, Wellesley College, Wellesley,
MA 02181





COMPOSITE SPECTRUM
for V778 Cyg



Appendix H

Emission Features in IRAS LRS Spectra of MS, S and SC Stars

submitted to the Astrophysical Journal 333:305-315

EMISSION FEATURES IN IRAS LRS SPECTRA OF MS, S AND SC STARS

Irene R. LITTLE-MARENIN

Air Force Geophysics Laboratory/Optical Physics Division,

Celestial Background, Hanscom AFB, MA 01731 and

Whitin Observatory, Wellesley College, Wellesley, MA 02181

Stephen J. LITTLE

Department of Natural Sciences, Bentley College, Waltham, MA 02254

Received: January 14, 1988

ABSTRACT

We find a progression of emission features due to dust grains observed in the IRAS LRS spectra of the 8-11 μm region in MS, S and SC stars that parallels their increasing C:O ratio and s-process enhancement. Strong S stars usually show a 9 to 14 μm emission feature which peaks around 10.8 μm whereas mild S or MS stars show a variety of features ranging from the typical 10 μm silicate emission to a 3 component feature, to the 10.6 μm S star feature. SC stars show either the S star feature or the SiC feature. A few S stars also show a broad, weak 9 to 15 μm emission feature. The infrared excesses in the 8-22 μm region correlate very strongly with the period of Mira S, MS, and SC variables (but not for semi-regular variables) and increase sharply for Miras with periods between 380 - 400 days. The excesses also correlate with mass loss rate for these stars. No 8-22 μm excesses or dust grain emission features are observed for variables including Miras with mass loss rates of $< 5 \times 10^{-6}$ Mo/yr.

I. INTRODUCTION

Stellar evolution theory predicts (Iben and Renzini 1983) and observations confirm that M stars evolve to MS- \rightarrow S- \rightarrow (SC)- \rightarrow C stars during the late stages of AGB evolution (Wood 1985) when helium shell flashing occurs and helium-burning products, primarily ^{12}C , s-process elements and technetium are mixed with the outer envelope during the third dredge-up phase. The C:O ratio of stars during the transition changes from ~ 0.4 (M stars) to ~ 0.6 (MS stars) (Smith and Lambert 1985, 1986) to ~ 0.8 (S stars) (Smith and Lambert 1986) to ~ 1.0 (SC stars) (Keenan and Boeshaar 1980; Dominy, Wallerstein and Suntzeff 1986) and finally to ~ 1.05 - 1.1 (C stars) (Lambert et al. 1986). At the same time the s-process elements are enhanced from solar abundances to as much as 10-100 times solar in the carbon stars (Smith and Lambert 1985, 1986; Smith and Wallerstein 1983; Dominy and Wallerstein 1986; Utsumi 1985). It is estimated that about 4-15 helium shell flashing episodes with subsequent mixing are necessary to change an M star into an S star or SC star (Smith and Lambert 1986; Mathews et al. 1986; Winters and Macklin 1987; Wallerstein and Dominy 1988) although some stars may skip over the SC evolutionary phase.

Many late AGB stars lose mass rapidly and develop extensive circumstellar dust shells (CDS). The changing photospheric composition of the AGB stars should be reflected in the composition of the dust grains found in the CDS (Little, Little-Marenin and Price 1987) since their lost photospheric material passes through the CDS on a time scale of < 1000 years -- a short time compared to the time of 10^4 - 10^5 years between He shell flashes (Iben and Renzini 1983).

II. ANALYSIS

IRAS obtained low resolution spectra (LRS) (IRAS Science Working Group 1986) of sources brighter than about 8 Jy in the 8-22 μm region in which the emission features of dust grains from silicates at 10 and 18 μm and SiC at 11.2 μm are found. We have analyzed 79 LRS of MS, S and SC stars to see if their changing photospheric composition produces different emission features.

The low resolution spectrometer scanned simultaneously two wavelength ranges, one extending from 7.7-13.4 μm and the other from 11.0-22.6 μm . The two spectrum halves in general do not agree at 12 μm unless a linear baseline is subtracted, contrary to the information provided in the Explanatory Supplement to the IRAS Catalogs and Atlases, Ch. 9 (1984). The four baseline values are stored as part of the header information for each spectrum or can be calculated by averaging the first and last 20 values of each spectrum half. We fit a blackbody energy distribution to the continuum underlying any features that might be present and subtract this black body distribution from the observed spectrum. This procedure allows us to study the spectral characteristics of the emission feature. We characterize the strength of the emission feature as the contrast, C_T , which we define as the percent of the emission above the underlying continuum at the wavelength of maximum emission. Besides the dust grain emission features, the CDS produces excess continuum emission above the stellar photospheric continuum. We define the 8 - 22 μm emission excess, Ex , as the percent of integrated flux in the 8 - 22 μm region above the photospheric continuum. We assumed a 2500 K photospheric temperature for all stars. Table 1 summarizes our findings. Column 1 gives the most common name (in alphabetical order of their variable star name if applicable) where CSS # = number in Stephenson's (1984) Catalog of S Stars. C

1633 is listed in Stephenson's (1973) catalog of carbon stars; however, its LRS spectrum does not show an SiC feature but instead a 3 component feature and we assume it to be an MS star. Columns 2 and 3 give the spectral type, variability class and period as listed in the General Catalog of Variable Stars (GCVS) (Kholopov 1985), Wing and Yorke (1977) or the Yale Bright Star Catalog (Hoffleit and Jaschek 1982). Column 4 lists the derived temperature of the underlying continuum in the 9-14 μm region. For about 80% of the stars with emission features the temperature lies between 600-1000 K. At times more than one temperature is needed to characterize the CDS which produces the 8-22 μm emission excesses, a hotter temperature ($T > 1500$ K) for the 8-9 μm region and a cooler temperature ($T < 500$ K) for the 14-22 μm region. Column 5 lists the contrast, C_{τ} , of any emission feature and column 6 gives the type of feature observed and, in parenthesis, the wavelength of peak emission. The various types of emission features, such as 'S' for the most common S star feature, the 3 component feature and a broad (br) 9-15 μm emission feature are discussed in greater detail below. 'Sil' refers to the 10 μm silicate emission feature observed in the LRS of M stars and SiC to the 11.2 μm feature observed in C stars. Dashes in column 5 and 6 indicate no emission feature is observed and a question mark (?) an emission feature that is difficult to characterize. Column 7 lists the emission excess, Ex , above the photospheric continuum in the 8-22 μm region. In column 8 we list the flux in Janskys at 8 μm as measured in the LRS since Gal et. al (1987) suggest that the strength of the 10 μm silicate emission feature in M variables correlates with the flux at 8 μm , i.e. that the more distant stars (lower $F(8 \mu\text{m})$) selectively show the stronger emission features. No such correlation appears to exist for the S, MS and SC stars except that, as expected at low flux levels, $F(8 \mu\text{m}) < 20 \text{ Jy}$.

only the stronger emission features with $C_T > 20\%$ are detectable above the noise. Column 9 lists the mass loss rates as calculated by Jura (1987); column 10 gives the percent of $10 \mu\text{m}$ silicate emission needed to match the observed S star dust grain feature (discussed below). An asterisk in column 11 indicates a remark at the end of Table 1.

We will exclude from the rest of the discussion the 6 stars listed in Table 1 as spectroscopic MS stars as defined in Little, Little-Marenin and Bauer (1987). These stars show neither enhanced s-process abundances nor Tc (Smith and Lambert 1986; Little, Little-Marenin and Bauer 1987). They are likely to be misclassified M stars, or their MS classification, if correct, is most likely produced by unusual atmospheric conditions. Their LRS are typical of non-variable or low-amplitude early ($< M4$) M stars with no indication of a CDS, i.e. no emission features are visible and their 8-22 μm fluxes are extensions of their photospheric fluxes ($T \sim 2000-4000 \text{ K}$). RT Aql is also excluded from the discussion since it is most likely a misclassified M star and not an MS star. It has no Tc and Keenan, Garrison and Deutsch (1974) observed no ZrO. Its LRS shows the typical 10 and 18 μm silicate emission features found in many variable M stars.

About one third of the remaining 72 spectra show only a smooth 8-22 μm continuum which can, for most stars, be matched with a 2000K to 3000K blackbody energy distribution representative of the photospheric temperatures of these stars. The other two-thirds of the spectra show emission features of weak to moderate strength. As expected from the studies of M stars, we find that 7 out of the 8 non-variable S and MS stars have featureless photospheric continua. Only BD-38°4770 shows a definite emission feature probably due to SiC. It is the only known S star with a pure SiC emission feature and needs

to be investigated further to see whether it is a misclassified C or SC star. It also may be an unrecognized variable star even though IRAS estimated only a 12% probability of it being variable in the infrared, similar to the probabilities observed for the other non-variable stars. Unexpectedly, four out of 23 (17%) S, MS and SC Mira variables show no emission features and no 8-22 μm excess. These are V865 Aql (S7,5e:, P=365^d), T Cam (S4,7e, P=373^d), U Cas (S3,5e, P=277^d) and S Her (M6(S) P=307^d). A few other stars show a cooler, featureless continuum including the two Miras, X And (S3,9 P=346^d T=1200 K) and R Gem (S3,6 P=370^d T=800 K), in which a small infrared excess is present but no dust grain emission feature is observed. Hence stars with featureless continua include all types of stars from the non-variables to the Miras.

III DISCUSSION

The S, MS and SC stars can be divided into three groups: a) 20 stars with featureless 2000 - 4000 K photospheric continua in the 8-22 μm region (discussed above); b) a few stars with featureless continua and cooler than photospheric temperatures (T between 1200 K and 700 K) in the 8-22 μm region; and c) 45 stars with emission features. A few stars defy the above classification scheme and are discussed in the remarks to Table 1.

The IRAS low resolution spectra are characterized according to the shape of their energy distribution and type of emission and absorption features observed in the 8-22 μm region. Spectra with typical oxygen-rich silicate dust grain emission features extending from 8-14 μm with a maximum around 10 μm are characterized as 2n where n=1-9 measures the strength of the 10 μm emission. Many also show the 18 μm emission due to the bending mode of silicates. Spectra with a carbon-rich, SiC dust grain emission features

extending from 10-14 μm and a maximum at 11.2 μm are characterized as 4n where n=1-9 measures the strength of the SiC feature. No other dust grain emission features were recognized in the LRS characterization since none were known; see the Explanatory Supplement to the IRAS Catalogs and Atlases, 1984, chapter 9, for a complete discussion of the 10 different classes. Among the S, MS and SC stars, we find three additional types of weak emission features 1) an emission feature extending from 9-14 μm that peaks in general around 10.8 μm but the maximum can vary from 10.3 to 11 μm , 2) a three component feature extending from 9-14 μm with peaks at 10 μm , 11 μm and 13.1 μm (Little-Marenin, Little and Price 1986), and 3) a broad, weak 9-15 μm emission feature with a poorly defined maximum around 11.4 μm . None of these three features match the narrower (smaller FWHM) spectral characteristics of the typical silicate or SiC emission.

1) The 10.8 μm S star feature

The emission features found in the spectra of S stars in general are weak with an average contrast, C_{τ} , of about 27%. In strong S stars, those with abundance classes between 4 and 9 (i.e. Sx,4 to Sx,9), emission features peak between 10.3-11 μm and have a FWHM value of about 2.4 μm . We will refer to this feature as the S star feature, and we list its wavelength peak in column 6, Table 1. Thomas, Robinson and Hyland (1976) noted this type of feature in the spectrum of π^1 Gru. The LRS of S Cas (S4,6) (Figure 1) illustrates a typical spectrum of this type. The top panel shows the observed spectrum, a 550 K black body energy distribution fitted to the continuum underlying the emission feature, and the difference spectrum (observed - black body) plotted along the wavelength axis. We know of no laboratory spectrum of grains that produces the S star emission feature. However, Gehrz et al. (1984) noted an

emission feature in Nova Aquilae 1982 with a peak at $10.5 \mu\text{m}$. The shape of the Nova Aquilae emission feature appears to be similar to that of S stars. The high abundances of heavier elements in the Nova (Snijders et al. 1984) suggests that both the S star and the Nova Aquilae feature are produced under similar conditions in CDS and/or by the same carrier. We find it unlikely that the feature is due to SiC as suggested by Gehrz et al. (1984) or due to silicates as suggested by Bode et al. (1984) since the wavelength dependence of the Nova Aquilae emission feature agrees with neither (see Figure 5 and 6 in Gehrz et al.). It is possible that silicates combined with an s-process element such as Ba, Zr etc may be responsible for the feature in both the S stars and Nova Aquilae. Unfortunately no s-process elemental abundances could be determined for Nova Aquilae. On the other hand, we find that the feature observed in S star LRS spectra can be modeled reasonably well by a co-addition of the $10 \mu\text{m}$ silicate feature and the $11.2 \mu\text{m}$ SiC feature. The percentage of silicate emission necessary to produce the co-added feature varies from star to star, but tends to lie in the 50%-70% range and is listed in Table 1, column 10. The percent of SiC equals 100 minus the percent of silicate. This simple co-added model fits the width of the feature reasonably well, but is less able to reproduce the smooth emission peak observed in S stars as can be seen in the bottom panel of Figure 1 where the normalized emission feature of S Cas is well modeled with a combined feature of 55% silicate and 45% SiC. It is unclear whether the co-addition of silicate and SiC emission is a valid characterization of the S star feature; it is usually assumed that SiC and silicate dust grains cannot co-exist in chemical equilibrium in CDS.

Wing and Yorke (1977) argue that surveys of S stars and MS stars are incomplete based on their analysis of IRC (Neugebauer and Leighton 1969) S

stars. It is possible ZrO bands were absent on the date of observation or were missed on objective prism plates. Hence, we have collected in Table 2, twenty-six variable stars which show the 10.8 μm S star feature but are classified as M stars. These stars should be re-investigated in order to see if the presence of the 10.8 μm feature can be used as a classification criteria for S stars.

2) the 3 component feature

Some of the S stars with emission features and abundance classes of 1 to 2, the Sx,1 class is also referred to as MS stars, show a 3 component feature with peaks at 10 μm , 11 μm and weakly at 13.1 μm and in some cases a longer wavelength feature that peaks around 19 μm . The intensities of the components relative to each other vary, but in general the ratio of the 10 to 11 μm feature lies between 1.0 and 1.4. These features are clearly different from the 10 and 18 μm silicate emission feature found in many M star spectra. The short wavelength side of the 3 component feature is similar to the M star 10 μm emission but shows considerably more emission longward of 10.5 μm with a FWHM (3 comp.)=2.7 μm as compared to a FWHM (10 μm)= 2 μm . In contrast, the 18 μm silicate feature is broader (FWHM=5.4 μm) than the 19 μm feature (FWHM=4.4 μm), but it is possible that we underestimate the width of the 19 μm emission since the feature is weak and the LRS do not extend beyond 22 μm . If the 3 component and the 19 μm feature are produced by a dust grain of differing composition and/or a different size distribution is not yet known. MgSiO annealed in vacuo can show structure around 10 μm at times with additional components at 9.2 and 11.2 μm (Nuth, Donn and Nelson 1986). Since the 3 component feature shows no peak at 9.2 μm we are probably not observing annealed MgSiO. However, it is possible that a similar process operating on a

different compound produces the 3 component feature. Figure 2 shows the 3 component feature in the LRS spectrum of RT Sco (S7,2) matched with a 700K blackbody energy distribution. The difference spectrum is plotted along the wavelength axis. The bottom panel of Figure 2 shows the composite 3 component feature of several Sx,1 and Sx,2 stars. It is very similar to the 3 component feature found in about 15% of the M stars with emission features (Little-Marenin, Little, and Price 1986). Since weak ZrO bands in MS stars can be missed on objective prism spectra, it is possible that all M stars with 3 component features are unrecognized MS stars.

3) The broad 9-15 μm feature

The three S stars, Z Ant, V635 Sco, and CSS 975, show a broad 9-15 μm emission feature. The poorly defined peak tends to have a maximum around 11.4 μm and features are identified as 'br' in Table 1, column 6 with the wavelength peak enclosed in square brackets. Roughly 30%-40% of variable stars with an LRS characterization of 14, 15, and 16 show this broad, weak type of emission. (An LRS characterization of 1n is supposed to indicate a blue featureless spectrum with $n=1-9$ being two times the spectral index. Only spectra characterized as 18 or 17 show, with few exceptions, no emission features. Over 50% of all the other spectra characterized as 1n tend to show weak, broad emission features.)

VI. MS STARS and SC STARS

Of the 26 MS stars listed in Table 1, only RS Cnc has a pure 10 μm silicate emission feature. Four other stars show various versions of the 3 component feature, five show the S star feature and three the broad 9-15 μm feature. Most of the rest of the stars have featureless continua which are matched with

photospheric temperatures with the exception of T Cet. Its spectrum shows an excess longward of $9 \mu\text{m}$, but no distinct emission feature.

It appears that the dust grain emission features found in MS stars span the range of features found among the M and S stars. Since M stars evolving to MS and S stars are estimated to be AGB stars experiencing the third dredge-up, which produces an increase in s-process elements and carbon, we suspect that the observed range of dust grain emission features in MS stars is related to the change in the photospheric composition of the parent star.

Among the 7 SC stars listed in Table 1, we find 3 (FU Mon, GP Ori and CSS 788) which show a photospheric continuum and the other four show emission features. In figure 3 we plot the observed LRS of S Lyr, UY Cen and R CMi along with blackbody energy distributions representative of their underlying continua and their difference spectra. The normalized difference spectra of the three SC stars are overplotted with different C star emission features (bottom panels). S Lyr and UY Cen show the $10.8 \mu\text{m}$ S star feature which can be matched by a 45 % and 35 % silicate plus 55 % and 65 % SiC feature, respectively (Figure 3a and 3b, bottom panels). In addition the spectrum of UY Cen is best understood as also having an absorption feature around $14 \mu\text{m}$ (Figure 3b) attributed in some C stars to C_2H_2 and HCN by Willems (1987). Similarly, FU Mon appears to show the C_2H_2 and HCN absorption feature but no emission feature. The apparent 8-9 μm emission feature seen in S Lyr (Figure 3a bottom panel) is an artifact because we assumed a single temperature for the CDS in the 8 - 22 μm region. A temperature of 2500 K is needed to fit the 8-9 μm region and a temperature of 640 K to fit the 10-22 μm region. S Lyr appears to be more closely related to the S stars since no obvious C star characteristics are present and Catchpole and Feast (1971) find that ZrO is

stronger in the spectrum of S Lyr than in UY Cen. UY Cen shows both S star and C star characteristics. R CMi may have a nearly pure SiC emission feature (Figure 3c bottom panel) seen in C star LRS, but its spectrum is very noisy and it is difficult to be certain. R CMi also has been classified as a marginal carbon star. A weak emission feature is present in the LRS of AM Cen, but the feature is too weak to classify accurately.

As found for the MS stars, the emission features observed in SC star spectra may reflect the changing photospheric composition of stars evolving to C stars. We have not distinguished between SC and CS stars.

V. STARS STRONG 10 μ m EMISSION

TT CMa, CSS 1146 and CSS 1259 have very strong 10 μ m silicate emission features, atypical of the other S stars, with a contrast C_r of 100%, 140% and 100% respectively. CSS 1146 appears to be incorrectly listed as an S star in Stephenson's (1984) catalog. Its spectrum appears to be late M (Allen et al. 1977; Pesch private communication). Nothing unusual is known about the two other stars; both TT CMa and CSS 1259 show LaO bands on objective prism plates. It is possible that the latter two objects are binary stars with components close in mass, as has been suggested for the C stars which show very strong 10 and 18 μ m emission features in their LRS (Benson and Little-Marenin 1987; Little-Marenin, Benson and Little 1987; Little-Marenin, Benson and Dickinson 1987). The silicate emission is hypothesized to come from an M star with a CDS which depresses its visible light so that the S star is predominant in the visible and near infrared region. Since the spectra of M and S stars are very similar in the 2-5 μ m region, it will be very difficult to spectroscopically distinguish between an M and S star component in 2-5 μ m spectral range where the cross-over in flux between the S star and the M star

component is estimated to lie. In IRAS color-color plots (see for example Zuckerman and Dyck 1986), TT CMa and CSS 1250 are located among the M stars and not among the other S stars suggesting that their CDS are more characteristic of the oxygen rich material of M stars than of the material located around S stars.

VI. PERIOD VERSUS 8 - 22 μm EXCESS

We searched for a correlation between the infrared 8-22 μm excess of S, MS and SC Miras and their period. We defined the 8-22 μm excess as the percent of integrated flux in the 8-22 μm region that lies above the estimated photospheric continuum and is listed in Table 1, column 8. We assumed a 2500 K photospheric temperature for all the stars since in the 8-22 μm region the shape of the black body energy distribution varies very little for $T > 2000$ K. We normalized the black body energy distribution to the observed spectrum at 8 μm , i.e. we are assuming that at 8 μm we are observing emission from the photosphere only. This is a reasonable approximation for spectra with weak emission features but it underestimates the excess for spectra with strong emission features since models for these have shown that the CDS can contribute significantly to the flux at 8 μm . Varying the adopted photospheric temperature from 2000K to 3000K produced an uncertainty in the derived 8-22 μm excess by about 10%. However, the uncertainties in the excesses are as much as 20% - 30% for stars with low S/N LRS (those with 8 μm fluxes of < 15 Jy) since it is difficult to determine the continuum temperature. It is also difficult to define weak emission features in these noisy spectra.

Figure 4 shows the 8-22 μm excess plotted against the period for Miras (open circles) and SR variables (crosses). A clear trend can be seen. S, MS

and SC Miras with $P > 400^d$ have excesses that are larger than 40% and Miras with $P < 370^d$ have excesses usually less than about 15%. In the 370-400^d range the amount of excess for Miras rises sharply. No trend with period is observed for the SR variables except that the few SR's with periods between 300-390^d show the same amount of excess as the Miras in this period range suggesting a fundamental similarity between these stars and the Miras. The major anomaly is TT CMa which has a strong 10 μm silicate emission feature and a very large excess and may be part of a binary system. Jura (1987), who correlated the ratio of the 2 μm IRC flux to the 25 μm IRAS flux versus period, reached a similar conclusion that the 25 μm excess for all S stars increases sharply for stars with $P > \sim 360$ days.

Figure 5 shows that our 8-22 μm excesses correlate fairly well with the mass loss rates for S stars as calculated by Jura (1987) for all types of stars - Mira, SR, Lb variables and non-variables. On the other hand only for Miras do we find that the mass loss rate correlates with period (Figure 6). For mass loss rates $< 5 \times 10^{-8} M_{\odot}/\text{yr}$ no dust grain emission features are observed and only W Cet and V441 Cyg show a very weak 8-22 μm excess. However, the presence and strength of dust grain emission features in the 8-22 μm region do not appear to correlate with mass loss rate. Whereas the mass loss rate varies by a factor of a hundred among the Mira MS and S stars, the contrast of the emission feature varies, seemingly randomly, by only a factor of two. For example, W Aql, the star with the largest mass loss rate of $4.5 \times 10^{-6} M_{\odot}/\text{yr}$ has one of the weakest emission features ($C_{\tau}=16$). Hence it appears that the amount of material emitting continuum radiation in the CDS is related to the mass loss rate (as expected) whereas the presence and strength

of grain emission features appear not to be driven directly by the mass loss rate.

Jura (1986) found that C star Miras with $P > 400^d$ tend to have larger mass loss rates. Hence, it appears that mass outflow increases significantly for S, MS, SC and C Miras with $P > 370$ days. On the other hand DeGiola-Eastwood et al. (1981) observed an increase in the infrared excess for M star Miras with $P > 200$ days, i.e. for significantly shorter periods than for the more evolved stars. Whether or not the same correlation between period and mass loss rate exists for M Miras as for the more evolved stars should be investigated. Also, the radioactive element technetium, as a tracer of the third dredge-up, is found predominately in M Miras with $P > 300^d$ (Little, Little-Marenin and Bauer 1987). It is likely that the onset of the third dredge-up should produce an increase in mass loss rate and infrared excess and should be observed for M Miras with $P > 300^d$ rather than for $P > 200^d$ as suggested by DeGiola-Eastwood et al. (1981).

Whereas 4 out of 23 (17 %) of S, MS and SC Miras have no 8-22 μ m excesses or emission features, we find that less than 2% of the ordinary M Miras have featureless photospheric continua. These M Miras (VX Aur, S Car, V581 CrA, S Gem, X Gem, RU Lib and RW Pup) as well as the MS and S Miras without emission features have $P < 400^d$ except for V581 CrA which has a very uncertain 1100 day period (Kholopov 1985). The significantly smaller percentage of M star Miras with featureless continua may indicate that for M Miras the mass loss rate or the transparency of CDS or some other factor differs significantly from that of MS, S, and SC Miras.

VII. CONCLUSIONS

We find that the emission features of the MS, S, and SC stars show a

progression of features with spectral class. Features in MS stars range from the 10 μm silicate emission and 3 component feature found in M star spectra, to the 10.8 μm S star feature. Strong S stars show a characteristic emission feature which peaks in the 10.3-11 μm range and SC stars show features characteristic of S and C stars. A few MS and S stars show a weak, broad 9-15 μm emission feature often found in M star LRS spectra. The exact nature of the carrier of the 3 component, the 10.5-11 μm feature and the broad 9-15 μm feature remains unidentified. However, the different emission features are likely to be related to the changes in photospheric composition observed in stars that evolve from M stars with $C/O < 1$ to C stars with $C/O > 1$ accompanied by a dramatic increase in s-process abundances. Since more and more of the available oxygen is tied up in CO as stars evolve from M \rightarrow S stars and s-process elements become more available, we propose that dust grains with different compositions are produced in the CDS. The 3-component feature and the typical 10.8 μm S star feature are also found in a few stars classified as M stars. Whether or not these stars are related in their photospheric composition to the MS and S stars needs to be investigated.

The 8-22 μm emission excess correlates with the period of pulsation for the Miras in our sample showing a dramatic increase in emission excess for periods between 370-400 days. No correlation between the period and 8-22 μm excess of SR variables is found. The excess emission all types of variables (Mira, SR and Lb) and non-variables correlates fairly well with their mass loss rates.

IRL-M would like to thank the Air Force Systems Command for a University Resident Research Fellowship to Air Force Geophysics Laboratory, OPC. SJL thanks Bentley College for an Assigned Time grant for research.

TABLE 1
 MS, S and SC Stars

No.	Name (1)	Sp. Class (2)	Var P (3)	Temp (4)	C_T (5)	feature (6)	Ex Flx(8) (7) (8)	M_O /yr (9)	% Sil (10)	Note (11)
<u>STRONG S STARS</u>										
1	X And	S 3,9e	M	346	1200	-- --	15 18	2.1(-7)		
2	BI And	S 8,8	SR	160	2500	-- --	<1 13	4.0(-8)		
3	Z Ant	S 5,4	SR	104	520	53 br[11.2]	75 22			*
4	W Aql	S 3,9e	M	490	650	16 S(10.8)	57 732	4.5(-6)	70	
5	V865 Aql	S 7,5e:	M	365	2500	-- --	< 2 30	4.7(-8)		
6	T Cam	S 4,7e	M	373	2500	-- --	< 2 61	5.0(-8)		
7	WX Cam	S 5,8	Lb		2500	-- --	<10 7	1.7(-7)		
8	BD Cam	S 5,3	Lb		2500	-- --	< 1 64	1.7(-8)		*
9	S Cas	S 4,6e	M	612	550	25 S(10.5)	>80 270	2.2(-6)	65	
10	U Cas	S 5,5e	M	277	2500:	-- --	< 8 8	4.6(-8)		
11	WY Cas	S 6.5pe	M	477	600	30 S(10.8)	55 44	7.5(-7)	50	
12	IW Cas	S 4.5,9e	M	396	650	20 S(10.8)	49 45		50	
13	TT CMa	S	M	314	650	100 sil.	>97 13			*
14	VX Cen	S 8,5e	SR	308	2500	wk ?	5 68			*
15	R Cyg	S 4,9e	M	426	750	24 S(10.4)	47 109	6.2(-8)	55	
16	AA Cyg	S 7,5	SRb	213	1000	wk wk	10: 50	8.1(-8)		
17	V441 Cyg	4,6	SRa	375	1200	wk?	13 12	4.2(-8)		
18	R Gem	S 5,9e	M	370	800	-- --	20 29	1.4(-7)		
19	DY Gem	S 8,5	SRa1145	700	34	S(11:)	42 22	1.1(-7)	45:	
20	π^1 Gru	S 5,7e	SRb 150:	750	28	S(10.7)	43 993		50:	
21	R Lyn	S 4,7e	M	379	2000	27 S(10.5)	10 26	6.2(-8)	--	
22	SU Mon	S 3,6	SRb		2500:	23 S(10.9)	9 24	6.3(-8)	30	
23	V521 Oph	S 5,4	SRb 320	3500	-- --	< 8 51	4.5(-8)			
24	RZ Sgr	S 4,4ep	SRb 223	700	wk --	35 41				
25	ST Sgr	S 5,5e	M	395	1000	23 S(10.8)	30 58	9.5(-8)	60	
26	ST Sco	S 4,6	SRa 195	800	24 br[11.6]	30 57	6.6(-8)			*
27	V635 Sco	S 7,6	Lb		2500	-- --	< 3 18			
28	UU Vel	S 7,8e	M	409	1500	60: S(11:)	20: 14		35:	
29	EP Vul	S 6,5	Lb		900	25 11.2	20 37	6.5(-8)		*
30	HD 191630	S 4,4	-----	2500	-- --	< 2 15				
31	BD-38°4770	S 4,6	-----	1000	22	SiC	20 15			*
<u>MILD S and MS STARS</u>										
32	W And	S 6,1e	M	390	950	23 3 comp	31 187	2.7(-7)		
33	RW And	S 6,2e	M	430	750	? ?	53 39	2.3(-7)		*
34	NO Aur	M2SIab	Lc		800	37 S(10.8)	39 /		50	
35	RS Cnc	M6IIIaSe	SRc 120:	1000	30	sil.	32 415			
36	V365 Cas	S 7,2	SRb 136	1200	28:	S(10.5)	20 24	7.9(-8)	60:	
37	T Cep	M 6.5e	M	388	800	11 br[11.3]	32 869			
38	T Cet	M5-6SIIe	SRc 159	700	wk?	--	22 220			
39	W Cet	S6,3-9,2e	M	351	1000	-- --	7 16	3.3(-8)		
40	TV Dra	M6p(S)	Lb		800	9 br[11.3]	27 66	7.1(-8)		
41	S Her	M6(S)e	M	307	2500	-- --	< 3 45			

42	ST Her	M6-7IIIIaS	SRb	148	650	14	S:(11:)	33	209		35:	
43	OP Her	M5IIb(S)	SRc	121	3500	--	--	< 1	80			*
44	R Hya	M6.5(S)e	M	389	760	11	br[11.4]	35	2068			
45	Y Lyn	M6SIb-II	SRc	110	950	37	S:(10.3)	40	135		90	
46	RR Mon	S 7,2e	M	393	800	30:	3 comp	41	19	1.5(-7)		
47	4o ¹ Ori	M3.2IIIIaS	SRb	30:	2500	--	--	< 1	113			*
48	HT Per	M6(S)	SR:	128:	600	27	S(10.5)	50	17		50:	
49	SU Pup	S 4,2e	M	340	800	30	3 comp	43	15			
50	RT Sco	S 7,2	M	449	700	20	3 comp	52	174			
51	DK Vul	S 4,2	SRa	370	800	?	?	16	19	1.6(-7)		*
52	HD 35155	S 4,1	-----	2500		--	--	< 6	10	2.9(-8)		
53	HD 49683	M4S	-----	3000		--	--	< 6	8	3.0(-8)		
54	HD 92681	S 5,2	-----	2500		--	--	< 1	13			
55	HD 110994	S 5,1	-----	3500		--	--	< 3	21			
56	HD 118685	S 6,2	-----	2500		--	--	< 2	34			*
57	BD-36 ^o 4827	S 5,2	-----	3500		--	--	< 2	12			

SC STARS

58	R CMi	SC5/10=C5,1	M	338	3500	50:	SiC:	15:	16			
59	UY Cen	SC6/8	SR	115	1200	23	S(11:)	9	63		35	*
60	AM Cen	SC	Lb		2500	v.wk	?	2	20			*
61	S Lyr	SCe	M	438	630	20	S(10.9)	42	54		45	*
62	FU Mon	C8,0J;CS	SR	310	4000	--	--	< 1	21			*
63	GP Ori	C8,0J,SC	SRb	370:	2500	--	--	<10	12			
64	CSS 788	SC;S5,8	---	---	3500	--	--	< 3	24			

S STARS WITH LITTLE INFORMATION

65	CSS 861	S			5:0	57	non S	52	15			*
66	CSS 929	Se			600	22	S(10.8)	51	60		50	
67	CSS 975	S			2500	45:	br[11.4]	20:	15			
68	CSS 1011	S	var		800	30:	S:(10.9)	26:	8		40:	
69	CSS 1043	Se			1000	28	3 comp:	26	21			
70	CSS 1146	S			380	140	sil	>290	32			*
71	CSS 1259	S			375	97	sil	>210:	6			
72	C 1633				850	25	3 comp	36	45			*

SPECTROSCOPIC MS STARS

73	CU Dra	M3III	Lb:		3000	--	--	0	92		=BS 5226	
74	NZ Gem	M3II-IIIIS	SR		3500	--	--	0	36		=BS 2967	
75	DE Leo	M2IIIabS	SRb		4000	--	--	<12	25		=BS 4088	*
76	GZ Peg	M4IIIS	Lb?		3500	--	--	0	124		=BS 8815	
77	BS 2508	M2IIIS	-----		3000	--	--	0	42			
78	BS 7442	M5IIIaS	-----		3000	--	--	0	31			

M STAR

79	RT Aql	M6eS	M	327	620	24	sil	42	83			*
----	--------	------	---	-----	-----	----	-----	----	----	--	--	---

Notes:

3 Z Ant: noisy; broad feat., max at 11.2 μ m and weak peaks at 10 and 13 μ m

8 BD Cam = BS 1105, excess shortward of 9.5 μ m

- 13 TT CMa: no 18 μm emission feature
- 14 VX Cen: weak broad 9.5 - 16 μm emission feature
- 16 AA Cyg: weak, broad emission feature
- 26 ST Sco: broad 9.5 - 15 μm emission feature
- 29 EP Vul: emission feature with peaks at 11.3 and 13 μm ; not SiC
- 31 BD-38^o4770: emission matches 11.3 μm SiC feature; maybe C star?
- 33 RW And: possible self-absorption at 10.5 μm
- 43 OP Her = BS 6702
- 47 4o¹ Ori: emission excess shortward of 9.5 μm
- 51 DK Vul: possible 9.5 - 15 μm emission or possible 9.5 μm absorption feature
- 56 HD 118685: emission excess shortward of 9.5 μm
- 59 UY Cen: absorption feature at 14 μm , probably due to C₂H₂ and HCN
- 60 AM Cen: very weak emission feature is present
- 61 S Lyr: LaO absorption at .74 and .79 μm ; possibly an S star.
- 62 FU Mon: possible C₂H₂ and HCN absorption feature at 14 μm
- 65 CSS 861: asymmetric 9-14 μm emission feature with peak at 10.4 μm
- 67 CSS 975: broad 9.5 - 15 μm emission feature
- 70 CSS 1146: late M not S
- 72 C 1633: classified as C star; emission feature more typical of MS stars
- 75 DE Leo: emission excess shortward of 9.5 μm
- 79 RT Aql: no ZrO, no Tc (Little-Marenin, Little and Bauer 1987); prob. M

colon (:) indicates uncertain value; wk = weak feature;

column 6: sil=10 μm silicate ft.; br=broad 9-15 μm ft.; S=10.8 μm S star ft.

Table 2
Stars with 10.8 um S star Feature

Name	Sp.Cl.	F(8μm)	Name	Sp.Cl.	F(8μm)
V	Aps M8	29	FZ	Hya M6	77
V429	Aql M2-M6	19	SV	Lib --	38
W	Aqr M6e	56	RS	Lyn M7	33
SV	Aqr Mb	52	EW	Peg M6	14
W	Ara MSIII	29	AE	Per M5	25
UX	Ara --	30	GH	Per M6.5	49
VY	Cas M6-M7	34	R	Psc M3e-M6e	25
VX	Cep M8	41	Y	Pup M7	43
V405	Cyg M6.5	42	SU	Sgr M6	
V702	Cyg M5	23	V1692	Sgr M9	22
V	Eri M6II	238	V	Tel Mc	95
AM	Gem M10	15	SU	Vel Mc	145
S	Gru M8IIIe	103	SZ	Vel M5e	40

REFERENCES

- Allen, D.S., Hyland, A.R., Longmore, A.J., Caswell, J.L., Goss, W.M., and Haynes, R.F. 1977, Ap.J., 217, 108.
- Benson, P.J., and Little-Marenin, I.R. 1987, Ap.J. (Lett), 316, L37.
- Bode, M.F., Evans, A., Whittet, D.C.B., Aitken, D.K., Roche, P.K., and Whitmore, B. 1984, M.N.R.A.S., 207, 897.
- Catchpole, R.M. and Feast, M.W. 1971, M.N.R.A.S., 154, 197.
- DeGiola-Eastwood, K., Hackwell, J.A., Grasdalen, G.L., and Gehrz, R.D. 1981, Ap.J., 245, L75.
- Dominy, J.F., and Wallerstein, G. 1986, Astrophys.J., 310, 371.
- Dominy, J.F., Wallerstein, G., and Suntzeff, N.B. 1986, Astrophys.J., 300, 325.
- Explanatory Supplement to the IRAS Catalogs and Atlases, 1984, Ed. C.A. Beichman, G. Neugebauer, H.J. Habing, T.E. Clegg, T.J. Chester. Washington, DC: US Govt. Print. Office.
- Gal, O., de Muizon, M., Papoular, R., and Pegourie, B. 1987, Astron. Ap., 183, 29.
- Gehrz, R.D., Ney, E.P., Grasdalen, G.L., Hackwell, J.A., Thronson Jr, H.A. 1984, Ap.J., 281, 303.
- Hoffleit, D., and Jaschek, C. 1982, Bright Star Catalogue, (Yale University Press: New Haven).
- Iben, I., Jr., and Renzini, A. 1983, Annu. Rev. Astron. Astrophys., 21, 271.
- IRAS Science Working Group. 1986, Atlas of Low Resolution Spectra, Astr. Ap., (Suppl.), 65, 607.
- Jura, M. 1986, Ap.J., 303, 327.

- Jura, M. 1987, (submitted for publication).
- Keenan, P.C., and Boeshaar, P.C. 1980, Astrophys.J.Suppl., 43, 379.
- Keenan, P.C., Garrison, R.F., and Deutsch, A.J. 1974, Ap.J. (Suppl.), 28, 271.
- Kholopov, P.N., ed. 1985, General Catalog of Variable Stars (4th ed., Moscow: Nauka).
- Lambert, D.L., Gustafsson, B., Eriksson K., and Hinkle, K.H. 1986, Astrophys.J. Suppl., 62, 373.
- Little, S.J., Little-Marenin, I.R., and Bauer, W.H. 1987, Astron.J., 94, 981.
- Little, S.J., Little-Marenin, I.R., and Price, S.D. 1987, Cool Stars, Stellar Systems, and the Sun, Fifth Cambridge Workshop (in press).
- Little-Marenin, I.R., Benson, P.J., and Dickinson, S.J. 1988, Ap.J. (accepted for publication)
- Little-Marenin, I.R., Benson, P.J., and Little, S.J. 1987, Cool Stars, Stellar Systems and the Sun, Fifth Cambridge Workshop (in press).
- Little-Marenin, I.R., Little, S.J., and Price, S.D. 1986, NASA Tech. Mem. 88342, p. 137.
- Mathews, G.J., Takahashi, K., Ward, R.A., and Howard, W.H. 1986, Astrophys.J., 302, 410.
- Neugebauer, G., and Leighton, R.B. 1969, Two Micron Sky Survey-a preliminary catalog, NASA SP-3047.
- Nuth III, J.A., Donn, B., and Nelson, R. 1986, Ap.J., 310, L83.
- Smith, V.V. and Lambert, D.L. 1985, Astrophys.J., 294, 326.
----- 1986, Astrophys.J., 311, 843.
- Smith, V.V., and Wallerstein, G. 1983, Astrophys.J., 27, 742.
- Snijders, M.A.J., Batt, T.J., Seaton, M.J., Blades, J.C., and Morton, D.C. 1984, M.N.R.A.S., 211, 7p.

- Stephenson, C.B. 1973, Publ. Warner & Swasey Obs., 1, No.4.
- 1984, Publ. Warner & Swasey Obs., 3, No. 1.
- Thomas, J.A., Robinson, G., and Hyland, A.R. 1976, M.N.R.A.S., 174, 711.
- Utsumi, K. 1985, Cool Stars with Excesses of Heavy Elements, Ap. Space Sc. Library, Vol 114., (eds M.Jaschek and P.C. Keenan) (Reidel:Dordrecht), p. 243.
- Wallerstein, G., and Dominy, J. F. 1988, Ap.J. (in press).
- Willems, F.J. 1987, (Ph.D. thesis, University of Amsterdam).
- Wing, R.F., and Yorke, S.B. 1977, M.N.R.A.S., 178, 383.
- Winters, R.R., Macklin, R.L. 1987, Ap.J., 313, 808.
- Wood, P.R. 1985, Cool Stars with Excesses of Heavy Elements, Ap. Space Sc. Library, Vol 114., eds M.Jaschek and P.C. Keenan (Reidel:Dordrecht), p. 357.
- Zuckerman, B. and Dyck, M.H. 1986, Ap.J., 311, 345.

FIGURE CAPTIONS

Figure 1. The observed spectrum of S Cas is matched with a 550 K blackbody energy distribution (top panel). The difference spectrum (observed-black body distribution) is plotted along the wavelength axis. The emission feature is typical of the S stars. The normalized difference spectrum is matched with a blend of 55% silicate + 45% SiC (bottom panel).

Figure 2. The observed spectrum of RT Sco is matched with a 700 K blackbody energy distribution (top panel). The difference spectrum (observed - blackbody energy distribution) is plotted along the wavelength axis. In the bottom panel the average 3 component feature with peaks at 10, 11 and 13.1 μm observed in some M stars can be compared to the very similar 3 component feature observed in mild S and MS stars.

Figure 3a. The observed spectrum of the SC star, S Lyr, is matched with a 640 K blackbody temperature (top panel). The difference spectrum is plotted along the wavelength axis. The normalized difference spectrum is overplotted with the spectrum of the C star C 2976 (Stephenson 1973). The long wavelength end of the emission feature of the two stars matches quite well. However, the short wavelength side of the feature can be matched by the co-adding a silicate and an SiC feature.

3b. The observed spectrum of UY Cen is matched to an 1800 K blackbody energy distribution (top panel). The difference spectrum is plotted along the wavelength axis. The normalized difference spectrum of UY Cen is overplotted with the difference spectrum of W Ori. A contribution of possible silicate emission to the spectrum of UY Cen at the short wavelength side can be seen.

An additional absorption feature around $14 \mu\text{m}$, attributed to C_2H_2 and HCN can be seen in both spectra.

3c. The observed spectrum of R CMi (smoothed over 5 points) is matched with a 3500 K blackbody energy distribution. The difference spectrum is plotted along the wavelength axis. The difference spectrum (smoothed over 3 points) is overplotted with an average SiC feature calculated from many C stars spectra. The two features match reasonably well. No additional emission at the short wavelength side of the feature (as is observed for the S stars) appears to be present.

Figure 4. The $8 - 22 \mu\text{m}$ excess is plotted versus the period of MS, S and SC Miras (open circles) and SR variables (crosses). The rapid onset of excess emission for Miras with periods > 370 days can be seen. Arrows on the data points indicate upper and lower limits.

Figure 5. The mass loss rate of Miras (o) and SR and Lb variables (x) is plotted versus their $8 - 22 \mu\text{m}$ excess. Stars with mass loss rates of $< 5 \times 10^{-6} M_{\odot}/\text{yr}$ show no emission features in their spectra and only W Cet and V441 Cyg show a weak excess. Arrows on the data points indicate upper and lower limits.

Figure 6. The mass loss rates of Miras (dots) and SR variables (x) are plotted versus their period. The mass loss rate increases with period for Miras but shows no correlation with period for the SR variables.

Addresses:

I.R. Little-Marenin, Whitin Observatory, Wellesley College, Wellesley, MA

02181

Stephen J. Little, Department of Natural Sciences, Bentley College, Waltham,

MA, 02254

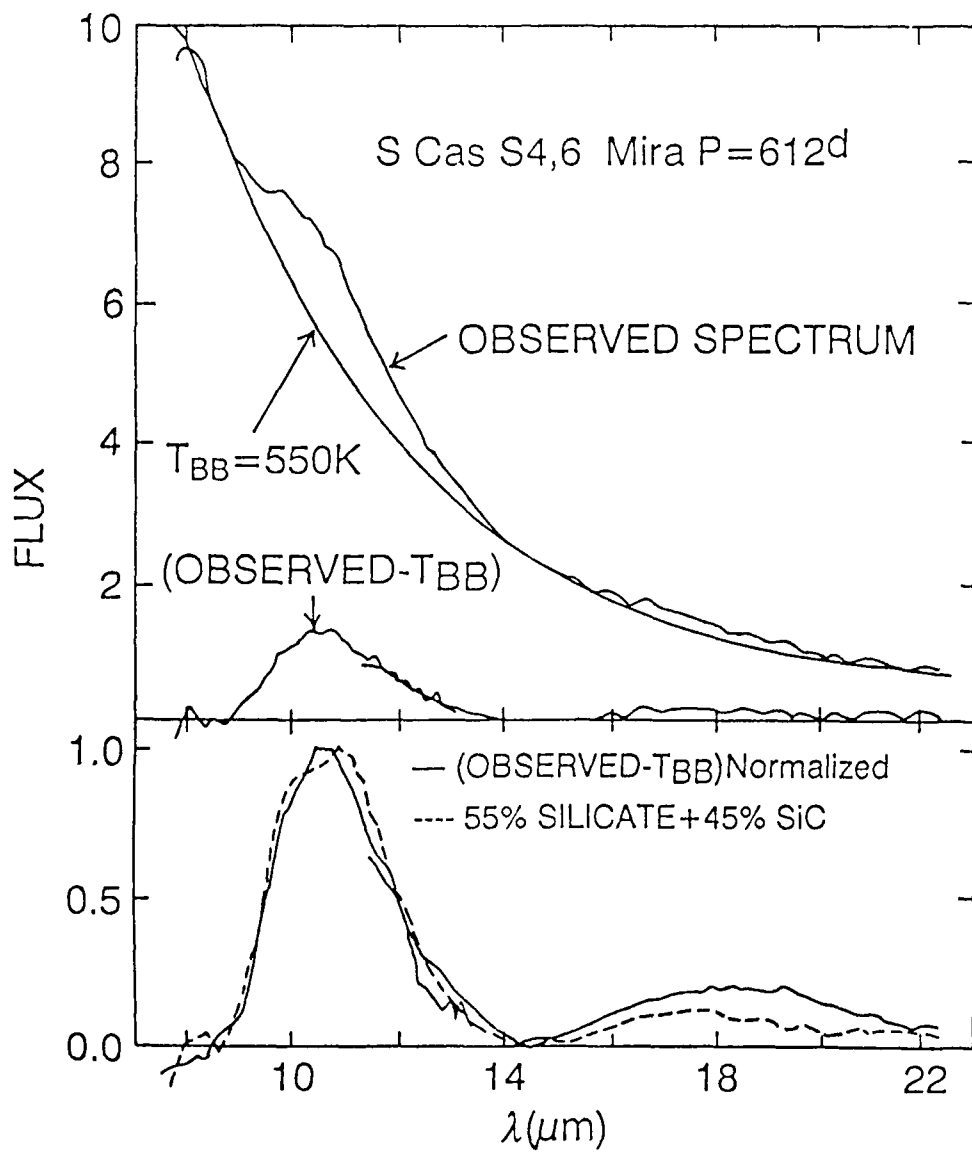


Figure 1

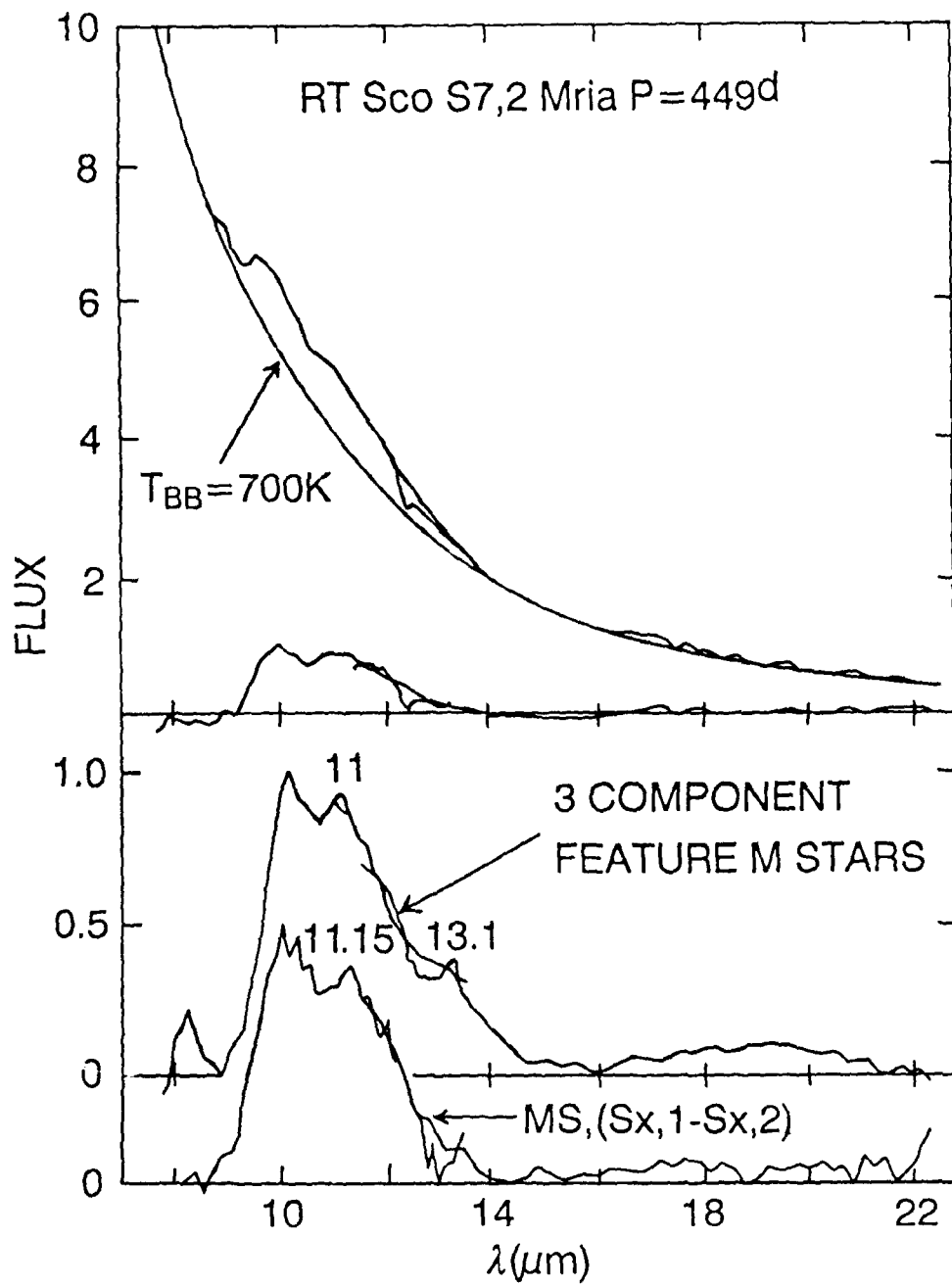


Figure 2

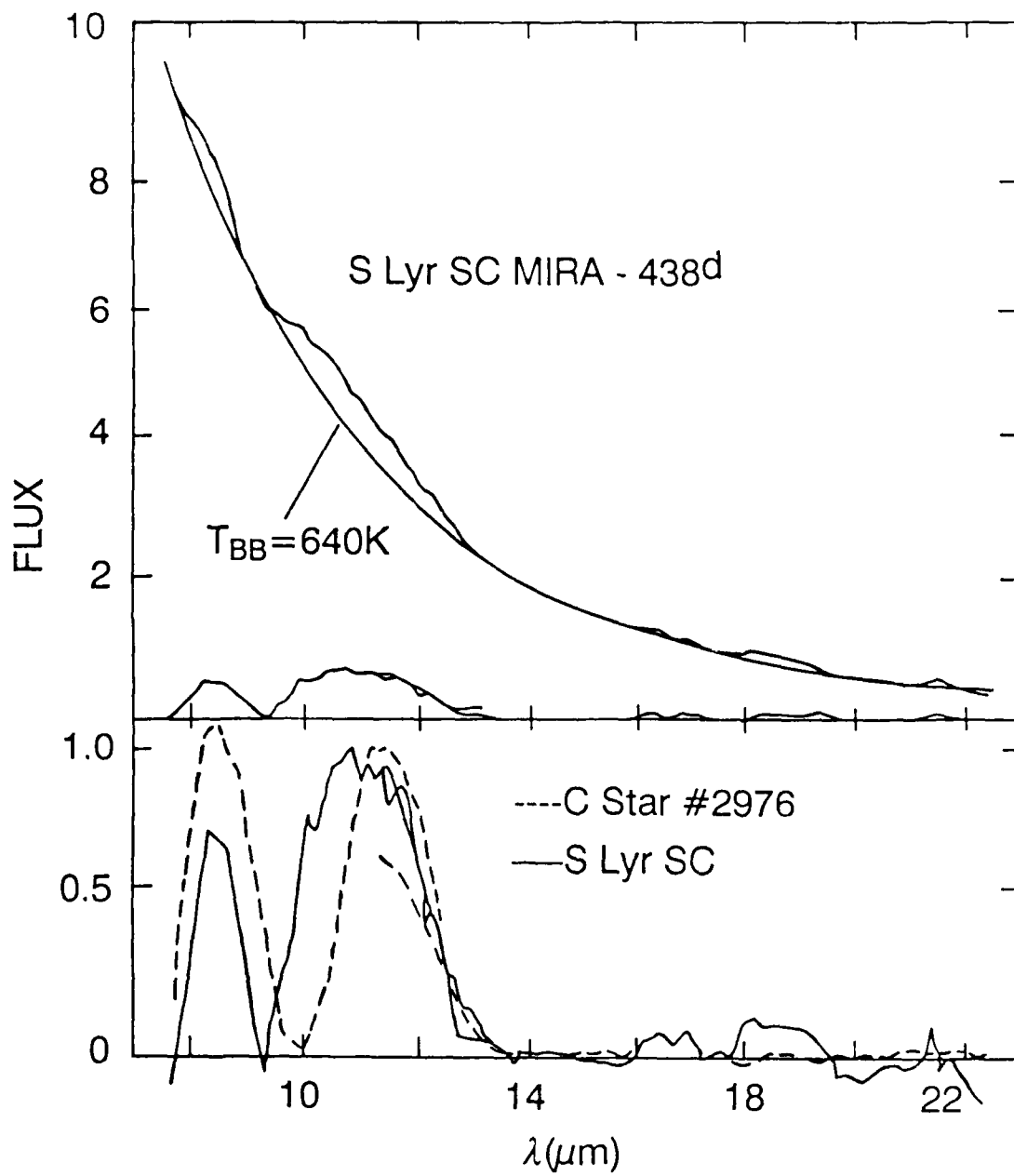


Figure 3a

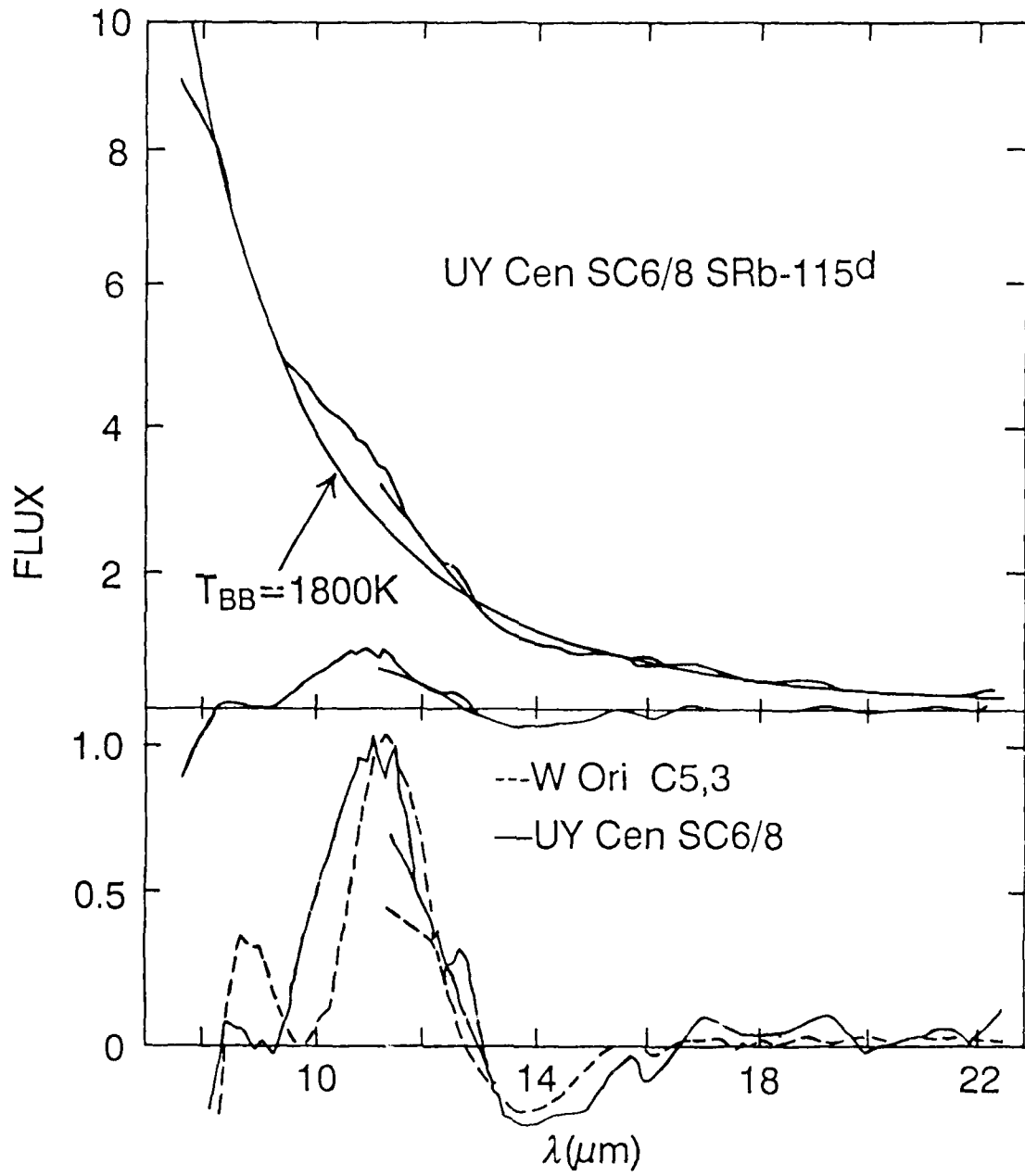


Figure 3b

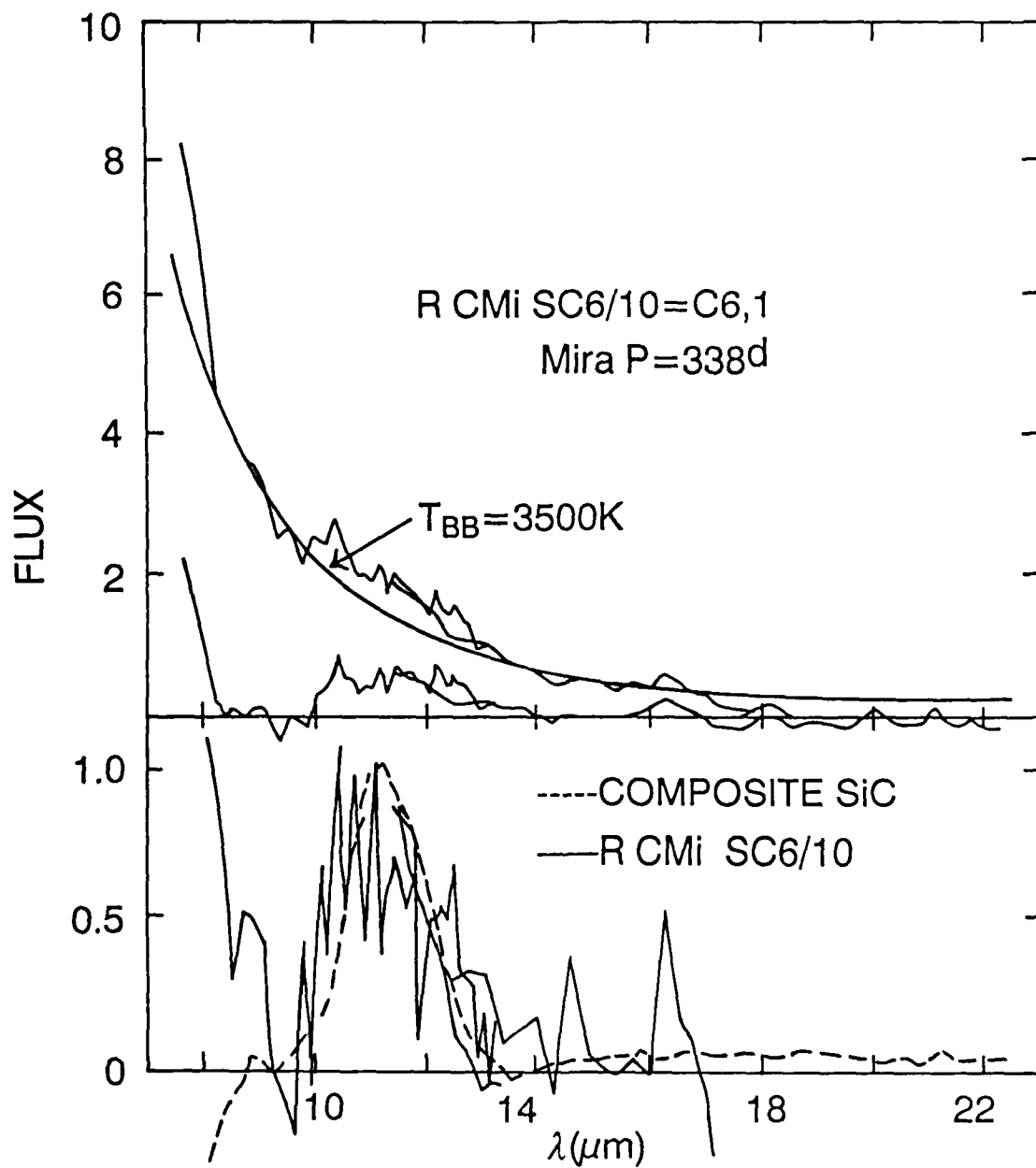


Figure 3c

MS, S and SC MIRAS and SR's

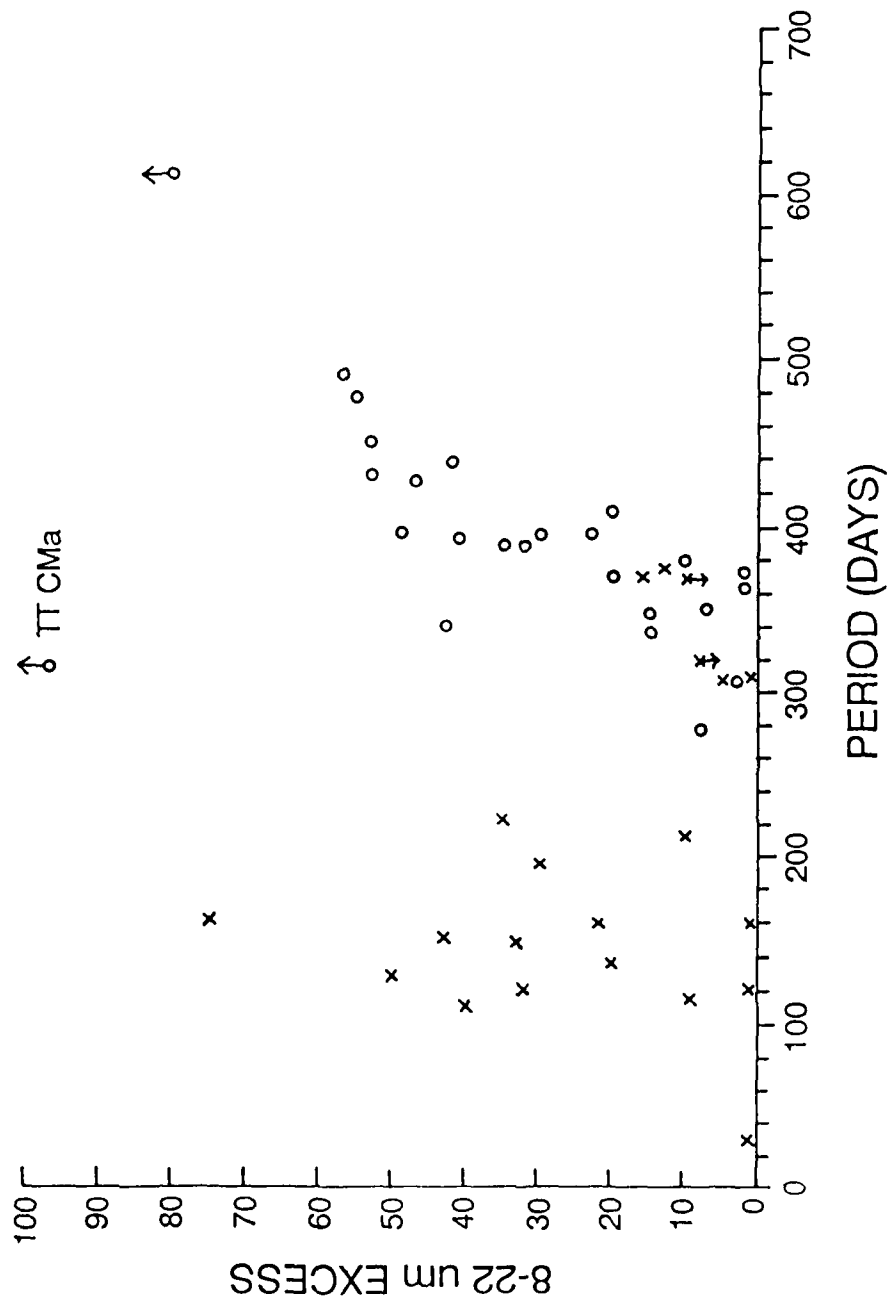
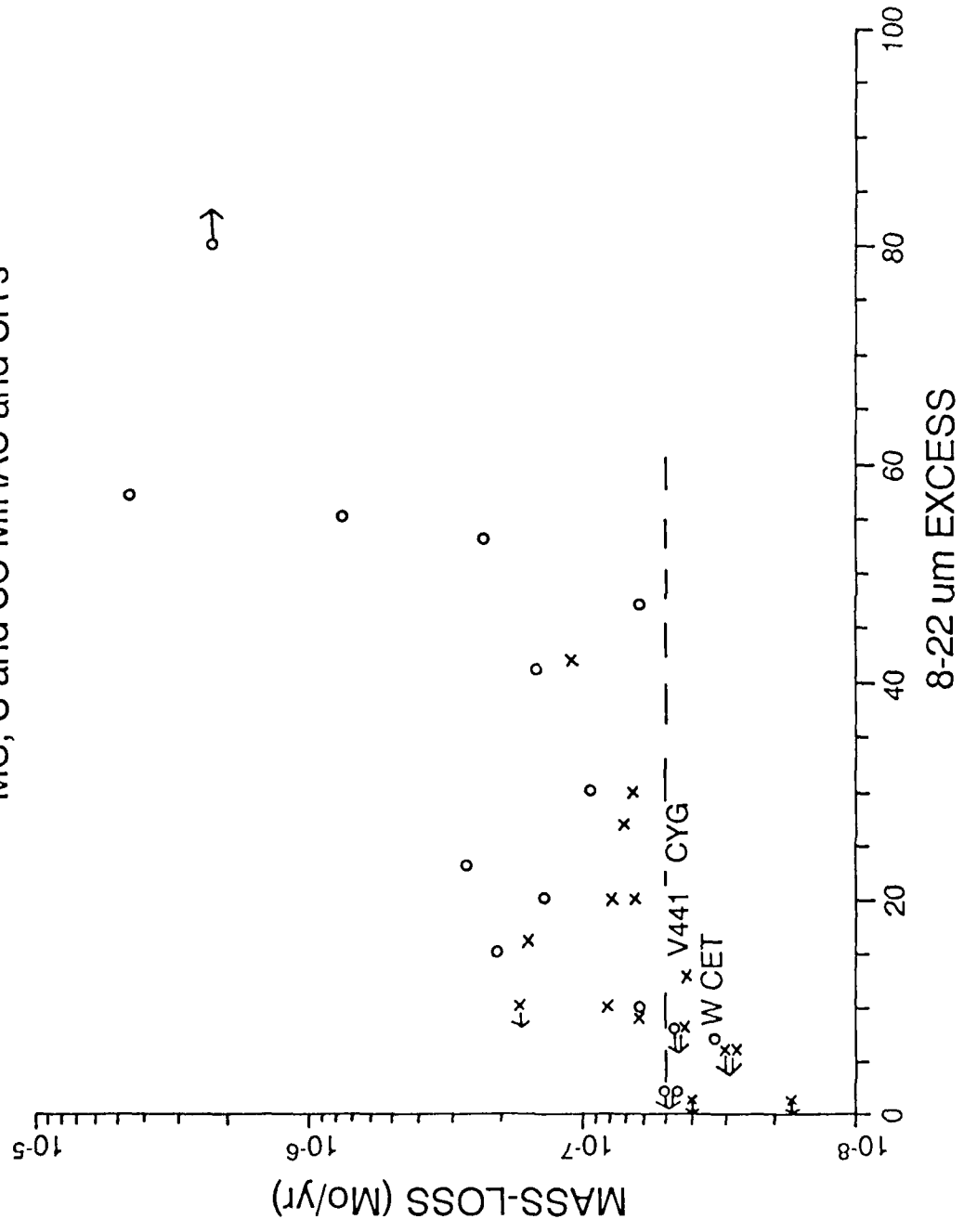


Figure 4

MS, S and SC MIRAS and SR's



MS, S and SC MIRAS and SR's

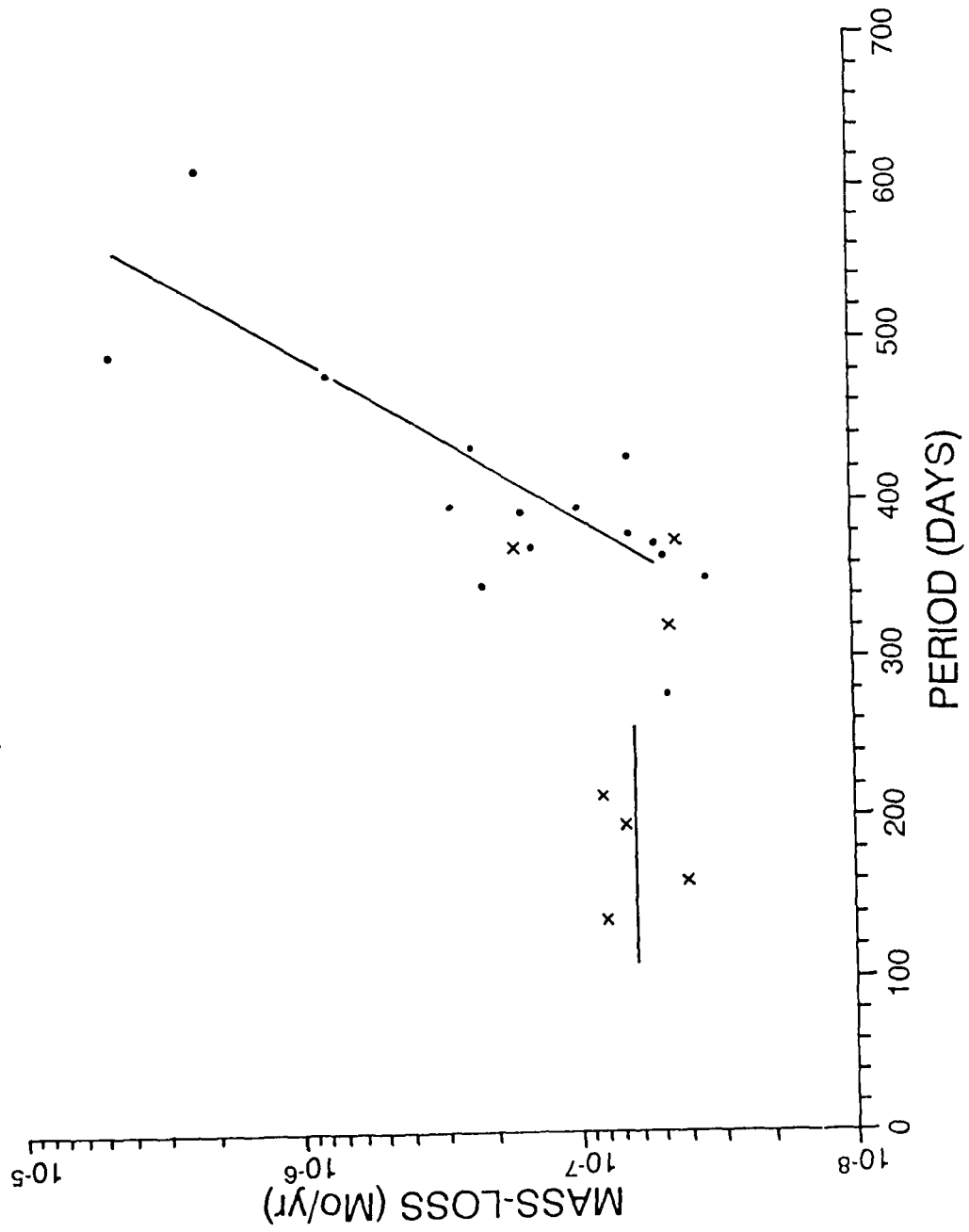


Figure 6

Appendix I

Papers Published as Part of a Conference Proceeding

Lecture Notes in Physics

Edited by H. Araki, Kyoto, J. Ehlers, München, K. Hepp, Zürich
R. Kippenhahn, München, H. A. Weidenmüller, Heidelberg
and J. Zittartz, Köln

254

Cool Stars, Stellar Systems, and the Sun

Proceedings, Santa Fe, New Mexico 1985

Edited by M. Zeilik and D.M. Gibson



Springer-Verlag

AN ANALYSIS OF IRAS LOW RESOLUTION SPECTRA (LRS) OF
CARBON AND M VARIABLE STARS

Irene R. Little-Marenin
Wellesley College
Wellesley, MA 02181

Charles Wilton
University of Wyoming
Laramie, WY 82071

IRAS, measured 250,000 point sources at 12, 25, 60 and 100 μm while simultaneously obtaining about 5000 low resolution spectra in the 8 to 22 μm region of point sources brighter than 20 Jy at 12 and 25 μm with a resolution of 0.1 and 0.25 μm . This region contains the spectral signature of silicate dust (around 10 and 18 μm) and of silicon carbide dust (around 11 μm), indicative of oxygen-rich and carbon-rich circumstellar shells produced by mass loss from their central stars. These dust grain features are in emission from optically thin relatively hot shells.

CARBON STARS

High and low quality LRS spectra of 269 known carbon stars exist. 85% of the high quality spectra show SiC dust in emission indicating that they are surrounded by circumstellar shells. The remaining 15% of the spectra show only a smooth continuum. We determined the wavelength dependence of the emission feature by subtracting the local background continuum. This background is best matched with multi-temperature black body curves ranging in temperature from 3000K (in the 8-10 μm region) to 450K (in the 13-22 μm region). This multi-component black body continuum can also be approximated by a fourth or sixth order polynomial fit in wavelength and was used in estimating the emission profile. The average excess emission above the local continuum is about 20% and ranges from less than 5% to about 40%. It does not appear to correlate with other photospheric parameters such as the color temperature, CN strength, the strength of the Merrill-Sanford bands due to SiC, in the blue region of the spectrum and the period of variability.

Overplotting the normalized SiC emission features of many carbon stars (Fig. 1a) shows that the shape of the SiC emission is very uniform among the carbon stars studied independent of the strength of the emission. The maximum emission occurs at 11.2 \pm 0.15 μm but minor

differences in the SiC profile do exist e.g. Y CVn. In 75% of the C stars spectra with SiC emission, we find a second emission feature around $8.2 \mu\text{m}$ (see Fig. 1a). If this emission is an artifact of the IRAS data or is real, is not known at this point. A feature around $8.7 \mu\text{m}$ has been observed previously and does appear to exist strongly in the spectrum of SS Vir and T Lyr.

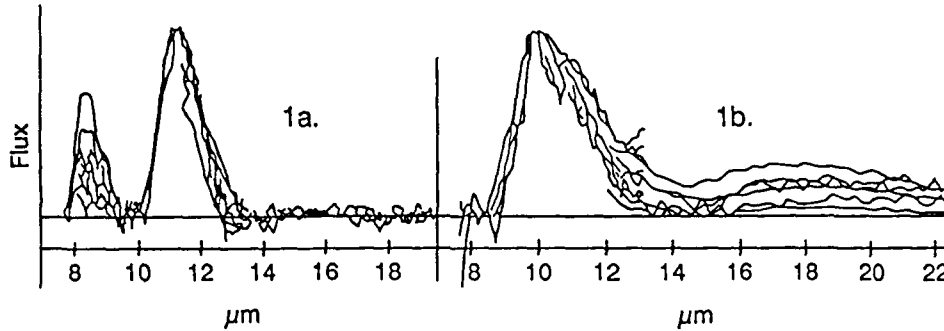


Figure 1a. The normalized SiC emission features of C stars are overplotted. The width of $0.15 \mu\text{m}$ on the short wavelength side is representative of the uncertainty in wavelength. The greater width of $0.4 \mu\text{m}$ on the long wavelength side occurs in the overlap region of the two cameras and represents the greater flux errors in this region.

Figure 1b. The normalized silicate emission features seen in M stars are overplotted. The emission profiles show greater variation than the SiC profiles.

M STARS

About 60% out of the 571 high quality LRS spectra of variable M stars (SR, Mira and Lb variables) show the silicate dust emission features above the continuum background around 10 and $18 \mu\text{m}$. As for the C stars we could match the continuum with two different black body curves; about 800K in the 8 to $10 \mu\text{m}$ region and about 400K in the 13 to $22 \mu\text{m}$ region (cooler than for the carbon stars).

Overplotting the normalized emission (with the local continuum subtracted) shows that there does appear to exist a fundamental silicate shape with a maximum around $9.9 \mu\text{m}$ but significant deviations from this shape occur (Fig. 1b) in the wavelength and shape of maximum emission as well as in the onset and ending wavelengths of the emission profile. In general the emission profile extends to shorter wavelength as the strength of the emission feature increased, starting shortward of $8 \mu\text{m}$ for very strong emission features.

The average excess emission ratio for M stars is about 30% and ranges from about 5% to greater than 70%. The large ratios are less re-

liably determined since the 10 μm emission correlates somewhat with the 18 μm emission making it difficult to establish the continuum background.

Only 3% of the high quality M star spectra which show a smooth continuum can be matched with black body temperatures representative of the stellar photospheres (2000K to 3000K). The rest show continua that can only be matched with multi-temperature black body curves ranging from 2000K to 800K in the 8 to 10 μm region to 800K to 400K in the 13 to 22 μm region indicating that we are receiving radiation from the circumstellar shell as well. The two temperature model is only an approximation to the real continuously decreasing temperature structure of the shell. To match the background and emission features correctly, we will need to integrate the equation of transfer through the circumstellar shell.

CARBON STARS WITH STRONG SILICATE EMISSION FEATURES

Four stars classified as carbon stars show the same strong 10 μm (and 18 μm) silicate emission feature as the M stars. These stars are BM Gem, V778 Cyg, RV Cen and Stephenson star number 1003. It is difficult to interpret these observations since the lifetime of material in transit through the circumstellar shell is on the order of years to decades. Hence material indicative of a C/O ratio less than one (silicate dust emission from the shell) should not simultaneously exist with photospheric material indicative of a C/O ratio greater than one as implied by the carbon star classification. There are several interpretations possible: a) the stars have been misclassified, b) we are observing a binary system with an M and C star component, c) the observed feature is not due to silicates despite the similarity in the profile, and d) we are actually observing very newly formed carbon stars still surrounded by oxygen-rich circumstellar shells.

This research was supported by the 1985 USAF-UES Summer Faculty Research Program/Graduate Student Summer Support Program sponsored by the Air Force Office of Scientific Research conducted by Universal Energy Systems, Inc. We would like to thank the Air Force Geophysics Laboratory and Dr. Stephan Price for making this opportunity available to us.

AN ANALYSIS OF IRAS LOW RESOLUTION SPECTRA OF S STARS

Stephen J. Little
Bentley College
Waltham, MA 02154

Irena R. Little-Marenin
Wellesley College
Wellesley, MA 02181

The Infrared Astronomical Satellite (IRAS) carried a low resolution spectrometer (LRS) with a wavelength response covering the 8 to 22 micrometer region. About 5000 LRS spectra exist of point sources brighter than 10 Jy at 12 and 25 micrometers. Spectra of 67 known S stars were identified by the IRAS catalogue search.

We have analyzed the 32 highest quality S star spectra and find that 19 show measurable emission features in the 9 to 13 micrometer region. Most of the emission features were relatively weak, the strongest being about 30% of the strength of the underlying continuum and the weakest about 10%. Four stars, Y Lyn, RS Cnc, W And, and RAFGL-2425, show emission features resembling the silicate features of M stars. One star, UY Cen, shows a nearly pure SiC feature. Most (14) S Star emission features were centered near 10.5 micrometers, intermediate between the silicate emission features of M stars and the silicon carbide (SiC) features of C stars (see the paper by Little-Marenin and Wilton at this conference).

The identification of the intermediate wavelength feature is at present unknown, but two possible interpretations may be suggested:

1) A previously unknown molecular species may occur in circumstellar shells only when stars are progressing from M to S to C by stellar evolution on the asymptotic giant branch, and while the photospheric ratio of C/O changes respectively from <1 to approximately 1 to >1 . We believe that the M to S to C change occurs on a time scale of greater than thousands of years, and that the circumstellar shell, with a lifetime of 10 to 100 years, should represent the chemical abundances in the photosphere. It has been suggested at this conference (see following remarks) that the unknown molecular species may be a form of polycyclic hydrocarbon. Our intermediate wavelength feature is similar to that observed by Gehrz, *et al.* (Ap. J., 281, 303, 1984) in Nova Aql 1982 as it evolved during its dust shell development phase.

2) The intermediate wavelength feature shown by our 14 S stars may be a blend of SiC and silicate emission. We are able to model the intermediate wavelength features of our 14 S stars with mixtures ranging

from silicate/SiC ratios of 80/20 to 50/50, see Table and Figure 1. This explanation is a difficult one to believe if one believes molecular equilibrium calculations which preclude simultaneous formation of silicate and SiC grains. The timescale of change for photospheric C/O ratios is much longer than the lifetime of material in the circumstellar shell.

We would like to thank the Air Force Geophysics Laboratory for their assistance during this research. One of us (IRL-M) would like to acknowledge support from the USAF-UES Summer Faculty Research Program, sponsored by the Air Force Office of Scientific Research, conducted by Universal Energy Systems Inc.

TABLE 1. A LIST OF THE STARS WE HAVE ANALYZED INCLUDING THE CLASSIFICATION OF THEIR SPECTRA AS A COMPOSITE OF SILICATE AND SILICON CARBIDE EMISSION.

STEPHEN- SON CAT.	NAME	SP. CL.	LRS*	COMPOSITE SiO/SiC	GCVS.
21	S Cas	S3,4-S5,8e	22	60/40	M-611
36	W And	S6,1e(M7)	22	100/0	M-307
110	-	M2S	43	50/50	-
156	DY Gem	S8,5(M)	42	compos.	SRa-1145
230	Y Lyn	M5 Ib-II(M6S)	43	100/0	SRc-110
351	RS Cnc	M6e Ib-II(M6S)	22	100/0	SRc?-120
414	Z Ant	S5,4	42	compos.:	SR-104
463	UY Cen	SC	43	10/90	SR-115
496	ST Her	M6-7S	41	50/50	SRb-148
505	-	Se	42	50/50	-
514	RT Sco	M6e-M7e(S)	22	70/30	M-449
586	ST Sgr	S5,5e	21	50/50:	M-395
594	S Lyr	SC	41	compos.:	M-438
597	W Aql	S4,9e	22	60/40	M-490
612	ZAFGL-2425	-	29	100/0	-
616	R Cyg	S3.5,9-S6,8e	22	60/40:	M-426
702	Pi ¹ Gru	S5,7:	42	60/40	Lb
739	WY Cas	Se	42	50/50	M-477
741	IW Cas	S4.5,9e	21	compos.:	M-396

* LRS CLASS: FIRST DIGIT: 2 = SILICATE EMISSION
 4 = SILICON CARBIDE EMISSION
 SECOND DIGIT: INCREASING STRENGTH OF EMISSION (1-9)

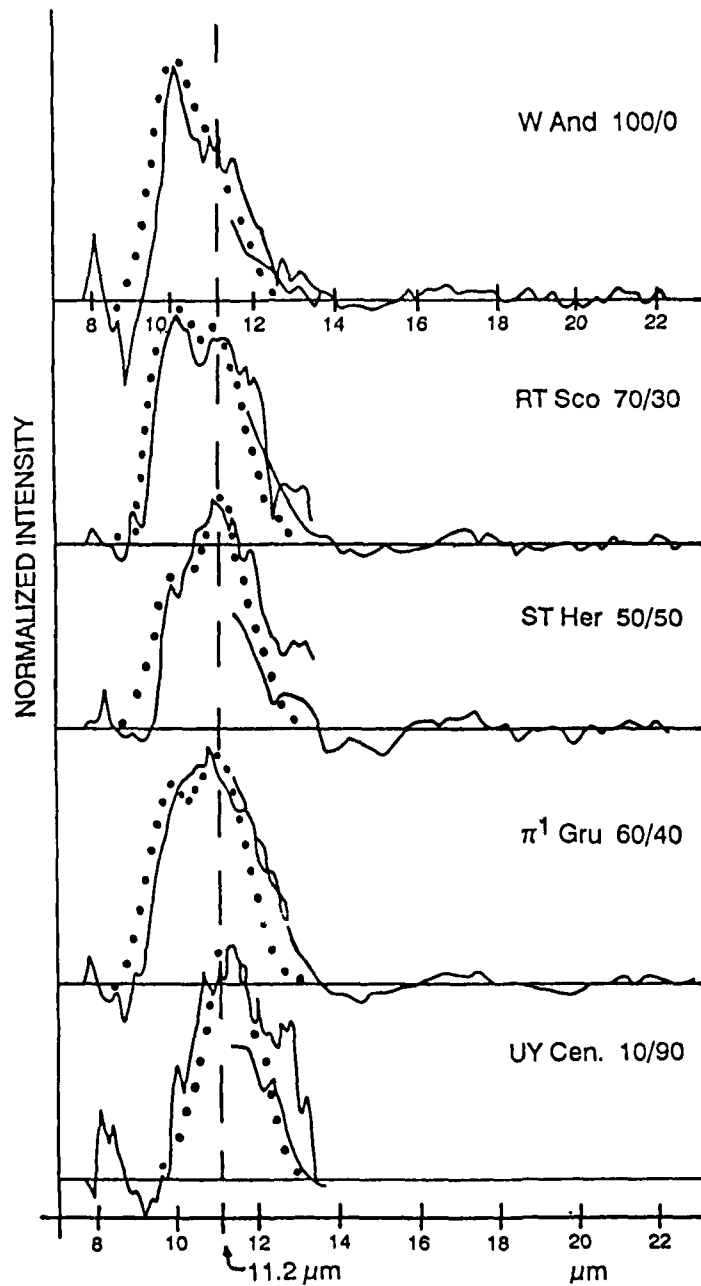


Figure 1. Normalized profiles of the emission feature in five S stars. The dotted lines are the modeled profiles for mixtures of silicate and SiC. The proportion to the right of the star name is the adopted mixture for each star.

HR 5110: AN ALGOL SYSTEM WITH RS CVn CHARACTERISTICS

I. R. Little-Marenin,¹ Jeffrey L. Linsky^{2,3}
Joint Institute for Laboratory Astrophysics, University of Colorado and National
Bureau of Standards, Boulder, CO 80309-0440

Theodore Simon³
Institute for Astronomy, University of Hawaii

¹JILA Research Fellow 1983-84; on leave from Wellesley College.

²Staff Member, Quantum Physics Division, National Bureau of Standards.

³Guest Observer, International Ultraviolet Explorer.

HR 5110 (HD 118216-BII CVn) is a close binary system ($P=2.6$) which is viewed nearly pole-on ($i=13^\circ$). A comparison of the characteristics of Algol and RS CVn systems to those of HR 5110 shows that HR 5110 can also be considered an Algol system. Because the primary star is relatively cool (F2 IV) and there is no apparent emission from an accretion disk, we are able to detect in IUE spectra the emission of an active chromosphere and transition region of the cooler secondary. HR 5110 is the only known Algol system for which the properties of the secondary star can be studied in detail. For a more complete discussion see Little-Marenin *et al.* (1986).

An interpretation of HR 5110 depends critically on knowing the spectral type and luminosity class of the two stars in the system. To accomplish this we obtained near-infrared JKLM photometry of HR 5110 on the 1.3-m telescope of the Kitt Peak National Observatory in 1980 February and June and also 1981 May. The best fit to the observed colors of HR 5110 for different types of primaries (F2 V to G0 V) and secondaries (G5 IV to K1 IV) is a F2 IV primary similar to σ Boo and a K0 IV secondary ($V_s - V_p = 1.88$) for which spots cover 35-40% of the surface. The determination that the K0 IV star is spotted comes from the infrared excess (from J to M'), which is fairly well matched with a blackbody curve of 3100 K and therefore is too hot to be produced by dust and has the wrong wavelength dependence to be produced by free-free emission. Our spectral synthesis differs from that of Shore and Adelman (1984), but is in agreement with the statistics found for Algol systems by Giuricin, *et al.* (1983); every F primary has a K secondary. We obtain from the Barnes-Evans relationship (Barnes and Evans 1976) an angular diameter of 0.47 milliarcsec for the spotted K0 IV star, corresponding to a radius of 1.9-2.7 R_\odot for a parallax of $0.027 \leq \pi \leq 0.019$. We conclude that the secondary fills its Roche lobe radius of 2.6 R_\odot , as originally suggested by Conti (1967).

We obtained IUE spectra during the latter (plateau) phases of the radio flares of 1979 May 29-31 and 1981 April 6, 56 hours after the first major event (Simon *et al.* 1980) and 26 hours after the second. We also observed HR 5110 in 1980 February and in 1983 August. The IUE archives yielded two additional spectra presumably taken when the system was quiescent. Unless an unobserved flare occurred on 1981 February, the IUE data appear to show correlations with phase with maximum flux

occurring near phase of 0.5, i.e. when we observed the side of the secondary star that faces the F star. The phases were calculated from an ephemeris having an epoch of JD 2445079.478 and period of 2.61328 days, obtained from the reanalysis of the orbit by Lyons, *et al.* (1984); we have adjusted the epoch so that an orbital phase of 0.0 corresponds to conjunction (K0 star in front).

To understand and model the variations in the emission correctly we must determine which star has the activity associated with it. Conti (1967) showed that the radial velocity variations of the Ca II emission are out of phase with those of the F star. This emission therefore defines the orbit of the secondary star. To establish from which star the upper chromospheric and TR emission originate, we analyzed a high-dispersion short wavelength spectrum SWP 13669 taken near quadrature centered on phase 0.27. This spectrum shows the He II, C IV, C II lines and, very weakly, the O I and Si IV lines in emission. We determined the shift in wavelength of the emission lines relative to the photospheric absorption lines of the F star by aligning the absorption lines of HR 5110 with those of Procyon (F5 IV-V). The two photospheric spectra match very well. Measuring next the wavelengths of the emission lines of HR 5110 relative to those of Procyon as a template, we determined an average velocity difference of $+40 \pm 10 \text{ km s}^{-1}$. At phase 0.27 the difference in radial velocity between the secondary and primary in HR 5110 is about $+45 \text{ km s}^{-1}$, in agreement with the velocity of the emission lines. The measured absolute velocity shifts of the emission lines, corrected for orbital motion of the Earth and the spacecraft, gave similar results. Hence this analysis shows unambiguously that the active chromosphere and TR phenomena in HR 5110 are located on the cooler K0 IV star and are not associated with the F star or with an accretion disk around the F star as in Algol systems. No emission lines are at the velocity of the F star.

Table 1 lists the average surface line fluxes on the assumption that all the flux in the binaries originates on their cooler components. UX Ari ($P=6^d.4$; K0 IV + G5 V) and HR 1099 ($P=2^d.8$; K0 IV + G5 IV) are both known as very active RS CVn binaries. The surface fluxes for HR 5110 and the two RS CVn stars are comparable and are much larger than the corresponding fluxes for the quiet Sun. It seems plausible to attribute the large surface fluxes for the secondary star in the HR 5110 system, like those for UX Ari and HR 1099, to rapid rotation. From the data presented by Vilhu and Rucinski (1983, their Table 3), we estimate that for stars with rotation periods of ~ 3 days the difference in UV line flux between an F8 star (0 Drs) and a K star (HR 1099) is about a factor of 10. This difference at a given rotational velocity in the strength of chromospheric and TR emission must be related to another parameter, e.g. the shallower depth of the convection zone in the F stars, and hence it is not surprising that in HR 5110 we find no evidence of emission from an active TR associated with the F2 IV primary even though the radii of both components are nearly the same so that their rotational velocities are nearly identical given synchronous rotation.

Table 1. Integrated line surface fluxes of the secondary components of HR 5110 and two RS CVn stars ($\times 10^5$ ergs cm^{-2} s^{-1}).

Star	Phase	$\frac{F(\Delta\lambda)^d}{f(\Delta\lambda)}$ ($\times 10^{+17}$)	N V	C II	Si IV	C IV	He II	Mg II k
			$\lambda 1240$	$\lambda 1335$	$\lambda 1400$	$\lambda 1549$	$\lambda 1640$	$\lambda 2796$
HR 5110	0.68-0.52	7.85	1.2-3.1	3.5-6.9	2.5-5.1	5.1-10.9	2.7-5.4	52-71
HR 1099 ^a	0.73	3.2	2.1	6.1	3.0	9.7	---	110
UX Ari ^a	0.61	4.6	1.9	4.4	2.5	6.5	3.5	68 ^b
Sun ^c	---	---	0.0086	0.046	0.025	0.058	0.031	6.8

^aSimon and Linsky 1980. Quiescent data.

^bSimon, et al. 1980. Quiescent data.

^cQuiet-Sun surface fluxes from Ayres and Linsky 1980.

^d $F(\Delta\lambda) = \left(\frac{4.125 \times 10^8}{\phi^2}\right) f(\Delta\lambda)$, where ϕ is the stellar angular diameter in milliarcsec.

Our observations of HR 5110 have shown that the behavior we observe is similar to that of rapidly rotating spotted RS CVn systems and hence must be determined primarily by the large rotational velocity of the KO star and dynamo action rather than being related to an accretion disk. Whether other secondaries of Algol systems have magnetic active regions is not yet known, since the UV spectra of the few systems that have been observed during primary eclipse (cooler star in front) appear to be dominated by an accretion disk around the primary.

We are grateful for support by the National Bureau of Standards Research Fellow program and for NASA grants to the Universities of Colorado and Hawaii.

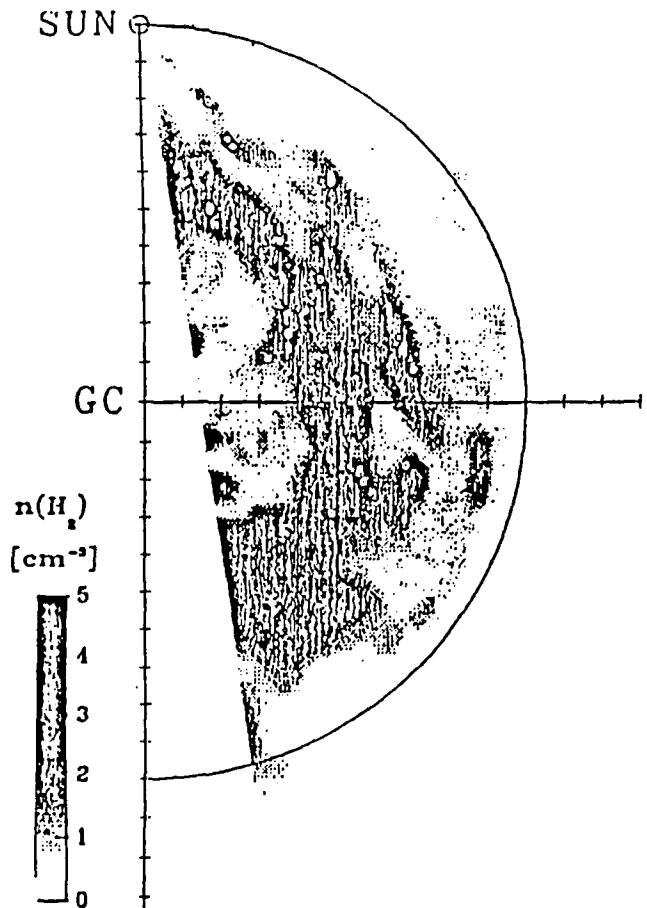
REFERENCES

- Ayres, T. R. and Linsky, J. L. 1980, *Ap. J.*, 235, 76.
 Barnes, T. G. and Evans, D.S. 1967, *M.N.R.A.S.*, 174, 489.
 Conti, P. S. 1976, *Ap. J.*, 149, 629.
 Gluricin, G., Mardirossian, F., and Mezzetti, M. 1983, *Ap. J. Suppl.*, 52, 35.
 Little-Marenin, I. R., Simon, T., Ayres, T. R., Cohen, N. L., Feldman, P. A., Linsky, J. L., Little, S. J., and Lyons, R. 1986, *Ap. J.*, in press.
 Lyons, R. W., Bolton, C. T., and Fraquelli, D. A. 1984, preprint.
 Shore, S. N., and Adelman, S. J. 1984, *Ap. J. Suppl.*, 54, 151.
 Simon, T. and Linsky, J. L. 1980, *Ap. J.*, 241, 759.
 Simon, T., Linsky, J. L., and Schiffer, F. H. III 1980, in *The Universe of Ultraviolet Wavelengths*, NASA Conf. Publ. 2171, p. 435.
 Vilhu, O. and Rucinski, S. H. 1983, *Astr. Ap.*, 127, 5.

Appendix J

Summer School on Interstellar Processes: Abstracts of Contributed Papers

Summer School on Interstellar Processes: Abstracts of Contributed Papers



October 1986

Proceedings of a Workshop Held at
Grand Teton National Park, Wyoming
July 3 - 7, 1986

NASA
National Aeronautics and
Space Administration

THE SHAPES OF THE CIRCUMSTELLAR "SILICATE" FEATURES

Irene R. Little-Marenin (AFGL and Wellesley C.)
Stephan D. Price (AFGL)

Around oxygen-rich stars we find that the spectra of most long-period variables (LPV) show an excess infrared emission which is attributed to circumstellar silicate dust grains. These grains produce emission features at about 10 and 18 μm due to bending and stretching modes of SiO respectively. It has been known (Forrest, Gillett and Stein 1975) that the spectral energy distribution of the 10 μm emission shows variations from star to star. With the availability of many IRAS Low Resolution Spectra (LRS) in the 8-22 μm region of M stars, we can now study the 10 μm feature to determine its uniformity (or lack thereof). For this analysis we assume that the 8-22 μm emission from these stars is produced by a) the stellar photosphere, b) a continuum emission from the dust grains and c) a strongly wavelength dependent dust grain emission term. By representing the first two terms with blackbody energy distributions and subtracting them from the observed spectrum, we are left with a remaining strongly wavelength dependent emission feature which we call the excess silicate or 10 μm emission.

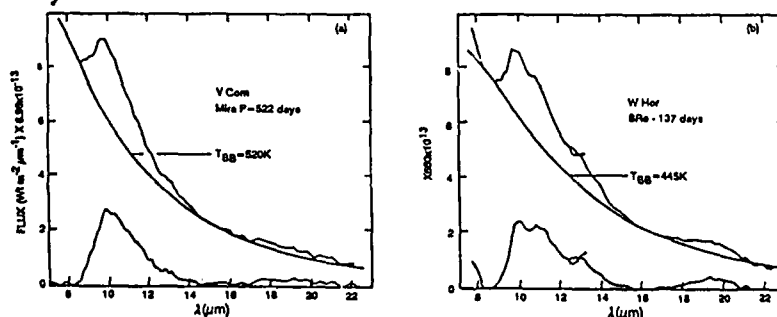


Fig. 1. Two M star LRS spectra (V Com and W Hor) are plotted together with black body energy distributions fitted to either side of the emission feature. The 10 μm excess (observed - local black body continuum) is plotted above the wavelength axis. The difference in the shape of the excess between the two stars is obvious.

The excess silicate emissions from about 130 LPVs can be divided into three groups characterized by similar spectral shapes. All three shapes are shown in Figure 2. The average silicate feature of semiregular (SRa,b,c) and irregular (Lb) variables is shown as a solid line. This feature extends from 8.4 to \sim 14.5 μm with a peak at $10 \pm 0.05 \mu\text{m}$. The FWHM is $2.1 \pm 0.15 \mu\text{m}$ but the feature is asymmetric with the ratio of the widths of the short wavelength (rising) branch compared to the long wavelength (falling) branch of 0.6:1.5 at half intensity. The rising branch shows only minor variations in wavelength from star to star whereas the wavelength at the FWHM point of the falling branch varies by $\pm 0.15 \mu\text{m}$. The average silicate excess of Mira variables is shown as a dashed line in Figure 2. The average feature extends from 8 to 14.5 μm with a peak at 9.75 μm and a FWHM of 2.3 μm . The feature is asymmetric but on the average has a less

steeply rising branch than the other LPVs giving a ratio of the rising width to the falling width of 0.75:1.5 at half intensity. However, the spectral shape of the silicate emission feature among the Miras shows much greater variation from star to star than that of the other LPVs. The shape of the emission from Miras ranges from one identical to the SRs and Lbs to a much broader one, extending from $<8 \mu\text{m}$ (the limit of the LRS detectors) to $\sim 14.5 \mu\text{m}$ with a corresponding shift in peak emission from 10 to $9.6 \mu\text{m}$ and an increase in the FWHM from 2.1 to $2.4 \mu\text{m}$. The long wavelength edge of the feature appears to vary very little among these Miras. Hence the difference in spectral shape between the Miras and the other LPVs is primarily due to the fact that in Miras the rising branch varies in wavelengths accompanied by a shift in the peak emission to shorter wavelengths. This shift to shorter wavelength correlates with the strength of the silicate excess. In general the greater the strength of the feature the shorter the wavelength of the rising branch. Unlike the results of DeGioia-Eastwood et al (1981), we find that the strength correlates only very weakly with period. This corroborates the conclusion reached by Vardya, De Jong and Willems (1981). At a given period the excess can vary by a factor of 4. The $18 \mu\text{m}$ emission feature is very similar in both types of profiles and extends from about 15 to $>22 \mu\text{m}$. Both these $\sim 10 \mu\text{m}$ and $18 \mu\text{m}$ features have been attributed to silicates.

The most interesting $10 \mu\text{m}$ emission occurs in stars which tend to show weak excesses but includes a few stars which have excesses comparable in strength to the stars with the other types of features (see Fig. 1a and 1b). There are relatively few stars in this group, but they constitute almost half of the stars with weak emission irrespective of their variability type. The feature has three components (dotted line Figure 2) with peaks at 10 , 11 and $13.1 \mu\text{m}$. The $10 \mu\text{m}$ peak is strongest in M stars and agrees in wavelength with the silicate peak of the SRs but it is narrower. The intensities of the 11 and $13.1 \mu\text{m}$ peaks vary greatly being at times quite weak. These stars show an emission excess at long wavelength which is significantly different from the $18 \mu\text{m}$ emission. It appears to extend from about 16 to $22 \mu\text{m}$ with a peak at about $19.5 \mu\text{m}$. If the 3 component feature is also due to silicates is not yet known. The peak at $8 \mu\text{m}$ seen in Figure 2 appears to be an artifact of our method of analysis. It disappears if photospheric temperatures are used to fit the shortest wavelengths of the LRS. This research is supported in part by a University Resident Research Fellowship from the Air Force Office of Scientific Research to the Air Force Geophysics Laboratory.

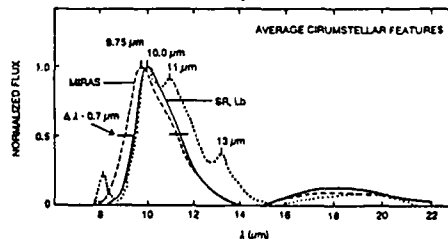


Fig 2. The three types of $10 \mu\text{m}$ excess.

REFERENCES

- DeGioia-Eastwood, K., Hackwell, J.A., Grasdalen, G.L., and Gehrz, R.D. 1981, *Ap.J.*, 245, L75.
 Forrest, W.J., Gillett, F.C., and Stein, W.A. 1975, *Ap.J.*, 175, 423.
 Vardya, M.S., De Jong, T., and Willems, F.J. 1986, *Ap.J.*, 304, L29.

Appendix K

Conference Digest: Second Haystack Observatory Meeting,
Paper Entitled Water Masers Around Two Short Period Miras:
R. Ceti and RZ Scorpii

NORTHEAST RADIO OBSERVATORY CORPORATION

HAYSTACK OBSERVATORY

WESTFORD, MASSACHUSETTS 01886

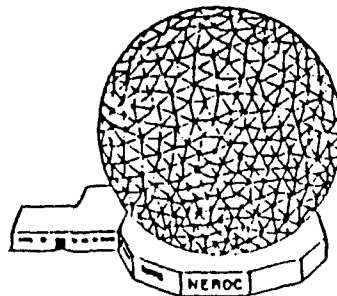
CONFERENCE DIGEST

Second Haystack Observatory Meeting

INTERSTELLAR MATTER

*A Symposium on Interstellar Molecules
and Grains*

in Honor of Alan H. Barrett



OPERATED UNDER AGREEMENT WITH
MASSACHUSETTS INSTITUTE OF TECHNOLOGY

WATER MASERS AROUND TWO SHORT PERIOD MIRAS: R CETI
and RZ SCORPII

IRENE R. LITTLE-MARENIN
AFGL/OPC, Hanscom AFB, MA 01731

PRISCILLA J. BENSON
Whitin Observatory, Wellesley College, Wellesley, MA
02181

DALE F. DICKINSON
Lockheed Palo Alto Research Lab, Palo Alto, CA 94304

ABSTRACT The 22 GHz water maser line of R Cet varies in phase with the infrared lightcurve but with a phase lag of 0.1 phase. The water maser emission of RZ Sco also appears to vary in phase.

We report the first detections of the water maser emission line at 22,235.080 MHz from two short period M star Mira variables: R Cet (M4e-M9, P=166^d) and RZ Sco (M3e-M4e, P=160^d) with the 37m Haystack Observatory¹ radio telescope. The intensity of the R Cet maser line has varied by about a factor of 10 from 4.2 Jy (1/23/85; phase=0.01) to 40.8 Jy (6/9/86; phase=0.21; $T_A^* = 3.40$ (0.09) K, $V_{LRS} = +31.20$ and $\Delta V = 0.64$) in phase with the visual lightcurve but with a phase lag of about 0.28 phase (Fig. 1a) corresponding to a phase lag of about 0.1 phase with respect to the K magnitude lightcurve. No other water maser lines are visible with flux > 1 Jy (3σ). The phase lag of 0.1 phase (about 16 days) with respect to the infrared suggests a collisionally pumped maser as proposed by Cooke and Elitzur¹. A maser pumped by the stellar radiation field should experience a negligible phase lag since the stellar radiation should transit through

¹Radio astronomy at Haystack Observatory of the Northeast Radio Observatory Corporation is supported by the National Science Foundation under grant AST78-18227.

WATER MASER EMISSION AROUND R CET AND RZ SCO

the water masing region (less than 70 AU) in less than 1 light day.

The intensity of the water maser line from RZ Sco also appears to vary in phase being below the detection limit of 1 Jy at phase=0.98 (5/19/87) and having an intensity of 7.2 Jy at phase=0.62 (3/23/87) (Fig. 1b). The line observed at phase=0.62 (3/23/1987) shows three components separated by 1.5 km s^{-1} . The strongest component is well fitted with a Gaussian: $T_{\Lambda}^* = 0.60 (0.05) \text{ K}$, $V_{\text{LRS}} = -163.87 \text{ km s}^{-1}$ and $\Delta V = 0.56 \text{ km s}^{-1}$.

Despite the suggestion by Feast et al.² that water masers are preferentially detected from apparent bolometrically bright (i.e. close-by Miras), we find that neither R Cet nor RZ Sco are exceptionally bright; $m_{\text{bol}} = 5.6 \text{ mag}$ (R Cet, $d = 800 \text{ pc}$) and $m_{\text{bol}} = 7 \text{ mag}$ (RZ Sco, $d = 1600 \text{ pc}$). The infrared colors of both stars are typical of other maser stars. However, both Miras have very asymmetric lightcurves and R Cet shows strong 10 and 18 μm silicate emission features (IRAS low resolution spectrum) indicative of a fairly optically thick circumstellar shell and a large J, H and K amplitude. These are characteristics of longer period Miras.

REFERENCES

1. Cooke, B., and Elitzur, M. 1985, *Ap.J.*, 295, 175
2. Feast, M. W. et al. 1982, *Mon. Not.*, 201, 439.

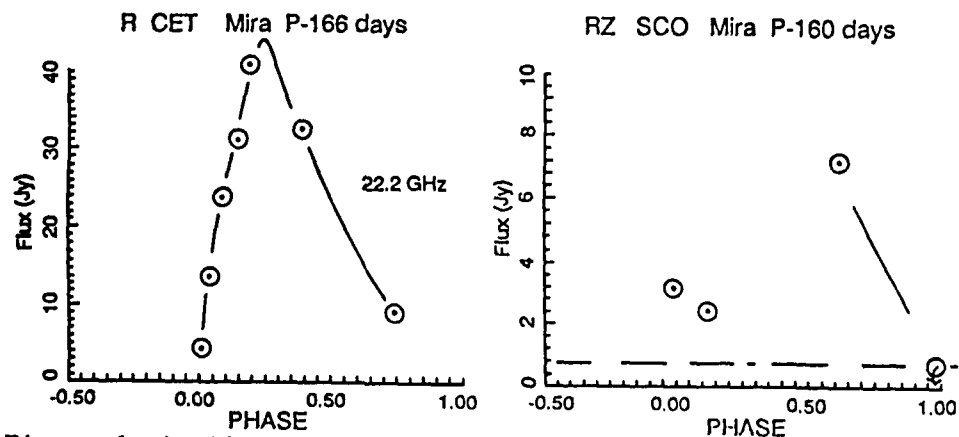
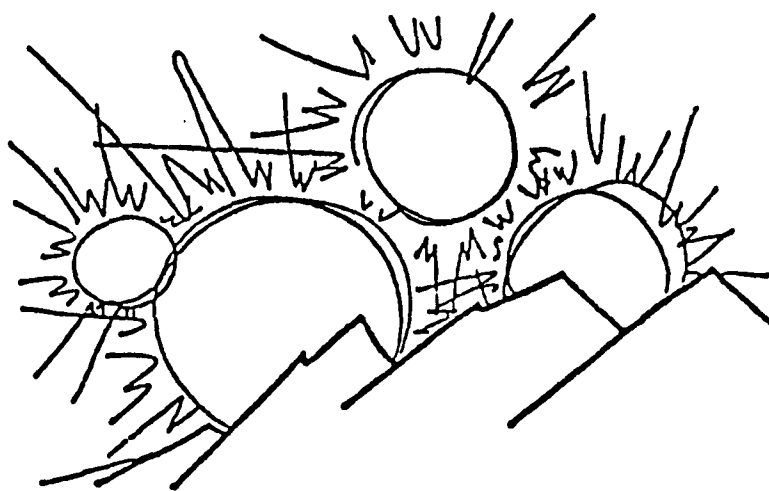


Figure 1a,b. The variation of water maser flux with phase

Appendix L

Emission Features in IRAS LRS Spectra of MS, S and SC Stars

Fifth Cambridge Workshop on Cool Stars,
Stellar Systems and the Sun



University of Colorado at Boulder, July 8-11, 1987

EMISSION FEATURES IN IRAS LRS SPECTRA OF MS, S AND SC STARS

Stephen J. Little (Bentley College)

Irene R. LITTLE-MARENIN (AFGL/OPC and Wellesley College)

Stephan D. PRICE (AFGL/OPC)

ABSTRACT We observe a progression of emission features in the 8-11 μm region in MS, S and SC stars that parallels their increasing C:O ratio and s-process enhancements.

Stellar evolution theory predicts that M stars evolve to MS \rightarrow S \rightarrow (SC) \rightarrow C stars during the late stages of AGB evolution when helium shell flashing occurs and helium-burning products (primarily ^{12}C and s-process elements) are dredged up and mixed with the outer envelope. The C:O ratio of stars during the transition changes from ~ 0.4 (M stars) to ~ 0.6 (MS stars) to ~ 0.8 (S stars) to ~ 1.0 (SC stars) and finally to ~ 1.1 (C stars). At the same time the s-process elements are enhanced from solar abundances to as much as 10-100 times solar in the carbon stars. Smith and Lambert (1985 Ap.J., 294, 326; 1986 Ap.J., 311, 843) estimate that 4-6 flashes are necessary to change an M star into an S star. Many late AGB stars lose mass and develop extensive circumstellar dust shells (CDS). The changing photospheric composition of these stars may be reflected in the composition of the dust grains since the lost photospheric material passes through the CDS on a time scale of 10-100 years -- a very short time compared to the time of 10^4 - 10^5 years between He shell flashes.

IRAS obtained low resolution spectra (LRS) of bright sources in the 8-22 μm region where the emission features of silicates (at 10 and 18 μm) and of SiC (at 11.2 μm) are found. We analyzed about 70 LRS of MS, S and SC stars in order to see if the changing photospheric composition produces unusual emission features in the 8-22 μm region. About one third of the spectra show only a smooth continuum which can (for most stars) be matched with a 2000K to 3000K blackbody energy distribution representative of the photospheric temperatures of these stars. These include, unexpectedly, a number of Mira variables with periods in the 250-400 day range such as T Cam, U Cas and V865 Aql.

Among the S stars, we generally find those with emission to have weak features with the exceptions of TT CMa, Steph1 612 and Steph1 674 which show very strong 10 and 18 μm emission. In general, S stars with abundance classes between 4 and 9 (i.e. Sx,4 to Sx,9) show an emission feature which peaks around 10.5-11 μm , i.e. it is neither due to the usual silicate emission observed in M stars nor due to SiC. We find this S star emission can be modeled reasonably well by co-adding the 10 μm silicate feature and the 11.2 μm SiC feature. The percentage of silicate emission contributed to the co-added feature varies from star to star, but tends to lie in the 50%-70% range. This simple co-added model produces a fit to the spectra that

reproduces the width of the feature well, but not the wavelength of peak emission. Figure 1 shows the observed LRS of S Cas (S4,6), a 640K blackbody energy distribution matched to the underlying continuum and the difference spectrum (observed- T_{BB}). The normalized difference spectrum of S Cas (bottom panel) is reasonably well modeled with a combined feature of 55% silicate and 45% SiC. It is unclear whether the co-addition of silicate and SiC emission is a valid description of the S star feature, or whether a dust grain of differing composition, e.g. an s-process element such as Zr, Y, Ba etc in combination with oxygen, may be responsible for the feature. We know of no laboratory spectrum of grains that have the emission feature shown by many S stars.

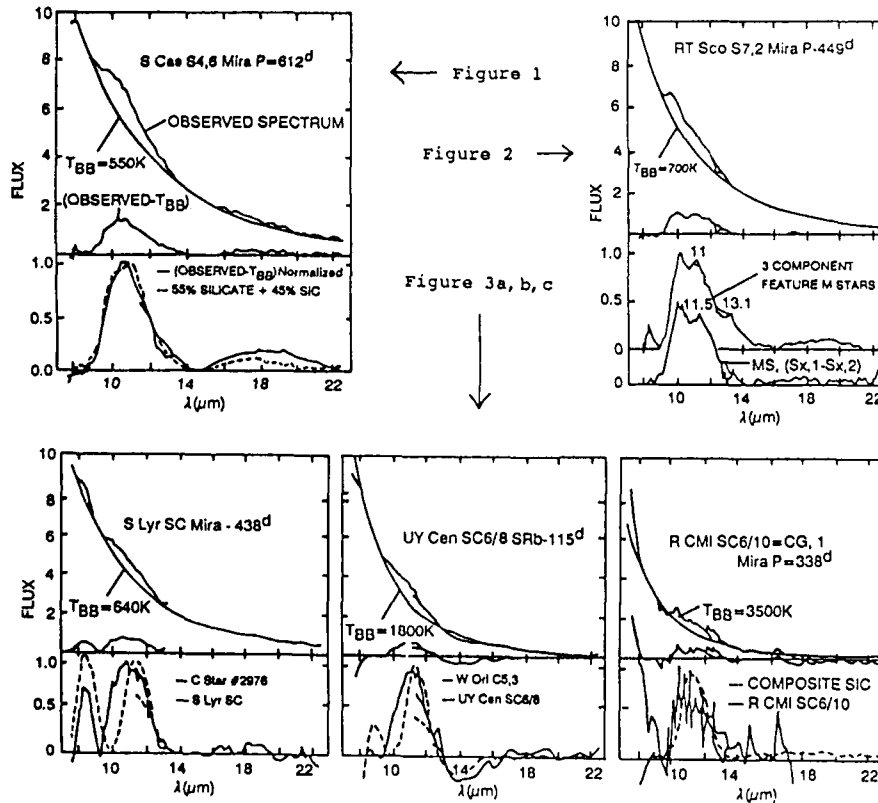
The S stars with emission features and abundance classes of 1 to 2 (Sx,1 class is also referred to as MS stars) usually show a three component feature with peaks at 10 μm , 11 μm and weakly at 13.1 μm . Figure 2 shows the observed LRS of RT Sco (S7,2) matched with a 700K blackbody energy distribution and the difference spectrum plotted along the wavelength axis. The bottom panel of Figure 2 shows the composite three component feature of eight Sx,1 and Sx,2 stars. It is very similar to the three component feature found in about 15% of the M stars with emission features except the 13.1 μm feature appears to be weaker in MS stars.

We interpret the three S stars with very strong 10 and 18 μm silicate emission features as probable binary systems. This is based on our similar attribution of silicate features found in C stars to a probable M star companion (Benson and Little-Marenin, *Ap.J.(Lett)*, 316, L37 and Little-Marenin, Benson and Little this volume). The 10 and 18 μm emission is hypothesized to come from an M star with a CDS which depresses the visible light so that the S star is predominant in the visible and near infrared region.

Of the 14 MS stars, we find 2 (Y Lyn and RS Cnc) with pure M star silicate emission and 5 with various versions of the three component feature. Only the MS supergiant NO Aur appears to show the typical 10.5-11 μm S star emission. Hence, the features found in MS stars appears to span the range of features found among the M and S stars as would be expected from stars in transition from M to S. We have excluded from the discussion 6 stars which we call "spectroscopic" MS stars (Little, Little-Marenin and Bauer 1987 A.J. (submitted)) because their stronger than normal Sr and Ba lines are apparently produced by atmospheric effects and not due to real s-process enhancements. All 6 stars show only a photospheric continuum. Among the 7 SC stars, we find 3 (FU Mon, GP Ori and Steph 442) which show only a photospheric continuum and 4 with emission features. Of these four, two (S Lyr and UY Cen) have the typical 10.5-11 μm S star feature and R CMi may have a nearly pure SiC feature. The emission of AM Cen is too weak to classify accurately. In figure 3 we plot the observed LRS of S Lyr, UY Cen and R CMi along with blackbody energy distributions representative of their underlying continua and their difference spectra. The normalized difference spectra of the three SC stars are overplotted with different C

star features (bottom panels). S Lyr and UY Cen have similar features to the typical 10.5-11 μm S star feature, but the one for UY Cen has its peak emission shifted more towards a longer wavelength. S Lyr shows an unidentified 8-9 μm emission feature seen in some C stars, and UY Cen shows an absorption feature at 14 μm probably due to $\text{C}_2\text{H}_2 + \text{HCN}$ seen in some C stars (Willems, 1987 Ph.D thesis). R CMi shows a feature close to a pure SiC spectrum, but the spectrum is noisy and hard to interpret. R CMi has been classified as a mild carbon star, and its emission appears to be more typical of many C stars than S stars.

In conclusion, we find that the emission features of the MS, S, and SC stars span the range from the 10 and 18 μm silicate emission found in pure M star spectra, to the 10.5-11 μm S star emission, to the 11.2 μm SiC emission of C stars as might be expected from stars in transition from an O-rich to a C-rich environment with increasing s-process abundances while on the AGB. The exact nature of the carrier of the three component and the 10.5-11 μm feature remains unidentified. The 3-component feature and the typical 10.5-11 μm S star feature are also found in a few stars classified as M stars (about 15%). If these stars are related in composition to the MS and S stars needs to be investigated further.



Fifth Cambridge Workshop on Cool Stars, Stellar Systems and the Sun, eds. J.L. Linsky and R. Stencel, (Springer Verlag: Heidelberg) 1987, p. 396
WATER MASERS ASSOCIATED WITH TWO CARBON STARS: EU ANDROMEDAE and V778 CYGNI

Irene R. LITTLE-MARENIN
AFGL/OPC and Whitin Observatory, Wellesley College

Priscilla J. BENSON
Whitin Observatory, Wellesley College

Stephen J. LITTLE
Department of Natural
Sciences, Bentley College, Waltham, MA

ABSTRACT We observed the 22.2 GHz H₂O maser line from the two C stars EU And and V778 Cyg. The intensity of the line has varied by more than a factor of 5 over several months and the line has shown additional weaker components. We interpret the system as being binary with a C and an M star component with a thick shell.

Seven carbon stars are associated with oxygen-rich circumstellar shells (CS) as deduced from the presence of strong 10 μ m and 18 μ m emission features in their IRAS low resolution spectra (LRS). Only four of these carbon stars are visible with the 37 m Haystack Observatory¹ radio telescope and a search for the 6₁₆-5₂₃ H₂O maser emission line at 22,235.080 MHz has proven successful for EU And and V778 Cyg. EU And (RA=23:17:41; Dec=+46:58:00 (1950)) was detected first on 13 December, 1986 with a flux of 8.2 Jy at $V_{LSR} = -29.4$ km s⁻¹ (Benson and Little-Marenin 1987). The intensity of the water emission has fluctuated by at least a factor of 8 over the last six months (Figure 1a) and at times has shown at least one other component at -31 km s⁻¹ (Fig 2a) and once possibly another at -26 km s⁻¹. V778 Cyg (RA=20:35:07; Dec=+59:54:48 (1950)) was first (weakly) detected on 23 March, 1987 with a flux of 1.9 Jy at $V_{LSR} = -16.8$ km s⁻¹. Since then the intensity of the maser has increased by at least a factor of 5 to a value of 10.9 Jy on 6/9/87 (Figure 1b). At times the line has shown two components (weaker in intensity by about a factor of 3 to 4) at -20.6 km s⁻¹ and -16.9 km s⁻¹ (Figure 2b). The weaker components also vary in intensity, but not necessarily in phase with the main water line. BM Gem (RA=07:17:56; Dec=-+25:05:03 (1950)) has been searched over a velocity range of +98+/-90 km s⁻¹ and NC#83 (RA=19:13:55; Dec=+54:12:06 (1950)) over a velocity of -180 to +180 km s⁻¹ with negative results.

The water masers are estimated to be located in spherically expanding circumstellar shells with weaker components arising from masers located in the near and far side of the shell. Half the velocity difference (i.e. about 2 - 2.5 km s⁻¹) should then represent the expansion velocity of the shell. Theoretical models of H₂O masing regions (Cooke and Elitzur 1985) predict expansion velocities of about 3-

¹Radio astronomy at Haystack Observatory of the Northeast Radio Observatory Corporation is supported by the National Science Foundation under grant AST78-18227.

6 km s^{-1} (corresponding to a terminal velocity of about 10 km s^{-1}) in agreement with our observations. The water masing region is estimated to be located from 7 to 70 AU from the central star. Hence the material outflowing from the central star will transit through the masing region in 6 to 120 years. The transit time of material through the silicate emitting region is estimated to be between 15-20 years (assuming an expansion velocity of 5 km s^{-1}) since models predict that the $10 \mu\text{m}$ emission comes primarily from a distance of about $10 R_*$ which corresponds for M star Miras to a distance of about 15-20 AU.

It is highly unusual to find an oxygen-rich CS (as indicated by the water maser and 10 and $18 \mu\text{m}$ silicate emission), around a carbon rich photosphere. There are two main interpretations possible for the data:

A) We are observing a binary systems with a C star and an M star component with a relatively thick circumstellar shell. The CS of the M star produces the 10 and $18 \mu\text{m}$ emission and the H_2O maser line. However, the CS absorbs the visible light of the M star so that only light from the carbon star is seen in the visible and near infrared region.

B) We are observing the transition of an M star to a C star so that we still observe the O-rich material in the CS for a brief time after the central star has already become C-rich.

We favor (A), the binary system hypothesis. First, EU And was recognized as a carbon star in the 1940's and is now classified as C4,4 (SR) and V778 Cyg was recognized as such in 1933 and is now classified as C5⁻,5 (Lb). The outflowing material has traveled about 45 to 50 AU's since first being classified and should have passed through the silicate emission region over 20-30 years ago, assuming that we observed both stars at the instance of transition from M to C without going through and S and SC phase. We consider this scenario highly unlikely. Only if the water masing region is $> 50 \text{ AU}$ could we still observe O-rich material in the CS. Secondly, for EU And, we find that the observed V_{LSR} of the maser emission differs from that of the C star by more than 10 km s^{-1} which we interpret as being due to the orbital velocity of the two components. However, for V778 Cyg the water maser velocity agrees with the velocity of the C star and may indicate that the orbital plane of the system is more highly inclined and/or that the M and C star components are presently moving across our line of sight and/or that the two components are more widely separated. Assuming typical C and M star Mira masses of $< 3 M_{\odot}$ ($M_1 + M_2 < 6 M_{\odot}$) and a separation of around $2 \times 30 \text{ AU}$ (so that the water masing region will be gravitationally bound to the M star), we estimate $P_{\text{orb}} > 200$ years. This value is reasonably consistent with $P_{\text{orb}} < \text{about } 190$ years for EU And if we assume an $v_{\text{orb}} > 10/2 \text{ km s}^{-1}$ and $a=30 \text{ AU}$ in a circular orbit.

V778 Cyg shows the typical strong CN absorption features of an Lb C star in the $0.8 - 1.08 \mu\text{m}$ region (Baumert 1972) implying that the M star is at least a magnitude fainter in this spectral region. No information on the near infrared spectrum of EU

And is available. Using the Rowan-Robinson et al. dust shell models for a typical carbon star (HV Cas) and for a typical M star with a relatively thick circumstellar shell (WX Ser), we find that the C star will dominate the emission shortward of about $5 \mu\text{m}$ and the M star with its shell will dominate longward of $5 \mu\text{m}$ (assuming nearly comparable luminosities for the two components as is expected for stars in a very similar evolutionary phase) (see Benson and Little-Marenin 1987). However, in order to model correctly the observed V778 Cyg flux of about 10 Jy at $1.08 \mu\text{m}$ (Baumert thesis) and the IRAS color corrected flux of 26 Jy ($12 \mu\text{m}$), 14 Jy ($25 \mu\text{m}$) and about 1.5 Jy ($60 \mu\text{m}$) for V778 Cyg, we will need to use a slightly optically thinner C star model than WX Ser. The $100 \mu\text{m}$ flux of 9.8 Jy (uncorrected) may be contaminated by the infrared cirrus.

REFERENCES

- Baumert, J. 1972, Ph.D. thesis, (Ohio State University)
 Benson, P.J., and Little-Marenin, I.R., 1986, *Ap.J.(Lett)*, 316, L37.
 Cooke, B., and Elitzur, M. 1985, *Ap.J.*, 295, 175)

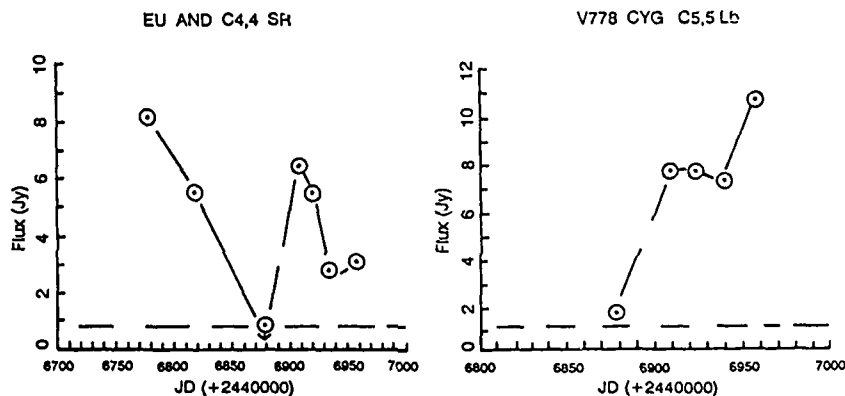


Figure 1a, b. The variation of the 22 GHz H_2O line as a function of Julian Date

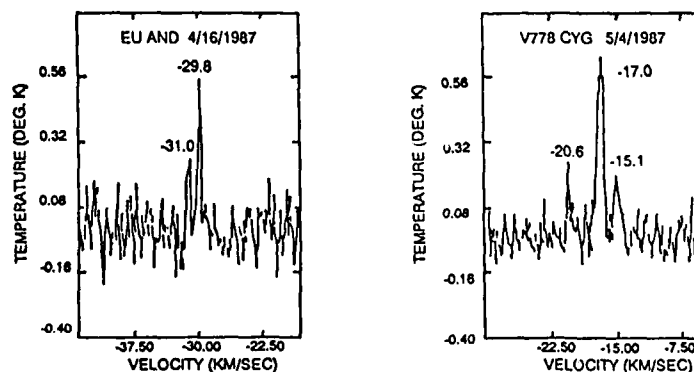


Figure 2a, b. The 22 GHz spectrum of EU And and V778 Cyg shows weaker components

Appendix M

New Late-Type Stars with Technetium, and Missing LRS Spectra of
IRAS C and S Stars, Pub. as Poster Paper Abstracts in Bull. AAAS

New Late-Type Stars with Technetium

S. J. Little (Bentley C.), I.R. Little-Marenin (AFGL, Wellesley C.), W. Hagen and L. Lewis (Wellesley C.)

We have added 89 stars to our list of late-type stars analyzed for the presence of the radioactive element technetium (Tc I, half-life = 200,000 yr). This brings the list of stars that have been analyzed up to 240 stars. We have found six new Mira variables which definitely show the presence of Tc I in their spectra. They are listed in Table 1 below. Three of these stars are pure M stars with periods of about 330 days. In addition we find 13 stars with the probable presence of Tc I lines. These stars are: R Aur, AA Cam, S CMi, V CMi, RS Cyg, RZ Her, T Hya, Y Lyn, V Mon, SW Peg, R Psc, RR Sgr, and TY Sgr. Nine other stars possibly show the presence of Tc I.

In the remaining 61 stars we find little evidence for the presence of Tc I lines. A large fraction of these 61 stars are not Mira variables, and many have a low amplitude of variation. Ten are supergiants, which we have never found to show the presence of technetium unless they are also MS stars.

TABLE 1. STARS DEFINITELY SHOWING Tc I LINES

W Cet	M-351	S6,3-S9,2e
R Col	M-328	M3e-M4e
T Gem	M288	S1.5,5e-S9,5e
V Gem	M-275	M4e(S)-M5e
RR Hya	M-343	M3.0e-M8e
RX Sgr	M-334	M5e

American Astronomical Society
Abstract submitted for the 168th (Ames) Meeting

Date Submitted _____

FORM VERSION 2/86

Missing LRS Spectra of IRAS C and S Stars

R.B. Culver (Colorado St. U.), I.R. Little-Marenin (AFGL, Wellesley C.), S.J. Little (Bentley C.), E.R. Craine (E/ERG)

We have made a study of IRAS low-resolution spectra (LRS) of both carbon and S type stars and have noticed that some of the brightest C and S stars have no LRS. In order to make an assessment of the number of missing spectra, we instituted a search of the IRAS point source and LRS catalog.

CARBON STARS: 337 identified carbon stars are listed in the point source catalog with flux densities >8 Jy at either $12 \mu\text{m}$ or $25 \mu\text{m}$. Of these 79 are not found in the LRS catalog with 59 having galactic latitudes $b > 2^\circ$ and therefore free from the clutter with galactic plane sources.

S Stars: 94 identified S stars are listed in the point source catalog with flux densities >8 Jy at either $12 \mu\text{m}$ or $25 \mu\text{m}$. Of these 28 have no LRS with 18 having $b > 2^\circ$.

The percentage of missing spectra for stars in the IRAS point source catalog with $b > 2^\circ$ is 19% for the carbon stars and 17% for the S stars. These percentages are far greater than the number expected to be rejected by source confusion (2-3%). All but one of the point sources were observed at least twice (most of them three times or more). The reason for the missing spectra remains unknown.

American Astronomical Society
Abstract submitted for the 188th (Ames) Meeting

Date Submitted _____

FOHM VERSION 2/88